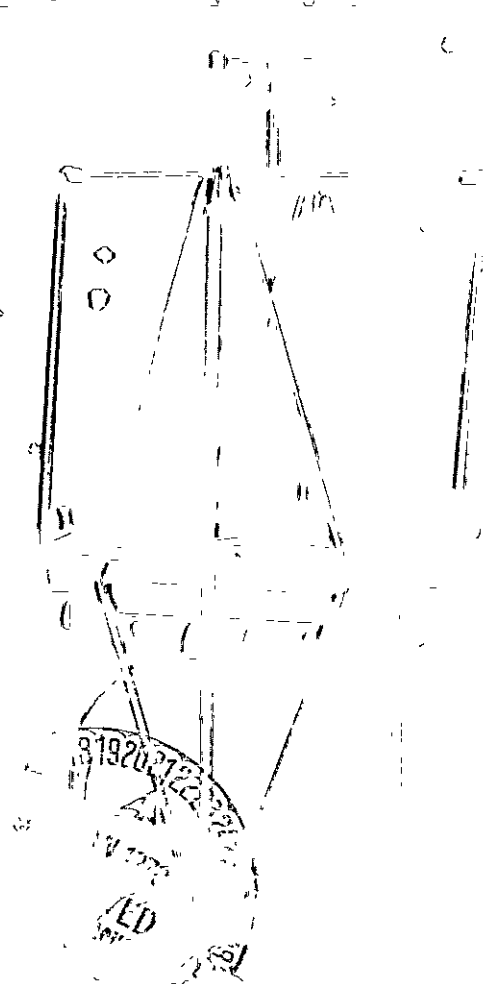


LUNAR LOGISTICS VEHICLE



FACILITY FORM 602	N70-17551	(ACCESSION NUMBER)	(THRU)
	<i>395</i>		<i>1</i>
	<i>CR-702078</i>	(PAGES)	(CODE)
		(NASA CR OR TMX OR AD NUMBER)	<i>31</i>
		(CATEGORY)	

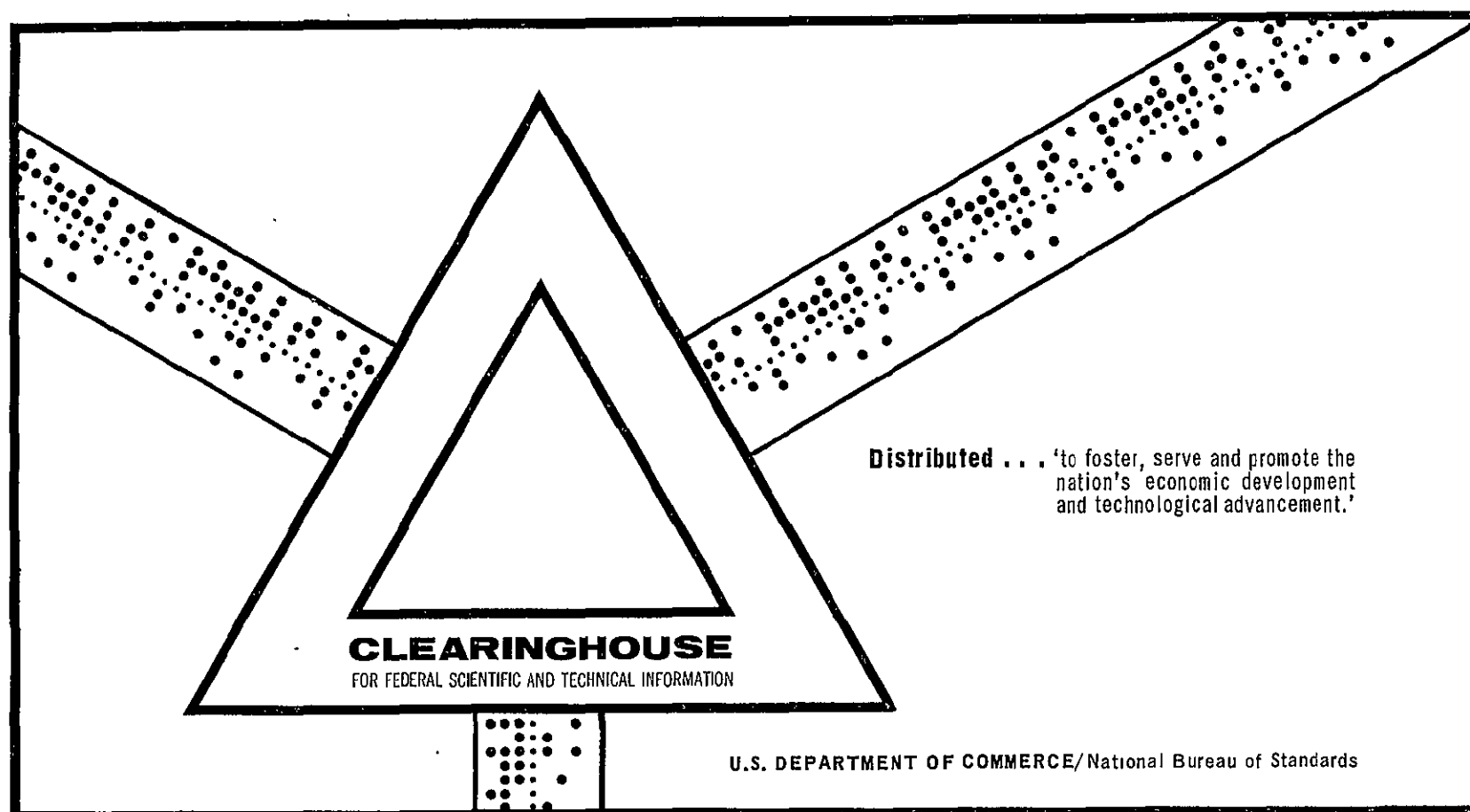
Reproduced by the
CLEARINGHOUSE
for Federal Scientific & Technical
Information Springfield Va 22151

LUNAR LOGISTICS VEHICLE

F. Davidson, et al.

University of Houston
Houston, Texas

September 1969



LLV

Lunar Logistics Vehicle


Houston - NASA MSC - Rice

Faculty Systems Engineering Institute

September, 1969

Final Report

Approved by:



C. J. Huang, Co-Director
University of Houston

Edited by:

F. Davidson
S. Dickerson
University of Houston



Bass Redd, Co-Director
NASA MSC, Houston, Texas

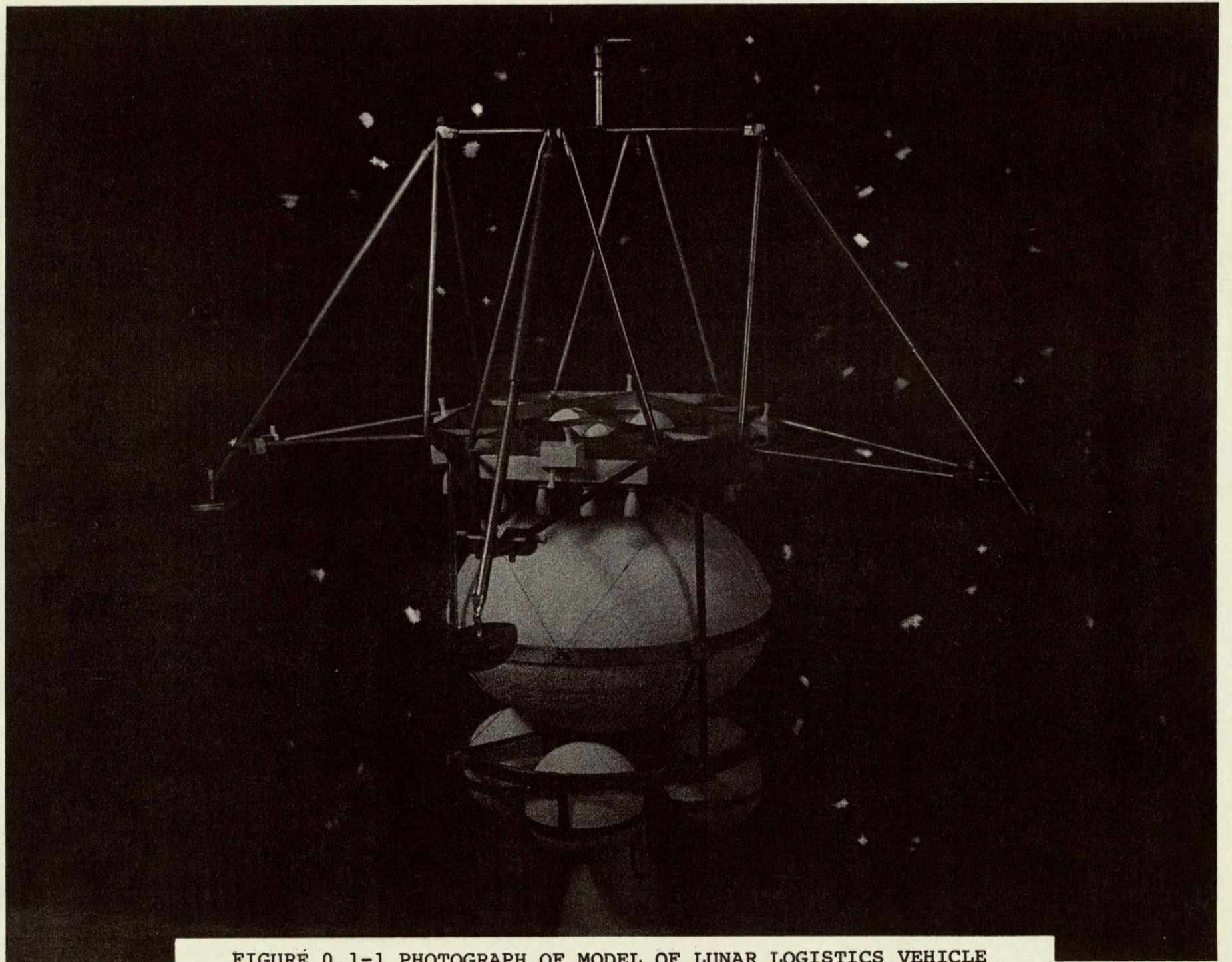


FIGURE 0.1-1 PHOTOGRAPH OF MODEL OF LUNAR LOGISTICS VEHICLE

FOREWORD

Steve Dickerson

0.1. Introduction

NASA, the University of Houston and Rice University intend that the Summer Faculty Programs in Systems Engineering acquaint the faculty of selected engineering colleges with the systems approach to complex design problems. The technique used is to involve the participating professors in a real conceptual design of a space system. See Figure 0.1-1. These summer educational experiences are based on Dr. William Bollay's initial graduate courses at MIT and Stanford. It is hoped that some of the major beneficial results of the program are the following.

- o The participants will have a better understanding of NASA's contributions, goals, and operations.
- o The participants will be able to organize new or modify existing design courses at their home institutions along the lines of the summer program.
- o The participants and their students will have a better appreciation of the contributions of other disciplines, including the non-engineering, and the need for effective cross fertilization.
- o A study of value to NASA will result.

0.2 Participants

Nineteen professors and instructors from eighteen different universities and colleges attended the program. By discipline there were three in electrical engineering, five in mechanical engineering, five in civil engineering, three in aerospace

TABLE 0.2-1 PARTICIPANTS AND STAFF

Dr. Floyd O. Calvert Research Institute University of Oklahoma	Prof. Thomas M. Perkins Engineering Technology Dept. Western Kentucky University
Dr. Jack H. Cole Mechanical Engineering Dept. University of Arkansas	Dr. Angelo J. Perna Civil Engineering Dept. Newark College of Engineering
Dr. Frederic M. Davidson Electrical Engineering Dept. University of Houston	Dr. George Pincus Civil Engineering Dept. University of Houston
Dr. Izydor Eisenstein Mechanical Engineering Dept. Purdue University	Dr. Charles G. Richards Mechanical Engineering Dept. University of New Mexico
Dr. Clift M. Epps Mechanical Engineering Dept. Texas Tech University	Dr. Joseph E. Robertshaw Physics Department Providence College
Dr. George E. Gless Electrical Engineering Dept. University of Colorado	Dr. Juda E. Rozenberg Civil Engineering Dept. Christian Brothers College
Dr. George F. Hauck Civil Engineering Dept. Tri-State College	Dr. Alvin M. Strauss Mechanical Engineering Dept. University of Kentucky
Dr. Frank J. Hendel Aeronautical Engineering Dept. California State Polytechnical College	Prof. Frank R. Swenson Mechanical & Aerospace Engr. Dept. University of Missouri
Dr. Benjamin Koo Civil Engineering Dept. University of Toledo	Dr. Jesse M. Wampler Geophysical Sciences Georgia Institute of Technology
Dr. Samuel J. Kozak Geology Department Washington & Lee University	
<hr/>	
C. J. Huang, Director Associate Dean of Engineering University of Houston	S. L. Dickerson, Associate Director University of Houston and Georgia Institute of Technology
A. N. Paul, Assistant Director Industrial Engineering Dept. University of Houston	D. B. Mackay, Faculty Advisor Dept. of Aerospace Engineering Rice University
Dennis Laue NASA Summer Intern Purdue University	Terrence Cheng Draftsman University of Houston

engineering, one in physics and two in geology. Table 0.2-1 contains a complete list of the participants. With one exception they had no previous experience in space system engineering.

0.3 Time Table

The program started June 9 and ended August 22, 1969. This eleven week period was broken into three phases, characterized roughly as the problem and alternative definition phase, alternative evaluation phase, and the reports preparation phase. Oral reports on project progress were prepared by the participants and presented at the end of each phase to members of the Engineering and Development Directorate at the Manned Spacecraft Center. The presentation for Phase III was a complete summary of the ~~entire~~ project and was open to the public. A chronological listing of the major milestones during the summer are given in Table 0.3-1.

TABLE 0.3-1 PROJECT MILESTONES

<u>Date</u>	<u>Milestones</u>
June 9	Program begins
June 13	Project teams organized, Phase I leadership selected.
June 27	Phase II leadership selected
July 1	Phase I oral review - statement of problem, alternative solutions, relevant technical material.
July 25	Phase III leadership selected
July 29	Phase II oral review- trade off studies and recommendation of basic design.
Aug 19	Final oral report -review of entire project and presentation of recommended LLV design.
Aug 22	All final report contributions due. Program ends.

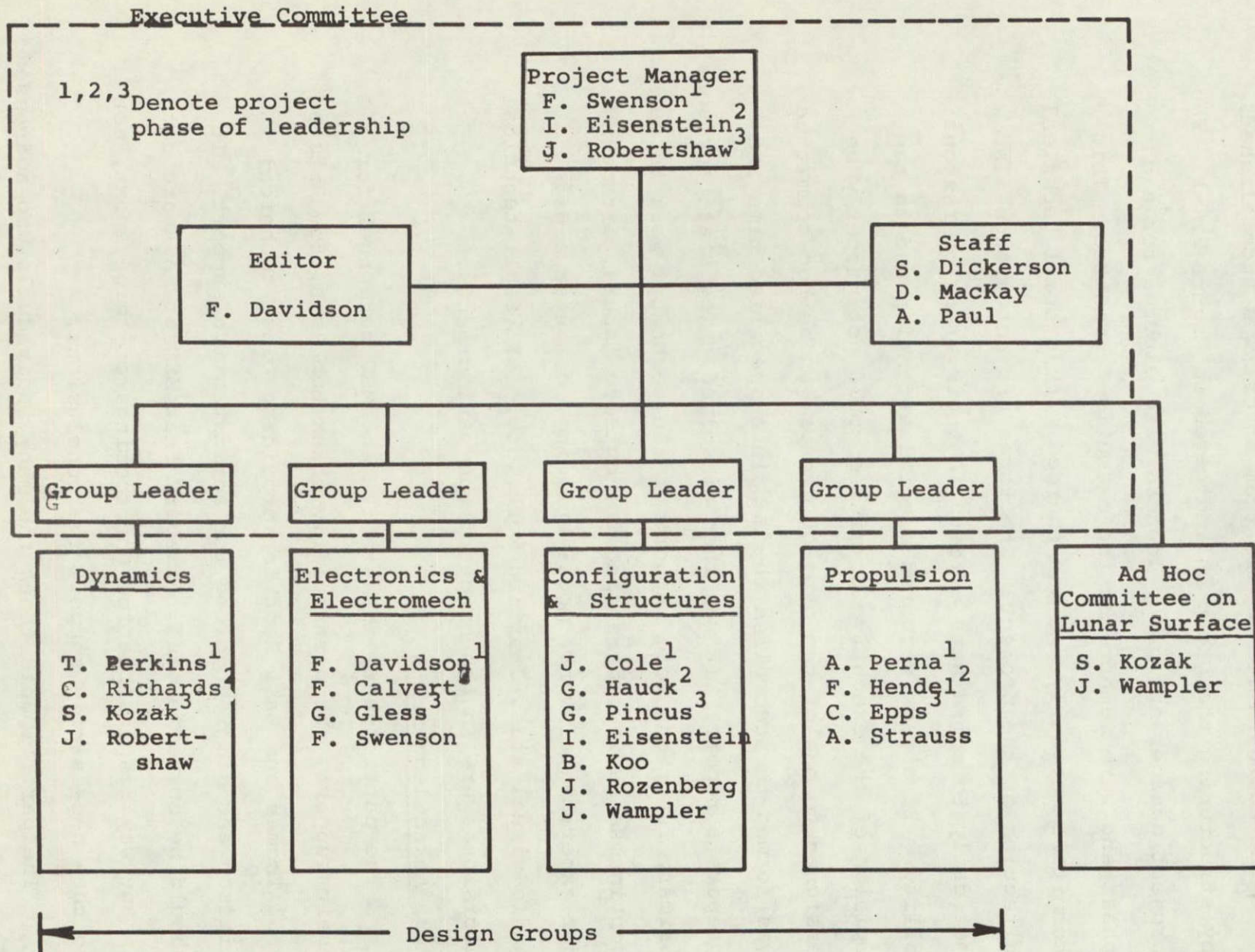
0.4 Organization

The coordination of the team effort was accomplished by structuring the group as indicated in Figure 0.4-1. The project manager and group leaders were elected for each phase and were members of the executive committee. This committee met daily and was charged with overall technical direction of the project. The three project groups also met daily to coordinate efforts in their areas of responsibility. If a task required special attention and in the opinion of the executive committee could not properly be assigned to one of the project groups, an ad hoc committee was formed to accomplish the task in a specified time and prepare a report. It was then dissolved. The staff advisors primary functions were support of the technical work through continuous review, arranging for outside inputs, arranging for experimental work, model building, computer aids, audio-visual aids, drafting work, etc. All final technical decisions were in the hands of the participants.

0.5 Acknowledgements

The participants and staff thank MSC personnel for their support. We particularly thank Bob Abel, Bob Bristow Paul Thomas and Bass Redd for providing close technical liaison and Jim Youngblood for administrative support. It should be borne in mind, however, that MSC or NASA are not in any way responsible for shortcomings of this report, nor do they necessarily support the conclusions.

The participants thank the many individuals who addressed



14

FIGURE 0.4-1 DESIGN GROUP STRUCTURE

the team to provide the essential background information. A list of the speakers, their topics and affiliations is given in Table 0.5-1.

Many others at MSC provided informal assistance to the group through individual consulting. Among these people are Arlie Fisher in the area of structural design, Jerry Smithson in propulsion, and Wilbur Wallenhaupt in flight operations.

Don Mackay, of Rice University, gave the group the benefit of his considerable industrial experience in aerospace firms.

We are indebted to the encouragement of Messrs. Francis B. Smith, Frank D. Hansing and Charles H. Carter of NASA Office of University Affairs; President Philip G. Hoffman, Mr. Paul Purser, Special Assistant to the President, and Dean C. V. Kirkpatrick of the University of Houston; Dr. Maxime Faget of NASA-MSC; and Vice President W. E. Gordon of Rice University.

Finally, we thank Mrs. Inez Law for tolerating twenty some bosses for eleven weeks.

TABLE 0.5-1 OUTSIDE SPEAKERS

<u>TOPIC</u>	<u>SPEAKER</u>	<u>AFFILIATION</u>
The Intermediate Size Lunar Logistic Spacecraft	P. G. Thomas	Engineering Analysis Office, MSC
Advanced Lunar Operations and ISLLS Payloads	A. J. Meyer	Adv. Missions Program Office, MSC
The Lunar Surveyor Program	C. Kirsten	Jet Propulsion Laboratory
Lunar Terrain	L. Wade	Mapping Sciences Lab., MSC
Costing	H. Mandell	Program Control Division, MSC
Main Propulsion and Reaction Control Systems	M. Lausten N. Chaffee	Propulsion and Power Division, MSC
Electrical Power Systems	D. Haines	Propulsion and Power Division, MSC
Communications and Instrumentation	J. Shephard	Space Electronics Systems Div., MSC
Structural and Thermal Consideration	A. Mackey	Structures and Mechanics Div., MSC
Landing Dynamics	George Zupp	Structures and Mechanics Div., MSC
Guidance and Control Systems	M. Jones Ed Chevers	Guidance and Control Div., MSC
Lunar Trajectory and Performance	B. Abel	Engineering Analysis Office, MSC

1969 NASA - ASEE Faculty Systems Engineering Institute
U. of Houston - - NASA MSC - Rice University Participants



(Left to Right) Third Row: D. MacKay Associate Director, F. Davidson, A. Strauss, R. Abel, F. Calvert, F. Swenson, C. Epps, A. Paul Associate Director, G. Hauck, B. Koo, G. Pincus. Second Row: J. Vitali NASA Washington Representative, J. Cole, C. Richards, J. Wampler, F. Hendel, S. Kozak, T. Perkins, J. Rozenberg, R. Bristow, A. Perna, D. Laue. First Row: S. Dickerson Associate Director, G. Gless, C.J. Huang Director, I. Eisenstein, J. Robertshaw, J. Youngblood, Director.

ABSTRACT

The preliminary design of an unmanned space vehicle that can land a payload of 2500 pounds on the moon is presented. The design is based on a maximum use of developed, space qualified hardware so that the vehicle can be made operational by 1973. The Titan III-D Centaur will be the launch vehicle. This booster combination can insert a 12,000 pound spacecraft into a translunar trajectory. Total program costs for an eight mission program would be approximately \$400,000,000, exclusive of payload costs.

Lunar touchdown 3-sigma landing dispersions of one kilometer relative to targeted geological features anywhere on the visible face of the moon are proposed. These can be obtained with the use of direct descent trajectories and terminal guidance corrections based on remote television transmissions. The vehicle can be safely landed in lunar slopes of up to 35 degrees with the aid of low touchdown velocities, held-down rockets, and a four-pad landing gear. Retro propulsion is provided by a main cryogenic stage that consists of a Pratt & Whitney RL-10A-3-3 engine, and is jettisoned after burnout at low altitude. Touchdown is accomplished with the use of a monomethyl hydrazine, nitrogen tetroxide vernier propulsion system that consists of sixteen modified Marquardt R-4D thrusters.

Other proposed major subsystems include a fuel cell and primary battery power supply, and a guidance and navigation system composed of the Lunar Module landing radar, inertial measuring unit, and modified guidance computer.

TABLE OF CONTENTS

FORWARD		
0.1	Introduction	ii
0.2	Participants	ii
0.3	Time Table	iv
0.4	Organization	v
0.5	Acknowledgements	v
PHOTOGRAPHS OF PARTICIPANTS		ix
ABSTRACT		x
TABLE OF CONTENTS		xi
LIST OF FIGURES		xiii
LIST OF TABLES		xvi
I.	INTRODUCTION	
1.1	Mission Objectives	1
1.2	Mission Constraints	2
II.	ALTERNATIVE SPACECRAFT DESIGN AND SELECTION	
2.1	Alternative Space Frame Configurations	6
2.2	Alternative Propulsion Systems	16
2.3	Summary of Guidance and Navigation System	18
2.4	Electrical Power System	23
2.5	Telemetry and Communications	25
2.6	Summary of Proposed Design	30
III.	FLIGHT CONTROL SYSTEM	
3.1	Guidance and Navigation System	35
3.2	Mission Profile	53
3.3	Some Trajectory Considerations	55
3.4	Landing Television System	78
IV.	PROPULSION	
4.1	Propulsion Requirements	100
4.2	Main Retro System	125
4.3	Vernier System	144
4.4	Reaction Control System	158
4.6	Propulsion Weight, Power Requirements and Costs	177
4.7	Trade-off Studies of Alternative Propulsion Systems	183
V.	ELECTRICAL POWER SYSTEM	
5.1	Introduction	197
5.2	Power System Requirements	198
5.3	Candidate Power Systems	205
5.4	Power System Comparison	207

5.5	Electrical Devices Battery	213
VI.	TELECOMMUNICATIONS	
6.1	Communication Subsystem Requirements	216
6.2	Communication Subsystem	223
6.3	Instrumentation Subsystem	229
6.4	Operational Considerations	234
VII	THERMAL CONTROL	
7.1	Thermal Control Requirements	238
7.2	Thermal Control System Design	247
7.3	Future Development	
VIII.	VEHICLE STRUCTURES AND SUBSYSTEMS	
8.1	Thrust and Retro Structure	263
8.2	Lander Structure	
8.3	Landing Gear	268
8.4	Payload Deployment	276
8.5	Vehicle Summary	
IX.	SOFT LANDING ANALYSIS	
9.1	Introduction	286
9.2	Static Stability	286
9.3	Dynamic Stability-- Energy and Momentum Methods	286
9.4	Solutions to Landing Equations of Motion	310
9.5	Dynamic Landing Model Tests	329
9.6	Probability of Safe Landing Analysis	336
X.	SYSTEM COST, SCHEDULE, AND RELIABILITY	
10.1	Cost Summary	347
10.2	Development Schedule	350
10.3	Reliability	351

LIST OF FIGURES		Page
0.1-1	Photograph of 1/10 Model of Lunar Logistics Vehicle	i
0.4-1	Design Group Structure	vi
1.2-1	Payload Envelopes	5
2.1-1	Initial Configuration Concepts	8
2.1-2	Comparison of Configuration Merit	9
2.1-3	Camel	11
2.1-4	Crushable Bowl Lander	11
2.1-5	Bottom Mounted Payload Lander (Separable)	12
2.1-6	Bottom Mounted Payload Lander (Integral)	13
2.6-1	1/10 Detail Drawing of Lunar Logistics Vehicle	30
2.6-2	1/10 Detail Drawing of Lunar Logistics Vehicle	31
3.1-1	Typical Earth Based Tracking Errors	37
3.1-2	Predicted Landing Site Miss Distance	40
3.1-3	Block Diagram of Guidance and Navigation System	49
3.2-1	Guidance and Navigation Mission Profile	54
3.3-1	Descent From Hover	58
3.3-3	Translation at Constant Altitude	58
3.3-2	ΔV to Descend from Hover	60
3.3-4	ΔV to Translate at Constant Altitude	65
3.3-5	Hop Trajectory	66
3.3-7	Approximate Trajectory Geometry	66
3.3-6	ΔV to Hop vs Hop Distance	71
3.3-8	Site Redesignation (Approximate)	73
3.3-9	Angle of Incidence vs Longitude	76
3.3-10	RL10 Tangential Trajectory	77
3.4-1	LLV Landing Television System	79
3.4-2	Earth Control System	81
3.4-3	LLV Landing Television System	86
3.4-4	Line-of-Sight Geometry in Along-Track Plane	88
3.4-5	Line-of-Sight Geometry in Cross-Track Plane	88
3.4-6	Line-of-Sight Geometry to the Lunar Horizon	90
3.4-7	Line-of-Sight Angles	91
3.4-9	Effective Fields of View	94
4.1-1	Characteristic ΔV vs F_0/W for High Energy Mission	101
4.1-2	Pictorial Representation of ΔV Requirements	102
4.1-3	ΔV for Midcourse vs Propellant Requirements	105
4.1-4	ΔV vs Weight of Propellant	107
4.1-5	Propellant for High Energy Mission with Throttleable RL 10	108
4.1-6	ΔV vs Altitude for LVPS Ignition for Hover at 100 ft.	112
4.1-7	Effect of Altitude on LVPS Propellant Requirements for Hover at 100ft.	112
4.1-8	ΔV vs LVPS Initiation Altitude	113
4.1-9	Effect of Target Velocity on Propellant Requirements for LVPS	114
4.1-10	Propellant Requirements for LVPS	115
4.1-11	Effect of Target Velocity in Propellant Weight for LVPS	116
4.1-12	Propellant Weight for LVPS	117

LIST OF FIGURES

(Continued)

4.1-13	Weight of Vehicle at Hover vs Weight of Propellant	119
4.2-1	Installation Drawing of RL10A-3-3	130
4.2-2	RL10 Propellant Control System	134
4.2-3	Pressurization of LOX and LH ₂	135
4.2-4	Effect of Increasing Area Ratio in RL10 on Performance	141
4.2-5	Estimated I _{sp} vs Thrust in RL10	142
4.2-6	Main Retro System	143
4.3-1	Vernier R-4D Engine	145
4.3-2	Initial Velocity and % Velocity Loss vs F/W ₀	148
4.3-3	Structure for Verniers and RCS	150
4.3-4	Helium Pressurization	152
4.3-5	Advanced Liquid Propulsion System	155
4.3-6	Helium Pressurization with Solid Gas Generated	156
4.4-1	RCS 4-1E Engine	159
4.4-2	Pulse Mode of RCS Operation	160
4.5-1	Attitude Control System	166
4.5-2	Gas Jet Thruster	170
4.5-3	Sequence of Rotation for Euler Equations	174
4.5-4	Commanded and Body Rates vs Time	174
4.7-1	Thermal Consideration in Vernier Design	191
4.7-2	All Propulsion Systems	194
5.2-1	Power Profile	201
5.2-2	Reactant & Tanhape Weight for Extended Survival	202
5.4-1	Schematic Illustration - Electrical Power System	208
6.1-1	Diagram of Telecommunications System	217
6.1-2	Diagram of Stored Program Data Processor & Signal Conditioning	219
6.2-1	Horizontal "Line" of TV Scan Signal	225
7.1-1	Surface Temperature for Vertical Oriented Radiator	242
7.1-2	Maximum Fuel Cell Power Output Permissible During Lunar Day	244
7.2-1	Insulation Heat Gain for Lunar Day	249
7.2-2	Insulation Heat Loss for Lunar Night and Transit	251
7.2-3	Thermal Switch Properties	254
7.3-1	Directional Emissivity Wall Configuration	260
8.3-1	LLV - General Landing Gear Configuration	270
8.5-1	Subsystems Configuration	278
9.2-1	Variation of Static Stability with C.G. Height to Landing Gear Radius Ratio	287
9.3-1	Back Legs, Front Legs Contact Initially	289
9.3-2	Vehicle Attitude at Initial Contact	290
9.3-3	Vehicle Attitude During Stability Rocket Firing	293
9.3-4	Vehicle Attitude at Initial Contact	295
9.3-5	Stability Rocket Thrust vs Surface Slope Angle	298
9.3-6	Stability Rocket Thrust vs Surface Slope Angle	299
9.3-7	Stability Rocket Thrust vs Surface Slope Angle	300
9.3-8	Stability Rocket Thrust vs Surface Slope Angle	301
9.3-9	Stability Rocket Thrust vs Surface Slope Angle	302

LIST OF FIGURES

(Continued)

9.3-10	Stability Rocket Thrust vs Surface Slope Angle	303
9.3-11	Stability Rocket Thrust vs Vertical Velocity	304
9.3-12	Stability Rocket Thrust vs Vertical Velocity	305
9.3-13	Stability Rocket Thrust vs Vertical Velocity	307
9.3-14	Stability Rocket Thrust vs Vertical Velocity	308
9.4-1	Primary and Secondary Strut Configuration	311
9.4-2	Computer Model Geometry	313
9.4-3	Touchdown Sequence & Stability Criteria	314
9.4-4	Variation of Landing Stability Boundaries with Touchdown Velocities	324
9.4-5	Variation of Landing Stability Boundaries with Touchdown Velocities	325
9.4-6	Variation of Landing Stability Boundaries with Touchdown Velocities	326
9.4-7	Variation of Touchdown Energy Absorbed with Surface Slope and Vertical Velocity	327
9.5-1	Landing Dynamic Model	331
9.5-3	Landing Dynamics Test Apparatus	331
9.5-2	Dynamic Model Photograph	332
9.5-4	Dynamic Test Apparatus Photograph	332
9.5-5	Experimental Results of Dynamic Model Simulation	334
9.6-1	Landing Uncertainty Circle vs Unhazarded Area	342
9.6-2	Circular Scan Area for .99% Probability of One Hazard Free Landing Site	343
9.6-3	TV Lens Angle vs Scan Radius	344
9.6-4	Effective Slope vs Probability of Slope Greater Than Effective Slope	345
10.2-1	Development Schedule	350
10.3-1	Functional Diagram	376
10.3-2	Logic Diagram	377

LIST OF TABLES

0.2-1	Participants and Staff	iii
0.3-1	Project Milestones	iv
0.5-1	Outside Speakers	viii
2.1-1	Preliminary Evaluation Matrix	9
2.1-2	Configuration Comparison Table	14
2.3-1	Alternative Guidance and Navigation Systems	19
2.3-2	Components of LLV Guidance and Navigation System	21
2.4-1	Electrical Power System Alternatives	23
2.4-2	Selection Criteria	24
2.5-1	Telecommunication Subsystem Requirements	28
2.5-2	Telecommunication Subsystem Candidates	29
2.6-1	Summary of Weights	34
3.1-1	Attitude Control Celestial Sensor Group	43
3.1-2	Physical Properties of Guidance and Navigation System Components used in Midcourse Correction Maneuver	45
3.1-3	List of Computer Programs	48
3.1-4	Guidance and Navigation System Box	52
3.3-1	AV Budgets for Lunar Descent (60 HR)	56
3.4-1	LTVNS Delay Time	83
4.1-1	AV Requirements for High Energy Mission	103
4.1-2	Burn Time for Midcourse Correction	104
4.1-3	Effect of Hover Attitude in Propellant Requirement for Touchdown	120
4.1-4	Propulsion System Penalty for Hop	121
4.1-5	Summary of Requirements for Propulsion	123
4.2-1	RL10A-3-3 Specification	126
4.2-2	RL10A-3-7 Specification	128
4.2-3	Main Difference in RL10A-3 Engine	132
4.3-1	Propellant Flow Rates for R-4D Engine	149
4.5-1	GH ₂ Budget for Attitude Control Set	172
4.6-1	Propulsion Weights	178
4.6-2	Propulsion Power and Energy Requirements	180
4.6-3	Estimated Cost	182
4.7-1	Trade-off Analysis of Retro Candidates	186
5.2-2	Summary of Energy Requirements	198
5.2-1	Electrical Load Summary	199
5.2-3	Peak Power	203
5.4-1	Candidate Power Systems	209
5.4-2	Advantage and Disadvantage Candidate Power Systems	210
5.4-3	Power System Weight	211
5.5-1	Performance of Explosive Devices Battery	213
5.6-1	Specifications for Fuel Cells & Battery System	214
6.1-1	Additional Telecommunication Requirement	218
6.1-2	Communication & Instrumentation Design Parameters	222
6.2-1	Communication Subsystem - Details	226
6.3-1	Instrumentation Subsystems - Details	230
6.3-2	Instrumentation Subsystems Comparison of Candidates	231

LIST OF TABLES

(Continued)

6.4-1	Candidate Landing Television System Cameras	235
7.2-1	Electronic Compartment A & B Thermal Control Design for Lunar Day	253
7.2-2	Electronic Compartments A & B Thermal Control Design for Lunar Night	253
7.2-3	Battery Compartment Thermal Control Design	256
8.3-1	Energy Absorption on One Landing Gear	274
8.5-1	Thrust and Retro Structure - Member Summary	280
8.5-3	Propulsion System Weight	281
8.5-4	Propellant Weights	281
8.5-5	Guidance and Navigation System Weight	282
8.5-6	Power System Weight	282
8.5-7	Communication System Weight	283
8.5-8	Instrumentation System Weight	283
8.5-9	Environmental Control System Weight	284
9.5-1	Similitude Parameters	329
9.5-2	Parameter Variations	333
9.6-1	Probability of Unhazarded Area	338
10.1-1	Estimated Subsystem Costs	347
10.1-2	Cost Buildup Summary	349
10.3-1	Failure Mode and Effects Analysis	367

CHAPTER I
INTRODUCTION

Joe Robertshaw

1.1 Mission Objectives

1.1.1 Types of Missions

The primary mission of the Lunar Logistics Vehicle (LLV) is to accurately soft-land a variety of payloads at any selected site on the visible face of the moon to support lunar exploration. The LLV is to be capable of performing in conjunction with separately-launched manned spacecraft and independently in unmanned missions. Some of the possible payloads are the Apollo Lunar Science Experiment (ALSEP), a shelter for the extension of astronaut stay-time, a lunar rover vehicle, lunar flying units, mobility supplies and propellants, life-support equipment, tools and equipment to be used by astronauts, a large stationary geological/geophysical package, an astronomical observatory, and various scientific payloads.

1.1.2 Mission Functions

The primary function of the LLV is to transport payload to the moon. However, it is desirable that the LLV systems be able to determine the condition of the payload after landing, verify deployment of the payload, and provide some support to the payload. Furthermore, if more than one spacecraft is to land at a given site, the LLV should have a beacon or transponder so that it can be easily located by following spacecraft.

1.1.3 Principles of Alternative Evaluation

The principle measure of effectiveness of the LLV system is

useful payload landed on the moon. Cost, mission success probability, development risks, flexibility in accommodating various payloads, ease of payload deployment, and growth potential were evaluated to aid in the selection of the configuration. It was assumed that there would be a total of eight missions.

1.2 Mission Constraints

1.2.1 Constraints Due to the Launch Vehicle and Trajectories

The LLV will be launched by a Titan III-D Centaur, which has the capacity to insert 12,000 pounds into a translunar trajectory. The LLV must be compatible with this launch vehicle and hence have a total weight of 12,000 pounds or less. The overall dimensions of the LLV are limited by the payload envelope of the Titan III-D Centaur which is about 300 inches long with a diameter varying from 120 inches to 150 inches. The LLV-Centaur interface is a 120-inch diameter structural ring with twelve hard points. The LLV must be able to withstand launch accelerations of 6g vertical and 2g horizontal.

The following trajectory ground-rules were laid down for the LLV:

Translunar Trajectory

60 to 120 hour trip time

60 hour:4500 fps hyperbolic excess velocity

120 hour:2500 fps hyperbolic excess velocity.

Midcourse Correction Budget

$\Delta V = 100$ fps

Lunar Phase

Orbital and/or direct descent

Landing site redesignation budget $\Delta V = 150$ fps

Constant attitude final approach

Hover: 20 seconds minimum

1.5% flight performance reserves

0 to 90 degree flight path angles with respect
to lunar horizon at initiation of retro

Maximum vertical landing velocity = 15 fps

Maximum horizontal landing velocity = 5 fps

It is desirable that the LLV land within a 3σ 1 km radius of the target, and it would enhance the effectiveness of the LLV if it had the capability, either built-in or through slight modification, to lift off after landing and "hop" to another site. Therefore, design considerations included the cost of a post-landing hop of 1 km.

1.2.2 Constraints Due to Payload

The LLV must interface with the payload through a structural ring. The C.G. of the payload is confined to a conical frustum 2.5 ft high located coaxially with the payload. The base diameter is 2 ft, and the top diameter is 1 ft. (See Figure 1.2-1.) It is desirable that the LLV payload capability be 2500 lb or more. The volume of the payload compartment must be compatible with the types of payloads mentioned in Section 1.1.1. In particular, the rover vehicle and lunar shelter provide upper limits to the payload envelope. The lunar rover is about 5 ft x 5 ft x 10 ft, and the shelter is 9 ft in diameter and 7 ft in length. Thus, the payload volume must be at least 7 ft high and wide enough to accommodate the lunar rover in a horizontal position, i.e. 10 ft or more.

1.2.3 Constraints: Due to Lunar Surface Conditions

It is desirable that the LLV be able to land in the rough terrain of the lunar highlands. Therefore, design considerations include safe landing on slopes up to 35° and among boulders of one foot diameter.

The LLV systems must function long enough in the extreme temperature conditions of the lunar environment to make immediate post-landing checkouts that determine the condition of the payload and success of payload deployment. It would enhance the effectiveness of the LLV ~~if~~ the life of the LLV systems could be extended. Therefore, design considerations included LLV system lifetimes up to 90 days and resultant costs.

1.2.4 Cost and Schedule Constraints

The LLV design objectives include low cost, maximum flexibility, and moderate growth potential. Maximum use of flight-proven systems such as those on Surveyor, Lunar Orbiter, and Apollo had to be made. There were to be few exceptions to this constraint.

The LLV is scheduled for use in the 1973-76 time period. Development time for any recommended systems must meet this constraint.

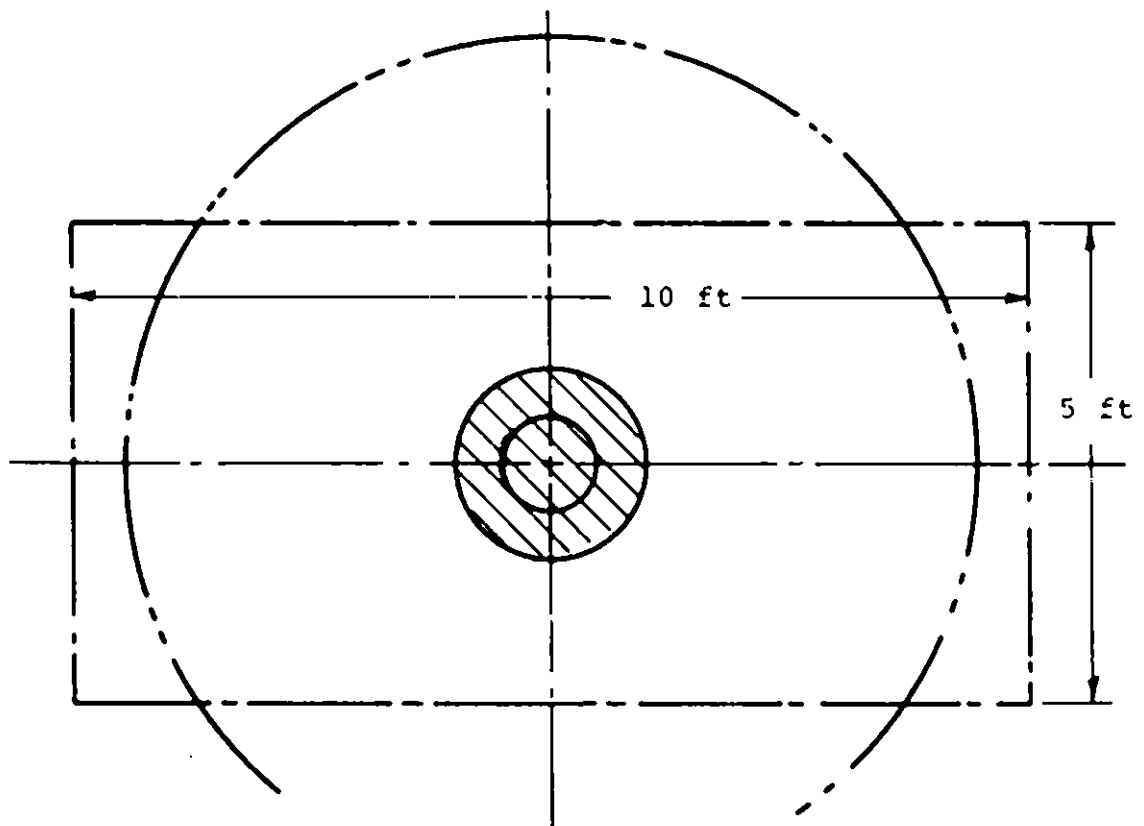
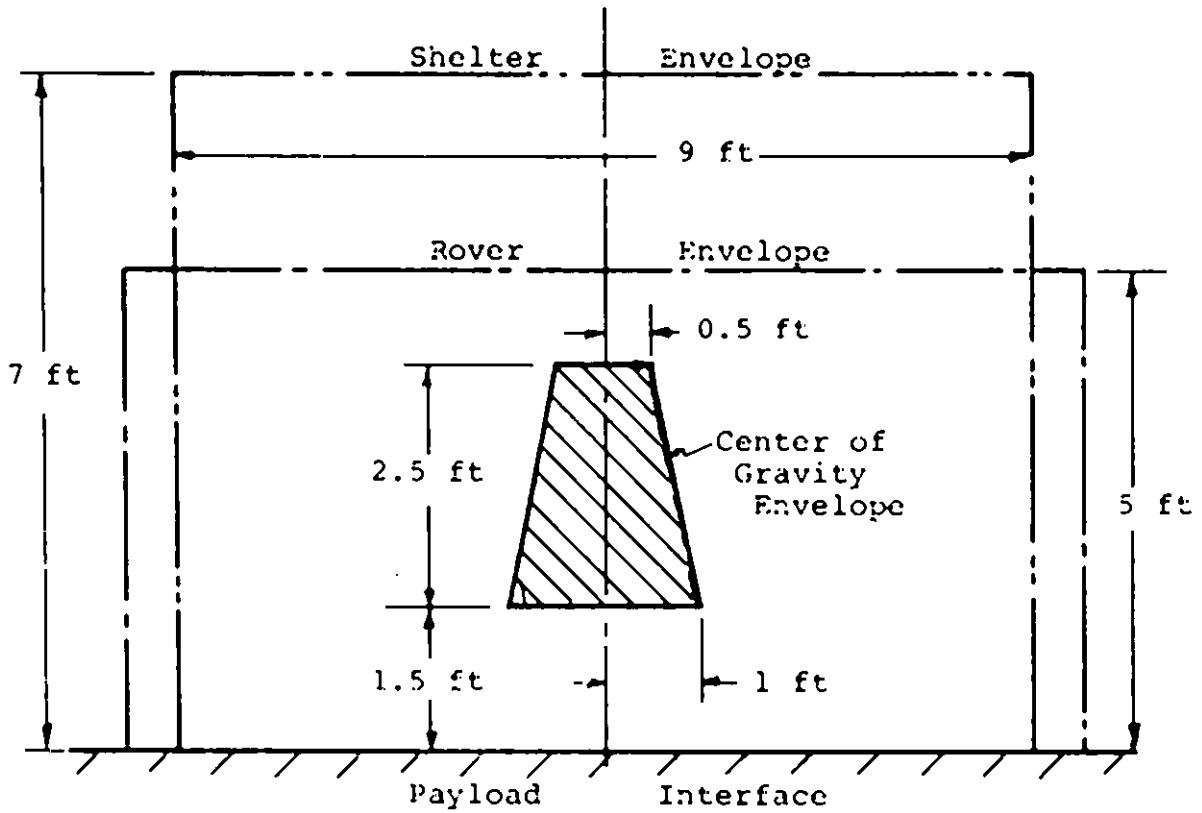


FIGURE 1.2-1 PAYLOAD ENVELOPES

CHAPTER II

ALTERNATIVE SPACECRAFT DESIGN AND SELECTION

George Hauck	2.1
Frank Hendel	2.2
Fred Davidson	2.3
Floyd Calvert	2.4
George Gless	2.5
George Pincus	2.6

2.1 Alternative Space Frame Configurations

In selecting a frame and packaging the various subsystems a truly infinite number of options are open to the structural designer, even with the constraints listed in the foregoing. Many basic configurations offer feasible solutions and each allows a variety of structural schemes and even more possibilities for geometric arrangement and component proportioning. Thus it should be noted at the outset that true optimization is impossible, and that the search must be directed to a good solution.

2.1.1 Alternative Landing & Payload Packaging Systems.

Any evaluation must proceed on a hierarchial basis, starting with a manageable number of quite general schemes, and ending with the selection of one well-defined system. This development took place in the following manner.

a. Basic Arrangement. A craft of the type considered consists essentially of a linear array of four elements: propulsion plant, landing device, equipment space and payload. The landing device may, however, in certain cases be removed from this array and attached to the sides of one or more of the other elements. The equipment may be stowed in several locations, e.g. some below the payload, some above.

Since important mass savings can be realized by jettisoning

the main propulsion plant before landing (at a slight structural penalty) this element clearly must be in the lowest location. The landing device, if in the array, must be at one of its ends, occupying the lowest position in the landed structure. This leaves the possibilities of bottom or top-mounted payload structures. In the flight configuration the propulsion plant can be attached to either end, but structural considerations clearly demand its location at the bottom of the configuration with respect to both lift-off and landing orientations. Thus the choice of possible arrangements of the four elements can rationally be narrowed to two, as follows:

<u>Top-Mounted Payload</u>	<u>Bottom-Mounted Payload</u>
Payload	Equipment Space
Equipment Space	Payload
Landing Device*	Landing Device*
Propulsion Plant	Propulsion Plant

Both of these arrangements promise advantages and were investigated more closely.

b. Initial Concepts. A number of promising initial concepts were developed for each of the two arrangement possibilities and are shown diagrammatically in Figure 2.1-1. Of interest were structural theme, packaging in the launch vehicle shroud, landing gear deployment and landing characteristics. The Configuration Group evaluated these seven concepts in a design conference, applying qualitative judgment with respect to general mission capability. The results are summarized in Table 2.1-1 and shown graphically in Figure 2.1-2. Four concepts were thought to warrant further deve-

*If part of the array.

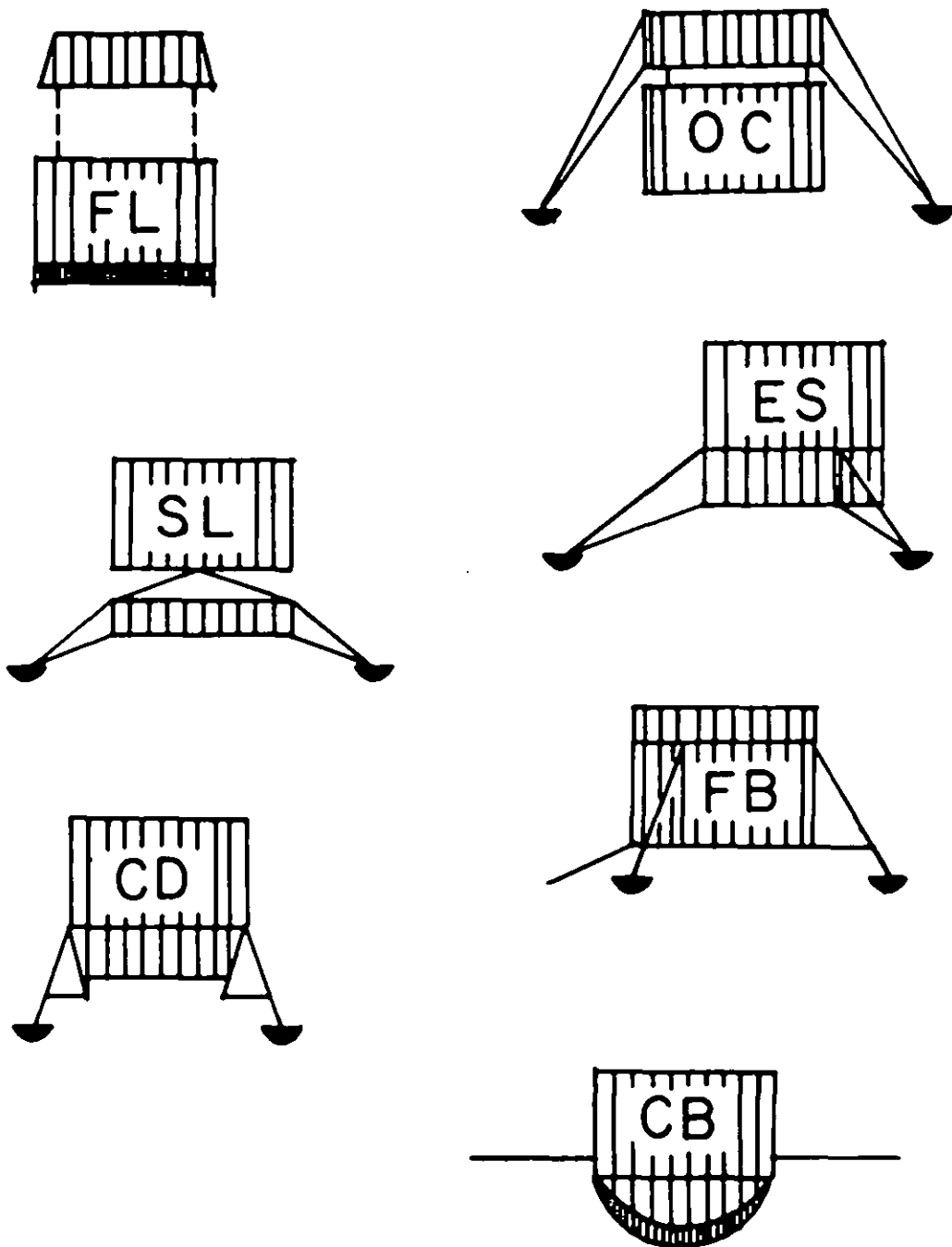


FIGURE 2.1-1 INITIAL CONFIGURATION CONCEPTS

VARIABLE	WT	FL	OC	SL	ES	CD	CB	FB
CAPACITY	5	10	8	5	5	8	8	8
STABILITY	4	9	8	9	4	6	10	7
SUPPORT	2	2	5	6	10	10	10	10
LIFT-OFF	2	0	2	3	10	9	8	10
OFF-LOADING	5	10	10	4	4	4	7	8
NOVELTY	3	7	6	2	10	9	5	7
SIMPLICITY	4	9	7	4	8	8	10	8
GROWTH	1	10	7	4	8	8	4	6
WEIGHTED TOTAL		211	182	127	171	189	211	207

TABLE 2.1-1 PRELIMINARY EVALUATION MATRIX

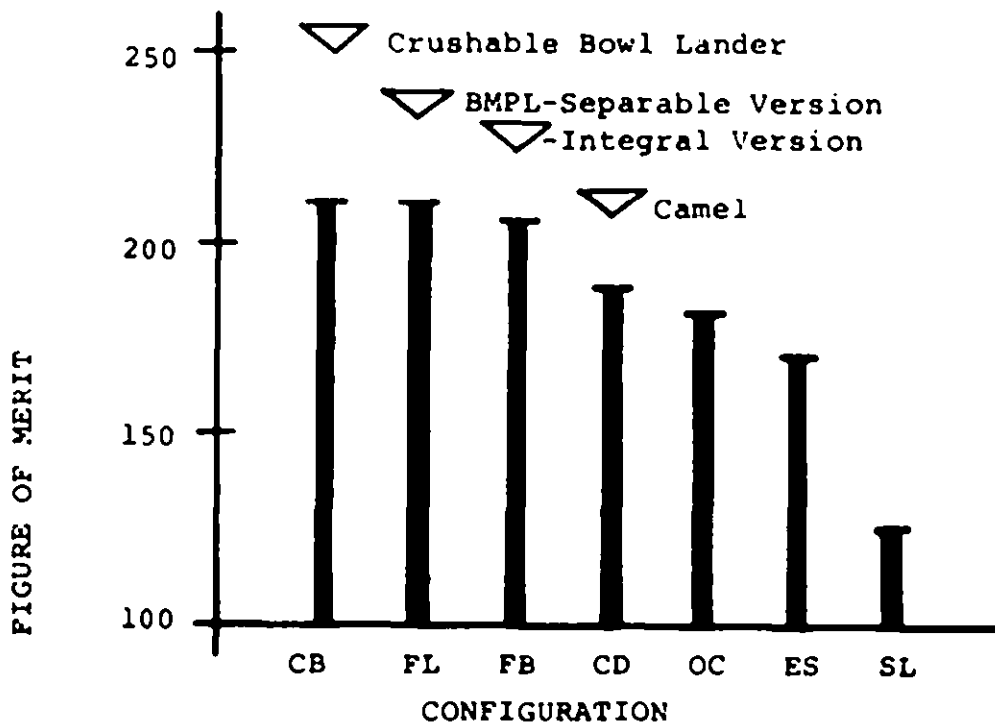


FIGURE 2.1-2 COMPARISON OF CONFIGURATION MERIT

lopment, namely:

(a) Crushable Bowl Lander (CBL), a vehicle using an approximately hemispherical shell covered with shock-absorbing material as a landing device; the payload may be top- or bottom-mounted.

(b) Bottom-Mounted Payload Lander (BMPL), a configuration that allows the payload to be dropped just prior to landing (Separable Version) or the vehicle to be landed intact (Integral Version).

(c) CAMEL, a top-mounted payload lander that maximizes the use of proven concepts, primarily of a modified, scaled-down Apollo LM type landing gear.

Further, two hybrids concepts were offered. One of these would employ basically the BMPL (Int.) structure in combination with the CBL landing concept by using a BMPL (sep) type landing device for the entire vehicle. The other combines essentially the BMPL (Int) and CAMEL concepts by shifting part of the support equipment, especially the vernier engines with their tanks, to the bottom, thus creating an Intermediate-Mounted Payload Lander (IMPL).

c. Candidate Configuration. The four primary concepts were developed to the extent of preliminary structural design, center-of-gravity determination, and deployment penalty estimates. An attempt was made to achieve sound and advantageous designs, but rigorous optimizations could not be carried out. The four competitive designs are indicated in Figures 2.1-3 through 2.1-6, and the estimated values of several pertinent parameters are summarized in Table 2.1-2.

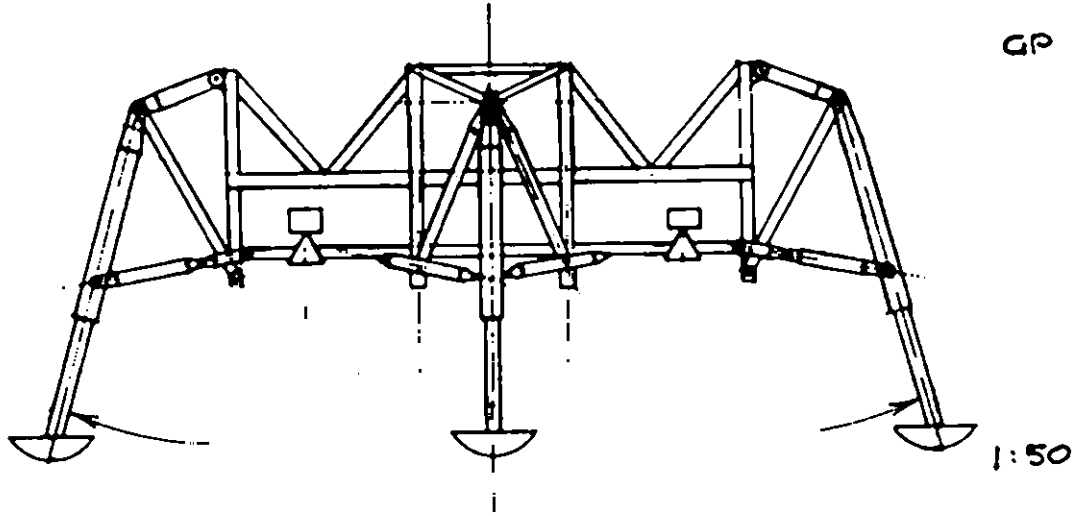


FIGURE 2.1-3 CAMEL

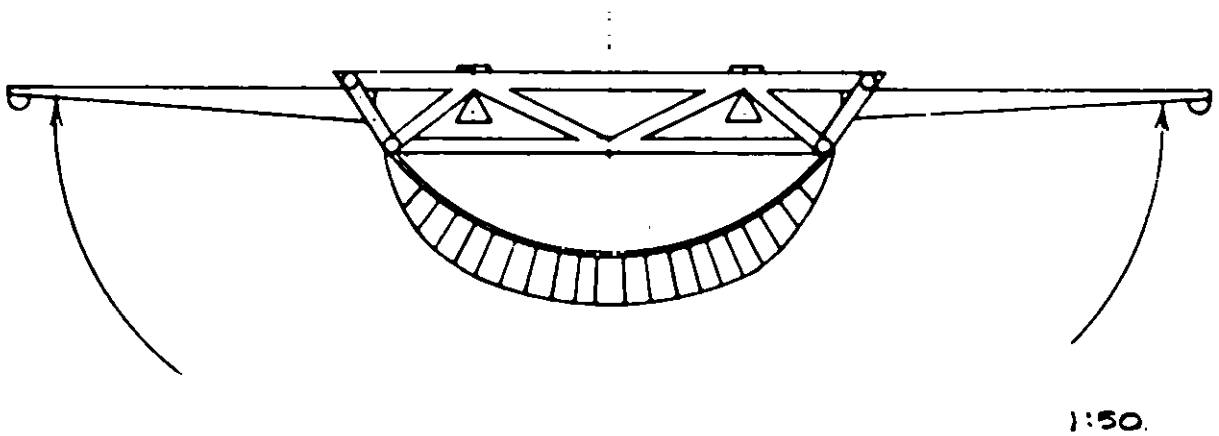
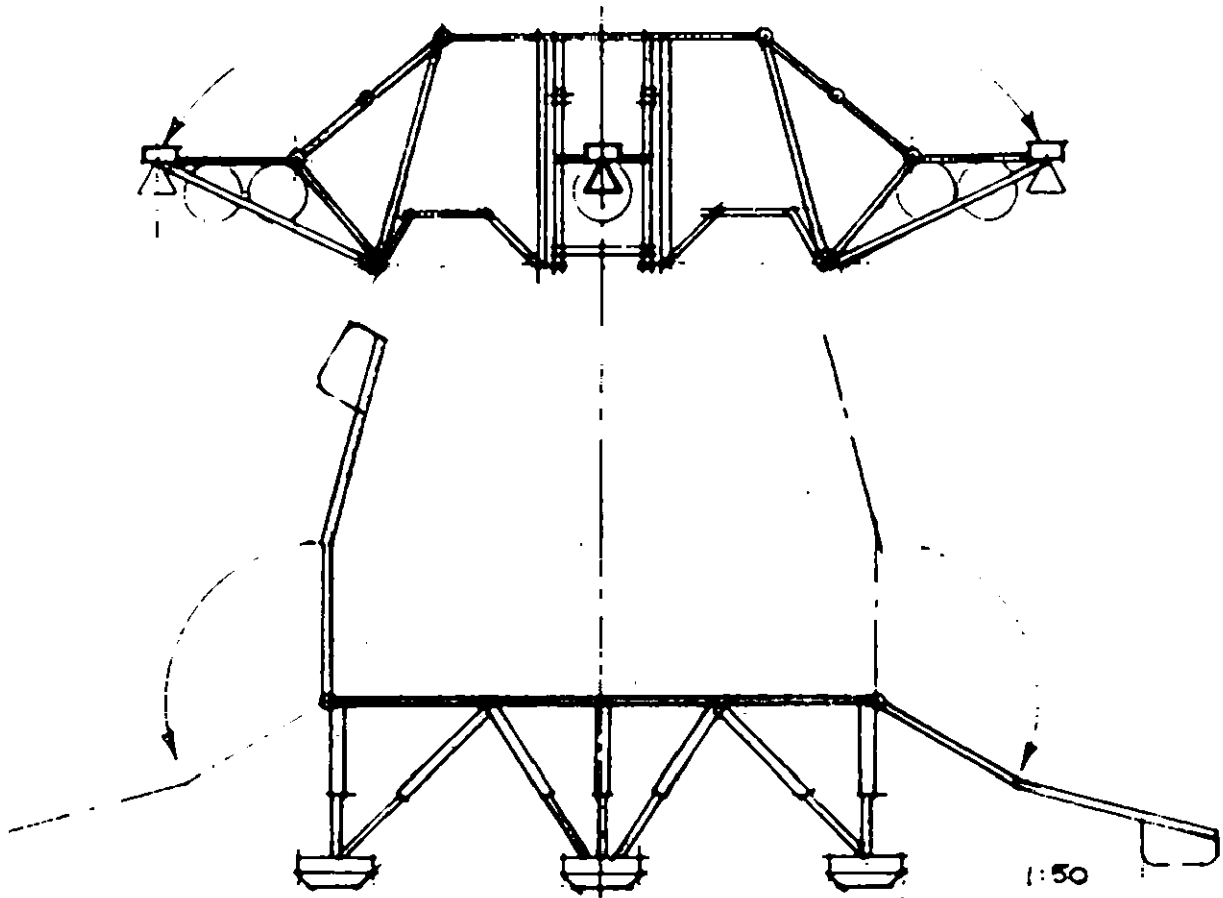
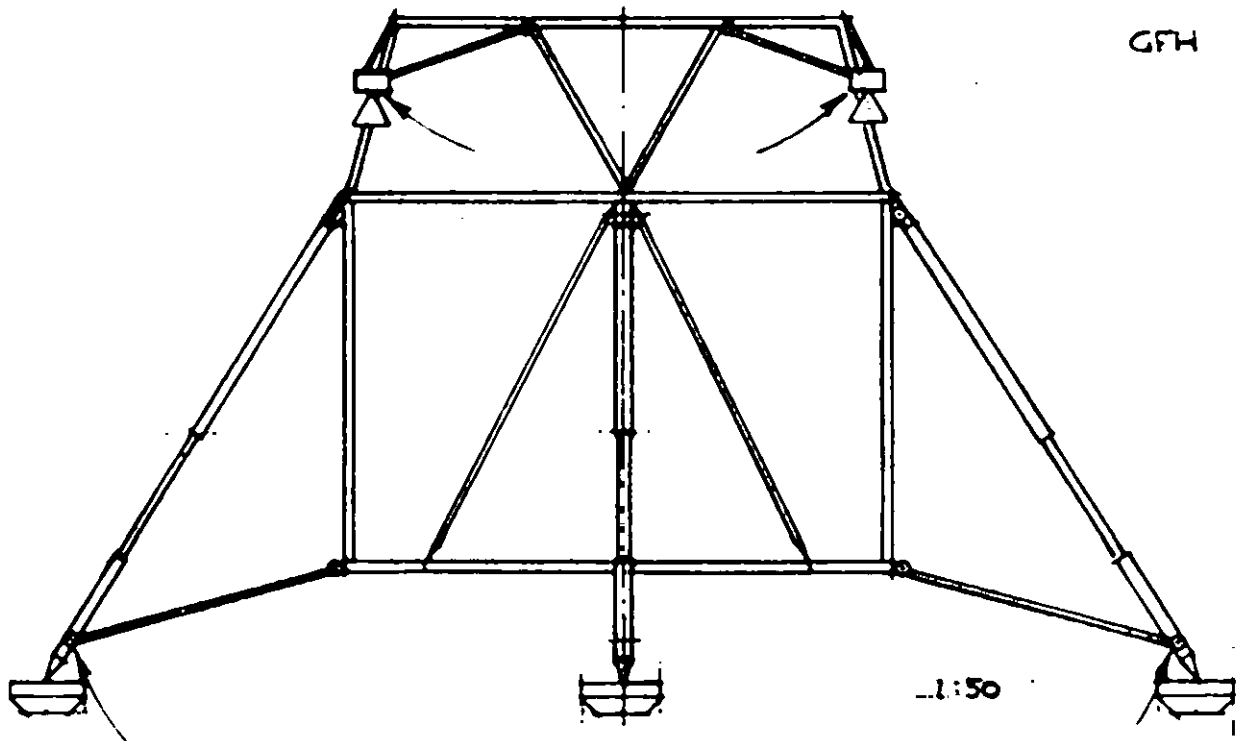


FIGURE 2.1-4 CRUSHABLE BOWL LANDER



BOTTOM MOUNTED PAYLOAD LANDER (SEPARABLE)

FIGURE 2.1-5



BOTTOM MOUNTED PAYLOAD LANDER (INTEGRAL)

FIGURE 2.1-6

TABLE 2.1-2 CONFIGURATION COMPARISON TABLE

	CAMEL	BMPL (INT)	BMPL (SEP)	CBL
Structural Weight (LBS)	605	605	475	770
RE-Fly Penalty (LBS)	<30	<30	N.A.	0
Stability Ratio H/R	1.6	0.93	0.81	0.97
Height of Payload (IN)	79	37	47	57
Ramp Penalty (LBS)	51	17	24	33

2.1.2 Evaluation and Selection

The CBL, BMPL, (Int.), BMPL (Sep.), and CAMEL each offer some unique advantages and drawbacks. Inspection reveals for each configuration favorable as well as unfavorable traits distinctive enough to aid in the selection process. The arguments are briefly tabulated below:

<u>Vehicle</u>	<u>Pro</u>	<u>Contra</u>
CBL	Landing stability	High Mass
BMPL (Int.)	Off-load ease	
BMPL (Sep.)	Low mass	Lack of PL Support
CAMEL	Conventionality	Off-load difficulty

In addition, it should be noted that the BMPL vehicles are subject to local hazard to the payload (while the equipment is endangered in the cases of the CBL and CAMEL). In addition to the obvious implication in regard to off-loading, thermal considerations, on the other hand, indicate a preference for mounting equipment on top to enhance its survivability.

A final aspect deserving attention is the low state of art in the matter of stabilizing arms used by the BMPL (Sep.) and the CBL. These devices would indubitably require lengthy development study.

In view of these arguments the Institute decided, upon recommendation by the Configuration Group, to propose the development of the BMPL (Int.), subject to reasonable modification. Upon a subsequent consultation with NASA, the one major modification decided on was the placement of most of the vehicle support equipment below the payload deck. The shift implies thermal control penalties for the vehicle, which are partially offset by a lowering of the center of gravity and improved thermal conditions for the payload. Structural penalties are not obvious: landing conditions favor original version; loads the modification; thus the differences are probably not appreciable. The recommended concept forms the basis for the design described in Chapter VIII, hereafter referred to as the Lunar Logistics Vehicle (LLV).

2.2 Alternative Propulsion Systems

2.2-1 Main Retro System.

The following candidates for the main retrograde (retro) rocket were considered and evaluated;

- (1) RL 10 engine (several models) which use LOX and LH₂ as propellants;
- (2) SRM-MSM a military solid propellant motor (classified) specially adapted for the LLV spacecraft;
- (3) Several military solid propellant motors (classified) readily available;
- (4) Surveyor solid propellant motor (used as a retro rocket); the following configurations were considered:
 - (a) three Surveyor motors in the first stage and one Surveyor motor in the second stage;
 - (b) four Surveyor motors in the first stage and one Surveyor motor in the second stage;
- (5) Descent engine of the Lunar Module (Apollo spacecraft);
- (6) Ascent engine of the Lunar Module (Apollo spacecraft);
- (7) Main engine of the Service Module (Apollo spacecraft);
- (8) Agena engine (several models).

The Section 4.7 shows the reasons why the trade-off analysis pointed out that the RL 10A-3-3 engine had to be selected in order to meet the payload requirement.

2.2-2 Vernier System.

The following candidates for a vernier system were considered;

- (a) A cluster of Apollo engines R-4D each 100 lb_f thrust;
- (b) A cluster of R-4D engines each 130-140 lb_f thrust (after increasing the feed pressure);

- (c) Bell 8570 engine of 325 lb_f thrust (not qualified);
- (d) Rocketdyne RS-21 engine of 300 lb_f thrust (not qualified);
- (e) New engines specially developed for LLV, throttleable from 500 lb_f to 50 lb_f;
- (f) Viking engine throttleable from 400 lb_f to 50 lb_f thrust (not developed).

The engines (a) through (e) use N₂O₄ and derivatives of N₂H₄ as bipropellants. The Viking engine will use N₂H₄ as a monopropellant and, hence, will have the lowest specific impulse.

Trading off the development costs, specific impulse, flexibility, weight, power consumption, and reliability and R-4D with a higher thrust was selected.

2.2-3 Reaction Control System.

The following candidates for a reaction control system were used:

- (a) Marquardt R-1E engine of 22 lb_f thrust (qualified for the MOL spacecraft);
- (b) Bell PBPS engine of 22 lb_f thrust
- (c) R-4D engines each 100 lb_f thrust for the use as verniers and, if specially canted, for roll control as well.

Trading off the development costs, flexibility, reliability, etc. the R-1E engine was selected.

2.2-4 Attitude Control System.

The following candidates for the attitude control were considered:

- (a) cold nitrogen gas jets;
- (b) cold hydrogen gas jets (boil-off from LH₂);
- (c) cold nitrogen/hydrogen gas jets;
- (d) cold hydrogen/oxygen gas jets (boil-off from LH₂ and LOX).

Considering that hydrogen gas is readily available and that it has the highest specific impulse, hydrogen jets were selected.

2.3 Summary of Guidance and Navigation System

2.3.1 Alternative Guidance and Navigation Systems.

Two basic types of guidance and navigation systems were considered - the surveyor type system, and a modified lunar module type system. The 3σ 1km landing dispersion radius specified necessitated a G&N system capable of altering the LLV preprogrammed descent trajectory, since inertial coordinates of possible landing sites on the lunar surface were not known to this accuracy. This requirement ruled out the use of a surveyor type G&N system.

The LLV mission was broken down into three phases - a coasting phase, a mid-course correction maneuver phase, and a terminal phase. Table 2.3-1 lists the types of G&N systems considered and indicates the choice made.

2.3.2 Components used in the LLV G&N system.

Once the type of system was selected, individual components were selected. Table 2.3-2 lists the components used in the selected system, and the function of each component.

TABLE 2.3-1 ALTERNATIVE GUIDANCE AND NAVIGATION SYSTEMS

Mission Phase	Type of Guidance and Navigation System	Advantages	Disadvantages	Choice
Coasting Phase	Inertial sensors servo loop control of attitude control system	Very accurate vehicle attitude, angular rate information	Gyro drift rate causes loss of attitude information and control as time increases, high electrical power requirements.	Celestial sensor (sun, Canopus) servo loop control over attitude control system
	Celestial sensor, servo loop control over attitude control system	Low electrical power requirements	Less accurate vehicle attitude, angular rate information	
Midcourse Correction	Inertial sensors, computer control of R. C. S.	Very accurate execution of midcourse maneuver	Requires complicated system that has high electrical power requirements	Inertial sensor, computer control of R. C. S.
	Celestial sensor, computer control of R. C. S.	Low electrical power requirements, less complicated system	Poor & limited angular orientation for midcourse maneuver, cannot sense vehicle accelerations	
Terminal Descent Phase	Inertial sensor, computer, television	Can alter descent trajectory to land in hazard free location	Poor information about altitudes, velocities of vehicle and never demonstrated as a workable system	

<p>Inertial sensor computer, landing radar</p>	<p>Can soft land vehicle with all velocity components less than 5 fps</p>	<p>No ability to deviate from pre-programmed landing site.</p>	
<p>Inertial sensors, computer, landing radar, television</p>	<p>Redundant, automatic soft landing system that can after descent trajectory to achieve a hazard free landing.</p>		<p>Inertial sensors, computers, landing radar television computer controls R. C. S., vernier, main retro propulsion systems</p>

TABLE 2.3-2

COMPONENTS OF LLV GUIDANCE AND NAVIGATION SYSTEM

ITEM	DIMENSIONS	WEIGHT	ELECTRICAL POWER REQUIREMENTS	FUNCTION
IMU and Navigation Base	12.5" diam. sphere; 14 " diam. ring 10" legs	45 lbs	100 watts	Provides angular rate, attitude, accelerations experienced by vehicle
IMU Pulse Torquing Assembly	2 1/2"x11"x13"	15lbs	90 watts	Resets gyros to desired orienta- tions on command from computer
Coupling Data Unit	5.5"x11.3"x20	35 lbs	50 watts	Converts analog sensor signals to digital computer inputs; computer outputs to analog control signals
Flight Computer	12"x18"x8"	50 lbs	100 watts (20 watts at reduced power)	Controls LLV during powered flight. Executes ground commands
Celestial Sensors	See Table 3.1-1	5.5 lbs	5 watts	Provides orient- ation information used by computer to control LLV attitudes during coasting phase of flight
Landing Radar	20"x24"x65" (antenna) 15.7"x6.75"x 7.35" (elec- tronics)	42 lbs	200 watts	Provides very accurate altitude, velocity infor- mation during low altitude phase of descent (<50,000 ft).
Power and Servo Electronics	24"x10"x3"	60 lbs	See Sec 5.6	Provides proper current, voltage, frequencies to all

electronics in the
vehicle

Transponder See Sec 6.2

Used in locating
LLV after landing

2.4 Electrical Power System

2.4.1 Alternative Electrical Power Systems

Five alternative electrical power systems were evaluated for the spacecraft. The five systems considered are listed in TABLE 2.4-1.

TABLE 2.4-1 ELECTRICAL POWER SYSTEM ALTERNATIVES

System	Power Generating Components
Batteries	Three Apollo LM ascent stage batteries, each 9 kw-hr capacity
Fuel Cells and Battery	Two radiation-cooled Allis Chalmers fuel cells, each 200 w rating; one Apollo LM ascent stage battery
Solar Cells and Battery	Solar array 30 square feet in area, orientable array; one Apollo LM ascent stage battery
RTG and Battery	Four SNAP 19 RTG modules, each rated 35 w for 90 days; one Apollo LM ascent stage battery
Fuel Cells	Two fuel cells, each rated 2 kw

2.4.2 Evaluation and Selection

Evaluation criteria which were used as the basis for selection of the electrical power system are listed in Table 2.4-2. A detailed comparison of the candidate electrical power systems is included in Chapter 5. The recommended electrical power system for the LLV spacecraft is the Fuel Cells and Battery system. One 200 watt fuel cell provides the nominal translunar coast phase electrical power and the silver-zinc battery provides supplemental power for peak power periods.

TABLE 2.4-2 SELECTION CRITERIA

System weight

System volume

Cost

Availability

Growth potential in mission length
and in mission power level

Lunar night survivability

Payload support and integration

Reliability - Redundancy

Complexity of interface problems

2.5 Telemetry and Communications

The telecommunications subsystem serves as the link between the spacecraft and its base on the earth. The subsystem must be able to receive information and commands and convert them into useful signals for operation of the vehicle. It must also be able to collect data and information from the spacecraft and its payload and transmit it to Manned Space Flight Network or Deep Space Network on earth. The specific requirements for various parts of the mission are outlined in Table 2.5-1.

2.5.1 Alternative Telecommunication Systems

One of the basic tenets in the design of the ~~in Luna~~ ~~Eogastina~~ ~~Vehicle~~ was to minimize development and qualification costs by maximizing the use of Surveyor, Lunar Orbiter, Apollo and other flight proven systems. If new systems are required, their introduction should result in substantial improvements or reduced costs.

One of the mission objectives is to land within one kilometer (30') of a point on the Lunar surface. Since the map error for a given point is usually much larger than one kilometer it became evident early in the investigation that guidance based on visible indications of the landing point would be necessary. All of the systems considered have real time television capability.

A summary of the data for each of the four systems considered is given in Table 2.5-2.

2.5.2 Evaluation and Selection

The criteria used for evaluation the final design were

1. Weight

2. Reliability
3. Cost
4. TV Capability
5. Data Rates
6. Power
7. Volume

Originally the tradeoff study was conducted with Surveyor, Apollo LM and Apollo CSM as the candidates. The CSM equipment is heavy and more complex than needed, and was eliminated. The LM system was ~~eliminated~~ when the following statement was discovered in the LM Apollo Operations Handbook, page 2.7-45: "S-band lunar stay antenna failed. Weakening of LM S-band signals (downlink) at MSFN loss or severe limitation of LMTV capability."

The Surveyor system, because of the extremely slow angular rates for the directional antenna and low uplink data rate, will not meet system requirements (more detailed system requirements are found in Section 6.1 and 6.2). However, it was learned that an Unmanned Lunar Rover concept using two television cameras was being developed by NASA. The equipment proposed for the Unmanned Rover seemed to be capable of meeting system requirements if suitably modified. A system was developed and is described in detail in Section 6.3.

A study of the data in Table 2.5-2 reveals that the modified Lunar Rover is equal to or better than the other three with the exception of the power requirements. The high power transmission periods are relatively short and thus additional energy requirement is correspondingly low. A prime advantage is the modulation capability for television which makes possible the elimination of some conversion equipment at the ground station. This point is discussed further in Section 6.4. A strong justification for using

Lunar Rover equipment is that some of the vehicle payloads are quite likely to be unmanned rovers and thus the two programs could complement one another. The Modified Lunar Rover telecommunication subsystem is thus recommended for the spacecraft.

TABLE 2.5-1 TELECOMMUNICATION SUBSYSTEM REQUIREMENTS

Mission Phase	Functions Required
Launch	Telemetry to send system performance data to ground.
Coast	Command signals to acquire the sun and canopus for navigation control.
Mid-course	Commands to align spacecraft with flight path and engine firing for ΔV correction.
	Telemetry to send system performance data to ground.
	Command signals to acquire the sun and canopus for navigation control.
Lunar Approach	Commands to align vehicle for television pictures and retro firing.
	Transmission of video signal from television camera for landmark recognition and hazard avoidance.
	Command signals to perform flight maneuvers to reach desired landing designation.
Post Landing	Telemetry to send system and payload data to ground.
	Turn on transponder if active one used.
	Commands to deploy payload.

2.6 Summary of Proposed Design

2.6.1 Spacecraft Design

The proposed design may be considered as a space frame enclosing a 9 feet diameter by 7 feet high cylindrical payload envelope. Four landing gears with 20 in. diameter pads are arranged at 90° to each other and placed perpendicular to the four longer sides of the octagon-shaped payload plane. (See Figures 2.6-1, 2.6-2, and D.1-1.

Each landing gear includes 3 members: a 150 in. long main compression strut running from the pad to the top of the structure and two shorter struts spanning from the main compression strut to the end points of the octagon longer sides. The main struts as well as the pads include crushable honeycomb material.

Eight diagonal members connect the top and bottom of the structure and there are no vertical elements between those two parallel planes. The octagon-shaped payload support structure includes transverse and stiffening elements within the octagon structure and on its plane. These elements are also used to attach the vehicle support equipment (guidance, communications, electronics, fuel cells and tanks, vernier propellant tanks,) to a 24 in. high envelope bounded on the top by the payload plane and on the sides by the octagon perimeter.

Channel sections are used for the elements forming the octagon payload support plane. The perimeter elements are subject to the largest loads and primarily function in simple bending in view of the intermediate and end support conditions. All other elements of the structure are tubes of up to 3.5 in. O. D. and wall thickness up to .146 in. Aluminum alloy 7075 is used throughout the structure.

TABLE 2.5-2 TELECOMMUNICATION SUBSYSTEM CANDIDATES - DATA SUMMARY*

	Surveyor	Apollo LM	Apollo CSM	Modified Lunar Rover
Weight-lbs**	106	163	271	101
Volume-ft ³ **	9960	12.80	20 50	11.80
W/O Antennas	1.21	2.45	3.14	1.09
Power-Watts***	100	156	233	171
	33	84	138	58
Data Rate-Kbits/sec				
Up-link	0.05	1.0	1.0	1.0
Down-link	4.4/0.017	51.2/1.6	51.2/1.6	102.4/0.24
Antenna Slewing Rate-degrees/sec	0.125/0.25	20	15	20
Transmitter TV Modulation-KHz	220	500	500	2000
Transmitter Power-Watts	10	18.6	11.2	10
	0.1		0.1/0.4	0.2

*Data taken from References 1-7, 6, Chapter VI

**Weight and volume values are for equipment only - no packaging is included. Total weight 152 lbs plus 85 lbs of cable harness and sensors.

***Power values given are for transmitter in high and low power /Recommended Subsystem

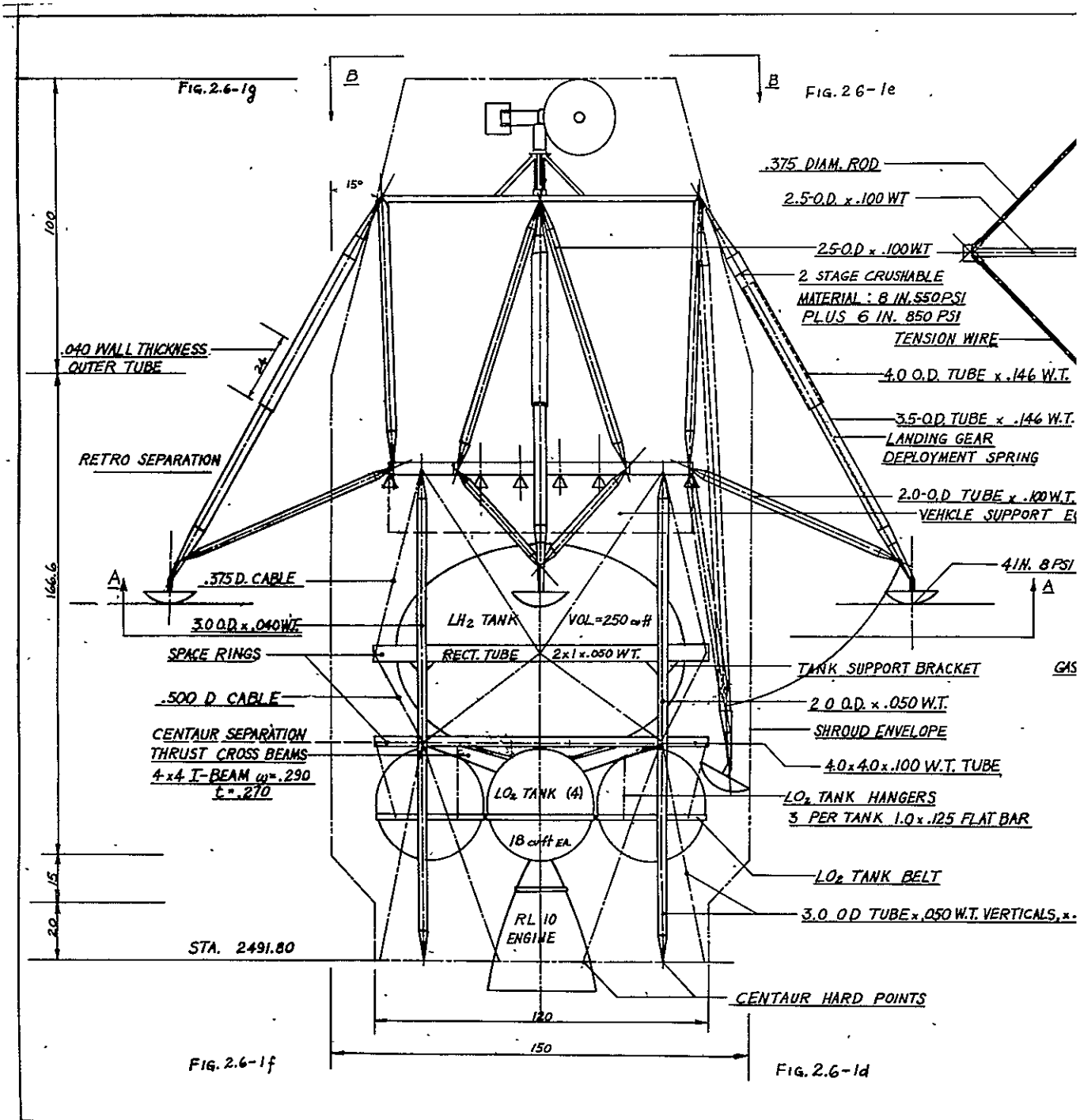


FIG. 2.6-1g

FIG. 2.6-1e

FIG. 2.6-1f

FIG. 2.6-1d

FOLDOUT FRAME 1

FIG. 2.6-1c

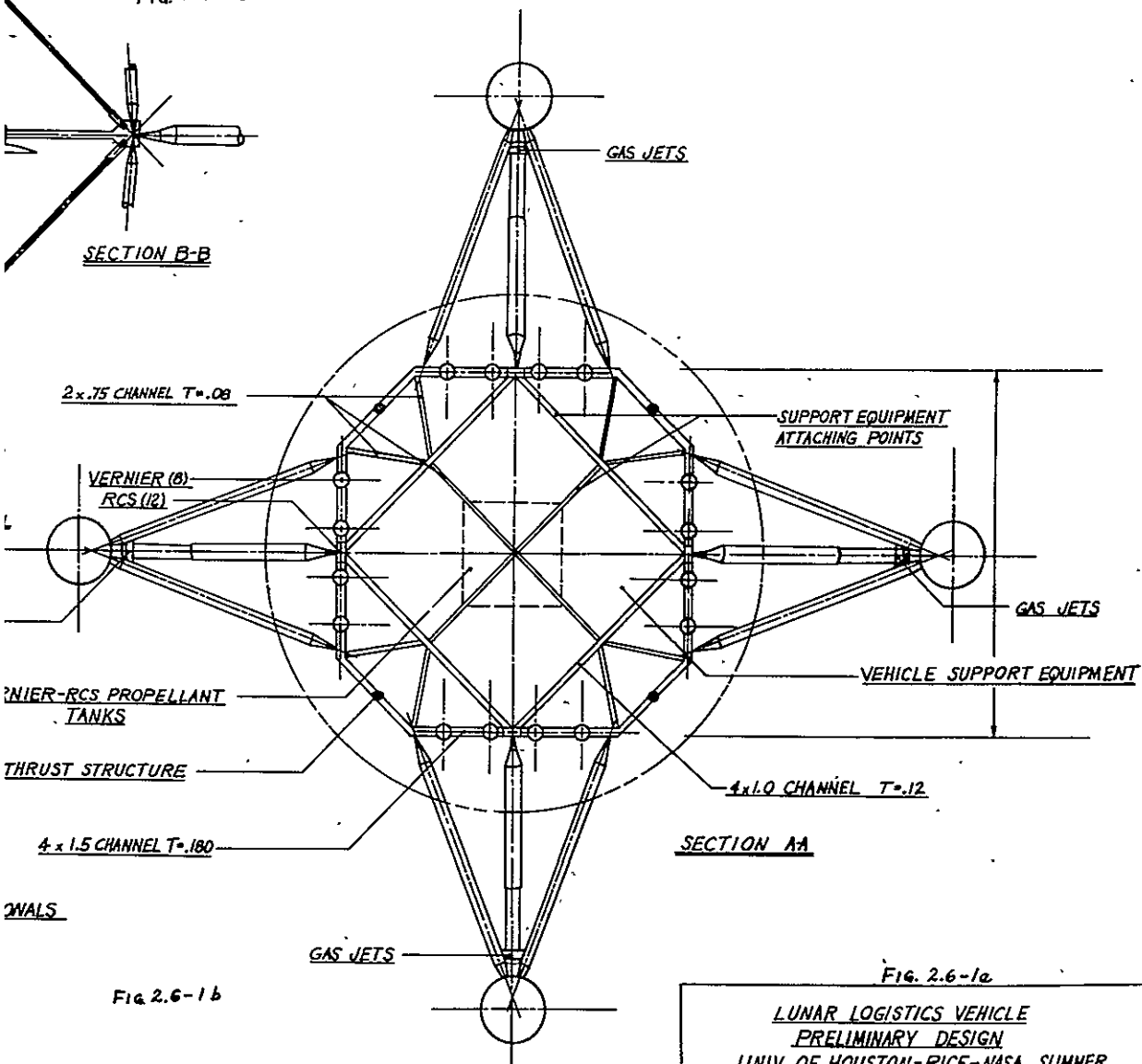
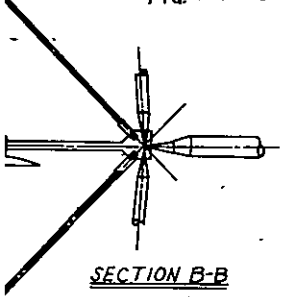
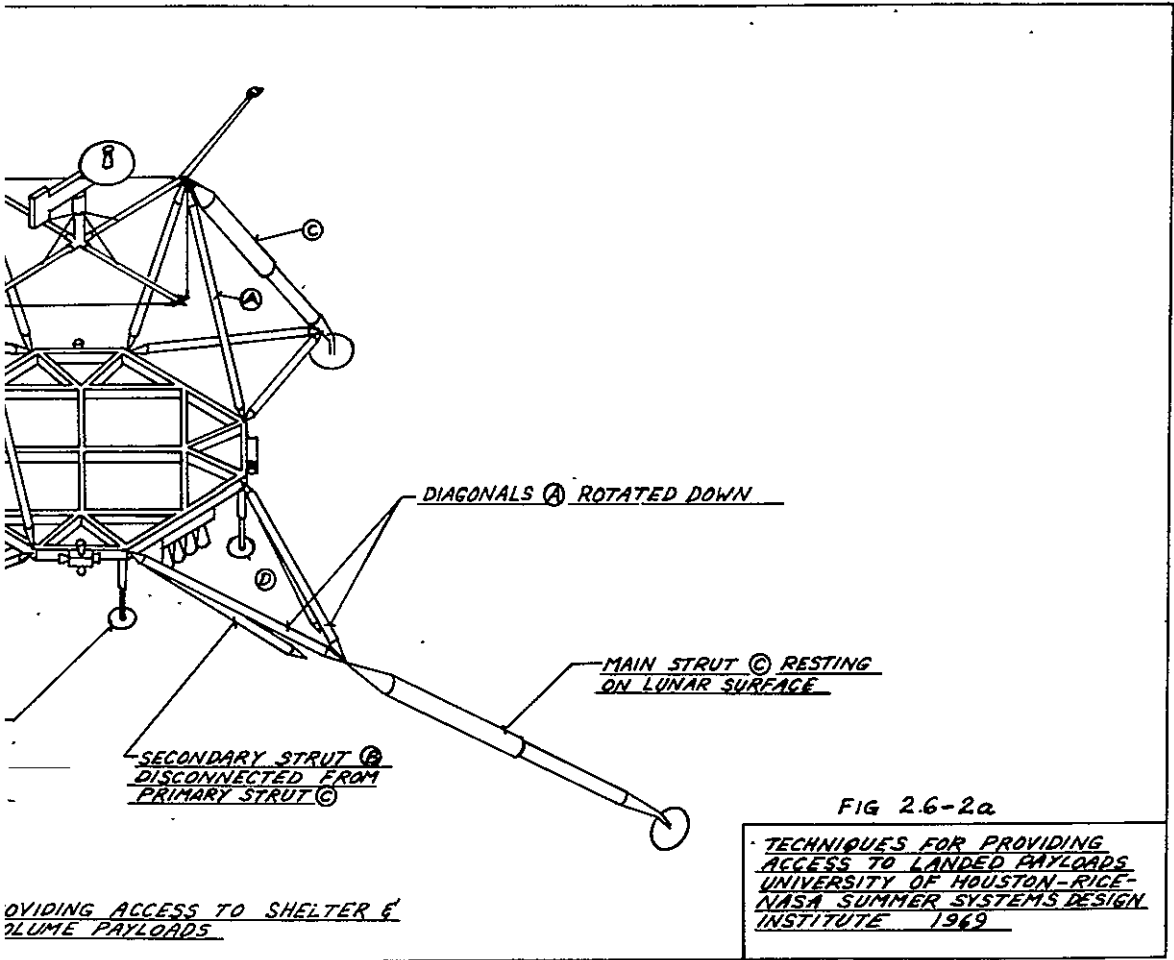


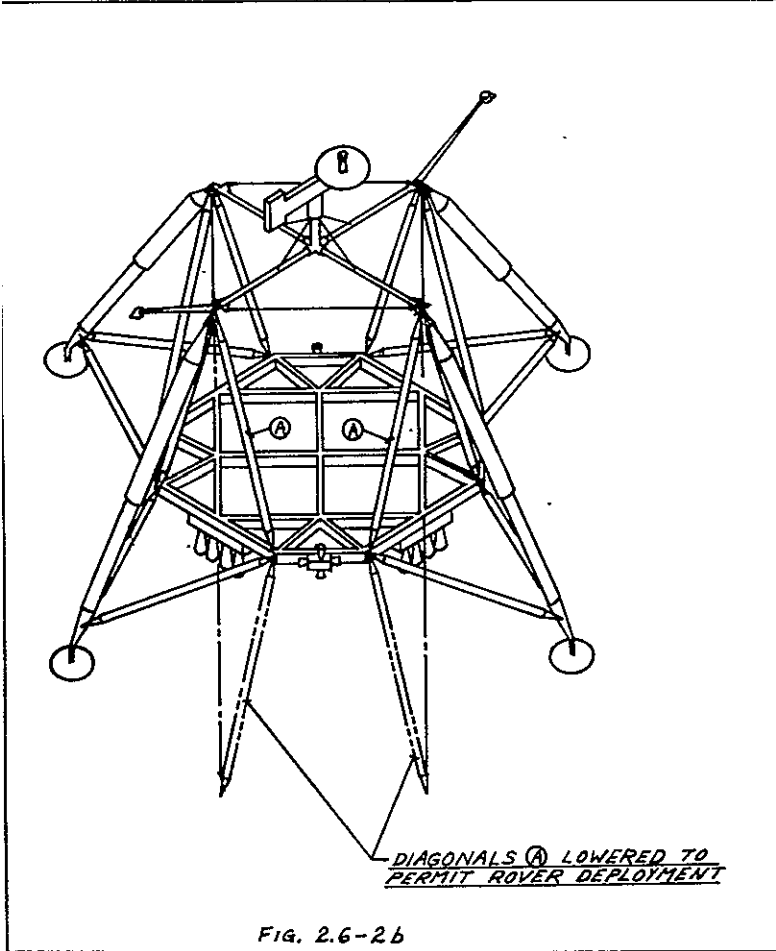
FIG. 2.6-1b

FIG. 2.6-1a

LUNAR LOGISTICS VEHICLE
 PRELIMINARY DESIGN
 UNIV. OF HOUSTON-RICE-NASA SUMMER
 SYSTEMS DESIGN INSTITUTE
 1969



FOI DOUT FRAME 2



MET/
OTHE

FOLDOUT FRAME 1

A 26 in diameter S-band steerable antenna is placed on the top of the vehicle at the intersection of the top cross-members. This antenna produces some bending in the top members but the magnitude of the bending stress is small in comparison with the stresses induced in the members at landing. Four tension wires complete the top structure and these are designed to balance the main cross-member loading.

Sixteen verniers, four on each side are attached to the four longer sides of the octagon payload support plane. These verniers feed from a common tank system located at the center of the payload plane. A total of 12 Reaction Control System Thrusters feed from the vernier propellant tanks are placed at the center of the longer sides and disposed in 4-4-2-2 groups. Small gas jets are attached to each landing gear to serve as an attitude control system that is used during coasting periods of the mission.

The thrust structure includes 3 in. O. D. round tubes and two support space rings. Four vertical members are continuous from the Centaur hard points to the middle of the short sides of the payload octagon structure. Diagonal elements span between the other 8 hard points on the centaur and the lower space ring. The upper space ring supports the hydrogen tanks with four brackets and also provides support points for the vertical and diagonal members to the lower space ring and to the payload support octagon structure.

2.6.2 Weight Summary

TABLE 2.6-1 gives a weight summary for the proposed Lunar Logistic Vehicle, support equipment, thrust structure, propellant, tanks and other elements necessary to implement the mission. These are tentative weights and subject to considerable refinement.

An itemized listing of all the weights is given in Section 8-6.

TABLE 2.6.1
SUMMARY OF WEIGHTS

<u>Ref. Table</u>	<u>Item</u>	<u>Weight (lbs)</u>
8.5.1	Lander Structure	330
8.5.2	Thrust Structure	250
8.5.3.	Propulsion System	933
8.5.4	Propellant	6378
8.5.5	Guidance and Navigation System	225
8.5.6	Power System	357
8.5.7	Communications System	111
8.5.8	Instrumentation	67
8.5.9	Environmental Control	196
	Payload	<u>2500</u>
	Total Launch Weight (Approximate)	11,400 lbs

CHAPTER III

FLIGHT CONTROL SYSTEM

Fred Davidson	3.1, 3.2
Joe Robertshaw	3.3
Frank Swenson	3.4

3.1 Guidance and Navigation System

3.1.1 Introduction

The objective of the LLV guidance and navigation system is to soft land the vehicle at the lunar surface within 1 kilometer of a preselected landing site, with a 99% probability of achieving the soft landing within the 1 kilometer distance from the chosen site. Several alternative guidance and navigation (G&N) systems were considered. These fell into two classes - the type of G&N system used on the Surveyor spacecraft, [1] and various G&N systems that contain a television system and involve some degree of earth based control of the spacecraft during the final phase of descent to the lunar surface [2,3].

The principle sources of error in any G&N system are the following:

1. Tracking errors that result in imprecise information about the trajectory the spacecraft is actually on.
2. Inertial measuring unit sensors errors that result in incorrect values of spacecraft velocity, acceleration, and attitude that are used by the guidance computer in determining the vehicle's state vector.
3. Powered maneuver execution errors caused by incorrect thrust vector alignment and engine thrust dispersions.
4. Map errors that result in incorrect inertial coordinates

for the selected landing site.

The largest source of errors in currently available navigation systems are errors in existing maps of the lunar surface. These range in magnitude from a few thousand feet in the best mapped region of the lunar surface to ten to twenty miles for poorly mapped regions near the extremities of the lunar front face and the entire rear face. There is little likelihood of significant improvement in lunar maps before the LLV is to be flown. The next largest errors are earth based tracking errors. Typical values of these errors [4] are shown in Figure 3.1-1. Inertial measurement unit (IMU) sensor errors [5] are typically 2 ft/sec velocity offset errors, 0.1 deg/hr non-acceleration sensitive gyro drift rates, 0.2 deg/hr/g acceleration sensitive gyro drift rates, and generally less than 60 arc sec gyro axis - spacecraft axis misalignment errors. Execution errors generally result in velocity residuals of 1-2 fps.

The Surveyor spacecraft guidance and navigation system consisted of three integrating rate inertial gyros (IRIG), one spring type accelerometer, sun and Canopus optical sensors, servo attitude control loops, an altitude marking radar, a velocity sensing three beam landing radar, and a logic sensing, control mode switching device. The logic sensing device received ground commands and performed the desired maneuvers via the control mode switching device. An automatic soft landing was achieved with the use of the landing radar and servo loops that controlled vernier engines. The system was designed to achieve a landing site dispersion radius of 14 kilometers [6], and could not deviate from the preprogrammed intended landing site once

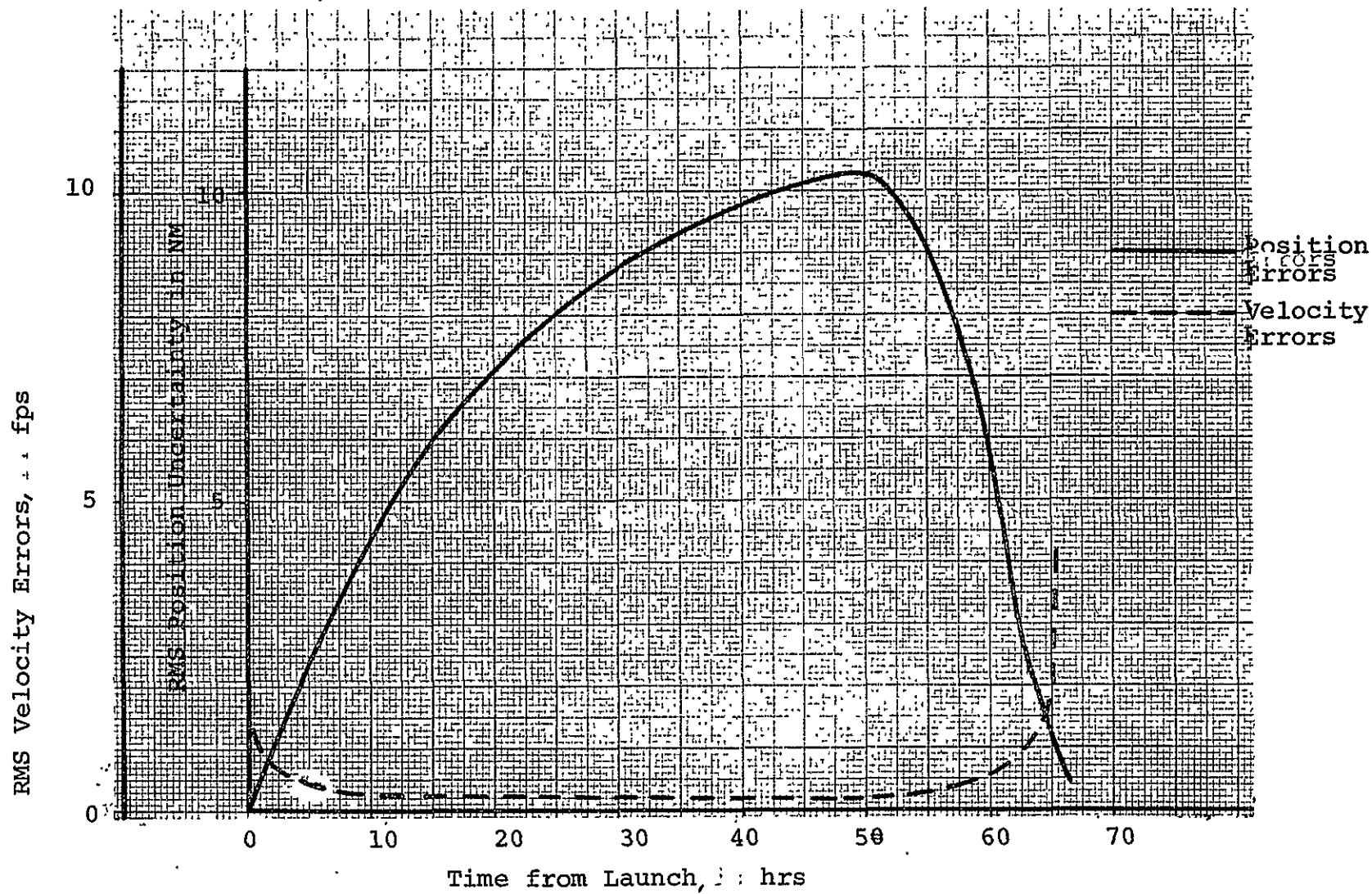


FIGURE 3.1-1 TYPICAL EARTH BASED TRACKING ERRORS

powered descent had begun.

A more accurate and versatile G&N system was used on the Apollo-Lunar Module spacecraft [7]. This type of system contains three IRIGS, three pulse integrating pendulous accelerometers (PIPA), an optical sextant, a landing radar and a flight computer. The system was capable of complete control over the spacecraft and could land the vehicle at any site selected by the astronaut with the use of the versatile flight computer. The LM G&N system is highly redundant since it is in a manned space vehicle and hence contains more equipment than would be needed on the LLV.

If inertial coordinates of the desired lunar landing site were known precisely, a sufficiently accurate G&N system without the ability to deviate from a preprogrammed landing location could be used. Since precise inertial coordinates of lunar surface sites are not available, the G&N system used on the LLV must be capable of altering the spacecraft landing location during the powered phase of its descent. This will allow the LLV G&N system to compensate for lunar surface map errors. This type of system could be constructed using a LM type G&N system with a television camera. An earth based operator could then change the vehicle's landing point once he determined that the vehicle would land in an incorrect location unless he altered its trajectory. The G&N system designed for the LLV was based on a combination of components found in the Surveyor and LM G&N systems. The details of the design are discussed in the following sections.

3.1.2 Coasting Phase Guidance and Navigation

The coasting phase of the LLV translunar trajectory begins with separation of the vehicle from the Centaur stage of the launch vehicle. Measurements must be made to determine very accurately the actual trajectory of the vehicle so that deviations from the nominal flight path may be corrected with mid-course maneuvers. Exact determination of the orbit and estimations of landing point dispersions require extensive calculation, and is best accomplished with ground based computers. Measurements of spacecraft velocities can be obtained from an onboard IMU or from an onboard transponder phase locked to ground tracking stations. The latter method provides better accuracy in measurements of the quantities needed for orbit determination. Figure 3.1-2 shows how tracking data improves the estimated landing point dispersion with time [6]. If the asymptotic value of the dispersion exceeds the required accuracy of 1 Km, a mid-course correction must be made. Precise orbit determinations generally cannot be made based only on IMU measurements because of gyro drifts that increase with time. The errors in velocity and position measurements become too large for accurate trajectory determination after only a few hours have elapsed from launch. Earth based tracking and trajectory determination then must be considered the primary LLV navigation system.

Attitude control over the spacecraft during the coasting phase of the flight is necessary for thermal control of sensitive electronic components, propellants, and stored cryogenics. It can be achieved with the use of attitude sensors, servo control loops and a cold gas jet system. The attitude sensors may be either the

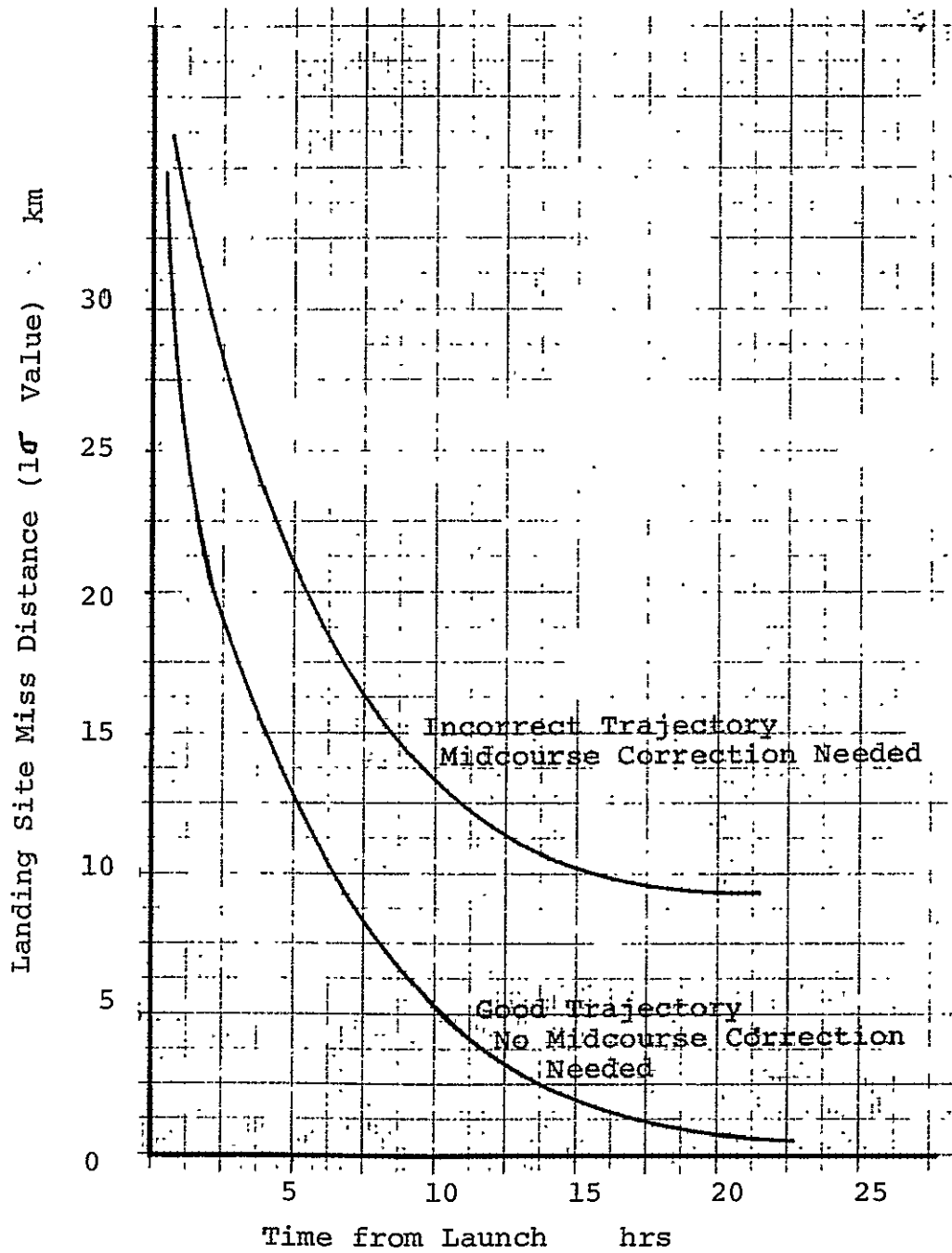


FIGURE 3.1-2 PREDICTED LANDING SITE MISS DISTANCE

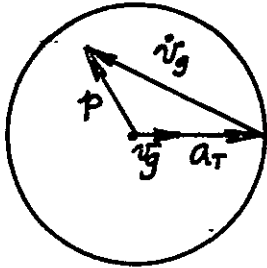
IRIGS in an IMU or a combination of celestial sensors. Use of an IMU is impractical because of the high power level required (25-200 watts) and the gyro drifts rates. Celestial sensors (e.g. sun sensor, Canopus sensor) require very little electrical power (less than 5 watts) and will control the spacecraft attitude to within a few tenths of a degree, depending on what dead bands are used in the attitude control system. The sun sensor and Canopus sensor used on Surveyor were selected in the LLV G&N system. The properties of these sensors are listed in Table 3.1-1. These sensors are coupled to the flight computer (discussed in the next section) with coupling data units that convert sensor analog signal outputs to digital computer inputs. The flight computer then issues commands directly to the appropriate cold gas jets.

3.1.3 Midcourse Correction Guidance

Once it has been established that the LLV is on an incorrect trajectory and will miss the intended landing site, a mid-course correction can be made. This usually consists of making a small change in the spacecraft's velocity which will cause it to land at the intended location. An accurate procedure has been established for mid-course correction maneuvers by the M.I.T. Instrumentation Laboratory [8]. It involves the determination of a velocity to be gained vector and a steering law that nulls this vector. The actual steering is done as follows, with the use of a combination of two steering laws:

Steering Law I.

The vehicle is orientated so the thrust acceleration vector is aligned with the velocity to be gained vector.



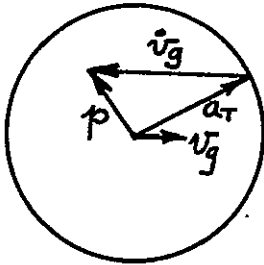
$$\dot{\vec{v}}_g = \frac{d\vec{v}_g}{dt}$$

\vec{v}_g = Velocity to be gained vector

\vec{a}_t = Thrust acceleration vector

Steering Law II.

The vehicle is aligned so that the thrust acceleration vector is directed in such a manner that the $\dot{\vec{v}}_g$ vector is opposite and parallel to the \vec{v}_g vector.

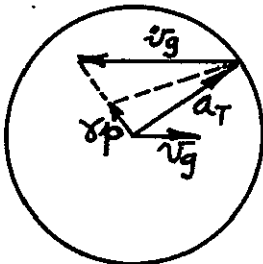


$$\dot{\vec{v}}_g = \frac{d\vec{v}_g}{dt}$$

\vec{v}_g = Velocity to be gained vector

\vec{a}_t = Thrust acceleration vector

These two laws are combined with a coupling constant γ to yield the steering law (Eq 3.1-1)



$$\vec{v}_g \times (\gamma \vec{p} - \vec{a}_t) = 0 \quad (3.1-1)$$

that minimizes the amount of propellant needed to perform the maneuver. Use of this type of steering required an accurate determination of the velocity to be gained vector and was accomplished with an IMU and onboard flight computer.

TABLE 3.1-1

ATTITUDE CONTROL CELESTIAL SENSOR GROUP

Item	Weight	Power Required	Scale Factor	Linear Region	Field of View	No. 11 Offset
Sun (pitch, yaw control)	0.4 lb	<1 watt	1.7 vrms/ deg	yaw: ± 2 deg pitch: ± 2 deg	yaw: 20 deg pitch: 10.5 deg	0.1 deg
Canopus (roll control)	5.0 lb	5 watt	2v/deg	± 2 deg	5 deg x 8 deg 5 deg adjustable by ± 15 deg	0.1 deg

Since this type of in flight guidance has been successfully used in the Apollo program, it was selected for the guidance system for the LLV. The procedures for its use are well developed and the hardware required is not excessive in terms of weight and electrical power requirements. Furthermore, use of an existing system will minimize the guidance and navigation system development costs for the LLV program.

The essential components of the G&N system for powered mid-course guidance are the existing Apollo-LM IMU, the LM coupling data units, and the LM G&N computer. The physical properties of these units are listed in Table 3.1-2. The guidance computer accepts information from either ground based controllers via telemetry or the onboard IMU through the coupling data units. It performs the necessary calculations, and is capable of direct control of the attitude control gas jets, the RCS system, the vernier propulsion system and the main retro engine. Mid-course maneuvers will be performed with the RCS system, since it offers the most accurate means of changing the spacecraft's velocity vector. A complete list of needed computer programs for the entire mission will be given in Table 3.1-3.

3.1.4 Terminal Guidance

The G&N system requirements are most severe during the terminal, or landing phase of the mission. The LLV must be slowed from a velocity in excess of 9,000 fps and brought to a soft landing at a chosen landing site. The system must contain a television camera for identification of the actual landed location. The television system will also allow an earth based operator to alter the landing trajectory if the LLV is on a trajectory

TABLE 3.1-2

PHYSICAL PROPERTIES OF GUIDANCE AND NAVIGATION SYSTEM
COMPONENTS USED IN MIDCOURSE CORRECTION MANEUVER

Item	Dimensions	Power Requirements	Weight
IMU	12.5" Diam Sphere	100 watts	45 lbs
Coupling Data Unit	5.5" x 11.3" x 20"	90 watts	35 lbs
Flight Computer	12" x 18" x 8"	100 watts*	50 lbs

*Computer can be run at reduced power of 20 watts if run at minimum clock speed.

which will cause it to land in an undesirable location. Several landing systems containing television were investigated and are discussed in Section 3.4.

The LLV soft landing system must furnish accurate horizontal and vertical velocity information to the flight computer. The IMU unit furnishes this data during the high altitude phase of the descent, but is not sufficiently accurate for the low altitude (less than 50,000 feet) terminal phase of the landing. Since this information is not obtainable from the television system, a landing radar must be included in the LLV G&N system. Two radar systems were considered--the LM landing radar and the Surveyor landing radar. Both have approximately the same accuracy in making measurements of velocities and altitudes, and are about equal in weight. However, the LM landing radar requires much less electrical power (maximum 200 watts) than the Surveyor radar (maximum of 590 watts), and hence should be the one used on the LLV.

The actual descent of the LLV is controlled by the flight computer [9]. Prior to initiation of powered descent, the vehicles state vector as determined from ground tracking is fed into the computer. The computer calculates the time at which powered descent should begin, based on a preprogrammed landing location. Once the main retro engine starts, the computer performs the following series of computations:

1. Calculation of the current state vector
2. Calculation of the position vector to the intended landing site.
3. Determination of the thrust level needed to keep the vehicle on the intended trajectory.

4. Computation of the throttle commands sent to the main retro engine.
5. Calculation of the gimbal angles, gimbal angle changes and angular rates to be used by the digital autopilot.

The digital autopilot is one section of the computer which directly controls the reaction control system by opening and closing the RCS engine valves.

The computer cycles through the listed calculations every two seconds. It determines the vehicle state vector from IMU data or from landing radar data. The intended landing site can be changed by alteration of the terminal point coordinates used in Step 2. This can easily be done by an earth based operator who can determine a new set of end point coordinates from TV data and then load these coordinates directly into the flight computer with a transmitted instruction to the vehicle. The details of this procedure will be discussed in Section 3.3. The IMU, landing radar and flight computer system can land the vehicle with velocity residuals of less than 5 fps.

3.1.5 Summary of Guidance and Navigation System

The essential components of the LLV G&N system are a LM type guidance computer, a LM landing radar, Surveyor sun and Canopus sensors, a television system, an Apollo-LM inertial measuring unit and pulse torquing assembly, and LM type coupling data units. The guidance computer need not have as great a capacity as the LM guidance computer, since it does not need to provide astronaut displays. The system is redundant in that it can safely land the vehicle if the television camera fails. The computer contains a variable speed clock which allows it to be

TABLE 3.1-3
LIST OF COMPUTER PROGRAMS

Coordinate system transformation routines
Celestial sensor lock-on program
Coast phase guidance program - uses celestial sensors
for attitude, angular rate information
IMU alignment program
Midcourse guidance - velocity to be gained, vector
determination, steering, thrusting programs
Vehicle state vector determination
Descent trajectory determination program
Powered descent thrusting program
Landing radar data processing program
Digital autopilot program
Steerable antenna programs (high gain communications,
landing radar antennas)
Subsystem monitoring programs (fuel, temperatures,
electrical power)
Ground command implementation program

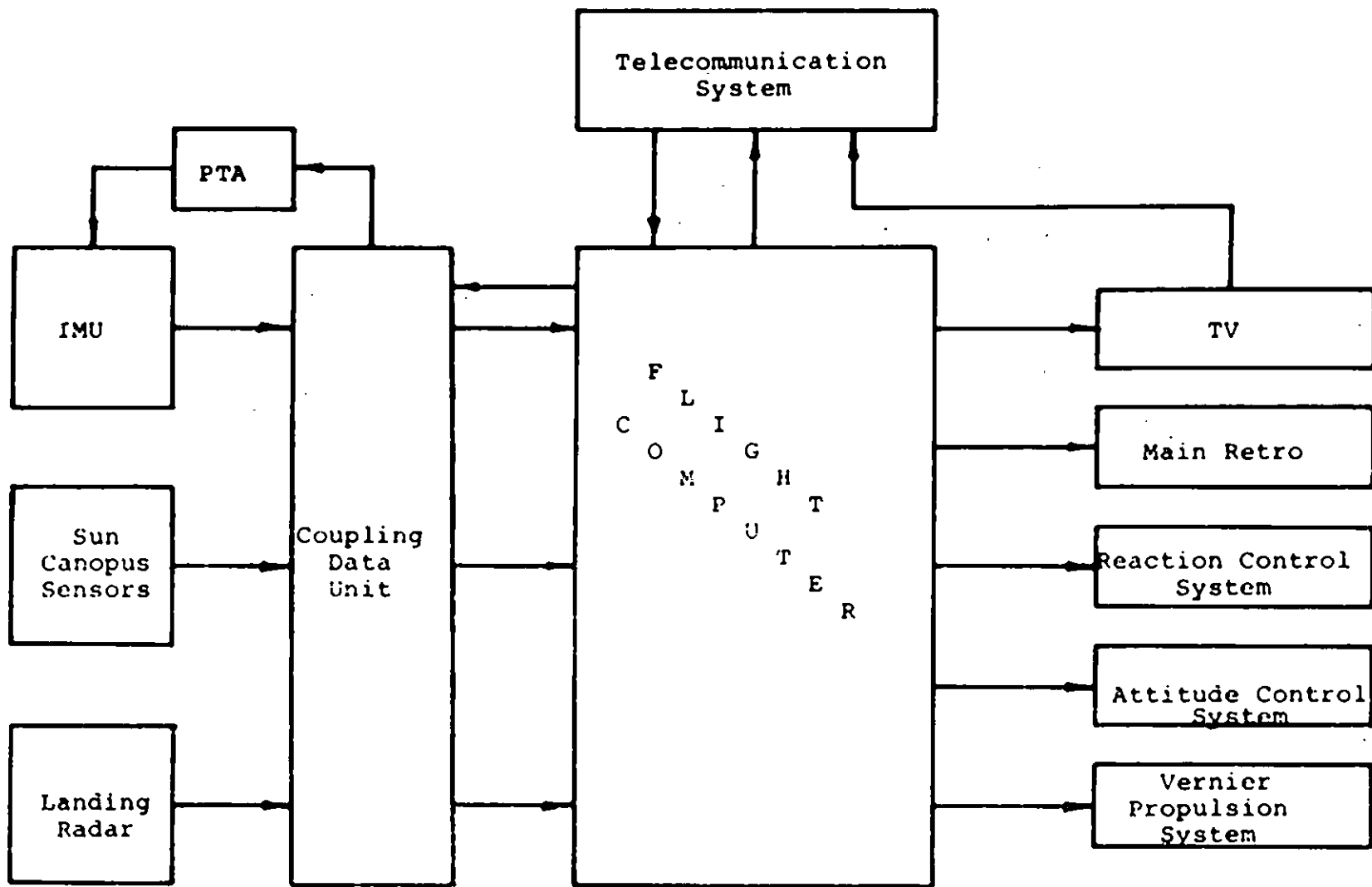


FIGURE 3.1-3 BLOCK DIAGRAM OF GUIDANCE & NAVIGATION SYSTEM

run at low power during the long coasting periods of the mission. During powered maneuvers, the clock is run at full speed and the computer is operated at full capacity. Table 3.1-3 gives a list of necessary computer programs. Figure 3.1-3 is a block diagram of the LLV G&N system.

The G&N system is physically located in the largest equipment box on the LLV. Table 3.1-4 lists the contents of this box. The power and servo electronics unit supplies power at the proper currents, voltages and frequencies to the G&N system and other electronic components in the spacecraft as well.

It is difficult to estimate the landing point dispersion ellipse that this system will produce. Since landing site redesignation with the use of a television camera and earth based operator has never actually been done on a flown mission, extensive simulation studies on the system will have to be carried out before the LLV G&N system is actually flown. The basic system without the television camera should nearly duplicate the accuracy of the Apollo LM system which gives a landing point dispersion ellipse of approximately 3 miles by 4 miles. The dispersion ellipse of the LLV system can be calculated from equations 3.1-2 through 3.1-9 [See Ref. 6].

$$\text{Semi-major axis} = \left[\frac{1}{2} (N_{t11} + N_{t12}) + \left[\left(\frac{N_{t11} - N_{t12}}{2} \right)^2 + N_{t12}^2 \right]^{1/2} \right]^{1/2}$$

$$\text{Semi-minor axis} = \left[\frac{1}{2} (N_{t11} + N_{t12}) - \left[\left(\frac{N_{t11} - N_{t12}}{2} \right)^2 + N_{t12}^2 \right]^{1/2} \right]^{1/2}$$

The matrix N_t is obtained from

$$N_t = N_g + N_{tr} \quad (3.1-3)$$

N_{tr} is the lunar miss covariance matrix, given by

$$N_{tr} = U J^{-1} U^T \quad (3.1-4)$$

U is a transition matrix which converts trajectory parameters into lunar coordinates. J^{-1} is obtained from

$$J^{-1} = [A^T W A + \Gamma^{-1}]^{-1} \quad (3.1-5)$$

A = matrix of first order partial derivatives

W = diagonal a priori weighting matrix

Γ = a priori covariance matrix on trajectory solution parameters

The matrix N_g is obtained from

$$N_g = G \sigma_I G^T \quad (3.1-6)$$

where G is transition matrix that converts spacecraft inertial system error matrix, σ_I , to lunar coordinates. σ_I is obtained from

$$\sigma_I = S \sigma_{s/c} S^T \quad (3.1-7)$$

S is the transformation matrix that converts spacecraft coordinates to inertial coordinates and

$$\sigma_{s/c} = \begin{pmatrix} \sigma_x^2 & 0 & 0 \\ 0 & \sigma_y^2 & 0 \\ 0 & 0 & \sigma_y^2 \end{pmatrix} \quad (3.1-8)$$

The elements of $\sigma_{s/c}$ are obtained from

$$\sigma_x^2 = \sigma_y^2 = [\sigma_\alpha^2 + (\sigma_g t)^2] \underline{1y1}^2 \quad (3.1-9)$$

TABLE 3.1-4.
GUIDANCE AND NAVIGATION SYSTEM BOX

Item	Dimensions	Weight	Electrical Power Requirements
IMU and Navigation Base	12.5" diam sphere 14" diam ring 10" long legs	45 lbs	100 watts
IMU Pulse Torque Assembly	2 1/2"x11"x13"	15 lbs	90 watts
Coupling Data Unit	5.5"x11.3"x20"	35 lbs	50 watts
Flight Computer	12"x18"x8"	50 lbs	100 watts (20 watts at reduced power)
Landing Radar Electronics	15.7"x6.75"x7.35"	25 lbs*	200 watts
Power and Servo Electronics	24"x10"x3"	60 lbs	†
Transponder Electronics	10"x6"x3"	16 lbs	90 watts

*Total landing radar weight including antenna is 42 lbs.

†Power consumption listed in Chapter V.

$$\sigma_z^2 = \sigma_b^2 + (\sigma_p |y|)^2$$

x, y, z are the spacecraft axes

σ_α = 3 σ attitude error minus the gyro error

σ_b = 3 σ thrusting bias uncertainty

σ_p = 3 σ thrusting proportionality uncertainty

σ_g = 3 σ gyro drift rate uncertainty

t = gyro drift time

\underline{v} = mid-course velocity correction error

Evaluation of these equations is beyond the scope of this study.

3.2 Mission Profile

The actual sequence in which the G&N system performs its functions is shown in Figure 3.2-1. This sequence permits the system to be run with a minimum expenditure of electrical power. The mission profile is designed to accommodate three mid-course correction maneuvers. The section of the profile enclosed by the dotted lines is to be performed each time a mid-course correction maneuver is made. The operation duration times for each component on the G&N system is shown in Section 5.2 which discusses electrical power requirements.

FIGURE 3.2-1
GUIDANCE AND NAVIGATION SYSTEM
MISSION PROFILE

Prelaunch Systems Check	-2:00:00	
Launch	0:00:00	
Centaur separation	0:10:00	
Residual rate dissipation	0:11:00	
Sun acquisition	1:00:00	Time - Hours: Minutes:
Canopus acquisition	2:00:00	Seconds
IMU shutdown	2:45:00	
Computer at reduced power	3:00:00	
C_{OAS_T}		
Computer power up	X:00:00=	
IMU start up	X:05:00	
IMU realignment	X:35:00	Three possible midcourse
State vector update	X:40:00	maneuvers, each lasting
Midcourse correction	X:41:00	for 1.5 hours. Actual
Sun acquisition	X+1:00:00	maneuver is made at X:41.
Canopus acquisition	X+1:25:00	
IMU shutdown	X+1:30:00	
Computer at reduced power	X+1:30:00	
C_{OAS_T}		
Computer power up	T-3:00:00	
IMU start up	T-2:55:00	
IMU realignment	T-2:30:00	
State vector update	T-2:45:00	
Maneuver to Retro fire		
attitude	T-2:00:00	
TV actuated	T-1:00:00	T = touchdown time
State vector update	T-:30:00	= 60 hrs, or 120 hrs
Landing radar on	T-:04:00	
Retro engine on	T-:03:00	
Vernier propulsion system		
on	T-:00:25	
Main retro burnout &		
jettison	T-:00:25	
Hover	T-:00:20	
Touchdown	T-:00	
Landing radar, IMU off	T+:01	

3.3 Some Trajectory Considerations

3.3.1 Direct vs Orbital Descent

The final descent to the lunar surface may occur by direct descent or via a lunar parking orbit. The direct descent provides more accurate landings (There is continuous tracking by earth stations, and there are less perturbations due to moon inhomogeneities.), and requires only a single impulse maneuver for touch-down. On the other hand, the lunar orbit descent makes the total lunar surface accessible, and the manned spacecraft program has furnished a wealth of experience with this mode of descent. The lunar orbit approach poses severe guidance problems since the descent trajectory is tangential in all cases (See Section 3.3.5).

The ΔV budgets for nominal direct and orbit descents are given in Table 3.3-1. The 60-hr mission sizes propellant requirements for the lunar orbit descent, and the 60-hr, -900 nm pericynthion altitude mission sizes propellants for the direct descent. The orbit descent has an appreciable ΔV penalty associated with it compared to the direct descent.

The direct descent is considered best for the mission.

3.3.2 Hover Penalty

One of the groundrules is a 20-sec minimum hover time. This requires a ΔV budget for the hover and also for the descent of the LLV from the hover altitude. The equation of motion of the LLV is

$$\dot{v} = \frac{T}{m} - g, \quad (3.3-1)$$

where \dot{v} is the time derivative of the velocity, T is the engine thrust, m is the mass of the LLV, and g is the acceleration due to lunar gravity. Since the initial and final velocities are

TABLE 3.3-1 ΔV BUDGETS FOR LUNAR DESCENT (60 HR)

	Orbit (60 nm)	Direct (hp = -900 nm)
Midcourse	100 fps	100 fps
Lunar Insertion	3,450	
Descent to 50,000 ft	71	
Braking	5,854	9,393
Redesignation	150	150
Final Approach	506	99
Hover	115	115
Touchdown	<u>50</u>	<u>50</u>
	10,296	9,907

both zero, we get for ΔV upon integrating Eq. 3.3-1 and using the definition of ΔV

$$\Delta V \equiv \int_0^t \frac{T}{m} dt = gt . \quad (3.3-2)$$

Since $g = 5.31 \text{ ft/sec}^2$, we get $\Delta V = 106 \text{ fps}$ for a 20-sec hover.

The optimal descent from hover is accomplished by letting the LLV fall freely until it reaches a height h whereupon the thrust is increased to maximum. The value of h is such that the LLV attains zero velocity at the lunar surface.

Consider Figure 3.3-1. We solve for the case of a spacecraft of mass m lifting off the surface with thrust T . At altitude h the thrust is decreased to zero, and the spacecraft coasts to an altitude H . The ΔV necessary for the (ascent) maneuver is the same as for the opposite (descent) maneuver. We assume that the accelerations are constant and that the change in mass of the spacecraft is small. The following relations hold.

$$v_1^2 = 2g(H-h) , \quad (3.3-3)$$

and

$$v_1^2 = 2a_1h = 2\frac{(T-mg)}{m}h , \quad (3.3-4)$$

where v_1 is the velocity at altitude h , and a_1 is the acceleration during the thrust phase. These equations lead to

$$h = \frac{mg}{T}H . \quad (3.3-5)$$

During ascent, $\dot{v} = \frac{T}{m} - g$, and therefore

$$\Delta V \equiv \int_0^t \frac{T}{m} dt = v_1 - v_0 + gt = v_1 + gt , \quad (3.3-6)$$

.....

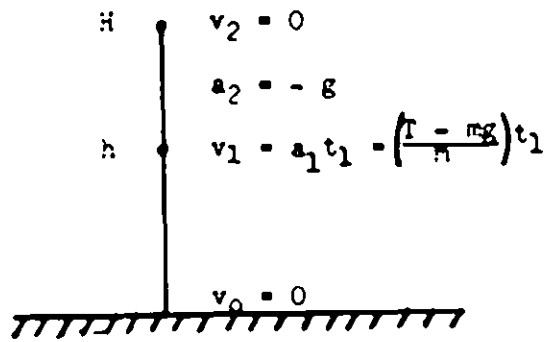


FIGURE 3.3-1 DESCENT FROM HOVER

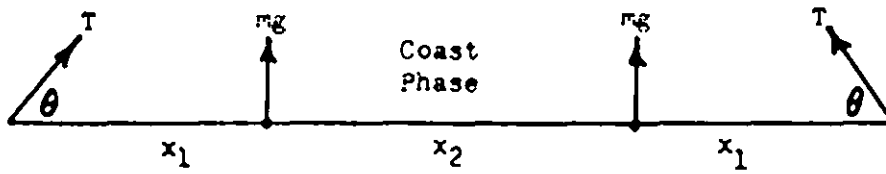


FIGURE 3.3-3 TRANSLATION AT CONSTANT ALTITUDE

Eliminating t in Eq. 3.3-6 and Eq. 3.3-7, and using Eq. 3.3-5 and Eq. 3.3-4, we get for the ΔV necessary to ascend to (or descent from) an altitude H

$$\Delta V = \left(\frac{2TgH}{T-mg} \right)^{1/2} . \quad (3.3-8)$$

ΔV vs H for various thrust to lunar weight ratios is plotted in Figure 3.3-2.

3.3.3 Post-landing Liftoff or "Hop"

It would be desirable for the spacecraft to have the capability to lift off and change its position. This may be accomplished in a variety of ways. We consider two kinds of hop program:

- (1) straight ascent, translation at constant altitude, and straight descent;
- (2) an optimal ballistic-type trajectory.

The ΔV required for ascent and descent is given by Eq. 3.3-8. The ΔV required for translation depends upon the thrust program. Consider first the following thrust program. The thrust is oriented at an angle θ to the horizontal so that the vertical component of the thrust is equal to mg , the lunar weight of the vehicle. This maintains the altitude constant. The horizontal component of thrust produces an acceleration and a translation. When one-half of the desired translation is accomplished, the thrust vector is reoriented so that the horizontal component points opposite to the velocity vector. When the spacecraft stops, the thrust is oriented vertically at a value mg . The minimum propellant solution for this program is described in [10]. The angle θ should be 45° , and the ΔV required is approximately

$$\Delta V = 4 \sqrt{gR} , \quad (3.3-9)$$

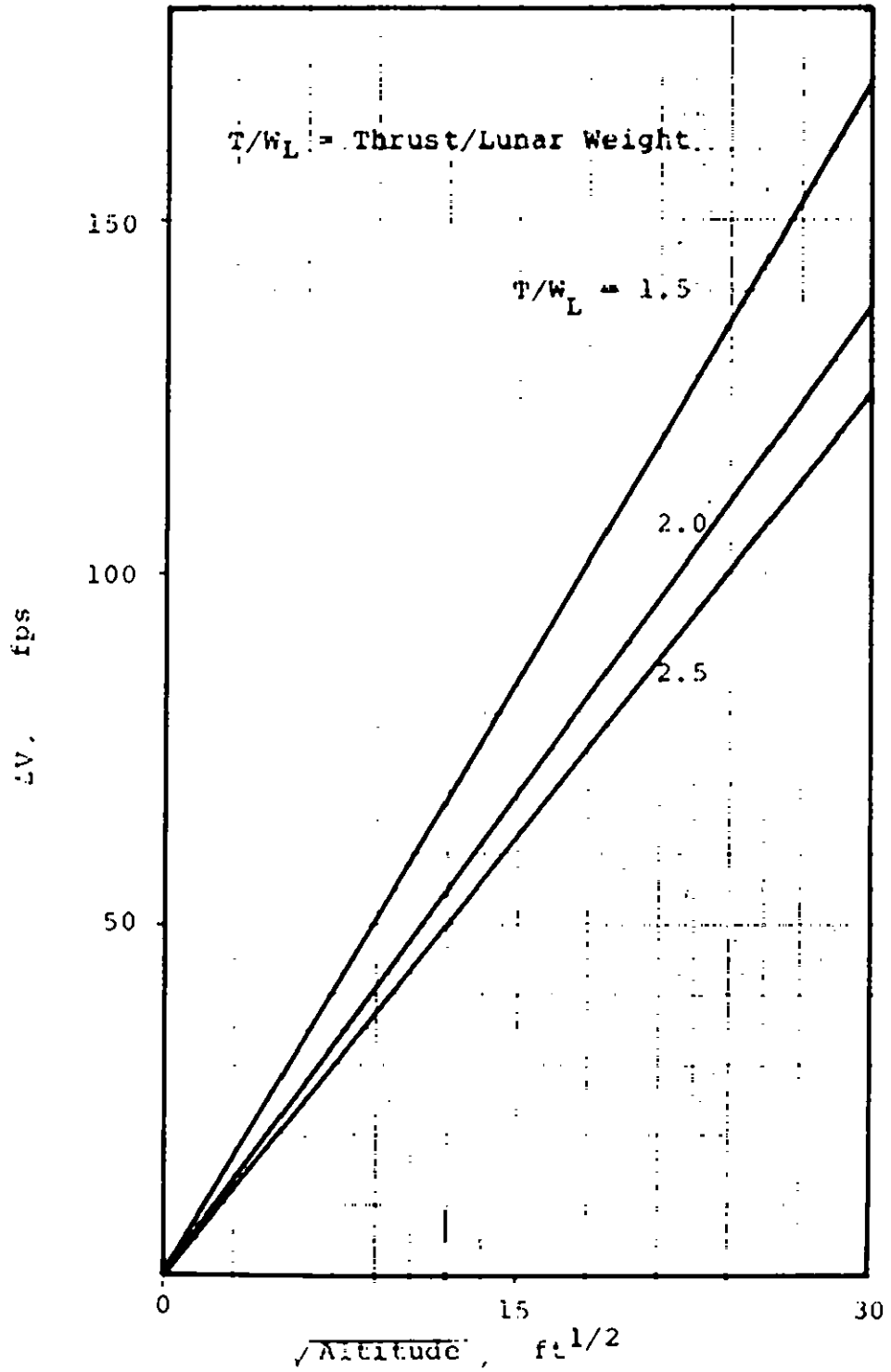


FIGURE 3.3-2 ΔV TO DESCEND FROM HOVER

where R is the translation distance. It is assumed that the change in mass is small during the maneuver.

The trajectory is more efficient if a coast phase is included. The thrust T is oriented θ degrees with respect to the horizontal such that the vertical component is $-mg$. This orientation is maintained for a distance x_1 , whereupon the thrust is set vertically so that the craft coasts at constant altitude and constant velocity v_2 for a distance x_2 . The thrust is then oriented at the angle θ with the horizontal so that the vertical component is opposite to the velocity vector. When the vehicle comes to a stop, the thrust is returned to the vertical position with a magnitude mg . We assume that the change in mass is small so that accelerations are constant. From symmetry the third phase translation distance is equal to the first phase translation distance x_1 . This program is represented in Figure 3.3-3.

The change in mass Δm is given by

$$\Delta m = 2\dot{m}_1 t_1 + \dot{m}_2 t_2, \quad (3.3-10)$$

where \dot{m} is the time derivative of m during the first and third phases, \dot{m}_2 is the time derivative of m during the second phase, and t_1 and t_2 are the times of the first (and third) and second phase, respectively. From the definition of the specific impulse I_s of the engine, we have

$$\dot{m}_1 = \frac{T}{g_e I_s}, \quad (3.3-11)$$

and

$$\dot{m}_2 = \frac{mg}{g_e I_s}, \quad (3.3-12)$$

where g_e is the acceleration due to earth gravity. The total distance traveled is-

$$R = 2x_1 + x_2 \quad , \quad (3.3-13)$$

where

$$x_1 = \frac{1}{2} v_2 t_1 \quad , \quad (3.3-14)$$

and

$$x_2 = v_2 t_2 \quad . \quad (3.3-15)$$

Eq. 3.3-14 follows from the assumption of constant acceleration.

Substituting Eq. 3.3-14 and Eq. 3.3-15 into Eq. 3.3-13 and using the value for v_2 produced by constant acceleration; i.e.,

$$v_2 = \frac{T \cos \theta}{m} t_2 \quad , \quad (3.3-16)$$

we get

$$R = v_2 (t_1 + t_2) = \frac{T \cos \theta}{m} t_1 (t_1 + t_2) \quad . \quad (3.3-17)$$

Solving Eq. 3.3-17 for t_2 , substituting into Eq. 3.3-10, and using

$$T \sin \theta = mg \quad , \quad (3.3-18)$$

we get, after arranging,

$$\frac{g_e I_s}{mg} \Delta m = \left\{ \frac{2}{\sin \theta} - 1 \right\} t_1 + \frac{R \tan \theta}{g t_1} \quad . \quad (3.3-19)$$

We find the minimum for Δm by setting the partial derivatives of Δm with respect to θ and t_1 equal to zero. The solution is

$$\theta = 30^\circ, \quad t_1^2 = \frac{R}{3\sqrt{3}g} \quad (3.3-20)$$

Using Eq. 3.3-17 and Eq. 3.3-20, we get the relation

$$t_2 = 2t_1. \quad (3.3-21)$$

Thus, the coast phase lasts for one-half of the total translation time.

Eq. 3.3-20 plus Eq. 3.3-19 yield for the minimum mass change

$$g_e I_s \frac{\Delta m}{mg} = 2\sqrt{\sqrt{3}} \frac{R}{g}. \quad (3.3-22)$$

Since

$$\Delta V = g_e I_s \ln \left(\frac{m+\Delta m}{m} \right),$$

$$\Delta V \approx g_e I_s \frac{\Delta m}{m}, \quad (3.3-23)$$

since we have assumed $\Delta m/m \ll 1$. Therefore, the minimum ΔV for translation using the above program is

$$\Delta V = \sqrt{4\sqrt{3}} g_e R = \sqrt{6.928} g_e R. \quad (3.3-24)$$

This relation is plotted in Figure 3.3-4.

If the thrust vector is allowed to change continuously during the translation at constant altitude, we may use the calculus of variations to determine the minimum ΔV . The problem is to minimize

$$\Delta V = \int_0^t [g^2 + \dot{v}^2]^{1/2} dt. \quad (3.3-25)$$

Eq. 3.3-25 may be derived in the following way. The basic equation

$$\dot{v} = \frac{\dot{F}}{m} - \dot{g}$$

is a vector equation. Thus, by the definition of ΔV ,

$$\Delta V = \int_0^t \frac{T}{m} dt = \int_0^t [g^2 + \dot{v}^2]^{1/2} dt,$$

where T is the magnitude of the vector \vec{T} .

The minimum ΔV is (See References [11] and [12])

$$\Delta V = \sqrt{2\pi g R} = \sqrt{6.283gR}. \quad (3.3-26)$$

Note that the ΔV given by Eq. (3.3-26) is only about 5% less than that given by Eq. (3.3-24).

The ΔV requirements for the three types of thrust program are plotted in Figure 3.3-4.

The optimum trajectory which is not limited to constant altitude may also be found by the calculus of variations. We can determine some properties of the trajectory by inspection. The minimum propellant program should include a coast phase (in this case, a ballistic path) since this saves propellant. The problem should be symmetric if we assume the change in mass is small. Also, in order to minimize gravity losses, the thrust should be as large as possible or zero. Thus, the trajectory should look like that in Figure 3.3-5.

To make x_2 , the ballistic range, a maximum, ϕ should be 45° . The basic equation of motion is

$$\ddot{\vec{v}} = \frac{\vec{T}}{m} - \vec{g}. \quad (3.3-27)$$

Thus, we seek to minimize

$$\Delta V = \int_0^{t_1} \frac{T}{m} dt = \int_0^{t_1} [\dot{v}_x^2 + (\dot{v}_y + g)^2]^{1/2} dt \quad (3.3-28)$$

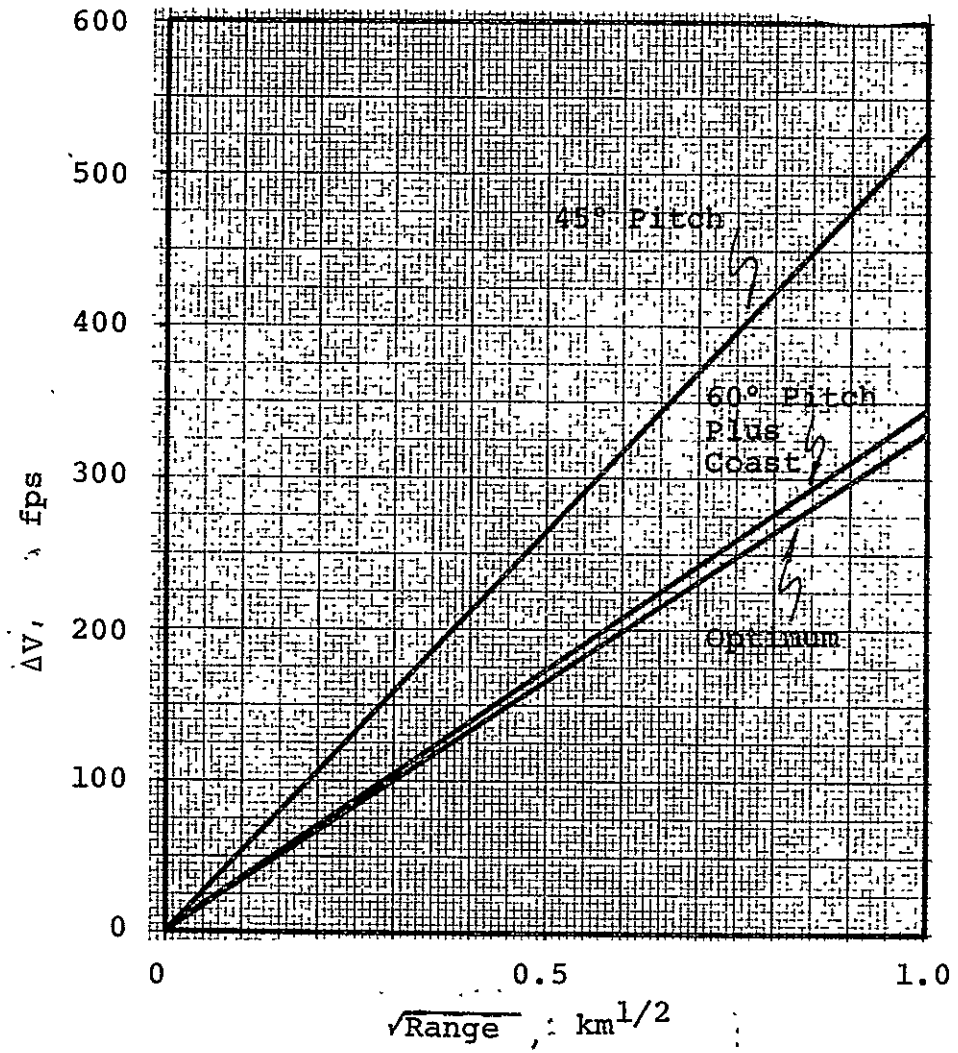


FIGURE 3.3-4 ΔV TO TRANSLATE AT CONSTANT ALTITUDE

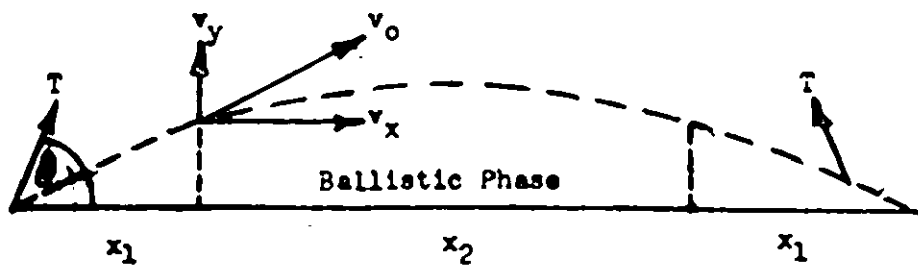


FIGURE 3.3-5 HOP TRAJECTORY

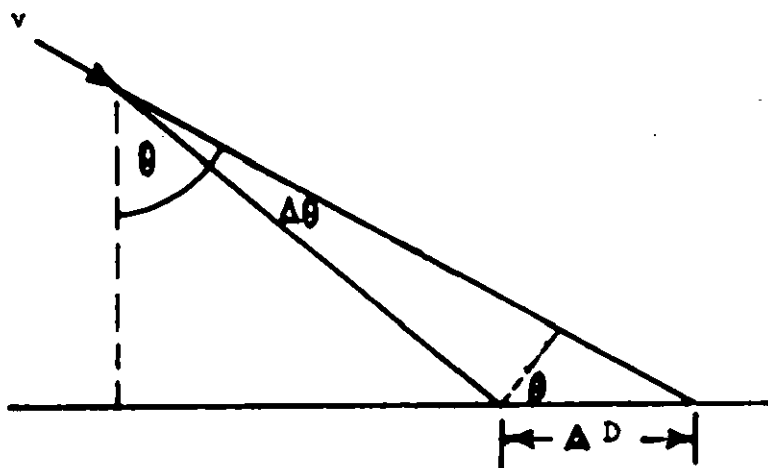


FIGURE 3.3-7 APPROXIMATE TRAJECTORY GEOMETRY

subject to the constraint

$$T = m[\dot{v}_x^2 + (\dot{v}_y + g)^2]^{1/2} = \text{constant} \quad (3.3-29)$$

and the boundary conditions

$$t=0: v_x = v_y = 0 ; t=t_1: v_x = v_y = v_0/\sqrt{2} . \quad (3.3-30)$$

In the above equations, the dot indicates time differentiation, the x and y subscripts are the horizontal and vertical components, respectively, and t_1 is the thrust time for the first phase. From the symmetry of the problem, the ΔV during the third phase of the trajectory is equal to that during the first phase. There is no ΔV required during the ballistic phase.

Let

$$\dot{\phi} = [\dot{v}_x^2 + (\dot{v}_y + g)^2]^{1/2} + \lambda(T - [\dot{v}_x^2 + (\dot{v}_y + g)^2]^{1/2}) , \quad (3.3-31)$$

where λ is a Lagrange multiplier. We also have the relations

$$m = m_0 - kt ; k = \frac{T}{g_e I_s} , \quad (3.3-32)$$

where g_e is the acceleration due to earth gravity and I_s is the specific impulse of the engine. We minimize ΔV by finding the solution to the Euler-Lagrange equations

$$\frac{d}{dt} \left(\frac{\partial \dot{\phi}}{\partial \dot{v}_i} \right) - \frac{\partial \dot{\phi}}{\partial v_i} = 0 , i = x, y. \quad (3.3-33)$$

After performing the indicated operations and arranging, we get

$$(1-\lambda m) \frac{\ddot{v}_x}{\dot{v}_x} + \lambda k - F(1-\lambda m) = 0 \quad (3.3-34)$$

and

$$(1-\lambda m) \frac{\ddot{v}_y}{(\dot{v}_y+g)} + \lambda k - F(1-\lambda m) = 0, \quad (3.3-35)$$

where

$$F = [\dot{v}_x \ddot{v}_x + (\dot{v}_y+g) \ddot{v}_y] / [\dot{v}_x^2 + (\dot{v}_y+g)^2]^{3/2} \quad (3.3-36)$$

Thus,

$$\ddot{v}_x / \dot{v}_x = \ddot{v}_y / (\dot{v}_y+g), \quad (3.3-37)$$

or

$$\ln \dot{v}_x = \ln(\dot{v}_y+g) - \ln c, \quad (3.3-38)$$

where c is a constant of integration. Then

$$c \dot{v}_x = \dot{v}_y + g. \quad (3.3-39)$$

From Eq. 3.3-27 we get

$$T_x = m \dot{v}_x, \quad T_y = m \dot{v}_y + mg \quad (3.3-40)$$

Thus, the optimum thrust program calls for

$$T_y = c T_x \quad (3.3-41)$$

that is, the thrust angle is constant.

From Eq. 3.3-39, we get

$$v_y + gt = c v_x + c_2 \quad (3.3-42)$$

where c_2 is an integration constant. Applying the boundary conditions (3.3-30), we get

$$c_2 = 0, \quad c = 1 + gt_1 \sqrt{2}/v_0. \quad (3.3-43)$$

Now

$$T^2 = T_x^2 + T_y^2 = (1+c^2)T_x^2 = (1+c^2)T^2/\cos^2\theta \quad (3.3-44)$$

Thus,

$$(1+c^2) \cos^2\theta = 1 . \quad (3.3-45)$$

Also,

$$\frac{v_o}{\sqrt{2}} = \frac{T \cos\theta}{m} t , \quad (3.3-46)$$

since we assume the acceleration is constant. Thus, we have the approximate relation

$$c = 1 + \frac{mg}{T \cos\theta} . \quad (3.3-47)$$

Using Eq. 3.3-45 and Eq. 3.3-47, we get after some arrangement

$$2\cos^2\theta + \frac{2mg}{T} \cos\theta + \left(\frac{mg}{T}\right)^2 - 1 = 0 ,$$

and, therefore,

$$\cos\theta = \frac{mg}{2T} \left(-1 \pm \left(\frac{2T^2}{m^2 g^2} - 1 \right)^{1/2} \right) \quad (3.3-48)$$

Now the range R is (See Figure 3.3-5)

$$R = 2x_1 + x_2 . \quad (3.3-49)$$

For our assumption of constant acceleration,

$$v_o^2 = 2v_x^2 = \frac{4T \cos\theta}{m} x_1 . \quad (3.3-50)$$

Also, for a ballistic trajectory, the range x_2 , for $\phi=45^\circ$, is

$$x_2 = v_o^2 / g . \quad (3.3-51)$$

Substituting Eq. 3.3-50 and Eq. 3.3-51 into Eq. 3.3-49, we get

$$R = \left(1 + \frac{mg}{4T\cos\theta} \right) \frac{2v_x^2}{g} \quad (3.3-52)$$

Also, from Eq. 3.3-40,

$$v_x = \int_0^{t_1} \frac{T_x}{m} dt = \cos\theta \Delta V_1 \quad (3.3-53)$$

Thus, the total ΔV is

$$\Delta V = 2\Delta V_1 = \frac{2}{\cos\theta} \frac{gR}{2 \left(1 + \frac{mg}{4T\cos\theta} \right)^{1/2}} \quad (3.3-54)$$

Eq. 3.3-48 and Eq. 3.3-54 determine the ΔV requirement for a hop of distance R for values of the thrust to lunar weight ratio. The ΔV requirement is plotted in Figure 3.3-6.

3.3.4. Site Redesignation

A landing site-redesignation ΔV budget of 150 fps is included in the main retro burn. To determine what change in range is possible with this ΔV , it would be desirable to consider the optimum thrust program to attain maximum (or minimum) range. This problem has been studied by Isaev [13]. The general results include a time varying thrust orientation with the magnitude of the thrust a maximum or zero; i.e., there may be a coasting phase. However, the thrust program for an actual spacecraft is highly dependent upon the guidance logic used. Therefore, in this section we shall be interested in obtaining an approximate description of the redesignation capability.

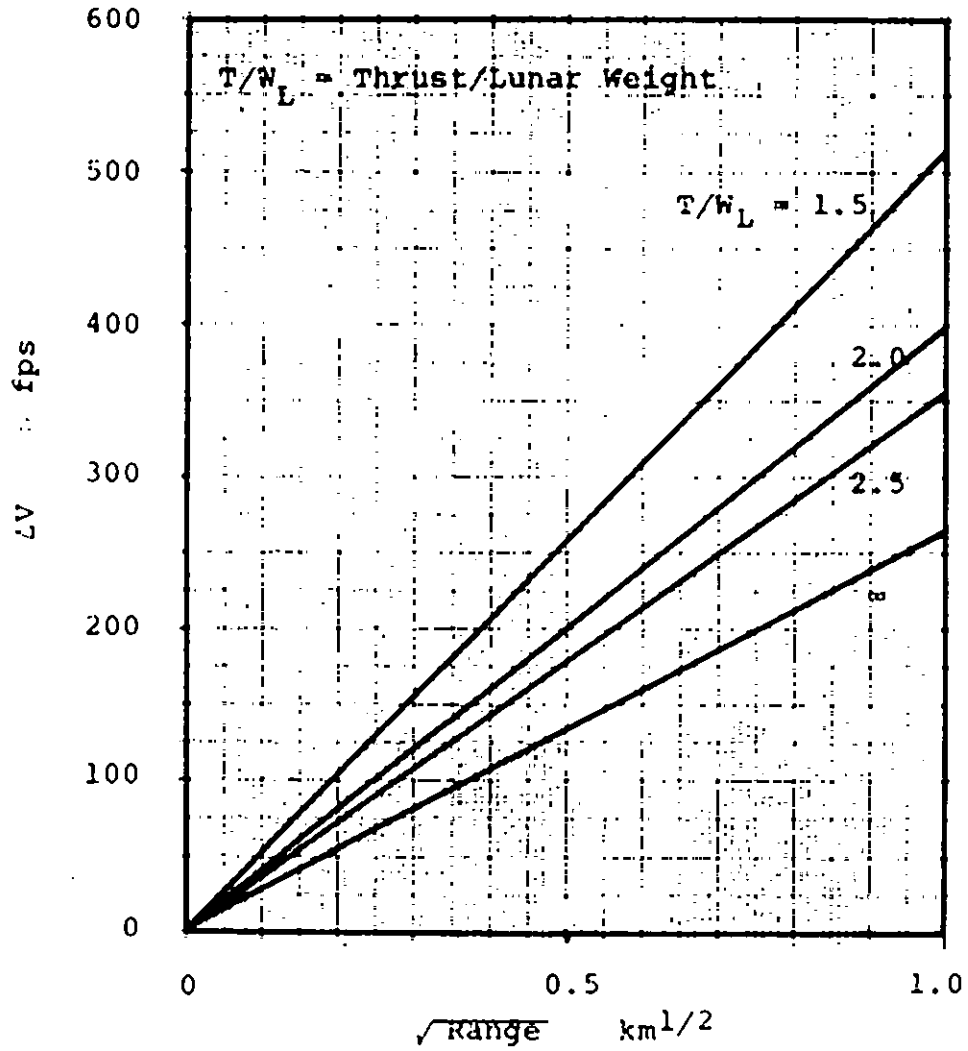


FIGURE 3.3-6 ΔV TO HOP vs HOP DISTANCE

A straight line trajectory is a good approximation to the main retro trajectory (see Figure 3.3-10). Consider Figure 3.3-7. If we neglect gravity losses, the ΔV along path r_1 is the same as that along r_2 . If $\Delta\theta$ is small, the difference in gravity losses between paths r_1 and r_2 is much smaller than 150 fps, the redesignation budget. Thus, to a sufficient approximation, we can assume that the entire redesignation budget can be used to change the angle of the trajectory. The change in range ΔD is then

$$\Delta D = \frac{r\Delta\theta}{\cos\theta} . \quad (3.3-55)$$

Assume that the ΔV is fed in impulsively and perpendicular to the trajectory at a distance r from burn-out. Then

$$\Delta\theta = \frac{\Delta V}{v} , \quad (3.3-56)$$

where v is the velocity of the spacecraft when the ΔV is added.

Thus

$$\Delta D = \frac{r\Delta V}{v\cos\theta} . \quad (3.3-57)$$

This relation is plotted in Figure 3.3-8. The values of r , v , and θ , as a function of time were taken from RL10 engine trajectories generated by a computer program and made available by the Manned Spacecraft Center of NASA. The zero nautical mile pericyynthion altitude, h_p , corresponds to a near tangential approach; whereas, the $h_p = -900$ nm corresponds to a near vertical approach.

Although we have assumed that the ΔV was added impulsively, in practice, the ΔV will be added over a portion of the trajectory. For example, if a nominal thrust of 10,000 lb were used, the ΔV could be added by pitching the thrust vector and increasing it

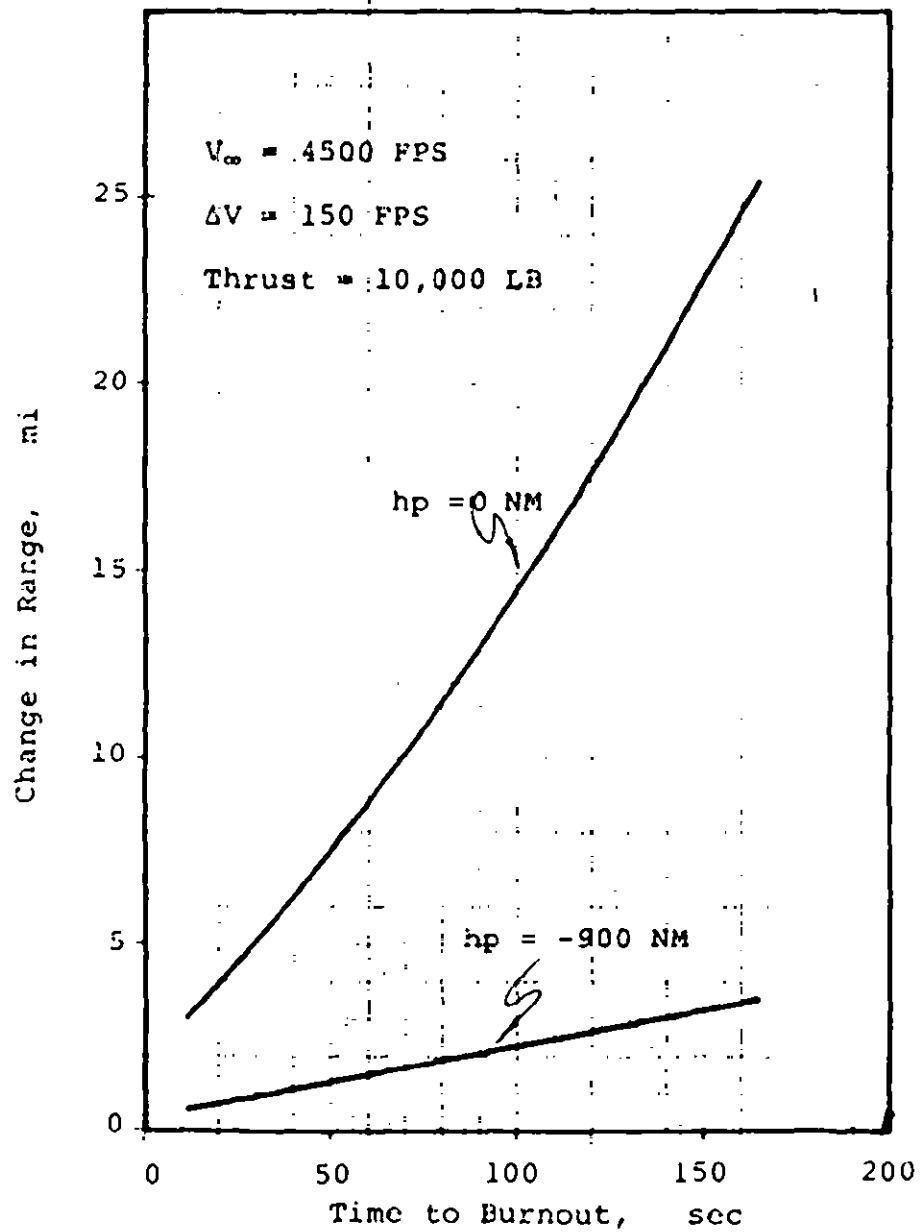


FIGURE 3.3-8 SITE REDESIGNATION (APPROXIMATE)

to 15,000 lb so that the thrust component along the trajectory remains at 10,000 lb.

It is estimated that the uncertainty in the position of the spacecraft at time of retro initiation, as determined by tracking, is about one-half mile. It is apparent from Figure 3.3-8 that this uncertainty can be nulled. However, there are map error uncertainties in lunar coordinates of the target. These may be as large as tens of miles, and they cannot always be nulled during the main retro phase.

3.3.5 Tangential Approaches

Figure 3.3-9 shows the angle of incidence (measured from the vertical) of the spacecraft trajectory as a function of longitude on the moon measured along the equator. Note that beyond 75° east no landing is possible for some trip times without paying a ΔV penalty to alter the trajectory. Also, the figure is drawn for nominal values. There is about a $\pm 7^\circ$ variation due to earth-moon distance variations, etc. Thus, about 20° of the eastern limb could require this ΔV penalty.

The tangential approach requires less ΔV than the vertical approach. Therefore, there is some ΔV available since the vertical approach sized the propellant requirements. However, the difference in propellant between the tangential and vertical missions for the RL 10 at a nominal thrust of 15000 lb is only about 40 lb. This is equivalent to a ΔV of about 100 fps. The velocity of the spacecraft is the order of 10^4 fps. Thus, we can turn it through an angle the order of 10^{-2} radian or one-half degree. Therefore, very little change in altitude is possible since we do not have

the capability to bend the trajectory so that it intersects the target and also make up for the increased gravity losses due to the steeper trajectory.

A computer program supplied by MSC was used to determine the inaccessible areas of the moon. For the 60-hr trip time the entire visible face of the moon was always accessible; however, for the 120-hr trip time the maximum longitude accessible sometimes got as low as 60° east. The uncertainty in the results of this program is about $\pm 5^\circ$. It thus appears that beyond 75° or 80° east, targeting will be extremely difficult, if possible at all, for some trip times.

Figure 3.3-10 shows an RL10 trajectory for a thrust of 15,000 lb, a tangential approach, and a high energy mission. The angle of the trajectory with the local horizontal is only about 8° . This poses problems for the guidance system. It would be desirable to raise the trajectory and make it steeper. However, as we have seen above, the ΔV penalty is large, and very little improvement can be made. Fortunately, the low angle also provides a high magnification for site redesignation (see Figure 3.3-8) so that this guidance problem is somewhat alleviated.

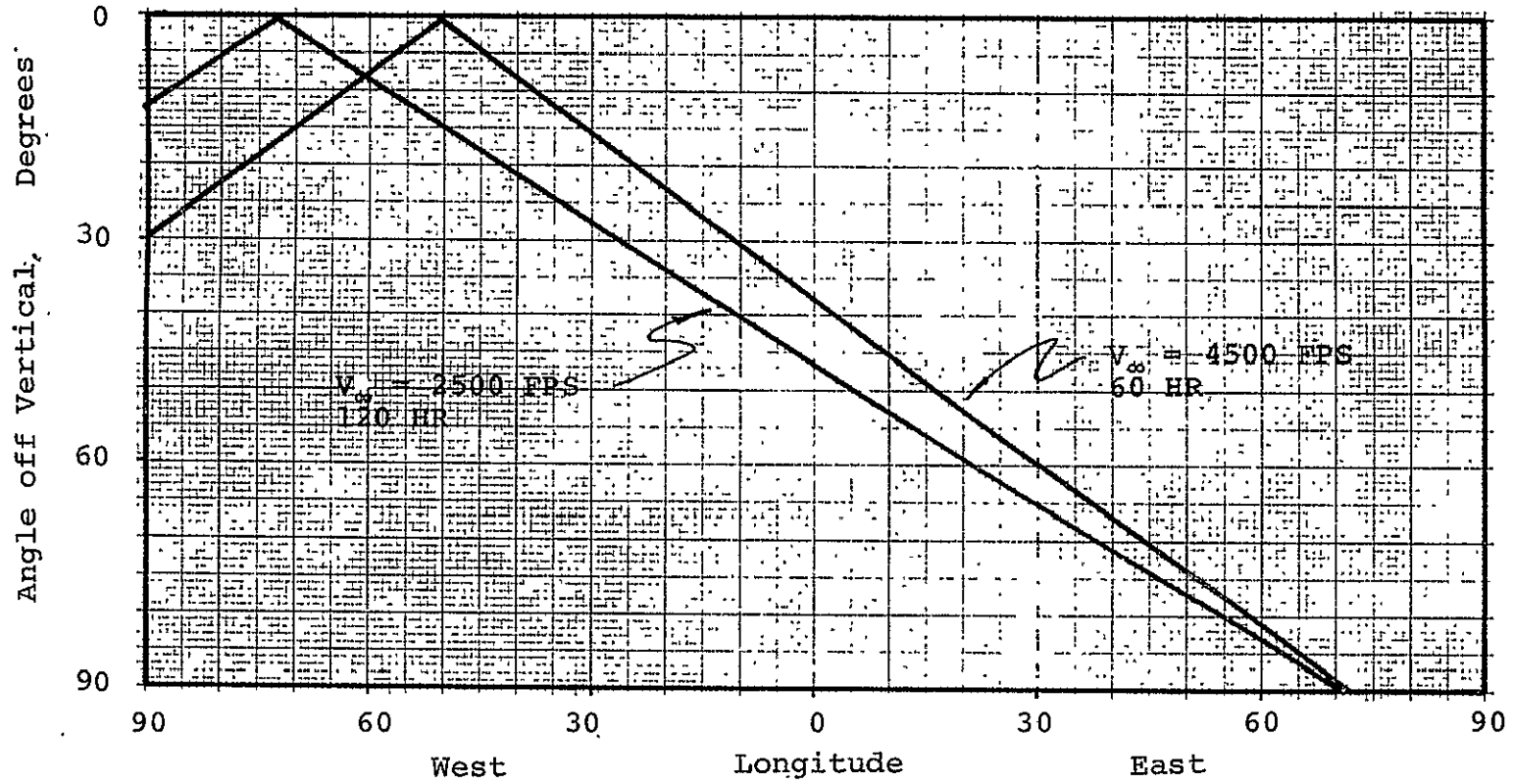


FIGURE 3.3-9 ANGLE OF INCIDENCE vs LONGITUDE

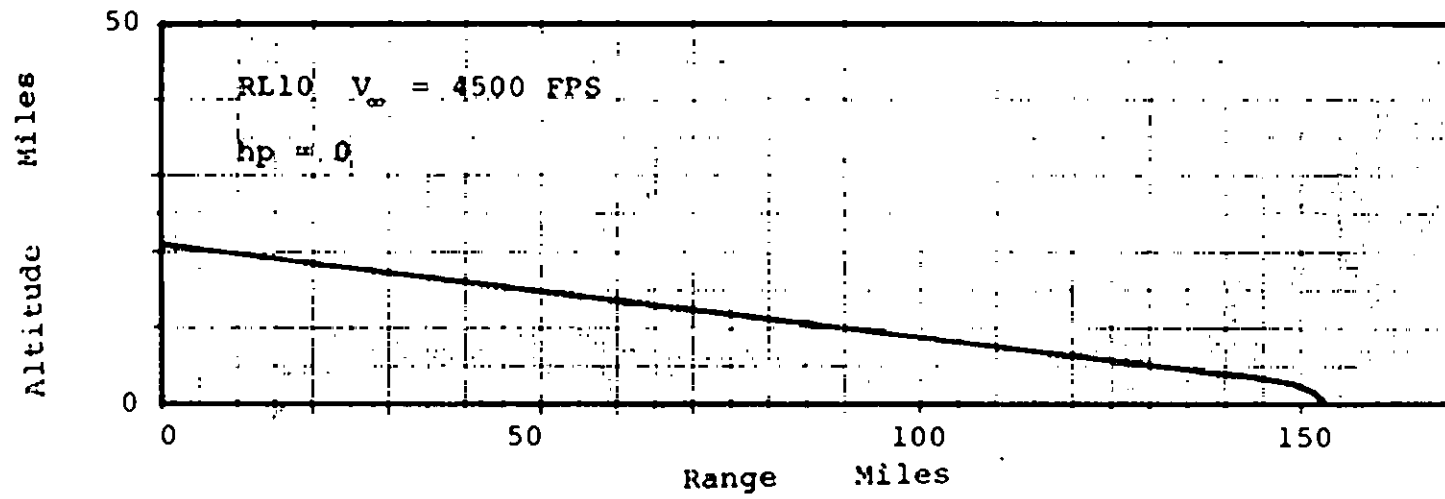


FIGURE 3.3-10 RL10 TANGENTIAL TRAJECTORY

3.4 Landing Television System (LTVS)

3.4.1 Introduction

The desired mission landing constraints of a 1 Km (3σ) landing point dispersion and a soft landing in the rough terrain of the lunar highlands produce terminal guidance system requirements that are more severe than those for the previously successful soft-landing United States spacecraft, the manned Lunar Module [14] and the unmanned Surveyor [1]. A Landing Television System (LTVS) is added to the standard guidance and navigation system on the LLV to provide an accurate landing system capable of avoidance of hazardous landing points.

The Landing Television System (LTVS) does not directly interact with the on-board G&N system, but rather the video data is transmitted back to earth for evaluation by a controller at Mission Control. The controller compares the video data with that for the nominal trajectory, redesignates a new landing point, and instructs the control center computer to calculate a new set of landing coordinates which are transmitted to the vehicle as superposed inputs to the G&N system.

Since the flight computer continually recalculates trajectory requirements from the latest set of landing coordinates and the terminal descent is initially preprogrammed, a loss of controller inputs will result in only a continuation of flight along the last updated trajectory. A block diagram of the on-board portion of the landing television and its interfaces with the G&N and telecommunications systems are shown in Figure 3.4-1.

Visual information from the lunar surface is sensed by the television camera which transforms it into electrical signals.

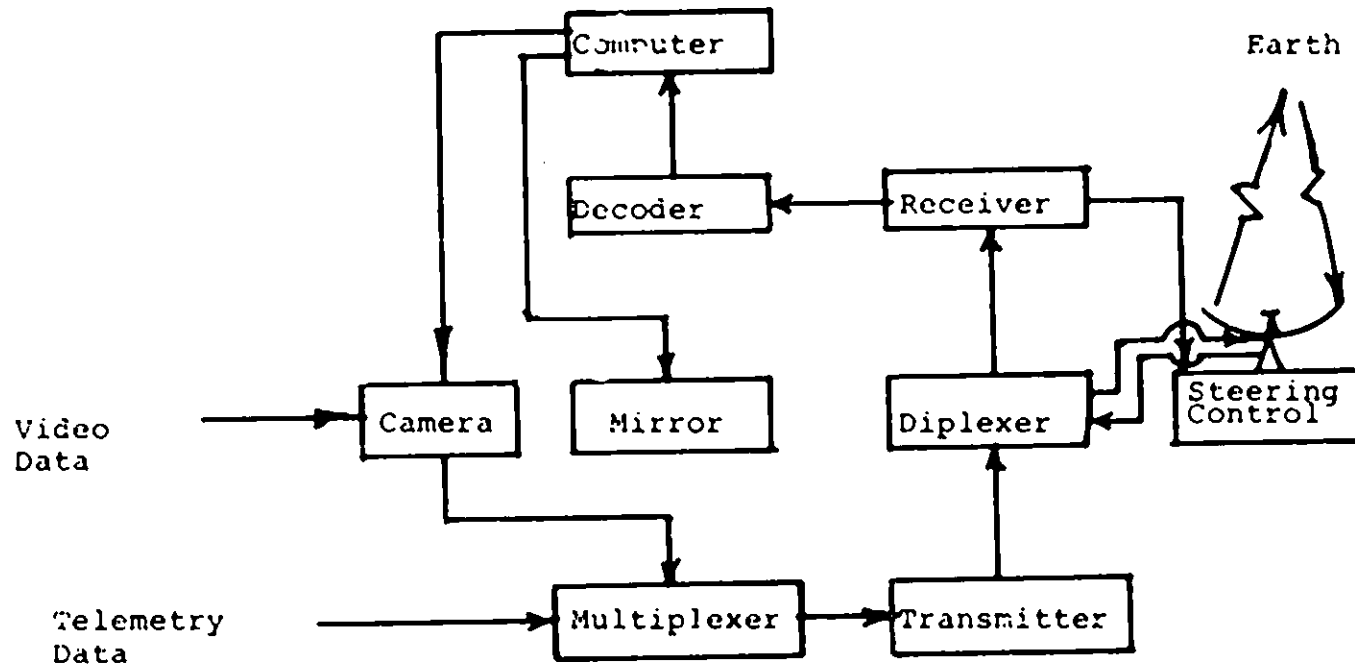


FIGURE 3.4-1 LLV LANDING TELEVISION SYSTEM.

This video signal and the horizontal and vertical synchronization pulses are then time multiplexed with the telemetry data. The multiplexer and the other telecommunications equipment is described in Chapter 6. The multiplexed output signal then passes through the transmitter, diplexer and steerable antenna and is transmitted to the earth-based control center. Command signals and new landing point coordinates are transmitted up-link from earth and pass through the diplexer and receiver to the command decoder and then into the flight computer.

The on-off and heater commands go to the TV camera. The firing signal to jettison the TV mirror goes to the mirror mounting bolt. This block diagram does not show the required interface with the vehicle power system. Also, the antenna steering is shown as controlled by the automatic gain control which occurs when the antenna is locked-on signals from the Earth based station.

The earth-based portion of the control system is shown as a block diagram in Figure 3.4-2. The signal from the LLV is received at one of the NASA's three large S-band antenna stations. The Goldstone (GDS) Station is shown since the 210-ft antenna has the highest gain of any of the three S-band receiver sites and since the Goldstone-to-Houston microwave communications link has a shorter transmission time delay than the links from Madrid or Canberra-to-Houston which must include relaying through the Communications Satellite Network, COMSAT.

At Mission Control in the Manned Spacecraft Center at Houston, Texas, the received signal is demodulated in the receiver and goes from there to video tape for permanent mission record and to the mission control computer for separation of the telemetry and

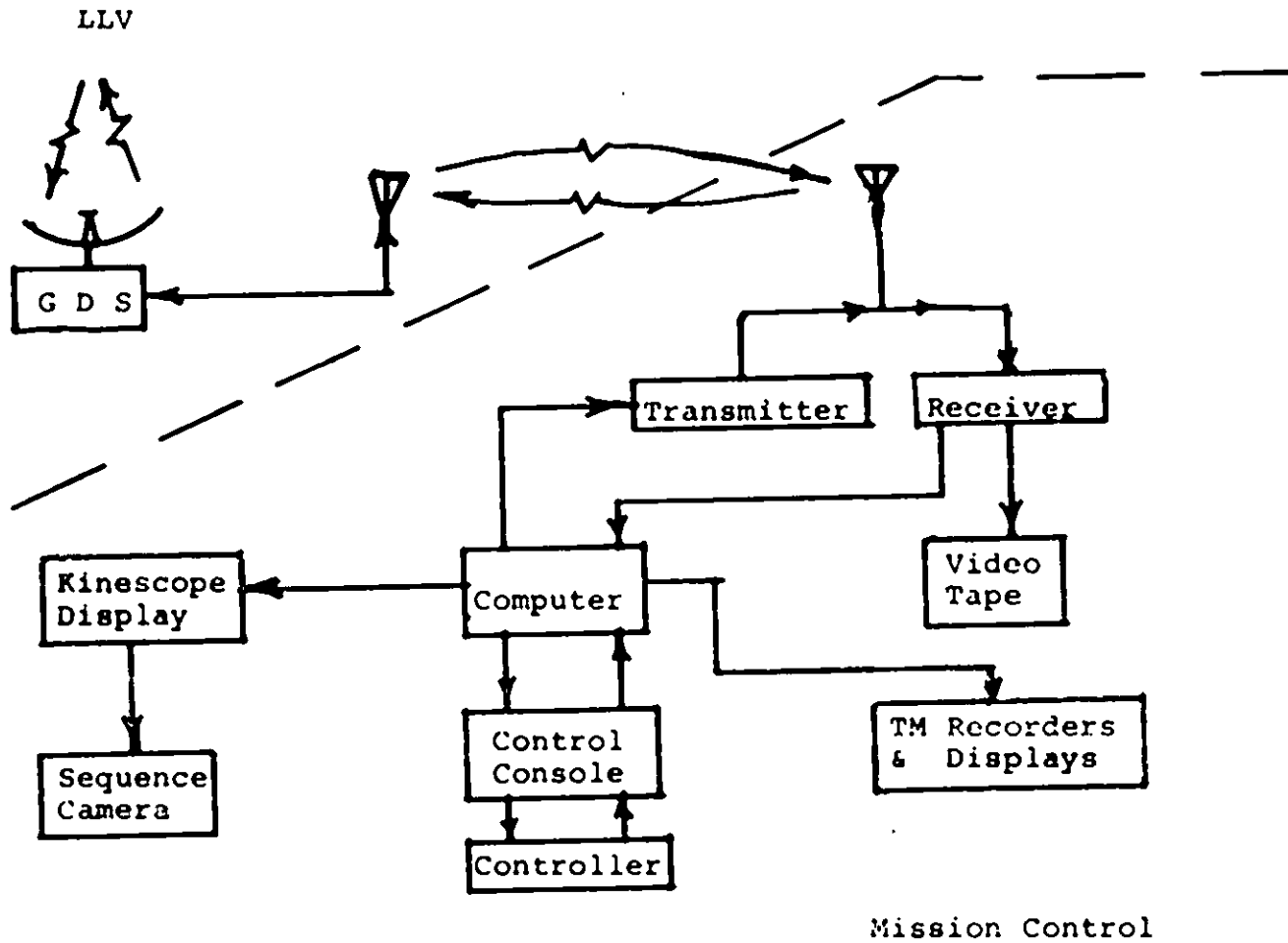


FIGURE 3.4-2

EARTH CONTROL SYSTEM

television signals. The telemetry data is both recorded and displayed for real-time interpretation. The television signal is sent to both a kinescope display where each frame is photographed by a sequence camera to provide a photographic record and to one or more control consoles. At the control consoles the relevant navigation and guidance telemetry signals and the video signals are displayed for real-time interpretation by one or more controllers.

The functions of the controllers during the terminal phase are similar to those for the pilots of the Lunar Module [11]. A partial listing of the controller activities is as follows:

1. Monitor the on-board guidance system performance.
2. Monitor descent engine ignition and engine gimbal alignments
3. Monitor propulsion quantities
4. Monitor programmed pitch attitude changes
5. Compare the range rate with the guidance boundaries at check times
6. Compare landmark locations with guidance boundaries at check time
7. Compare landing radar altitudes with guidance boundaries at check times.
8. Redesignate the trajectory to remain within guidance boundaries
9. Evaluate landing area for acceptance or rejection
10. Redesignate the landing area to avoid hazardous landing sites
11. Null all rates except descent for touchdown
12. Evaluate landing point for location of hazards
13. Roll the vehicle to avoid hazards at the landing point

Functions 4, 5, 6, and 8-13 are all performed in part of the basis of video information from the landing television system.

The planning of the mission includes the preparation of the nominal trajectory information, lunar maps and landing strategy necessary for the successful performance of these functions.

The redesignation functions can be performed by the technique suggested by Meissinger [3]. A cursor is moved by the controller to the desired landing point. The cursor location and the on-board predicted landing point and the present flight point are compared by a computer program. New guidance system target inputs are calculated and are transmitted to the G&N System on-board the vehicle, once an execute command is given.

Previous studies [3, 15] have shown the importance of stability considerations in earth-based closed-loop guidance with long time delays. Table 3.4-1 is an estimation of the total time delay for terminal phase guidance to the lunar surface

TABLE 3.4-1 LTVS DELAY TIME

Earth-to-moon transmission (Round Trip)	2.61 sec.
Earth station transmission time (MAI) or CNB)	0.3 sec.
Operator delay time [13]	1.7 sec.
Signal processing time	<u>0.1 sec.</u>
TOTAL TIME	6.7 sec.

The system for redesignation may be further stabilized by sufficient spacing between a fixed number of redesignation opportunities which are referred to as terminal course corrections to emphasize their relative correspondence to the mid-course corrections. By providing adequate spacing between the terminal course corrections the controller is prevented from repeating the command for a maneuver before it is completed. The number of terminal course corrections require for a given landing point accuracy will be dependent on the shape of each trajectory that is flown. A general detailed study of this dependency is strongly

recommended, and a detailed study for each mission is recommended as a task in the planning of each mission.

The number of controller activities, short duration of the mission terminal phase and time sharing of the activities prevent the functions of the controller being completed by one individual. The monitoring activities (1, 2, 3 and 4) are handled at a single controller station. The comparison, evaluation redesignation, null of rates and roll activities are sequential or closely enough related to be time shared by a controller with map matching assistance by a navigator. The tasks of the navigator are to select nominal trajectory overlays and match these map overlays with the video map from the LTVS. When the overlay and the map are aligned and at the same scale, the nominal trajectory display is projected at the controller's console as a superposed image on one of the video screens. The predicted updated position of the vehicle is also superposed on the same screen as a traveling point of light or as a line with a moving end. The updated position coordinates are calculated by the control computer as the time-varying solution of a smoothing updated trajectory equation.

The layouts and displays of the consoles, and the training of the control personnel are recommended as topics for further study. Each trajectory should be treated as a manned spacecraft trajectory and be fully planned and simulated.

The performance levels for controllers are similar to those required for Lunar Module pilots and the controllers could be an assignment of off-flying-status astronauts. The training and experience of the earth-based controller would be a preliminary step to the training of controllers to perform the same functions

from the lunar surface.

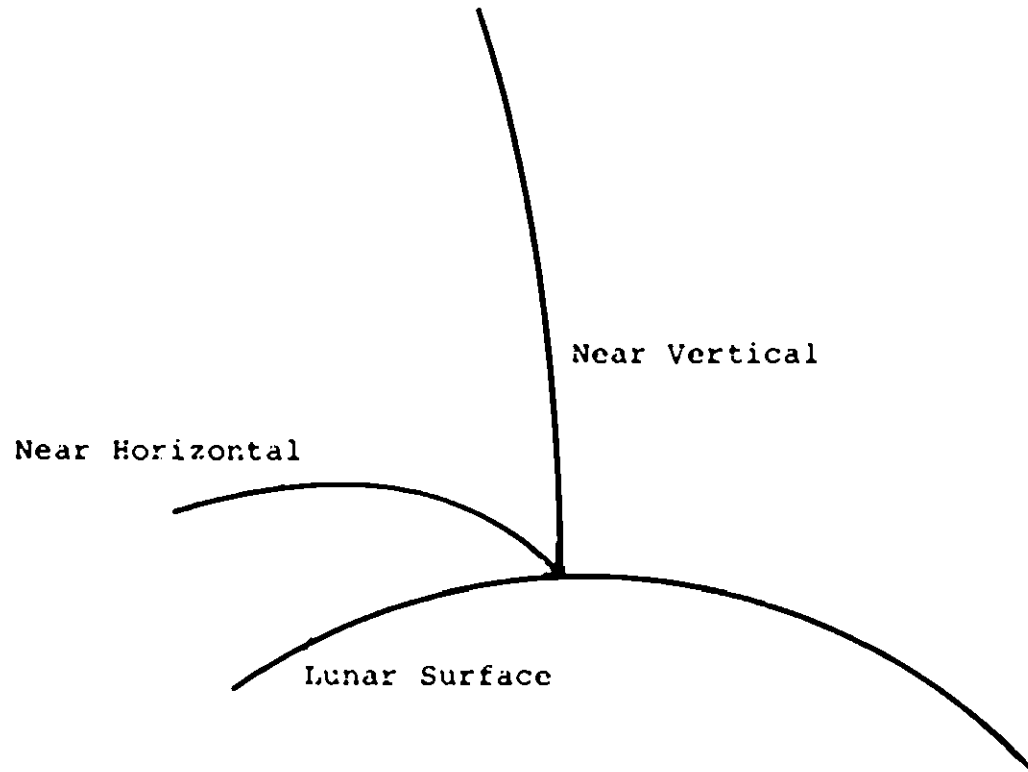
3.4.2 System Performance Parameters

The mission constraint of an LLV landing area location being anywhere on the near lunar surface leads to the requirement for a range of both near-vertical-and near-horizontal-approach trajectories. These two types of trajectories are illustrated in Figure 3.4-3. From considerations of approach navigation, the near-horizontal trajectory is the more severe as the landing area is either beyond the horizon at so low an angle that lineal distortion prevents landmark identification. The approach navigation is accomplished by sightings on landmarks near the vehicle but considerably uprange of the landing area and therefore have unknown map errors of position relative to ~~the~~ landing area. In the succeeding discussion the television system parameters are discussed in terms of the requirements for near-horizontal approach.

The TV system parameters to be specified from guidance requirements are:

1. TV camera field of view
2. Number of horizontal scan lines per TV frame
3. TV frame rate
4. Video frequency bandwidth

Of these parameters, the field-of-view (FOV) is most directly related to visibility requirements. In both the near-vertical and near-horizontal approach, the LTVS is used to evaluate the trajectory from landmark sightings and to evaluate the trajectory from the landmark sightings and to evaluate the landing area for landing hazards, craters, blocks and steep slopes. The TV camera lens FOV is specified from the requirements of scan area for approach



LLV LANDING TRAJECTORIES

FIGURE 3.4- 3

navigation and scan area for location a minimum-hazard landing point.

The scan area is determined from the geometry of the TV field-of-view. The field-of-view geometry can be determined from a consideration of the simpler geometry of a line-of-sight from the LLV to a land mark (LMK) on the lunar surface as shown in Figure 3.4-4 and 3.4-5.

The notation is forward surface range, R ; radius of the moon, r_m altitude, H ; slant range, s ; lunar angle, ϕ ; along-track line-of-sight angle with respect to the local vertical at the spacecraft, α ; elevation angle of the LLV with respect to the local horizontal at the LMK, θ ; cross-track line of sight angle, γ ; lateral surface range, W ; cross-track slant range, S_L ; cross-track lunar angle, ζ ; and cross-track LLV elevation angle ρ .

The relationships between the geometrical along-track parameters are:

$$\phi = \frac{R}{r_m} \quad (3.4-1)$$

$$\tan \alpha = \frac{\sin \phi}{\left(1 + \frac{H}{r_m}\right) - \cos \phi} \quad (3.4-2)$$

$$\frac{H}{r_m} = \frac{\sin(\phi + \alpha)}{\sin \alpha} - 1 \quad (3.4-3)$$

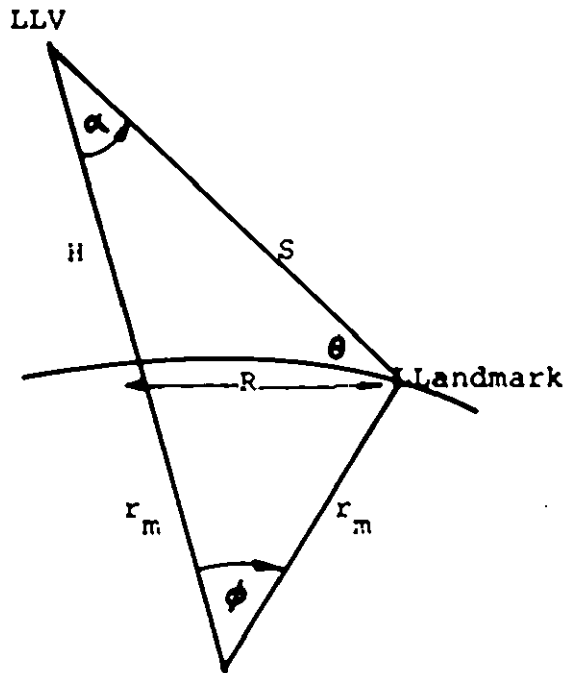
$$\frac{s}{r_m} = \frac{\sin \phi}{\sin \alpha} \quad (3.4-4)$$

and

$$\theta = \frac{\pi}{2} - \alpha - \phi \quad (3.4-5)$$

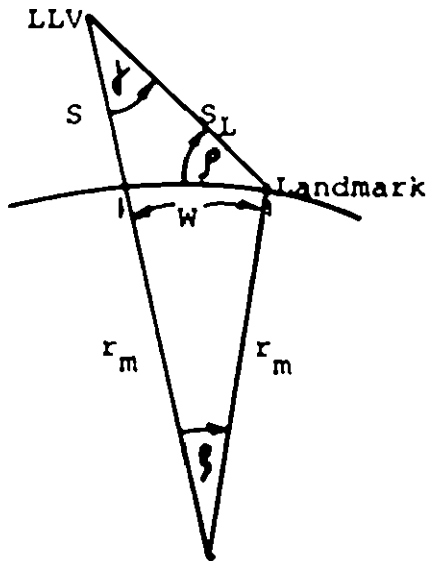
and for the cross-track parameters:

$$\zeta = \frac{W}{r_m} \quad (3.4-6)$$



LINE-OF-SIGHT GEOMETRY IN ALONG-TRACK (H-R) PLANE

FIGURE 3.4-4



LINE-OF-SIGHT GEOMETRY IN CROSS-TRACK (S-W) PLANE

FIGURE 3.4-5

$$\tan \gamma = \frac{\sin \zeta}{\left(1 + \frac{S}{r_m}\right) \cos \zeta} \quad (3.4-7)$$

$$\frac{S}{r_m} = \frac{\sin(\zeta + \gamma)}{\sin \gamma} - 1 \quad (3.4-8)$$

$$\frac{S_L}{r_m} = \frac{\sin \zeta}{\sin \gamma} \quad (3.4-9)$$

and

$$\rho = \frac{\pi}{2} - \gamma - \zeta \quad (3.4-10)$$

The relationships for Equations (3.1-11) in along-track parameters and the corresponding Equation (3.4-7) are plotted in Figure 3.1-7.

The slant range to the lunar surface is a maximum when the LLV elevation angle is zero. At this range the line-of-sight is to the lunar horizon, for either the along-track or the cross-track geometry. The lunar horizon line-of-sight geometry is shown in Figure 3.4-6. The relationships for a line-of-sight to the along-track horizon are:

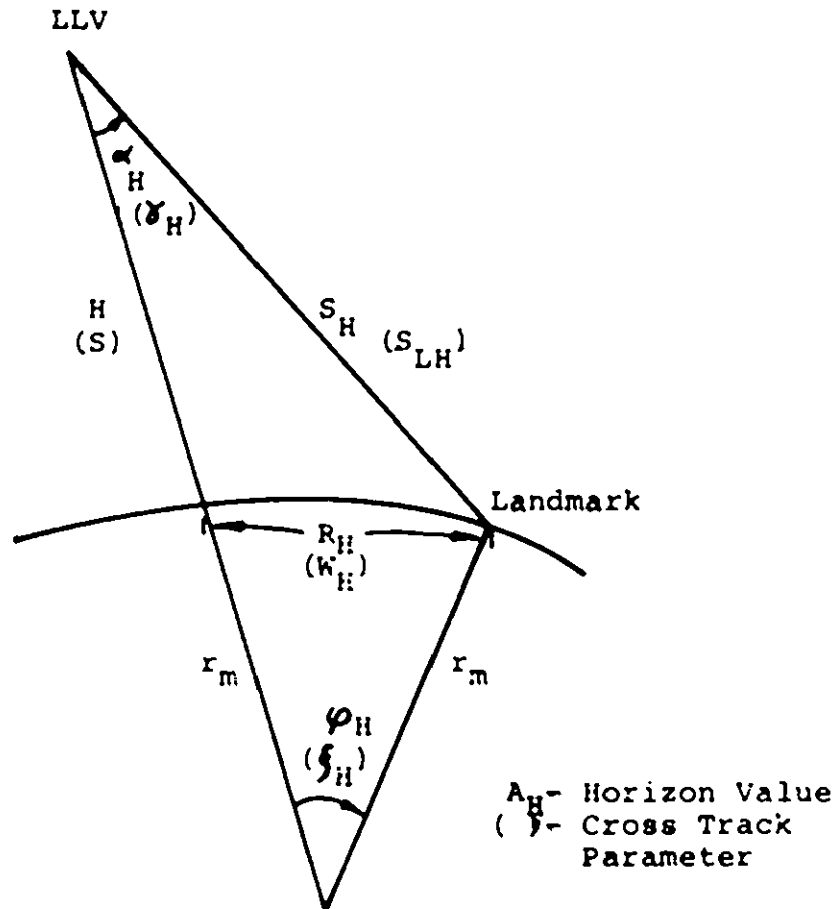
$$\phi_H = \cos^{-1} \left(\frac{1}{1 + \frac{H}{r_m}} \right) \quad (3.4-11)$$

$$\frac{S_h}{r_m} = \left(1 + \frac{H}{r_m} \right) \sin \phi_H \quad (3.4-12)$$

$$\alpha_H = \sin^{-1} \left(1 + \frac{H}{r_m} \right) \quad (3.4-13)$$

$$\theta_H = 0 \quad (3.4-14)$$

The corresponding cross-track relationships can be found by renaming the parameters.



LINE-OF-SIGHT GEOMETRY TO THE LUNAR HORIZON

FIGURE 3.4 -6

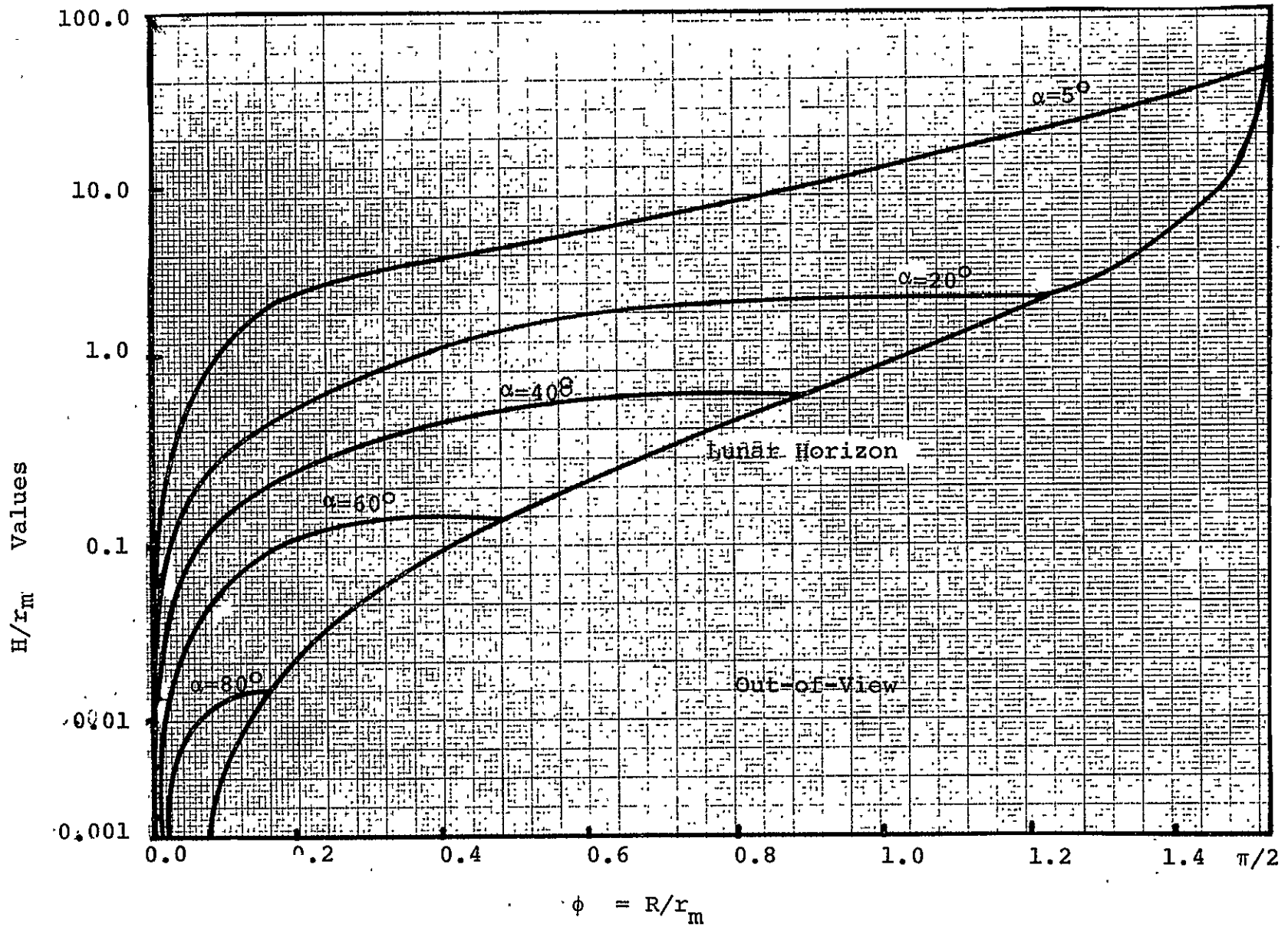


FIGURE 3.4-7 LINE-OF-SIGHT ANGLES

3.4.3 Effective Field-of-View

The effective field-of view for the TV camera is smaller than the lens field-of-view because of the non-circular format of the television field. As shown in Figure 3.4-8, a standard 4x3 rectangular format superscribed within the circular cross-section of the conical lens view field reduces the effective values, β and γ , for a lens FOV, Ψ , where:

$$\beta = \tan^{-1} (0.8 \tan \Psi) \quad (3.4-14)$$

and

$$\gamma = \tan^{-1} (0.6 \tan \Psi) \quad (3.4-15)$$

These relationships are plotted in Figure 3.4-9

In the LTVS, the larger angle, β , is oriented along-track to the trajectory and γ is oriented cross-track.

A camera lens system FOV can be selected for a required scan area at an altitude, H , and line of sight angle, α , by finding the effective FOV's, β and γ , from Figure 3.4-7 by entering at normalized altitude $\frac{H}{r_m}$ and finding dimensionless surface ranges ϕ_1 and ϕ_2 for $\alpha + \frac{\beta}{2}$, and $\alpha - \frac{\beta}{2}$ respectively, and ζ , for an $\alpha = \gamma$. The dimensionless along-track range is then $\phi_1 - \phi_2$ and the dimensionless cross-track range is 2ζ .

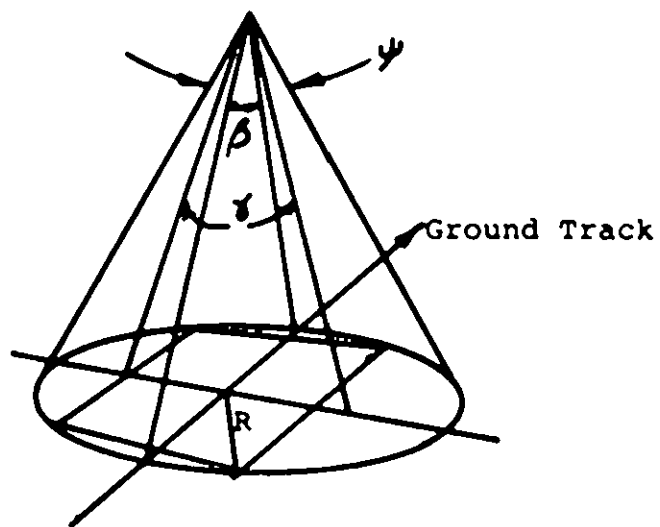
The corresponding scan area is then approximately equal to the following.

$$A = 2.0RW \quad (3.4-16)$$

and

$$A = 2(r_m)^2 (\phi_1 - \phi_2)W \quad (3.4-17)$$

Previous studies for NASA [7,8,9,20] show that the scan area required for recognizing landmarks patterns is dependent on the vehicle altitude, phase angle of the line-of-sight with respect to the sun



GEOMETRY OF EFFECTIVE FIELDS-OF-VIEW

FIGURE 3.4-8

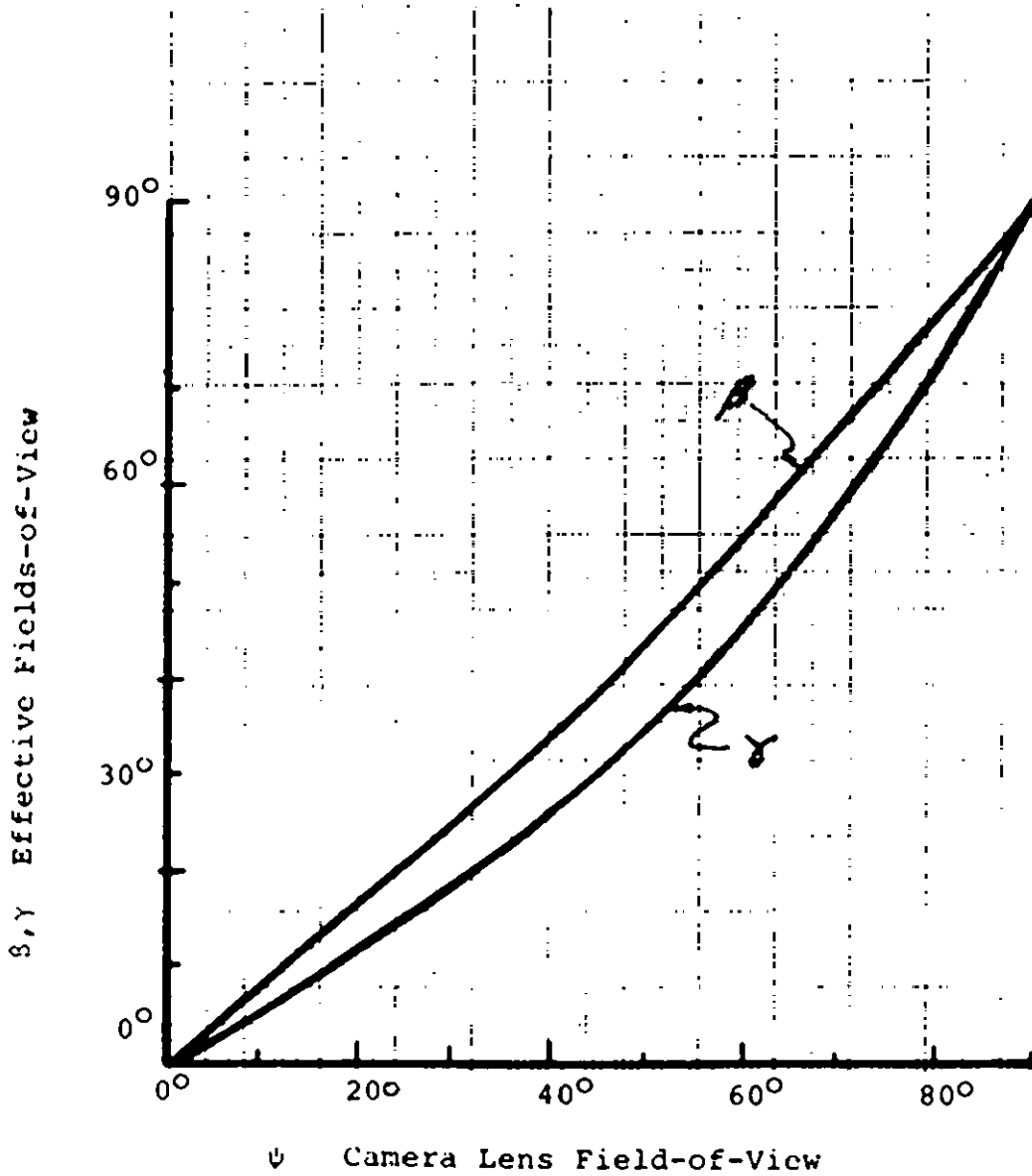


FIGURE 3.4-9 EFFECTIVE FIELDS-OF-VIEW

line to the landmark, sun elevation angle, and the slant range to the object as well as the camera resolution for each scan line. The required scan areas are determined from the requirements for approach navigation and for avoiding hazards in the landing area. The scan area required for finding in the field-of-view at least on hazard-free landing site in the lunar rough highlands is determined from Figure 9.6-2.

3.4.4 Resolution

The vertical resolution of the TV camera system is estimated by dividing the effective along track field-of-view, in radians, by the number of horizontal scan lines which result in the angle subtended by each scan line. This value is then degraded by multiplying by 0.7, which is commonly accepted value [21] for the ratio of the number of active lines in a television format to the total number of horizontal lines. Finally, the resulting values is multiplying by the number of lines required by the television viewer to detect and recognize an object. A commonly accepted value is 3 lines [21] in the view region of sharpest focus of the viewers. The distance relationship of the practical resolution of the TV system bases on the above consideration is then

$$\frac{\Delta R}{S} = 2.10 \frac{\beta (\text{rad})}{N_L} \quad (3.4-18)$$

where

ΔR = minimum resolved distance on the lunar surface

S = surface slant range

β = effective along-track field of view

N_L = number of horizontal scan lines per television frame

The horizontal resolution is limited by the response rate

of the television scan to changes in scene contrast between two adjacent points in the scene. The horizontal resolution is also constrained by the available bandwidth of the associated communications system as shown in the approximate Equation 3.4-18 [17],

$$f = \frac{a N^2}{A} P \quad (3.4-19)$$

where f is the bandwidth frequency, P is the number of frames per second, N is the number of horizontal lines per frame and (aN) is the equivalent number of horizontal lines for a determined horizontal resolution. The frame rate, P , that is required for the LTVS depends on the relative motion allowable between frames, the amount of video map information required for evaluation of the trajectory, permissible additional delay time, compatibility with commercial television systems so that scan conversion is not required, and as is shown in Equation 3.4-27, the frequency bandwidth of the associated telecommunications equipment. The selection of the Landing Television System hardware is discussed in Section 6.4

3.4.5 LTVS Performance

The use of a landing television system is an addition to present guidance and navigation strategies for lunar landings. Its inclusion in the LLV design is justified on the basis of increased mission effectiveness. The effectiveness measure, E , for the LLV design is the landed payload, W_L multiplied by the probability, P_s , of a successful mission. P_s is the product of the probabilities of a sequence of n successful events as follows:

$$E = W_L P_s \quad (3.4-20)$$

$$E = W_L (P_1 P_2 \dots P_{n-3} P_{n-2} P_{n-1} P_n) \quad (3.4-21)$$

where P_1 is the probability of a successful launch, P_2 is the probability of a successful trans-lunar injection, P_{n-3} is the probability of a successful last mid-course correction, P_{n-2} the probability of terminal descent to the selected landing area, P_{n-1} , the probability of a soft landing; and P_n the probability of successful post-landing operation. A decrease in the maximum possible delivered payload is a penalty associated with the addition of the LTVS to the vehicle. Associated benefits are the increases in the probability, P_{n-2} , of landing in the desired area and probability, P_{n-1} , of a successful soft landing.

The change in the effectiveness is shown in Equation (3.4-22).

$$dE = \left(\frac{\partial E}{\partial W_L} \right) dW_L + \left(\frac{\partial E}{\partial P_{n-2}} \right) dP_{n-2} + \left(\frac{\partial E}{\partial P_{n-1}} \right) dP_{n-1} \quad (3.4-21)$$

The relative increase in effectiveness is

$$\frac{dE}{E} = \frac{dW_L}{W_L} + \frac{dP_{n-2}}{P_{n-2}} + \frac{dP_{n-1}}{P_{n-1}} \quad (3.4-22)$$

If the change in effectiveness is positive, the system should be included; if negative, the LTVS should be deleted.

3.4.6 Recommended Studies

Continuation studies should be made of the following:

1. Terminal course corrections required for near-vertical and near-horizontal trajectories.
2. Landing area viewing time for near-vertical and near-horizontal trajectories.
3. Vehicle redesignation capabilities for open-loop landing systems with long time delays.
4. Vehicle redesignation capabilities with multiple full throttle engine burns.

REFERENCES

1. Surveyor Final Engineering Report, Hughes Aircraft Co., Vol II, 1968.
2. T. Y. Feng, C. A. Wasynczuk, "Terminal Guidance for Soft and Accurate Lunar Landing for Unmanned Spacecraft", J. Spacecraft 5, 644, 1968.
3. H. F. Meissinger, "Lunar Landing by Command Guidance in the Presence of Transmission Time-Delay", Proc. of AIAA Conference on Guidance and Control, Aug 12-14, 1963, Mass. Institute of Technology, Cambridge, Mass.
4. R. C. Duncan, "Guidance and Control for Atmospheric Entry" U.C.L.A. short course notes on Re-entry and Planetary Entry, Physics and Technology, March 1966.
5. Apollo IV Guidance and Navigation Error Analysis, TRW Systems Group Report, Feb. 1968.
6. J. J. Ribarich, "Surveyor Spacecraft Landing Accuracy", J. Spacecraft 5, 768, 1968.
7. Apollo Lunar Landing Mission Symposium, June 25-27, 1966, Manned Spacecraft Center, Houston, Tex.
8. F. H. Martin, R. H. Battin, "Computer Controlled Steering of the Apollo Spacecraft," AIAA Guidance, Control and Flight Dynamics Conference, Aug 14-16, 1967, Huntsville, Alabama.
9. Apollo Operations Handbook Lunar Module, Grumman Aircraft Engineering Corp, Beth-page, N. Y., 1968.
10. J. D. Kraft, F. Santora, A. Jazwinski, F. Martikan, and R. Salinger, "Descent to and Ascent from the Lunar Surface", Lunar Flight Handbook NASA SP-34, Part 2 (1963) p VII - 21.
11. R. K. Cheng, "Lunar Terminal Guidance", Lunar Missions and Exploration, C. T. Leondes, R. W. Vance, Ed., John Wiley (1964), p 348.
12. J. N. Sivo, C. E. Campbell, V. Hamza, "Analysis of Close Lunar Translation Techniques", NASA TR-R-126 (1962).
13. V. K. Isaev, "L. S. Pontryagin's Maximum Principle and Optimal Programming of Rocket Thrust", Automat. Telemekh. 22 No. 8 (Aug. 1961) p 986-1001.
14. D. B. Cheatham and F. V. Bennett, "Apollo Lunar Module Landing Strategy", Apollo Lunar Landing Mission Symposium, June 25-27, 1966, Manned Spacecraft Center, Houston, Texas, NASA TMX-58006, pp. 175-240.

15. W. A. Finley, "A Technique for Lunar Landing Site Selection by Earth-Based Control", Space Technology Laboratories, Inc. 9350, 2-54, January 1963.
16. S. L. Dickerson and A. N. Paul, "Man-Machine, System Design", Paper presented at AIEE National Conference, May 16, 1968. Houston, Texas.
17. D. C. Swanan, "Section IV. LM Landing", Study Report, Apollo Applications Program, Lunar Surface Mission Planning, Volume 2, November 1, 1967, Bell Telephone Laboratories.
18. A. V. Bernard, Jr., "Landing Site Selection Criteria", Apollo Lunar Landing Mission Symposium, June 25-27, 1966, NASA TM X-58006.
19. G. T. Keene, Final Report, Lunar Photo Study, Contract NASA 3826, Eastman Kodak Company, Rochester, N. Y., 1 October 1965.
20. K. Ziedman, Lunar Landmark Visibility Study, TRW Systems Memorandum (69) 7246.4-36, July 28, 1969.
21. D. G. Fink, Principles of Television Engineering, 1st Edition, McGraw-Hill Book Company, Inc., New York, 1940.

CHAPTER IV

PROPULSION

Angelo Perna 4.1
Frank Hendel 4.2-4.7

4.1 Propulsion Requirements

The following section contains the analysis of the mission requirements for the LLV study as they relate to the "on board" propulsion system. The mission requirements were defined to meet the below-listed operational objectives:

- (1) High Energy Mission ($V_{\infty} = 4500$ fps; $h_p = -900$ nm)
- (2) Midcourse Correction: $\Delta V = 100$ fps
- (3) Site Redesignation: $\Delta V = 150$ fps
- (4) Minimum Hover Time @ 100 ft: 20 sec
- (5) Hop Possibility After Landing
- (6) ΔV Budget to Include 1 1/2% FPR

Based on data (See Figure 4.1-1) obtained from NASA consultants [1] a ΔV budget was prepared for the mission and is presented in Table 4.1-1. All propulsion systems investigated for use on the LLV were compared based on this ΔV budget.

In order to facilitate engineering analysis, parametric studies were undertaken to determine the effect of performance variables of individual propulsion subsystems on propellant requirements for a given mission objective. These studies are presented in graphical form in the pertinent sections.

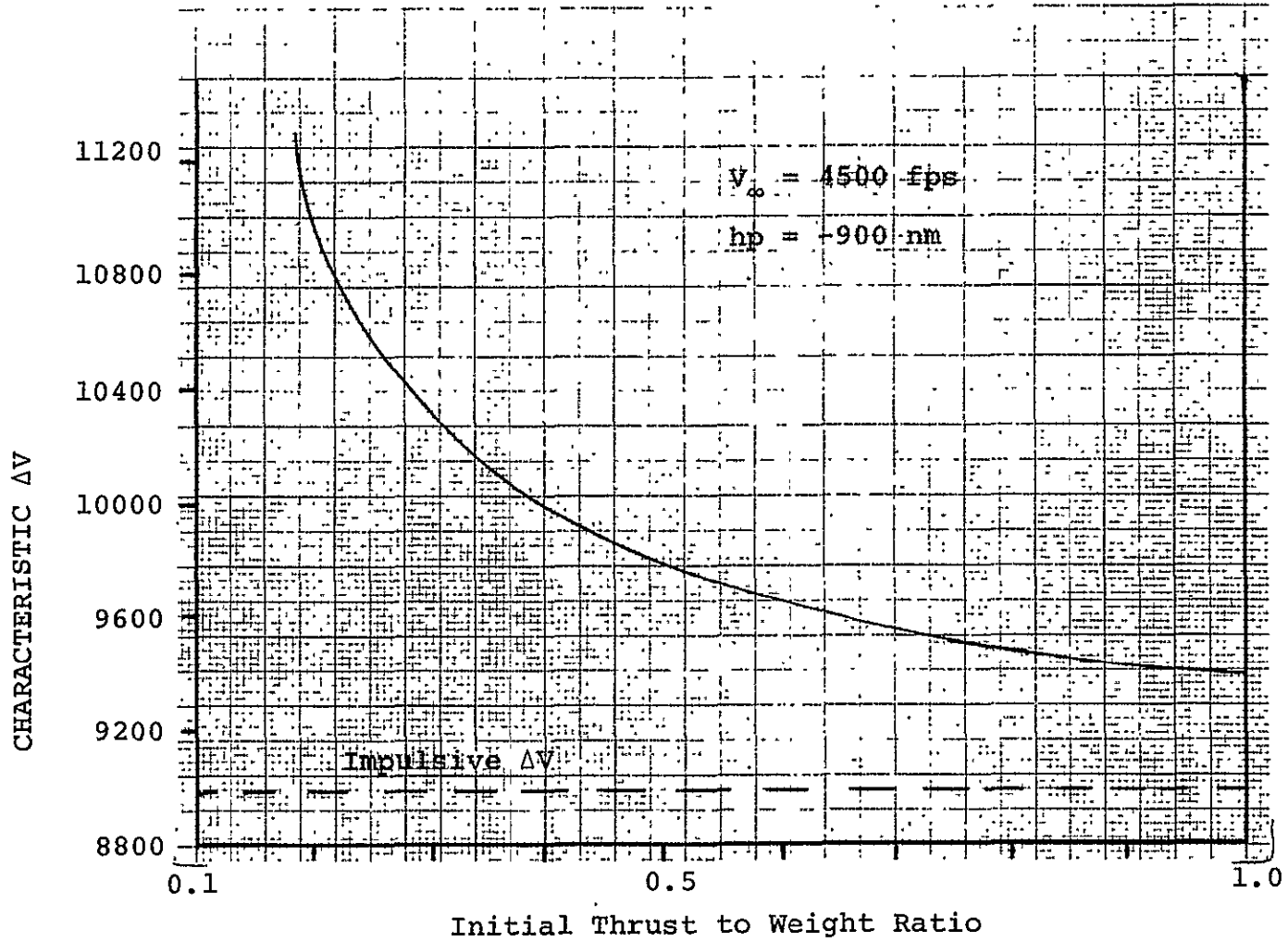


FIGURE 4.1-1 CHARACTERISTIC ΔV REQUIREMENTS vs INITIAL THRUST TO WEIGHT RATIO FOR HIGH ENERGY MISSION

Midcourse Correction
AV = 100 fps

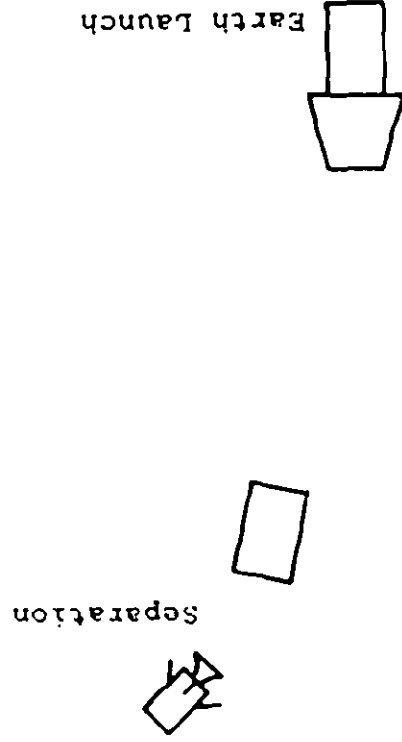


FIGURE 4.1-2 PICTORIAL REPRESENTATION OF TV AV MISSION REQUIREMENTS

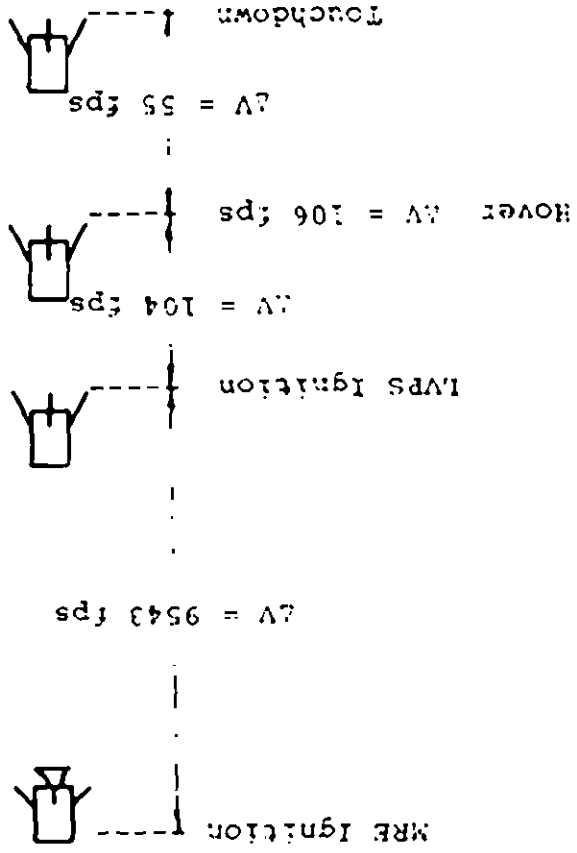


TABLE 4.1-1 PROPULSION SYSTEM ΔV REQUIREMENTS
FOR HIGH ENERGY MISSION

Propulsion Maneuver	Propulsion System	Reqd.	ΔV FPR****	Total
Midcourse Correction	RCS*	100.00	1.50	101.50
Retro Phase	MRE**	9392.75	143.00	9535.75
Site Redesignation	MRE	150.00	2.25	152.25
Terminal LVPS				
Initiation to Hover	LVPS***	104.36	1.57	105.93
Hover	LVPS	106.00	2.00	108.00
Hover to Touchdown	LVPS	55.00	1.00	56.00

* Reaction Control System

** Main Retro Engine

*** Liquid Vernier Propulsion System

**** Flight Performance Reserves

4.1.1 Midcourse Correction

The first major maneuver to be accomplished by a propulsion subsystem after separation from the launch vehicle is to correct for any error in the trajectory. The maximum ΔV budgeted for this operation is 101.5 fps. Although this maneuver can theoretically be performed by any of the propulsion subsystems (See Figure 4.1-3) the propulsion group recommends and has designed for the Reaction Control System (RCS) to accomplish this correction. The maneuver requires more propellant with the RCS system than the Liquid Vernier Propulsion System (LVPS) or the Main Retro Engine (MRE). The finer control and alleviation of plume problems more than compensates for the extra propellant (approximately 5 lbs) required. In addition the time available for the budgeted ΔV for midcourse correction (See Table 4.1-2) is maximized.

The amount of on board propellant for this task was calculated to be 133 lbs. This amount includes 3 per cent residuals.

TABLE 4.1-2 MAXIMUM BURN TIME FOR MIDCOURSE CORRECTION

System	F lbs	M lbs	t sec
RCS			
Two R-1E Engines	44	12000	840.00
LVPS			
Two R-4D Engines	200	12000	186.50
MRE			
RL10A3-3	15000	12000	2.70
Throttlicable	5000	12000	7.44

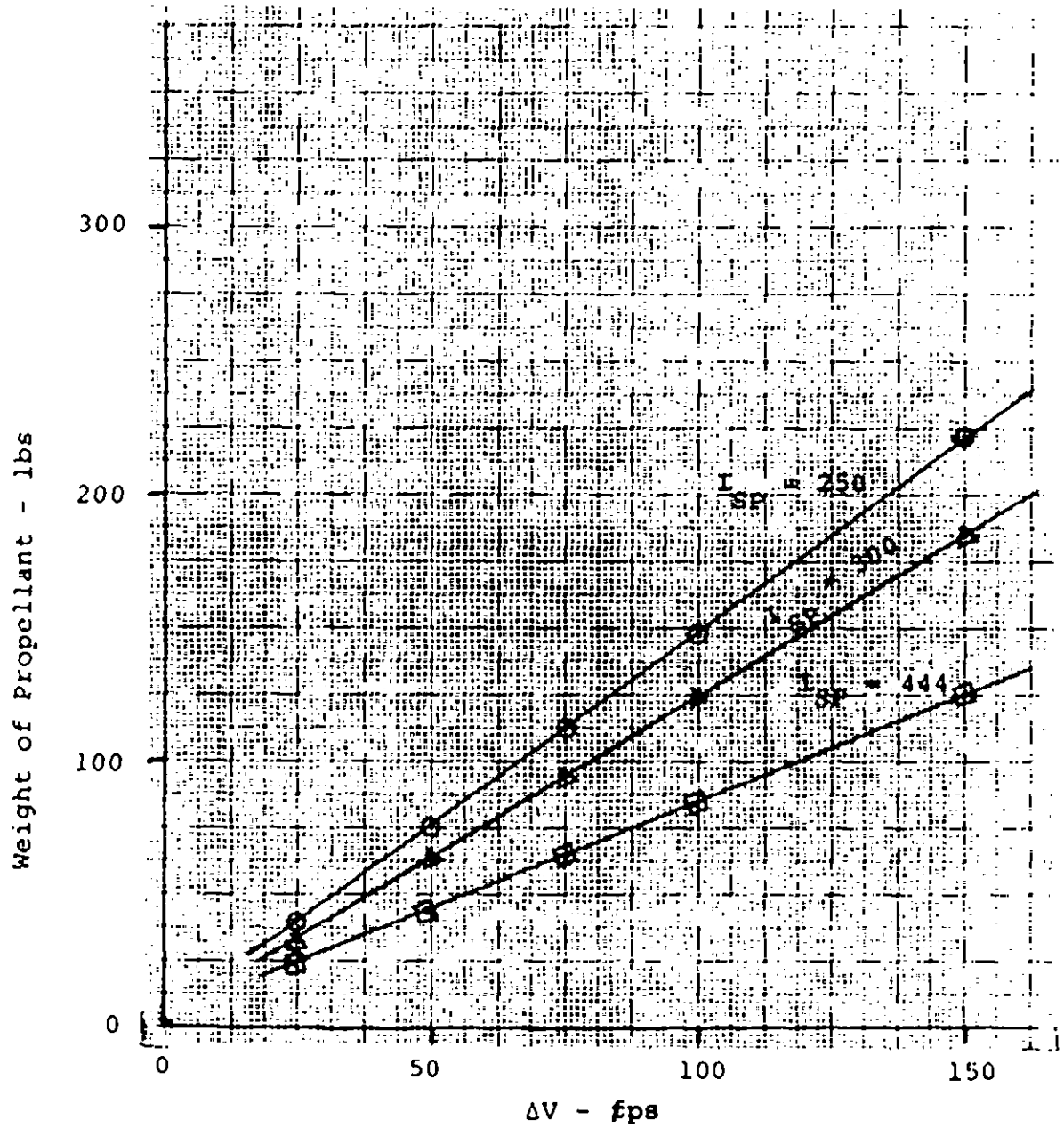


FIGURE 4.1-3 EFFECT OF ΔV REQUIREMENT FOR MIDCOURSE
VS PROPELLANT REQUIREMENT

4.1.2 Main Retro Engine Burn Phase

During the retro phase the majority of the ΔV budget is used. For the high energy mission the total ΔV requirement in the MRE is 9688 fps with 152.25 fps of the ΔV requirement being for site redesignation.

For the above ΔV value the burnout velocity of 99 fps at 200 feet altitude is achievable. This burnout point maximizes the use of the MRE while minimizing the requirements on the LVPS.

The site redesignation budget is for correcting last minute trajectory errors as well as for any gross changes in the touch-down landing site.

Parametric studies based on operating characteristics of various engines were developed for the previously listed MRE mission profile and the results are presented as a series of graphs and tables on the following pages.

Analysis of the results indicate a throttleable (3/1 ratio) RL10A3-3 is the best candidate engine for the retro phase of the mission. Although the RL10A3-3 is presently a qualified fixed thrust (15000 lb) engine, it has been flight certified for the throttleable condition. The upgrading of the engine to flight qualified status should cost approximately five million dollars which can be justified in terms of increased payload and mission flexibility. An additional increase in payload can be realized by extending the engine nozzle 19 inches at a cost of 35 pounds which increases the I_{sp} to 449 and results in a propellant savings of 0.5 per cent.

It should be pointed out that since the recommended engine

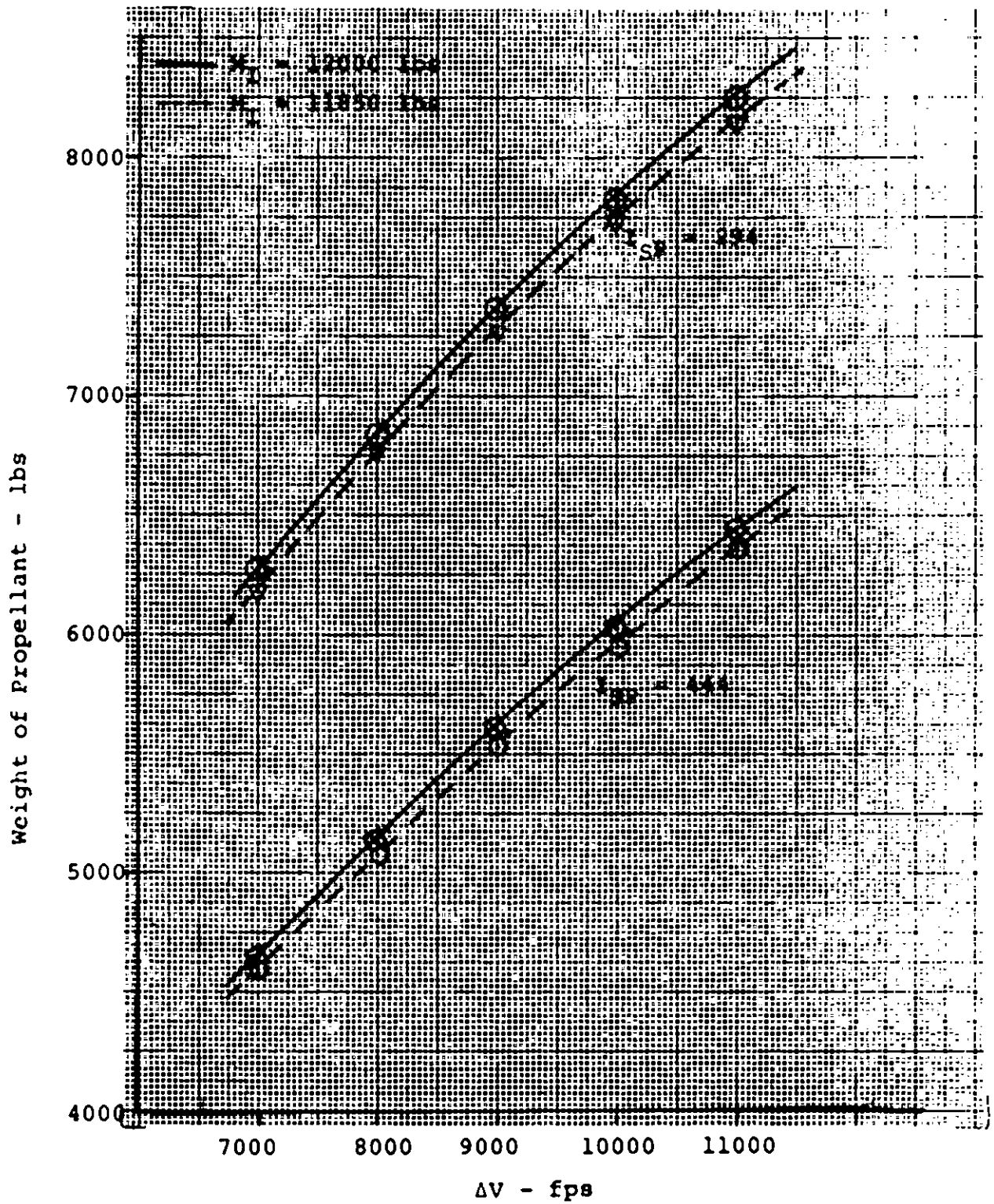


FIGURE 4.1-4 ΔV VS WEIGHT OF PROPELLANT REQUIRED

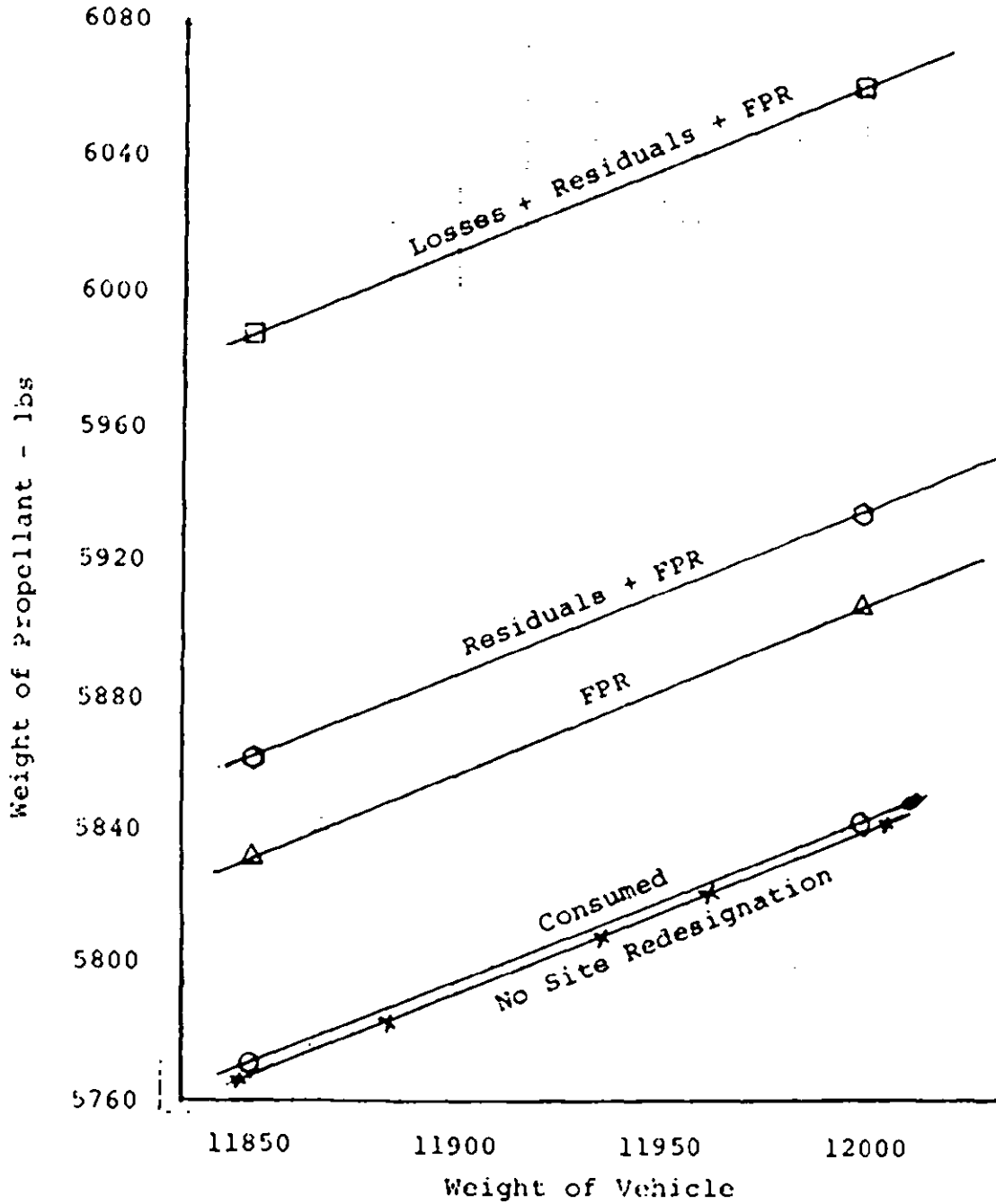


FIGURE 4.1-5 PROPELLANT REQUIREMENTS FOR HIGH ENERGY MISSION WITH RL10 THROTTLEABLE ENGINE.

burns a mixture of cryogenics, liquid hydrogen and oxygen, propellant penalties are involved. These weight penalties are as follows:

(1) Insulation of Tanks [2]

$$H_2 = 71 \text{ lbs}$$

$$O_2 = 12.5 \text{ lbs/tank}$$

(2) Transit Boil off [2]*

$$H_2 = 35 \text{ lbs}$$

$$O_2 = 35 \text{ lbs}$$

(3) Engine Burn losses

$$H_2 = 30 \text{ lbs}$$

$$O_2 = 16 \text{ lbs}$$

(4) Additional Volume required for Above

$$H_2 \quad \text{Boil off} \quad 8.31 \text{ ft}^3$$

$$\quad \quad \text{Engine loss} \quad 6.83 \text{ ft}^3$$

$$O_2 \quad \text{Boil off} \quad 0.51 \text{ ft}^3$$

$$\quad \quad \text{Engine loss} \quad 0.24 \text{ ft}^3$$

(5) Additional Tank Weight [3]

$$H_2 = 10 \text{ lbs}$$

$$O_2 = 0.5 \text{ lbs/tank}$$

Improvements in insulation and engine operation characteristics can reduce these losses significantly, resulting in larger payloads.

The total weight of propellant for this phase of the mission is 5861 pounds, which includes 0.5 per cent residuals.

* Based on a 60 hour mission. For a 120 hour mission the transit boil off losses double and items 4 and 5 should be scaled up appropriately.

4.1.3 LVPS Terminal Phase Initiation

After MRE burnout at a velocity of 99 fps and an altitude of 200ftthe LVPS R-4D engines remove any ΔV remaining. A reduction in weight of approximately 900 pounds is achieved at LVPS ignition by dropping the MRE stage with associated tanks and support structure. This operation reduces the propellant requirements by reducing the weight of the vehicle by about 16 per cent. The ΔV required prior to hover is 106 fps based on a hover altitude of 100 ft. Results of studies based on engine and vehicle parameters are presented in Figure 4.1-6 to Figure 4.1-12. Analysis of the results indicate a propellant requirement for this mission task of 60 pounds with 3 per cent residuals.

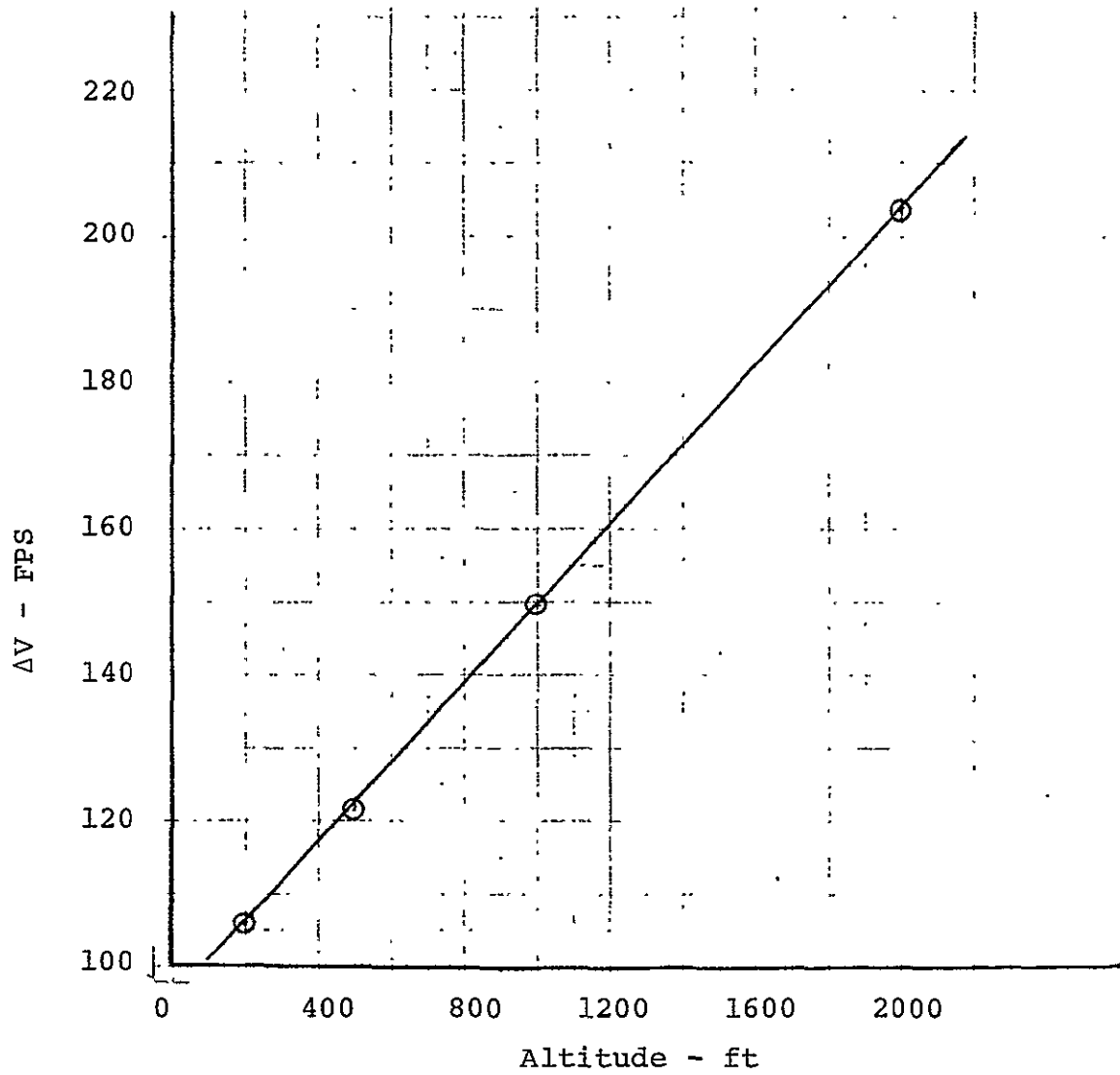


FIGURE 4.1-6 ΔV VS ALTITUDE FOR LVPS IGNITION FOR
HOVER AT 100 FT

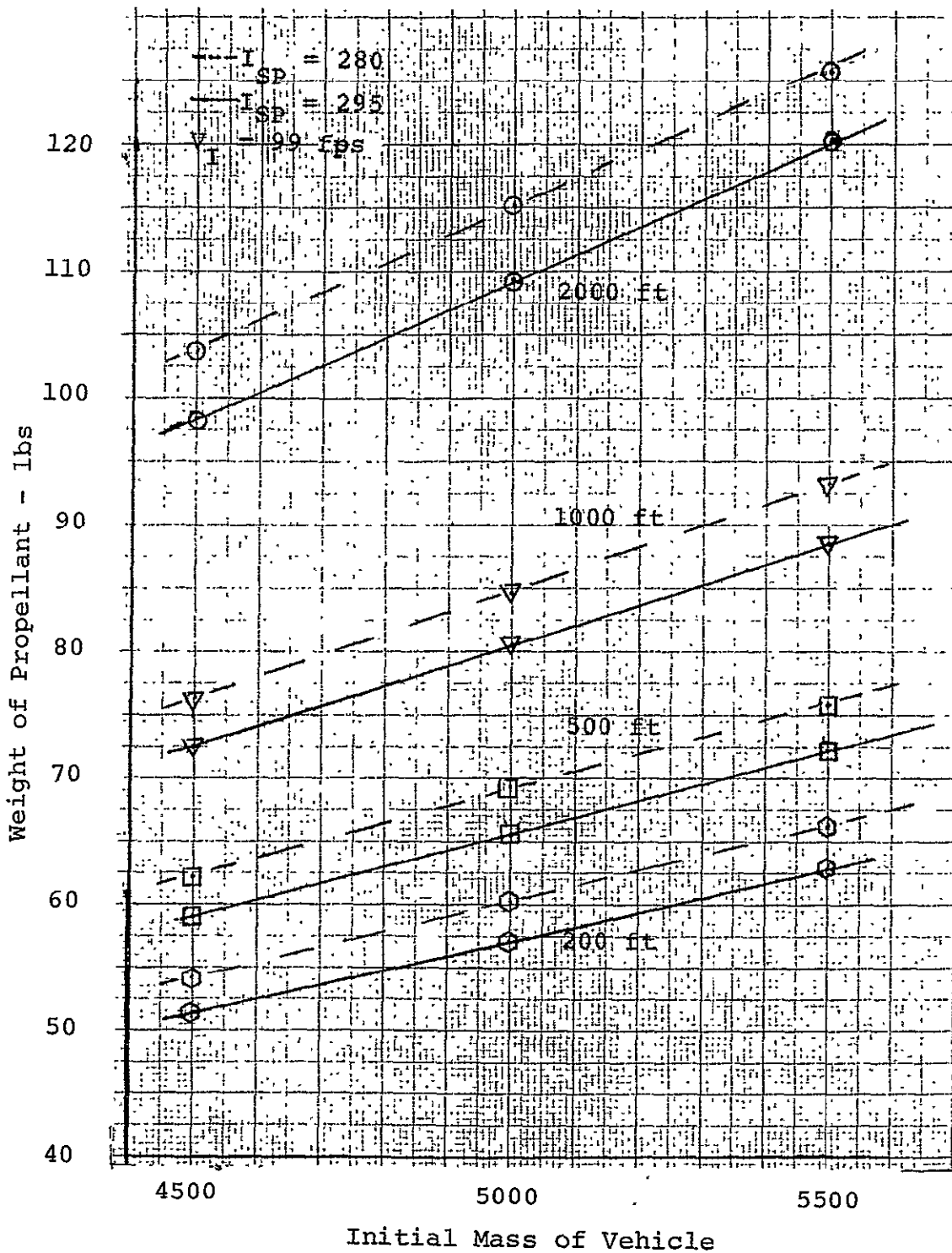


FIGURE 4.1-7 EFFECT OF ALTITUDE ON LVPS PROPELLANT REQUIREMENTS FOR HOVER AT 100 FT

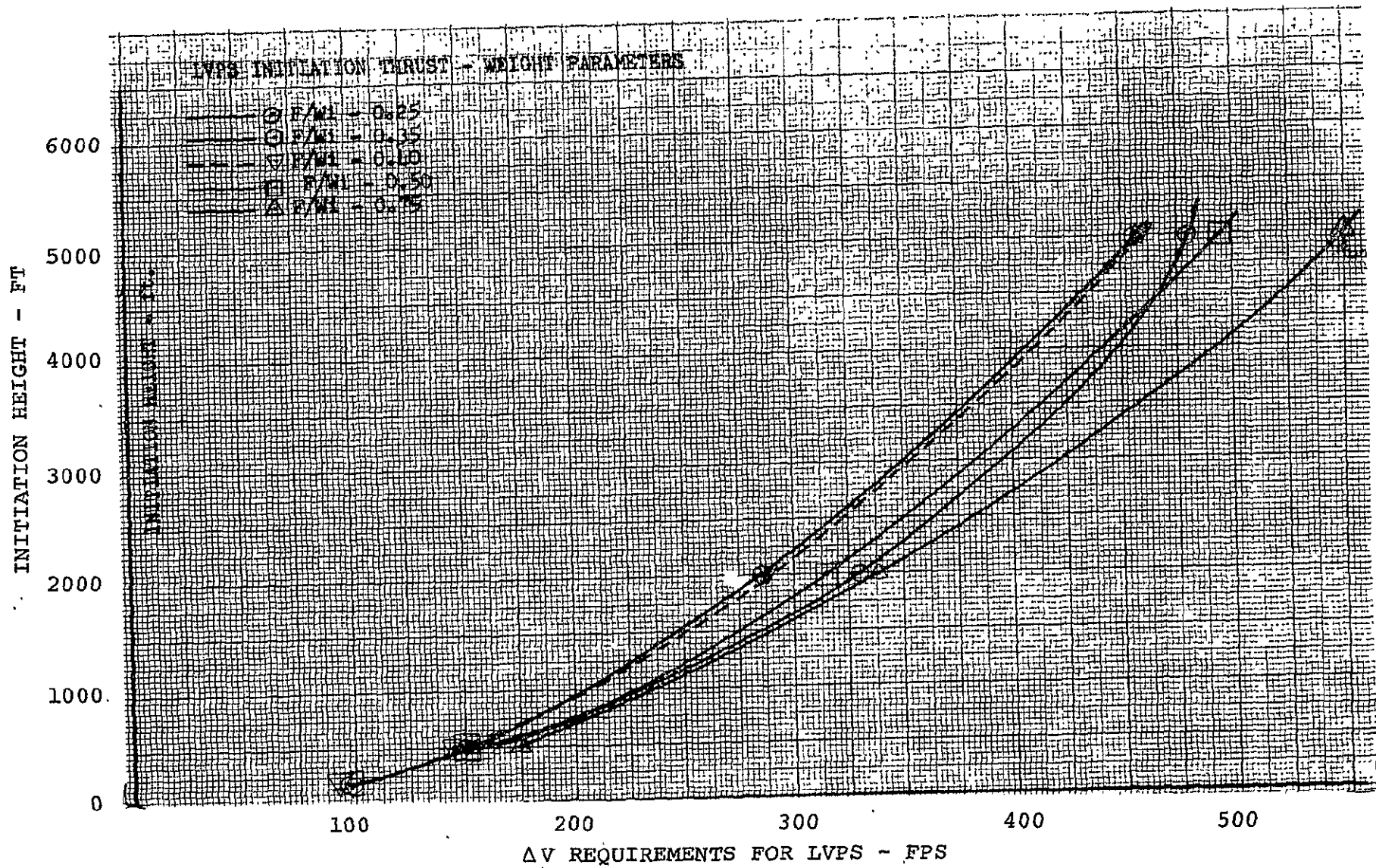


FIGURE 4.1-8 ΔV vs LVPS INITIATION ALTITUDE FOR VARIOUS THRUST TO INITIAL WEIGHT RATIOS

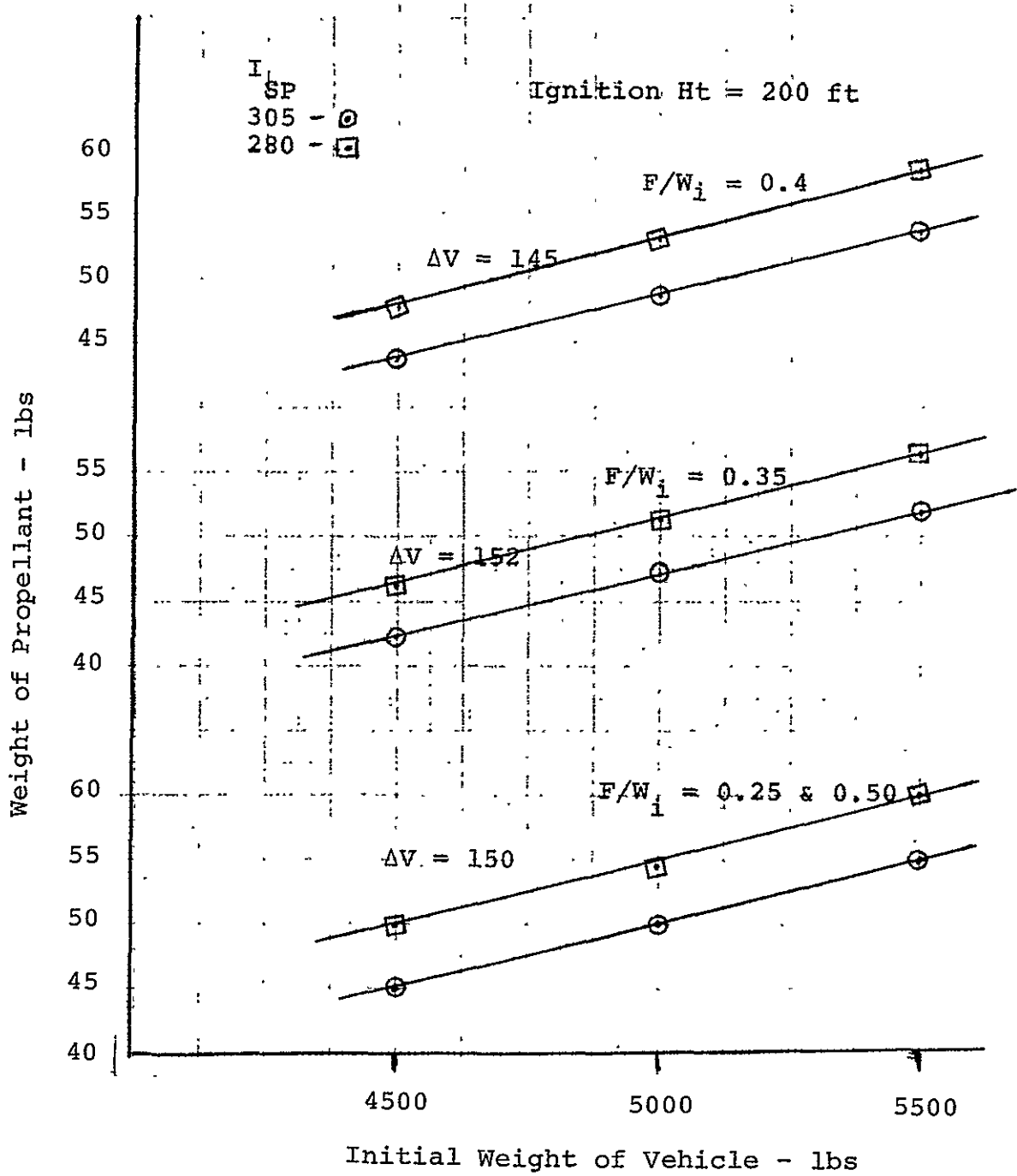


FIGURE 4.1-9 EFFECT OF TARGET VELOCITY ON PROPELLANT REQUIREMENTS FOR LVPS

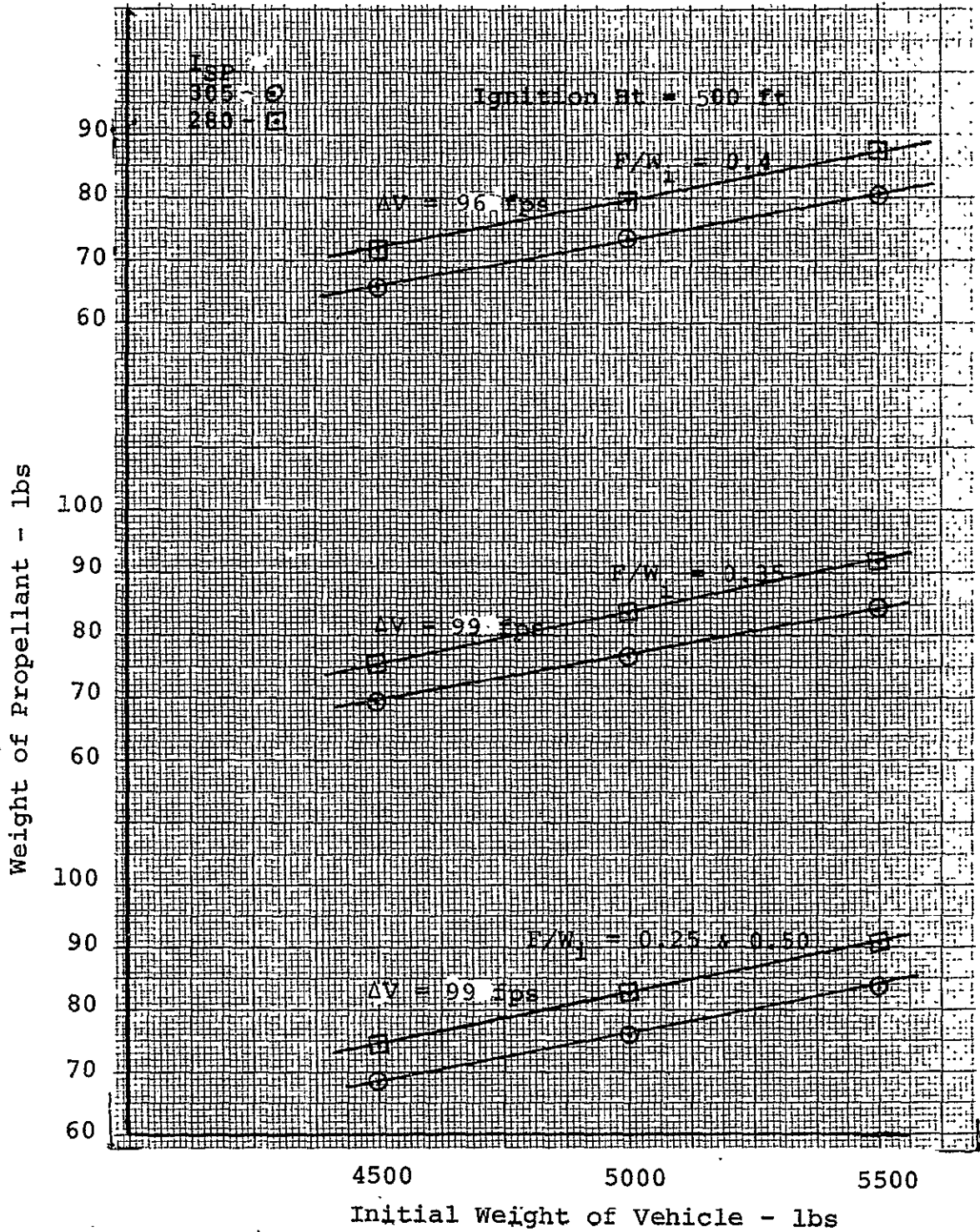


FIGURE 4.1-10 EFFECT OF TARGET VELOCITY ON PROPELLANT REQUIREMENTS FOR LVPS

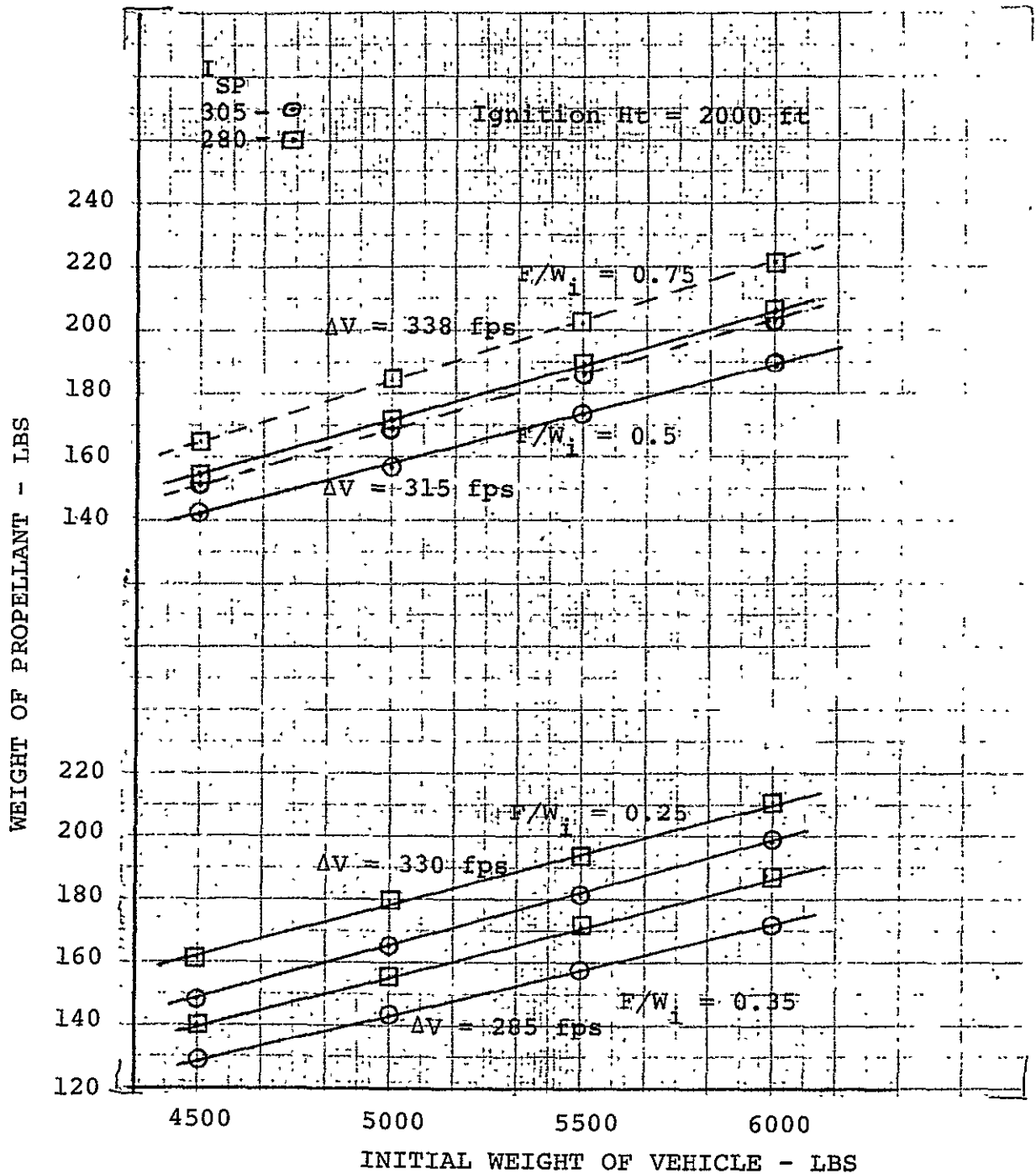


FIGURE 4.1-11 EFFECT OF TARGET VELOCITY ON PROPELLANT WEIGHT FOR LVPS

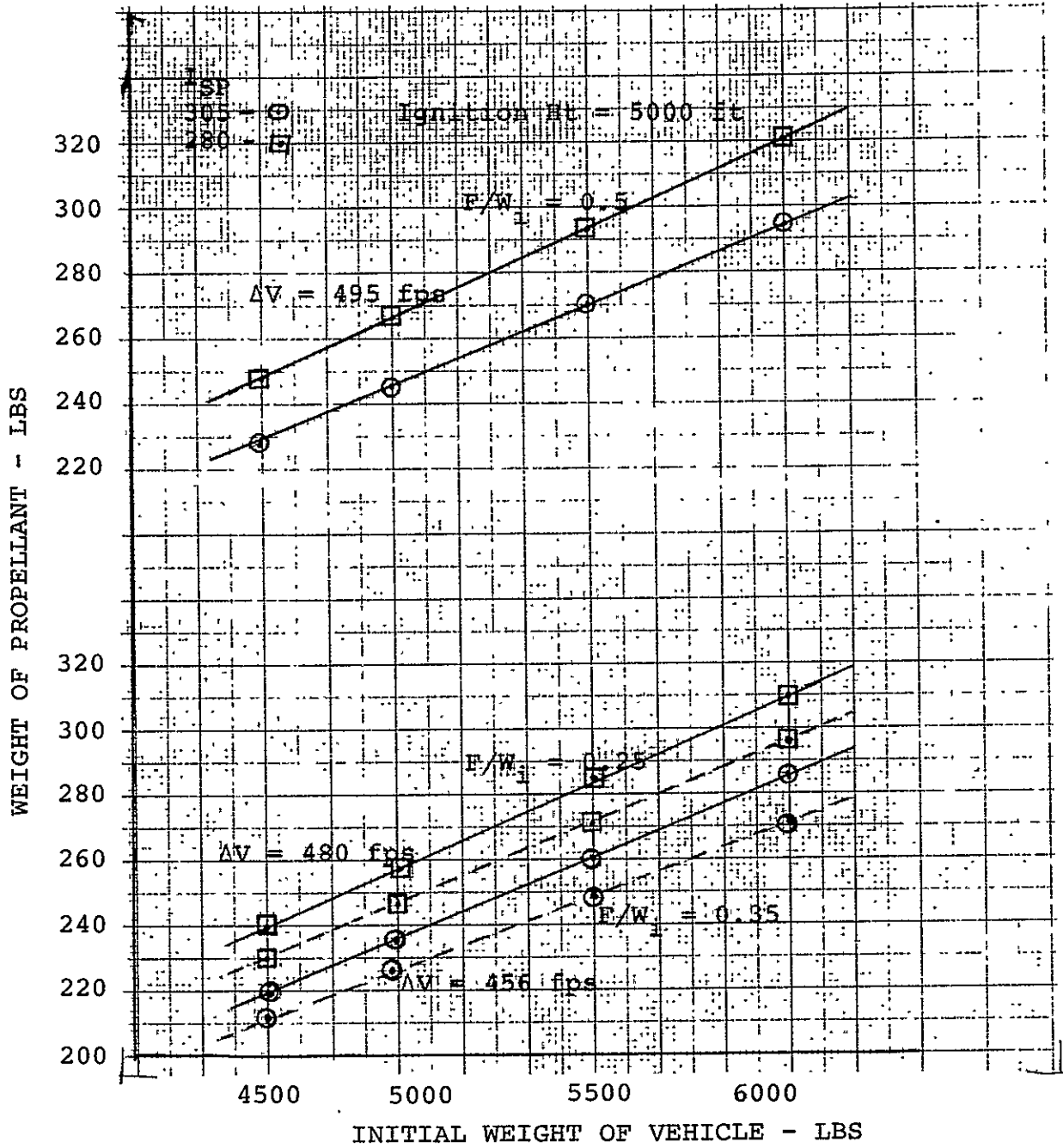


FIGURE 4.1-12 EFFECT OF TARGET VELOCITY ON PROPELLANT WEIGHT FOR LVPS

4.1.4 Hover Maneuver

The primary purpose of the hover capability incorporated in the mission is for orientation of the LLV for landing and slight translational movement for small hazard avoidance. This maneuver is accomplished with the LVPS and RCS engines. The minimum ΔV requirement for 20 second hover is 106 fps. Figure 4.1-13 gives the results of a parametric study on hover requirements. Since the majority of the ΔV requirements are in the MRE, the hover propellant requirements change very little with altitude. In actuality the hover altitude only affects the LVPS terminal phase from hover to touchdown since the MRE is targeted for burnout at the proper altitude and a ΔV of 99 fps (See Table 4.1-3). The hover phase of the mission was targeted for 100 feet altitude, to achieve a balance between propellant expenditure and TV requirements, and requires a programmed amount of propellant of 60 pounds, including 3 percent residuals. Although the work study directive asked for only 20 second minimum hover time, an additional amount of propellant should be programmed into a contingency budget for increasing the time for this maneuver.

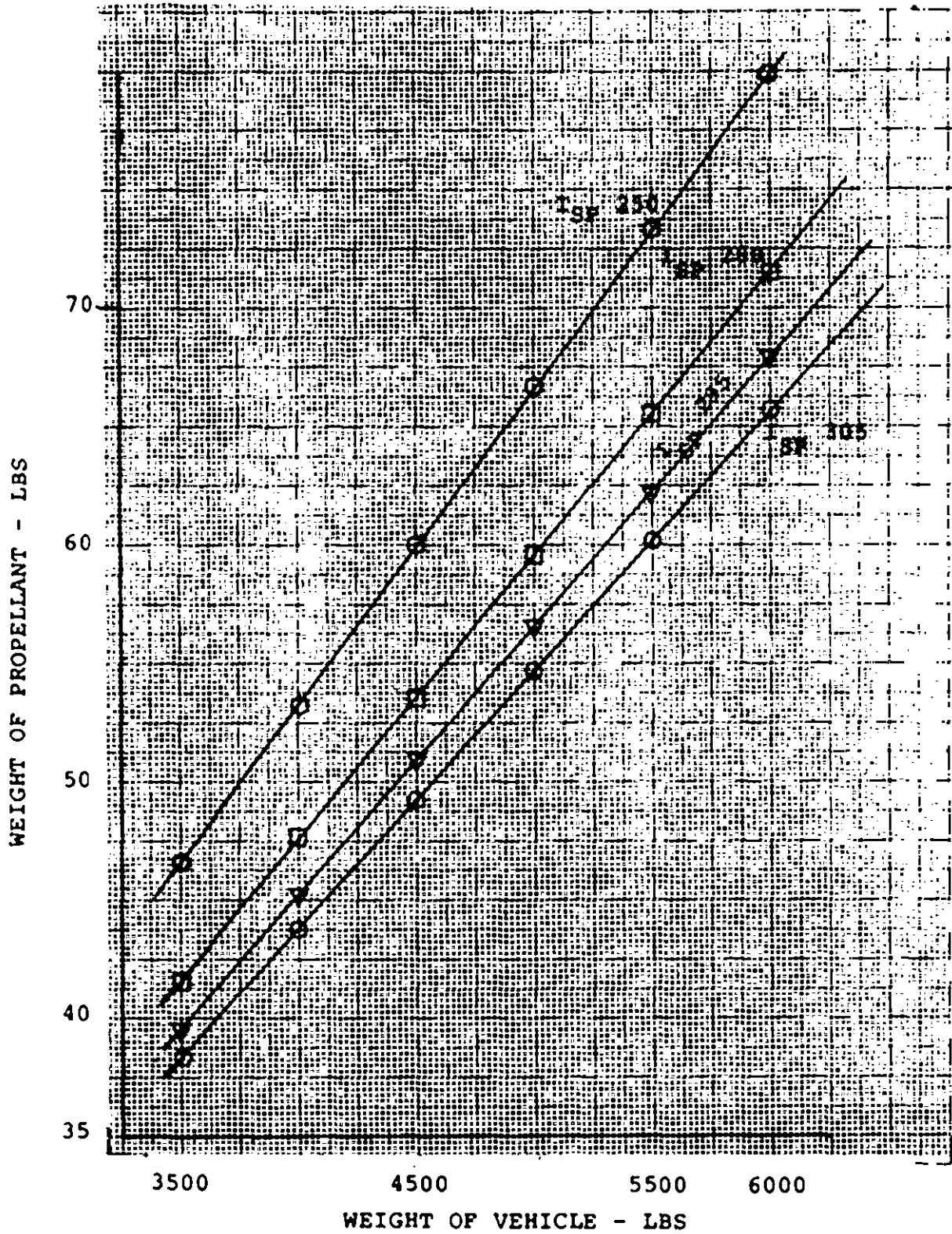


FIGURE 4.1-13 WEIGHT OF VEHICLE AT HOVER VS
WEIGHT OF PROPELLANT REQUIRED

4.1.5 End of Hover to Touchdown

The final prelanding phase is immediately at the conclusion of the hover phase. This mission objective was analyzed utilizing various hover heights. The results of this are presented in Table 4.1-3. Examination of these results shows one should hover as close as possible to the ground for minimum propellant requirements. Although this last phase allows for a maximum touchdown velocity of 15 fps, the calculations were based on a landing velocity of zero fps which allows for some excess in the propellant requirement. The programmed budget for this final maneuver is a AV of 56 fps (optimum AV is 42 fps) and the propellant requirement based on all previous maneuvers being carried out is 30 lbs including 3 per cent residuals.

TABLE 4.1-3 EFFECT OF HOVER ALTITUDE ON PROPELLANT
REQUIREMENTS FOR TOUCHDOWN MANEUVER

Mass @ End of Hover	Hover Height	AV	I _{SP}	Propellant Required End Hover-Touchdown
lbs	ft	fps*	sec	lbs**
5000	100	42.63	292	23.30
5000	500	97.44	292	53.10
5000	800	117.74	292	64.10
5100	100	42.63	292	23.76
5100	500	97.44	292	54.16
5100	800	117.74	292	65.37

* Includes FPR

** Includes 3% Residuals

4.1.6 Post-Landing Propulsion System Operation

One of the proposed functions for the LVPS after landing was a hop of one km with the possibility of this maneuver taking place up to ninety days after touchdown. Parametric studies (See Figure 3.3-6) were undertaken in conjunction with the Dynamics Group in order to determine the ΔV budget and thus the propellant weight for this operation. The results of the study are based on an optimum trajectory (ballistic) and a simple case trajectory (a square traverse). Table 4.1-4 lists the results of the investigation. No attempt was made to integrate electrical, thermal or structural penalties into the study. The penalty paid for this maneuver is mainly in the extra propellant the LVPS must carry. The additional tank weight represents eleven pounds, and the additional propellant volume can be accommodated by utilizing available qualified tanks.

The recommendation of the Design Institute is that this maneuver not be programmed into the mission.

TABLE 4.1-4 PROPULSION SYSTEM PENALTY FOR PROPOSED HOP

Distance	1 km Maximum
Landed Weight	5000 lbs
Thrust/Weight Ratio	0.44
ΔV Budget	
Ballistic	360 fps
Square	429 fps
Mass of Propellant*	
Ballistic	203 lbs
Square	227 lbs
Additional Tank Wt	11 lbs

*No FPR or Residuals Included

4.1.7 Summary

An analysis of the propulsion requirements for a soft landing of a Lunar Landing Vehicle based on a high energy mission ($V_{\infty} = 4500$ fps and $h_p = -900$ nm) was undertaken, and the propellant requirements based on the below-listed subsystems is presented in Table 4.1-5.

- | | |
|-----------------------------|--|
| (1) Main Retro Engine | One P & W RL10A3-3
Throttleable (3/1 ratio) |
| (2) Liquid Vernier System | Sixteen Marquardt R-4D Engines |
| (3) Reaction Control System | Twelve Marquardt R-1E Engines |

The above systems were chosen to be the best qualified from the following considerations:

- (1) Availability
- (2) Cost
- (3) Reliability
- (4) Minimum Propellant Requirements
- (5) Growth Potential

TABLE 4.1-5 SUMMARY OF REQUIREMENTS FOR PROPULSION SYSTEM

Propulsion Function	Propulsion System	ΔV Programmed fps	Propellant Programmed lbs	I_{SP} sec
Midcourse	RCS	101.50	138.30	280
Main Retro Phase Bulk ΔV	MRE	9535.75	5796.66	444
Site Redesign.	MRE	152.25	64.73	444
Losses			116.00	
Intermediate	LVPS	106.00	60.00	292
Hover	LVPS	108.00	60.00	292
Final	LVPS	56.00	30.00	292
Attitude (Roll-Pitch-Yaw)	RCS	--	50.00	270
Contingencies for Extended Hover Time and Minor Translation LVPS Variations RCS Variations Increased Hover Height Launch Vehicle Separation Posigrade prior to Retro			61.70	

Equations Used in Calculations

$$F = I_{SP} \dot{W} \quad (1)$$

$$Ft = I_{SP} W \quad (2)$$

$$\Delta V = I_{SP} G \ln \frac{M_I}{M_I - M_P} \quad (3)$$

$$\Delta V_{GL} = gt$$

$$\Delta V = V_I + V_{GL}$$

Where

M = Weight, lbs

$W_I = M_I$ = Initial Weight, lbs

M_P = Propellant Weight, lbs

F = Thrust, lb_f

I_{SP} = Specific Impulse, sec

t = Time

\dot{W} = Mass flow Rate, lbs/sec

G = constant = 32.2 ft/sec^2

ΔV_{GL} = Velocity Gravity Losses, fps

ΔV_I = Initial Velocity, fps

ΔV = Characteristic Velocity, fps

g = Acceleration of gravity, ft/sec^2

4.2 Main Retro System

The main retro (retrograde) power plant removes the bulk of the ΔV during the terminal descent of the LLV. The site re-designation (up to \approx 6 miles) is also performed by the main retro at lower approaches to the lunar surface with or without the help of the verniers and the reaction control system (RCS).

After the main retro has performed its mission, it is jettisoned together with its tanks (which may still contain some unused propellants).

RL-10 Engine. The reason why the RL-10 has been selected as the main retro is shown in Section 4.7. This engine was originally developed for the Centaur and Saturn S-IV programs [1,2,3,4] and proved to be very reliable. The engine uses LOX and LH_2 at a mixture ratio of 5.0 which with the engine length of 70.2 inches gives a thrust level of $15,000 \pm 300 \text{ lb}_f$ and a vacuum specific impulse of $444 \text{ lb}_f\text{-sec}/\text{lb}_m$.

Tables 4.2-1 and 4.2-2 show the specifications and performance of two different engine models: RL 10A-3-3 (Fig. 4.2-1) and RL 10A-3-7. The first one has a minimum of three restarts and is in general non-throttleable, while the second has 50 restarts and is throttleable from $15,000 \text{ lb}_f$ to 1500 (idle condition) lb_f thrust at a specific impulse of $420 \text{ lb}_f\text{-sec}/\text{lb}_m$. Pratt & Whitney proved that the 3-3 model can idle with a thrust of 400-700 lb_f , depending on the pressure in the propellant tanks [2]. Thus, when the retro fires and is shut down for a short time, it can idle during that time without the rotation of the

TABLE 4.2-1 RL10A-3-3 LIQUID ROCKET ENGINE SPECIFICATION
 VACUUM PERFORMANCE (1)

Thrust Rating	15000 ± 300 lb
Specific Impulse, Nominal	444 sec
Specific Impulse, Minimum (3σ)	439 sec
Mixture Ratio, Nominal (Factory Setting)	5.0 ± 2.00%
Acceleration Time (From Start to 90% Rated Thrust)	2 sec maximum
Start Impulse (To 2 sec from Start and 540°R)	14,200 ± 4000 lb-sec
Shutdown Time (From Removal of Start Signal to 5% Rated Thrust)	0.15 sec maximum
Shutdown Impulse	1180 ± 150 lb-sec (based on 380 sec run duration)
Mission Start Capability	3 minimum
Nominal Running Time per Start	450 sec
Service Life	4000 sec
Thrust Vectoring (Gimbal Range)	±4.0 (square pattern)
Geometric Thrust Axis Location (From Gimbal Point)	±1/16 in
Including Standard Equipment, Shall Not Exceed	290.0 lbs
Type--Regeneratively-cooled, turbopump-fed liquid-oxygen, liquid-hydrogen rocket engine	
Maximum Engine Diameter (at room temperature)	39.67 inches
Maximum Engine Length (at room temperature)	70.23 inches
Maximum Radial Projection from Centerline	20.25 inches
Fuel Specification, Liquid Hydrogen	Preliminary Specification MIL-P-27201

TABLE 4.2-1 (Contd)

Oxidizer Specification, Liquid Oxygen	MIL-O-25508A
Helium Specification, Gaseous Helium	Bureau of Mines Type A
Nozzle Area Ratio	57:1

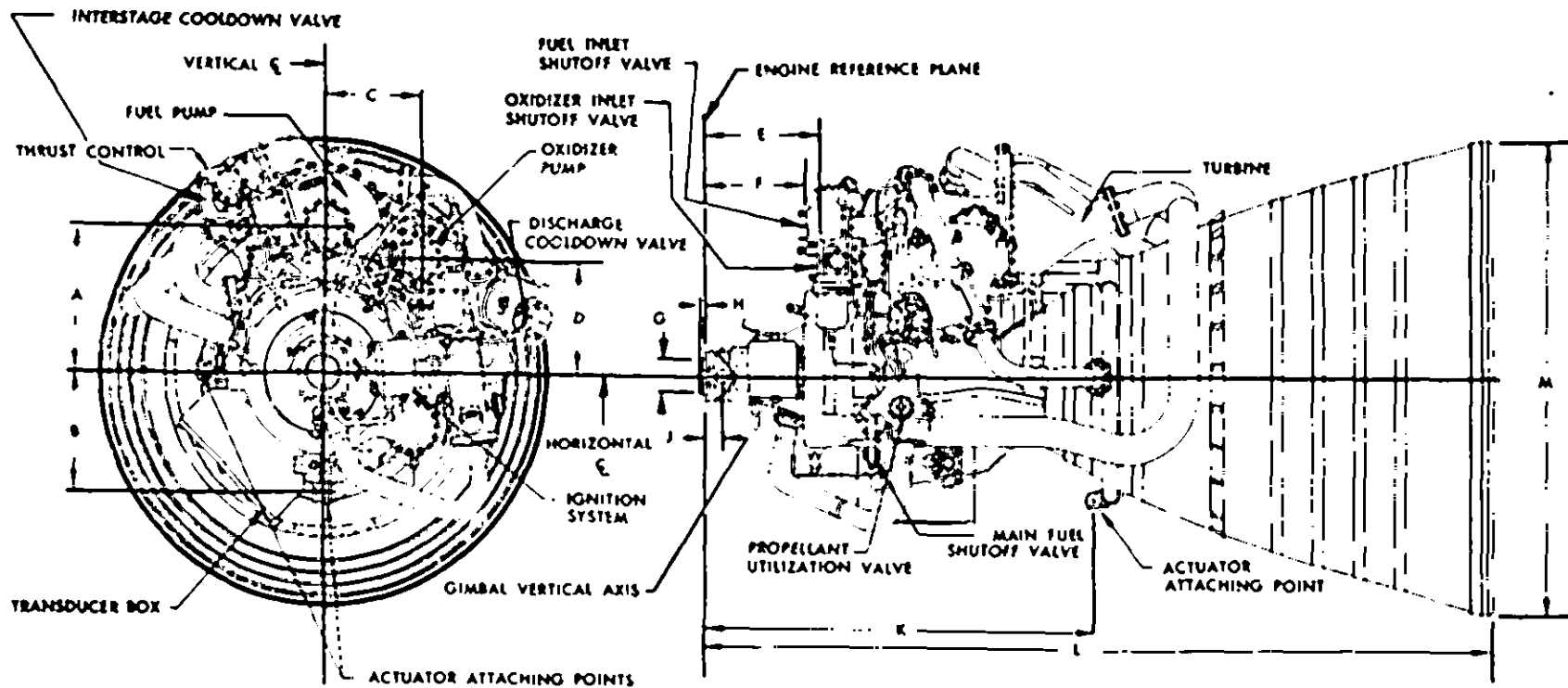
TABLE 4.2-2. RL10A-3-7 LIQUID ROCKET ENGINE SPECIFICATION

VACUUM PERFORMANCE [1]

	Rated	Pumped Idle	Tank Head Idle
Thrust Rating (Throttleable, pumped idle to rated)	15,000 ± 300 lb	1500 ± 150 lb	*
Specific Impulse, Nominal	444 sec	435 sec	410 sec
Specific Impulse, Minimum (3σ)	439 sec	430 sec	405 sec
Mixture Ratio, Nominal (Factory Setting)	5.0 ± 2.00%	5.0 ± 5.00%	*
Acceleration Time (From Start to 90% Maximum Thrust)	2 sec maximum	*	*
Start Impulse (0 to 95% Thrust and 540°R)	3450 ± 1000 lb-sec	1850 ± 500 lb-sec	
Shutdown Time (From Removal of Start Signal to 5% Rated Thrust)	0.15 sec max	0.095 sec max	
Shutdown Impulse	1180 ± 150 lb-sec	285 ± 50 lb-sec	
Nominal Running Time	900 sec	900 sec	900 sec
Minimum NPSP required at engine inlet:			
Fuel	2 psi	0 psi	0 psi
Oxidizer	4 psi	0 psi	0 psi

TABLE 4.2-2. (Contd)

Number of Starts During Service Life	50
Service Life	4000 sec
Thrust Vectoring (Gimbal Range)	±6.0° (square pattern)
Geometric Thrust Axis Location (From Gimbal Point)	±1/16 in
Including Standard Equipment, Shall Not Exceed	315 lbs
Type--Regeneratively-cooled turbopump-fed liquid-oxygen, liquid-hydrogen throttleable rocket engine	
Maximum Engine Diameter (at room temperature)	39.7 inches
Maximum Engine Length (at room temperature)	70.2 inches
Maximum Radial Projection from Centerline	20 inches
Fuel Specification, Liquid Hydrogen	MIL-P27201A
Oxidizer Specification, Liquid Oxygen	MIL-O-25508D
Helium Specification, Gaseous Helium	Bureau of Mines Type A
Nozzle Area Ratio	60:1



A - 11.750	D - 9.419	G - 2.876	K - 32.874
B - 10.172	E - 9.603	H - 0.240	L - 70.10
C - 8.128	F - 8.738	J - 1.500	M - 39.56

DIMENSIONS ARE NOMINAL IN INCHES AT ROOM TEMPERATURE

FIG. 4.2-1. INSTALLATION DRAWING OF THE RL 10A-3-3 ENGINE [1]
RECOMMENDED FOR I.I.V

turbine. It also has been demonstrated that the 3-3 model can be throttled down to 5000 lb_f.

The 3-7 engine requires a very low NPSH which is 2 psi for LH₂ pump and 4 psi for the LOX pump, while the 3-3 engine requires 6 and 10.5 psi, respectively. Both engines can start within 2 seconds and shut down within 0.15 seconds. The 3-3 engine has a nominal running time of 450 seconds while the 3-7 engine is doubling this figure. The thrust vectoring (gimbal range) in the first engine is $\pm 4^\circ$ while in the other one it is $\pm 6^\circ$.

The model 3-3 weighs 290 lbs, costs \$300,000 and is qualified. The model 3-7 weighs 315 lbs, costs \$400,000, has been extensively tested, demonstrated its capability, but is not qualified. Although it is better to use a throttleable engine as the main retro of the LLV, lower NPSH for the pumps, longer running time, 47 additional restarts, and a higher gimbal range are not required. Hence, only throttling of the RL 10A-3-7 must be qualified. It is estimated that such qualification should cost between \$5,000,000 and \$10,000,000. Table 4.2-3 summarizes the differences between these two engines.

Throttling of the main retro helps in site redesignation during the retro phase descent. The throttleable retro can bring the spacecraft to an altitude of a few hundred feet above the lunar surface, while in the case of the non-throttleable engine the height should be greater and the descent to the lower altitude must be accomplished by verniers and RCS as described in

TABLE 4.2-3. MAIN DIFFERENCES IN RL10A-3 ENGINES

Engine Type	RL10A-3-3	RL10A-3-7
Thrust, lb _f	15,000 ± 300	15,000 ± 300
Throttleable	No*	Yes to 1500 ± 150
NPSH for LH ₂ , psi	6	2
NPSH for LOX, psi	10.5	4
Gimbal range	±4°	±6°
Restarts	3	50
Running time, sec.	450	900
Weight, lbs	290	315
Cost, \$	300,000	400,000
Qualified	Yes	No

* Throttleability from 15,000 down to 5,000 was demonstrated.

the next section. In general site redesignation and terminal descent can be performed with the RL 10A-3-3 engine when throttling it to 5000 lb_f. However, this is not as convenient as with the 3-7 model which is fully throttleable.

Both engines use a regeneratively-cooled thrust chamber assembly and a turbopump feed system. Fig. 4.2-2 shows the flow diagram of this system. LH₂ flowing through the nozzle and thrust chamber tubes cools the walls and absorbs heat, which fully vaporizes the cryogenic liquid. GH₂ then enters the injector to the thrust chamber where it meets the spray of LOX. A small flow rate of GH₂ is used to pressurize (after reducing its pressure by the pressure regulator) the LH₂ tank, as shown in Fig. 4.2-3.

The LH₂ pump brings the pressure of the fuel to 900 psia, while the LOX pump brings the pressure of the oxidizer to only 450 psia. The higher pressure of LH₂ is necessary for the regenerative cooling of the nozzle and thrust chamber.

Propellant Tanks. Cryogenic tanks holding LH₂ and LOX must be properly insulated; this includes all tubes and valves attached to the tanks. The tanks and valves must be properly supported to reduce the heat inputs which otherwise will increase the boil-off [5, 6, and 7].

Pressurization of Tanks. Pressurization of the LOX tanks is accomplished by diverting a very small flow rate of LOX from the pump outlet to a heater below the rocket nozzle. The heater can be in the form of a coil or in the form of a hollow ring of the

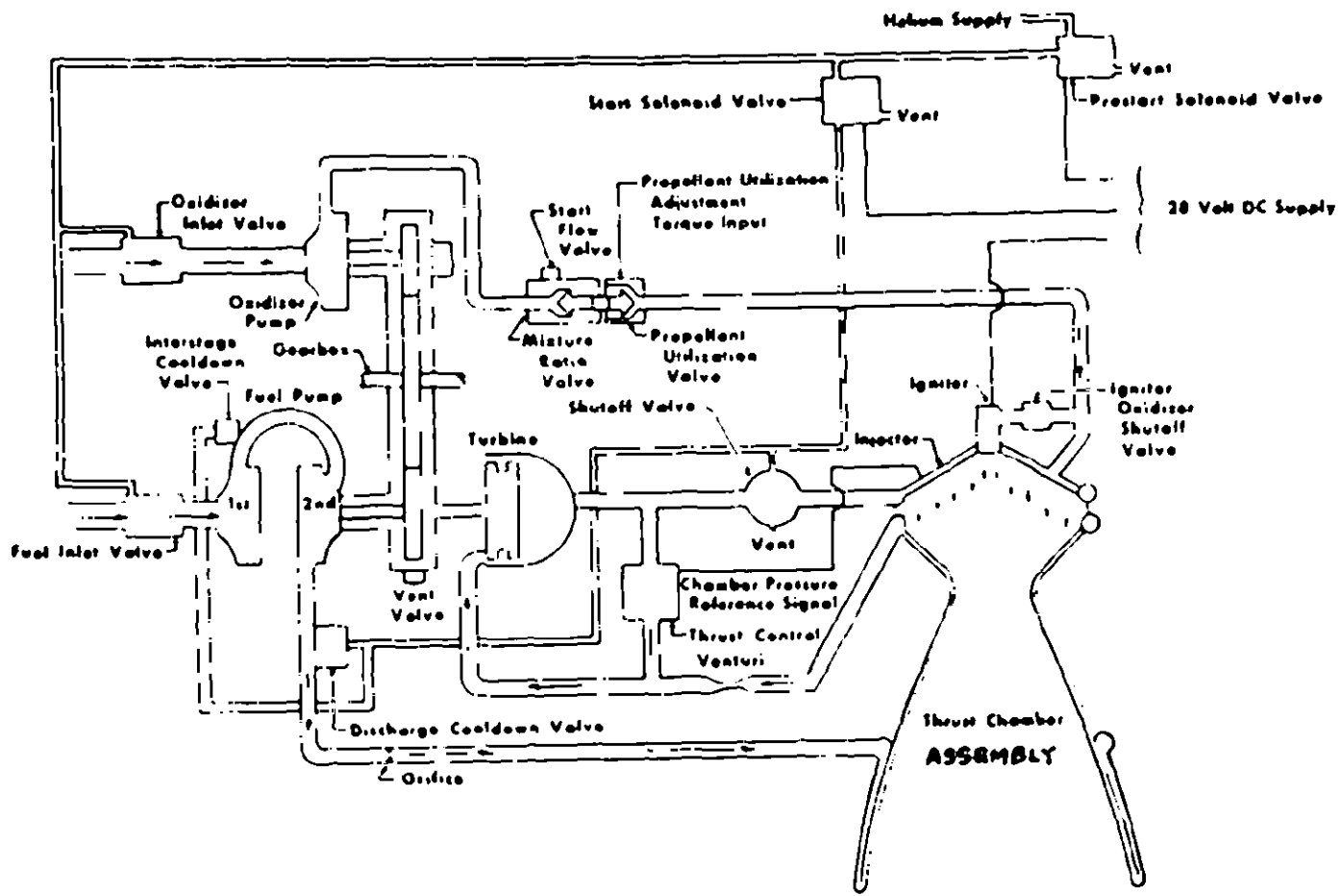


FIGURE 4.2-2. RL10 PROPELLANT CONTROL SYSTEM [2]

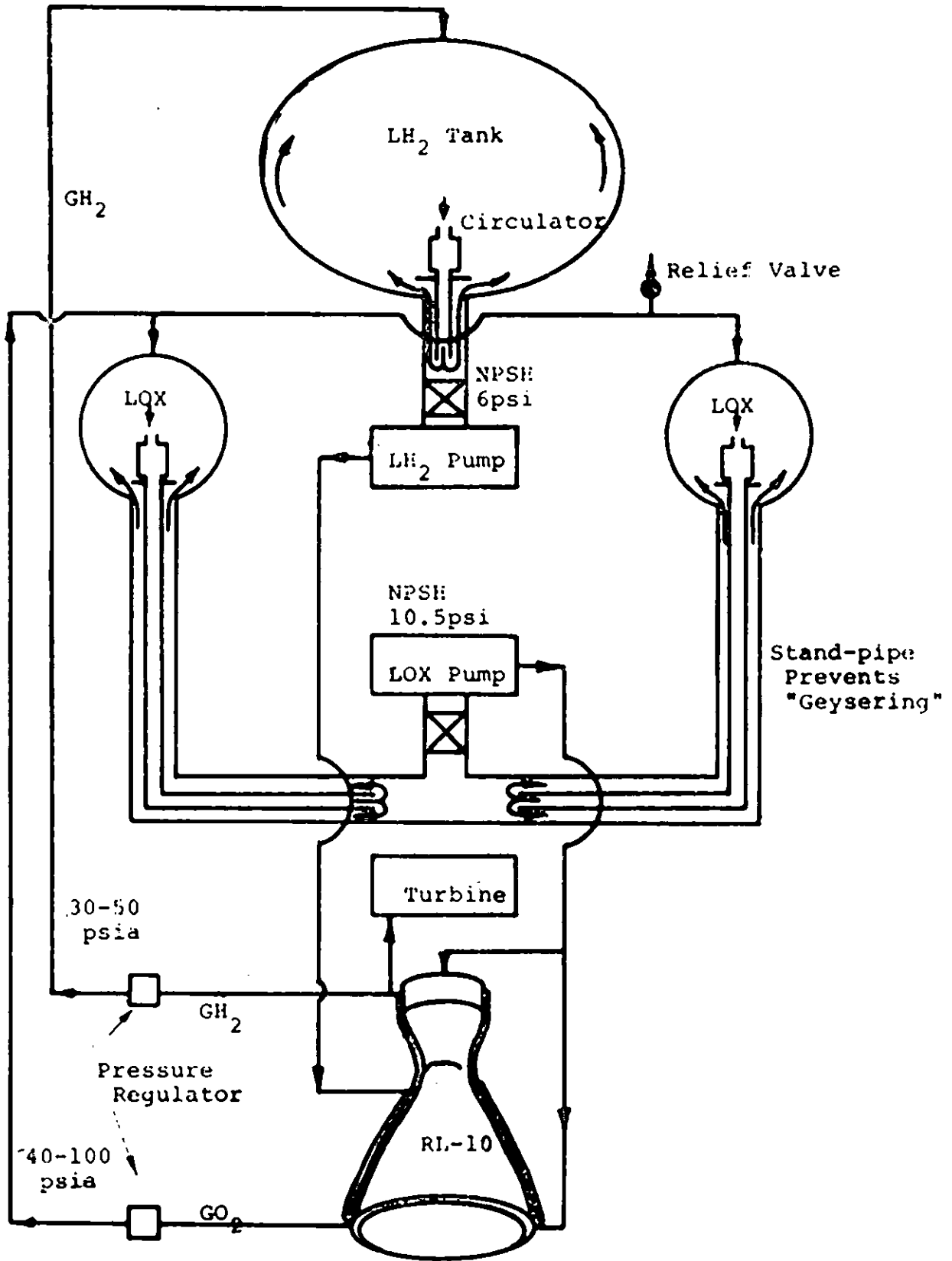


FIGURE 4.2-3. PRESSURIZATION OF LOX AND LH₂ TANKS

size of exit area periphery as shown in Figure 4.2-3. Pressure regulator, such as sonic flow control nozzle in the GO_2 line, will reduce the pressure of the evaporated oxidizer to between 40 and 100 psia (as required). At the same time the pressure regulator regulates the flow of LOX to the heater.

As the engine exhaust gases are not immediately hot after the start of the engine, it may become necessary to increase the pressure in the LOX tanks prior to the start of the engine. This can be accomplished by an increase in the setting of the relief valve of the LOX tanks. During most of the lunar trajectory the relief valve should be set at not over 50 psia; however, several hours before firing the retro the relief valve should be set to open at 100 psia. This will insure a build-up of pressure in the LOX tanks due to boil-off, and this, in turn, will provide a good NPSH to the LOX pump during the first few seconds of engine operation, i.e. during transient condition when LOX in the pressurization stream is not yet fully evaporated. Alternative systems of LOX tanks pressurization will require gaseous helium and would make the pressurization system much heavier.

Figure 4.4-1 shows the utilization of the hydrogen from the LH_2 tank for the attitude control jets. This figure also shows the lines which have to be severed by a guillotine cutter or quick disconnect at the time when the RL 10 engine and the tanks are jettisoned. The lines should be severed on one side of the propellant tanks so that the remaining pressure in the tanks will cause a side thrust on the mass that is being jettisoned. This

will push the mass away from the descending trajectory of the spacecraft so that the spacecraft will not land on top of the jettisoned mass.

Circulation of LH_2 and LOX. In weightless conditions, liquid cryogenic propellant behavior during extensive period of flight causes a problem in the location of bubbles (from ullage gas and boil-off) and the unequal heat inputs from outside [8]. It has been found that liquids behave as if they were covered by a contractible membrane in uniform tension. This tension acts along the surface and tends to make its surface as small as possible. The force-per-unit length acting normal to any line drawn in the surface is defined as the interfacial or surface tension. During and shortly after the formation or destruction of new surfaces, the apparent surface tension may differ somewhat from its equilibrium value. This modified surface tension is called the dynamic surface tension.

When a liquid drop comes in contact with a solid surface, three angles are formed in a plane perpendicular to the three-phase line in the solid surface. The angle measured within the liquid between the solid and the tangent to the liquid-gas interface at the three-phase line is called the contact angle. The value of the contact angle is related to the relative magnitude of the microscopic adhesive and cohesive forces.

Most researchers consider that in zero-gravity the bubbles of the gas or vapors congregate in the middle of the tank; others, however, found that the bubbles, especially in cryogenic liquids, congregate on the surface of the tank. Surface bubbles could create

a problem caused by external heat inputs (from supports of the tanks, piping connections, and non-perfect insulation). The overall heat transfer coefficient through the bubbles is different than through the liquid. This causes overheating of certain parts of the tank walls, which, in turn, causes evaporation of some liquid when during a space maneuver the cryogenic liquid will come in contact with the warmer wall by a sloshing movement. Such sloshing may produce a large quantity of vapors which could result in a too rapid increase in tank pressure to be relieved by relief valves.

In order to prevent the sudden increase in pressure, each tank containing LOX or LH_2 is provided with a circulator (Figure 4.2-3), which will circulate the cryogenic propellants, at least one minute every few hours. In the Apollo spacecraft, fuel cells require cryogenic tanks with hydrogen and oxygen under supercritical (or near supercritical) high pressure conditions. These tanks have circulators (called fans) which require 26.4 watts motors in the oxygen tank and 3.6 watts in the hydrogen tank. Each tank has two circulators. Taking under consideration the sizes of the LLV cryogenic tanks and the viscosity of the liquids one 30 watt circulator for the LH_2 tank and one 72 watt circulator for each LOX tank were selected.

These circulators are shown in Figure 4.2-3. Each takes suction from the middle of the tank and discharges the liquid into the tubes leading toward the propellant pumps (as described below). The propellant in each tube then returns to the respective tank and flows around a baffle toward the periphery of the

tank, mixing up the bubbles and the liquid.

The circulators should not be used too often as they cause some heating of the cryogenic propellant and, in turn, an increase in boil-off.

Geysering Effect. The term "geysering" is applied to that phenomenon which occurs in a cryogenic liquid system when a column of liquid in long vertical lines is expelled by the release of vapors at a rate in excess of that rate which may occur as a normal function of bubble release. The result is an expulsion of liquid from the vertical line. Refilling the line by gravity action from the tank above the line results in a pressure surge analogous to water hammer. The pressure surges produced as a result of geysering can be very large, and damage feed lines, valve supports, etc.[9]. In weightless conditions geysering is no problem; however, when the ullage maneuver necessary to settle the cryogenic propellants before the retro will fire, geysering may become a problem.

The usual approaches to minimize this problem are: (1) helium injection, (2) subcooled topping, and (3) cross-feed circulation. The first two methods waste either helium or the cryogenic propellant. The third method was adopted with a certain change. It is shown in Figure 4.2-3 and utilizes circulators to cause the movement of the liquid in the tubes below the tanks.

Helium System. The RL-10A engine requires gaseous helium in an amount of 0.044 lbs for pneumatic valve actuation at each start. After each actuation helium is removed overboard.

Helium is taken from the GHe tank which is mainly used to pressurize the vernier and RCS propellant tanks (Figure 4.4-4).

Growth Potential. The growth potential of the RL-10A system lies in the possibility of extending the nozzle of the engine and thus increasing the specific impulse of the propellant combination. This increase and the associated with it weight penalty are shown in Figure 4.2-4 and 4.2-5. The increased specific impulse will permit a reduction in propellant weight [10].

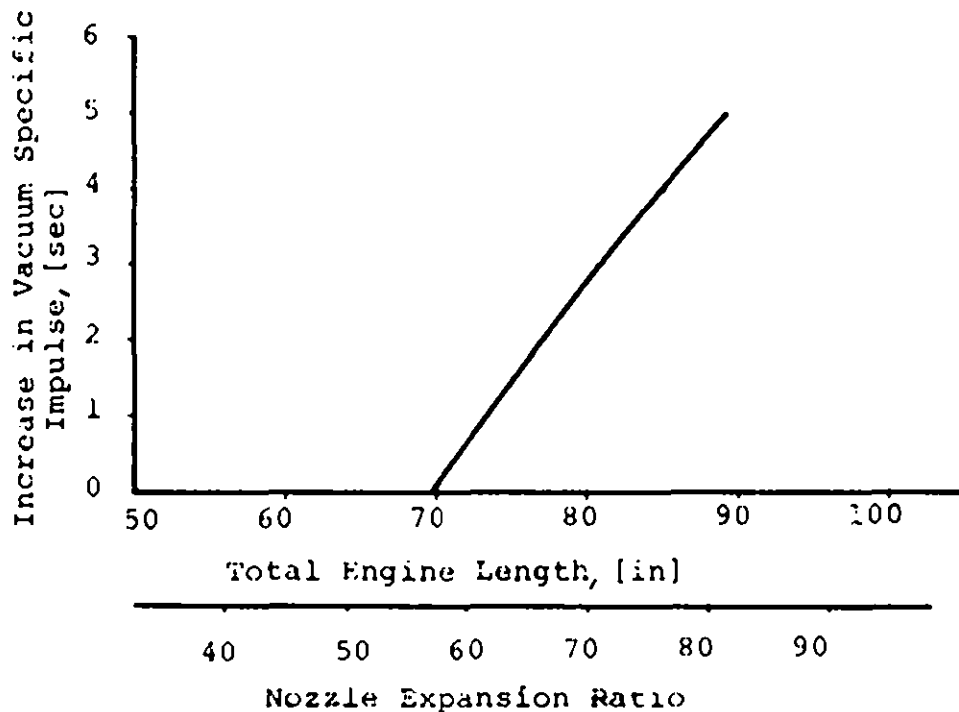
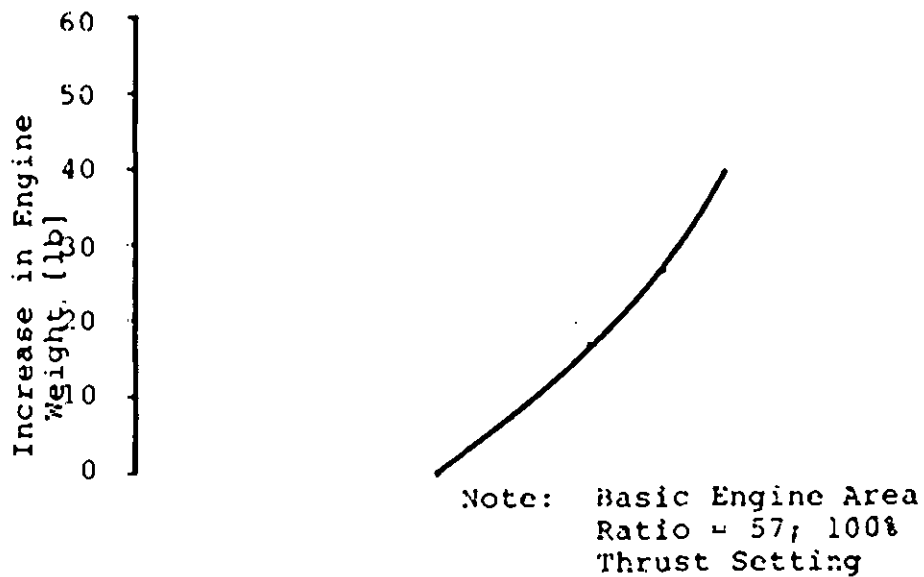


FIGURE 4.2-4 EFFECT OF INCREASING AREA RATIO IN RL-10 ON PERFORMANCE [3, 10]

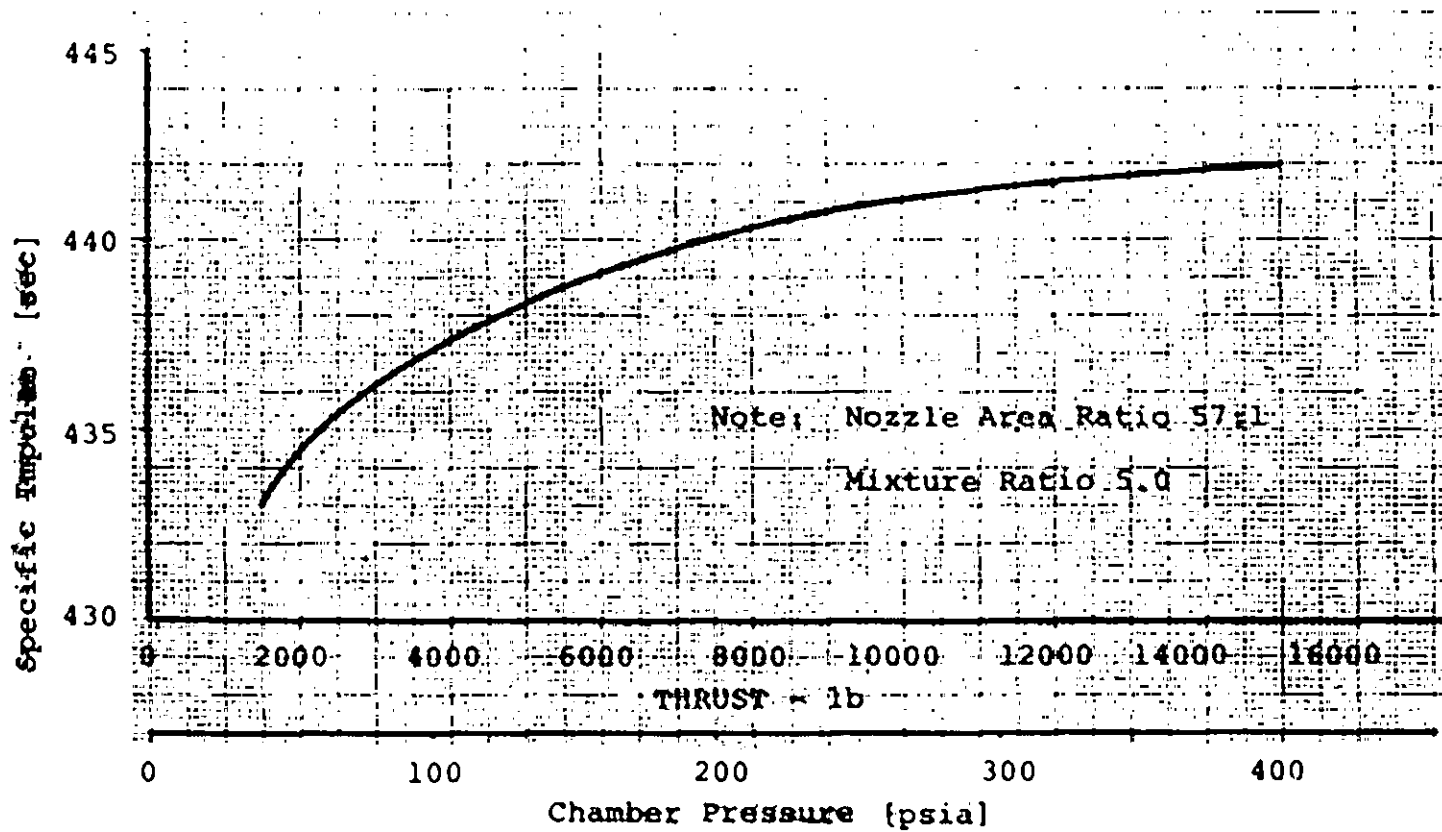


FIGURE 4.2-5 ESTIMATED SPECIFIC IMPULSE VS THRUST IN RL-10 [3, 10]

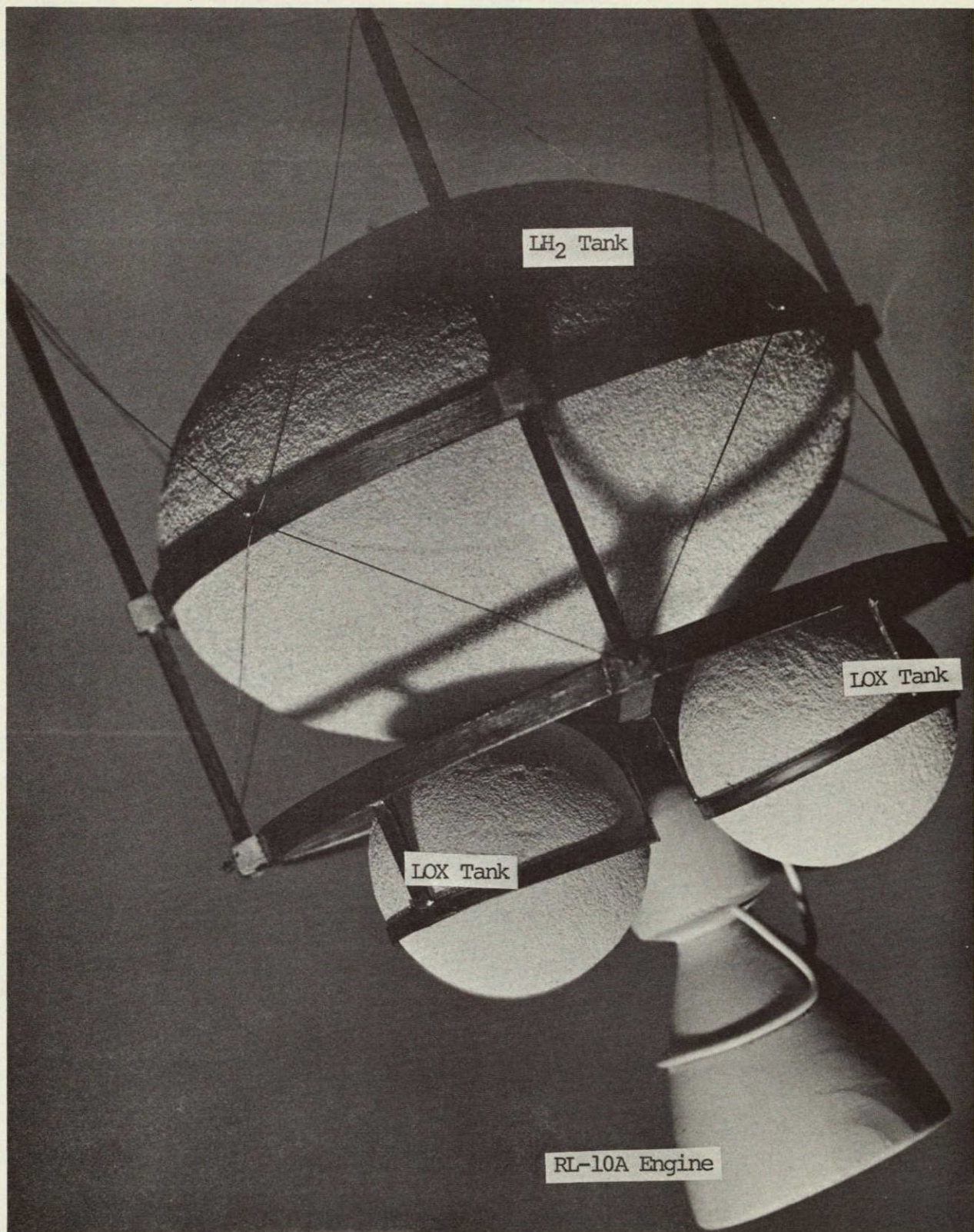


FIGURE 4.2-6. MAIN RETRO SYSTEM
(Photograph of a Model)

4.3 Vernier System

The vernier system consists of 16 engines, two propellant tanks, one helium tank, and appropriate tubing, valving, instrumentation, and heaters. The propellant and helium tanks are common with the reaction control system.

Engines. The verniers are the same Marquardt R-4D liquid engines which were used in the Apollo Service Module and Lunar Module [11]. These engines use N_2O_4 as the oxidizer and either MMH (monomethyl-hydrazine) or a 50% blend* by weight of hydrazine and UDMH (unsymmetrical dimethyl-hydrazine) as the fuel.

Figure 4.3-1 shows the engine assembly which weighs 5.25 lbs. It consists of a radiation-cooled thrust chamber, an injector, and two solenoid operated propellant injection valves. The design incorporates a preigniter chamber where initial combustion occurs. The purpose of this chamber is to minimize overpressurization or "spiking," which is a transient condition, but if sufficiently severe, can lead to destruction of the engine.

Spiking is caused by the formation of unstable intermediate products of low-temperature combustion, which occurs when the engine is cold. In vacuum of space, the injected propellants immediately flash by adiabatic evaporation and lower the temperature of the spray. The lower temperature produces a mixture of vapors, liquids, and solids of both the fuel and the oxidizer. Under these conditions, the initial reaction rate is apparently very

* This blend is often referred to as Aerozine.

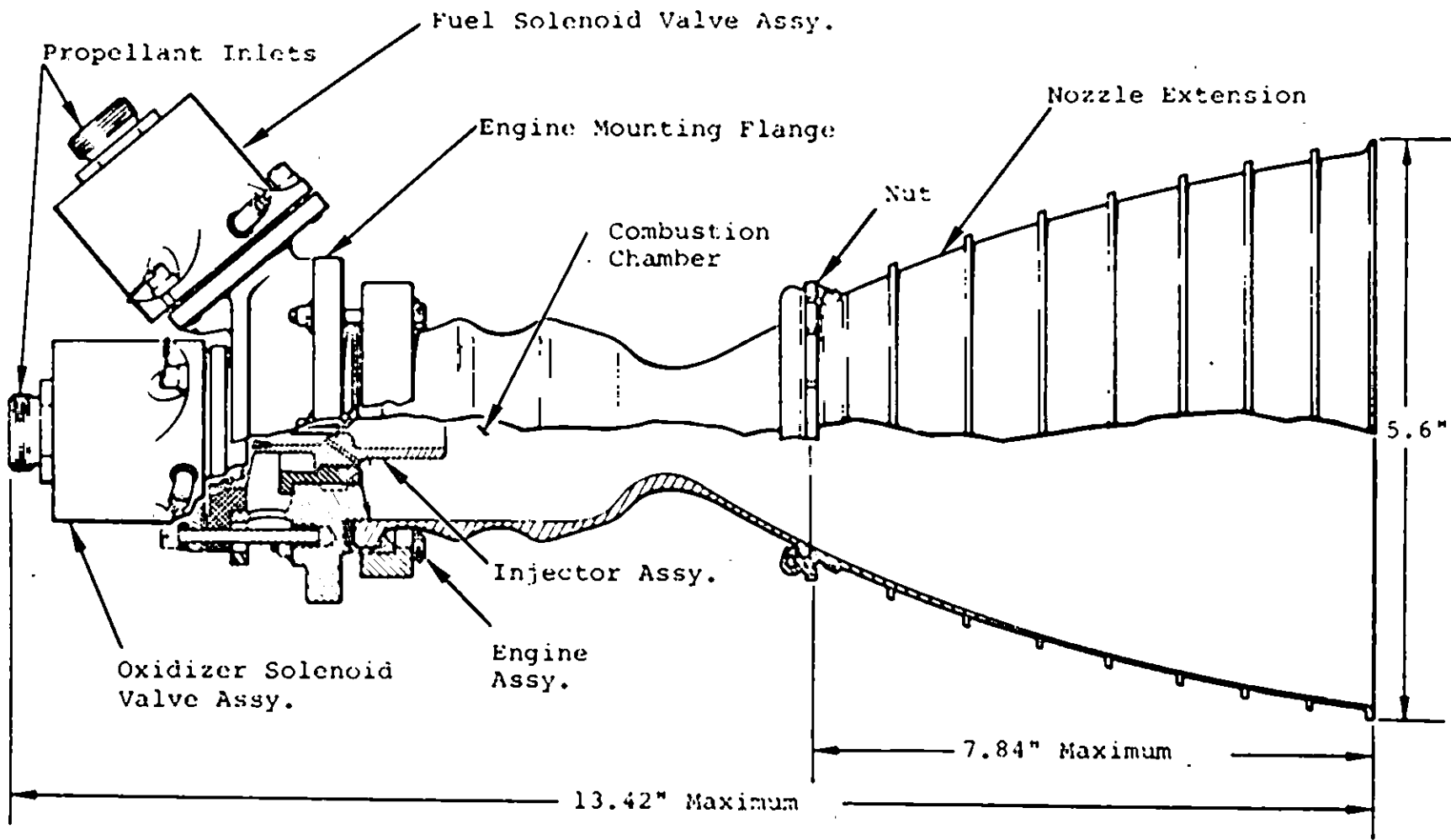


FIGURE 4.3-1 VERNIER R-4D ENGINE (11)

slow, thus allowing an explosive mixture to accumulate. That is why it is very important to preheat the engine up to 30 minutes before firing. In the Lunar Module these engines were preheated with electrical heaters to between 138° and 140°F.

To further minimize spiking the preigniter chamber is prepressurized by fuel lead.

When the engine propellant valves receive an "open" command, approximately 9 milliseconds are required for both valves to fully open. Propellants flow immediately through the valves into the injector and reach the combustion chamber about 11 milliseconds after the "open" command, with ignition occurring approximately 1 millisecond later. In steady-state operation the chamber pressure is 100 psia, the delivered vacuum thrust is 100 lb_f and the delivered specific impulse is 290 lb_f -sec/ lb_m . In pulsed operation all these values are somewhat lower.

Marquardt Corporation has demonstrated [12] that higher flow rates of propellants can be used by increasing the inlet pressure to 300 (or even to 600) psia. This resulted in 185 (or 297) psia chamber pressure and a correspondingly higher thrust level, but a lower specific impulse of 276 sec. These conditions required a modification of the injector to reduce the propellant pressure drop.

In the LLV design it was decided to increase the flow rates of propellants to a value which will not require any modification of the R-4D engine. An increase of thrust level to 140 lb_f is considered compatible with the existing, qualified model of the engine. The following calculations show the thrust levels for the

Apollo R-4D engines, modified R-4D engines, and the LLV verniers. Using equations 4.5-6 and 4.5-3.

$$\dot{V} = I_S \dot{W} = C_F A_T P_C$$

For a constant C_F and A_T we obtain up to 0.496 lb/sec for the new propellant flow rate (Table 4.3-1).

Quads. The verniers will be used only during the last part of the terminal descent, i.e. (1) from the retro engine burn-out to hover, (2) for hover, and (3) from hover to the final touchdown. Figure 4.3-2 shows the need for a thrust of at least 2000 lb_f, which increases the thrust to mass (or earth weight) ratio to 0.4 in order to greatly reduce the gravity loss during the first phase of the descent with verniers. This phase will be done with 16 verniers arranged in quads (Figure 4.3-3), each quad attached to the "mouse-house" (a nickname used in Apollo).

The hover and the final descent phase require a thrust of less than 1000 lb_f, because at that time the lunar weight of the spacecraft is slightly below 1000 lb_f. The reduction of the thrust can be done by changing the steady-state mode of engine operation to a pulsed mode and/or by shutting off two verniers in each quad.

Landing on Slopes. The touch-down on the lunar surface requires special consideration, especially if the slope of the surface is between 15° and 35°. Small stabilization solid rockets firing upwards (as described in Section 9.3) and/or the verniers firing downwards can be used to reduce angular rates after touchdown. Although no analysis has been conducted, allowing the attitude control system to continue operation for a few seconds after initial lunar contact may reduce the tendency to

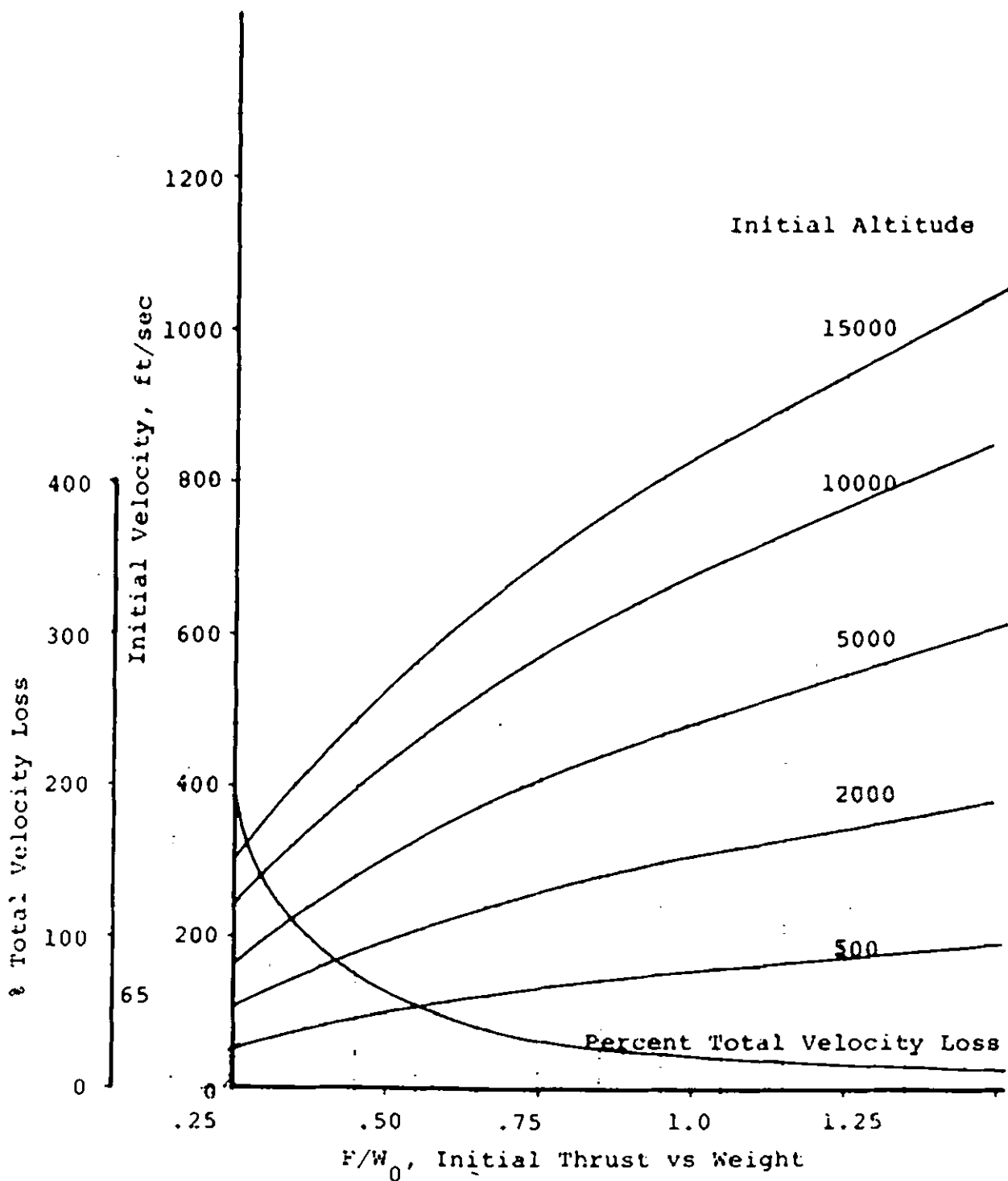
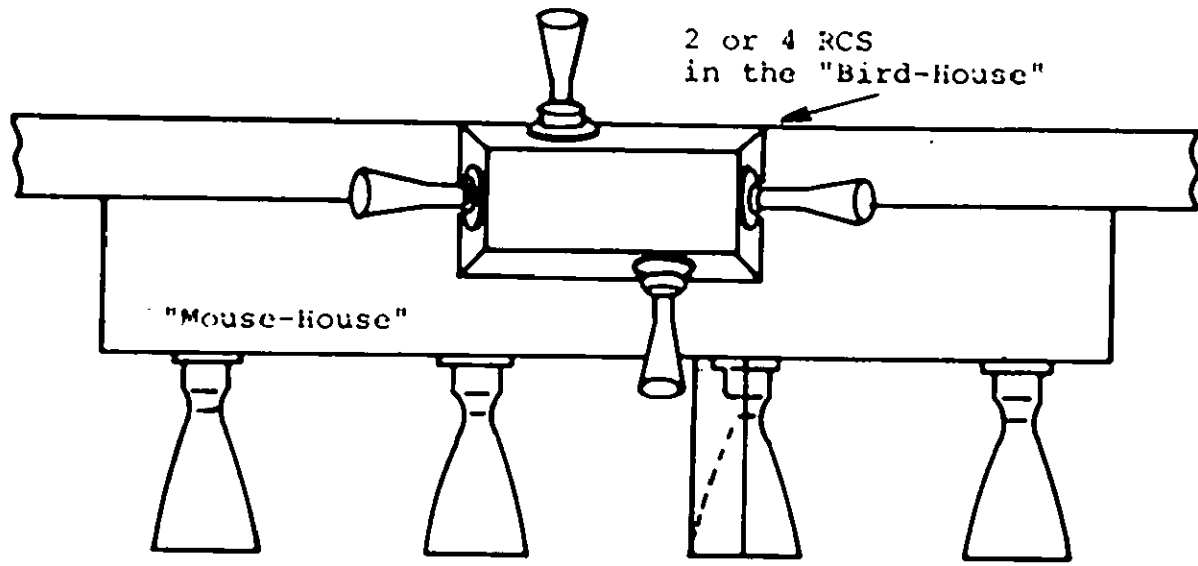


FIGURE 4.3-2 INITIAL VELOCITY AND PERCENT VELOCITY LOSS AS A FUNCTION OF F/W_0 FOR AN INITIAL FLIGHT PATH ANGLE AT -80°

(from R. W. Abel of NASA MSC).

TABLE 4.3-1. PROPELLANT FLOW RATES FOR R-4D ENGINES [12]

Engine	Thrust, lb _f	Chamber Pressure, psia	Delivered Specific Impulse, sec.	Flow Rates lb/sec.
Apollo	100	100	290	0.345
Modified	185	185	276	0.670
LLV Vernier	130	130	283 estimated	0.460
LLV Vernier	140	140	282 estimated	0.496
LLV Vernier (growth potential)	185	185	276 estimated	0.670

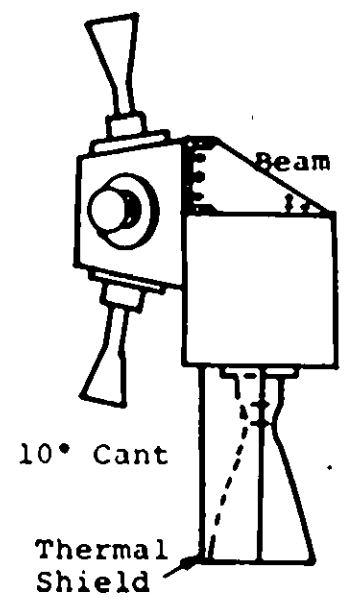


2 or 4 RCS
in the "Bird-House"

"Mouse-house"

R-4D
Verniers--140 lb_f
(100-160 lb_f)
13.38" x 5.60" dia.

R-1E
RCS--22 lb_f
9.6" x 4.25"



Beam

10° Cant

Thermal
Shield

FIGURE 4.3-3 STRUCTURES FOR VERNIERS AND RCS

overturn on landings. During this period the verniers would resist LLV angular rates imparted by the landing gear.

The firing of the verniers on the lunar surface will cause some dust to ~~reduce visibility~~. This, however, does not present any problem, because at that time the television system will not be used for command guidance.

Tanks. Propellant and helium tanks and the pressurization system are shown in Figure 4.3-4.

Helium in gaseous form, in an amount of 2.5 lb is in a tank made of Ti 6Al-4V alloy similar to the sphere used on the Surveyor spacecraft [3]. Its proof pressure is 8400 and burst pressure is 11,000 psig.

GHe is used to pressurize the tanks for propellants for both the verniers and the reaction control system (RCS engines). The helium pressure for these tanks is held by the pressure regulators at 295 psia.

A small amount of GH_2 is also used to operate several pneumatic valves of the RL 10A engine. Another pressure regulator reduces the helium pressure to between 440 and 500 psia (while its temperature is between 300° and 600°R). When the RL 10A engine is jettisoned the helium line must be severed upstream of the pressure regulator. This is best done by a pyrotechnically

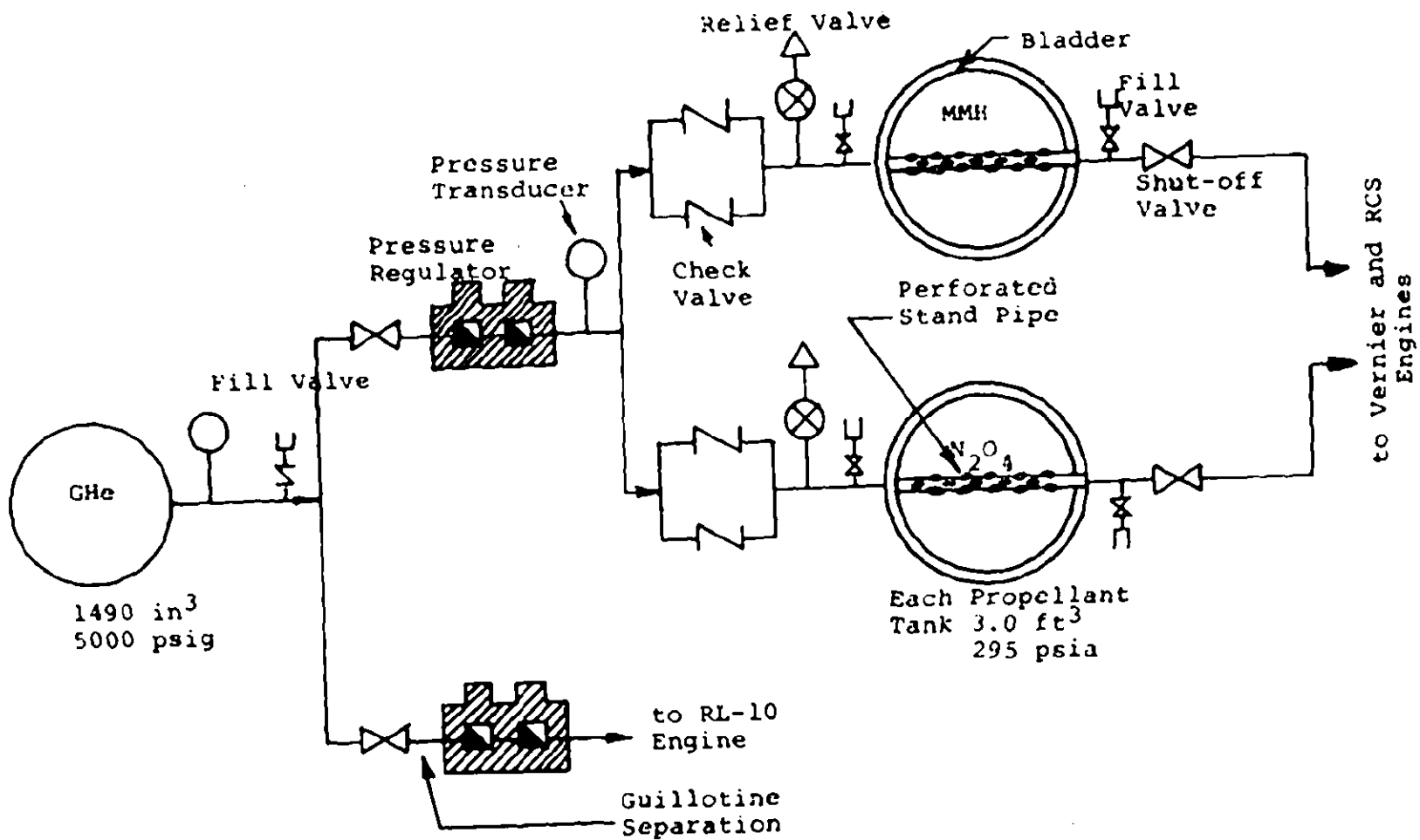


FIGURE 4.3-4. HELIUM PRESSURIZATION SUB-SYSTEM

operated guillotine after the isolation valve (upstream of the severance location) is closed by a solenoid.

The propellants are MMH (154 lb) and N_2O_4 (246 lb). Because of the difference in densities these propellants can be stored in identical tanks. The tanks selected for these propellants are both spheres each of 5,195 in³ (3 ft³) volume for an operating pressure of 295 psia. Similar tanks were used on Gemini for MMH and N_2O_4 [14].

Each sphere weighing 11.5 lbs has a diameter of 21.9 inches, has a proof pressure of 500 psia and a burst pressure of 670 psia. The tanks were manufactured by Rocketdyne Division of North American Rockwell Corp. from Ti 6Al-4V alloy. Each tank requires an expulsion bladder and a perforated stand pipe.

Growth Potential. The above tanks can be replaced by larger 22.0 inch diameter spherical tanks, each having a volume of 5,575 in³ and an operating pressure of 300 psig. The tanks were also made of Ti 6Al-4V alloy and although the burst pressure was higher than of the tanks described previously, the weight was only 8.0 lbs per tank. The tanks were manufactured by Fansteel, Inc. These tanks (designation No. 103172) were used on Gemini for the positive expulsion of fuel and oxidizer.

The higher operating pressure will permit higher flow rates to verniers, especially if they are modified to reduce the pressure drop across the injector valves.

Extended hover time and hop capability require more propellants for verniers and RCS engines and hence larger propellant and helium tanks.

Instead of using three new tanks consideration may be given to a novel system called by the Jet Propulsion Laboratory (of California Institute of Technology) ALPS or Advanced Liquid Propulsion System. This system with certain modifications is shown in Figure 4.3-5.

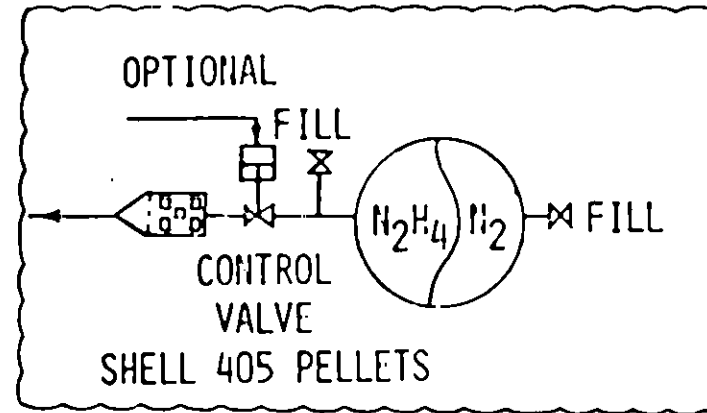
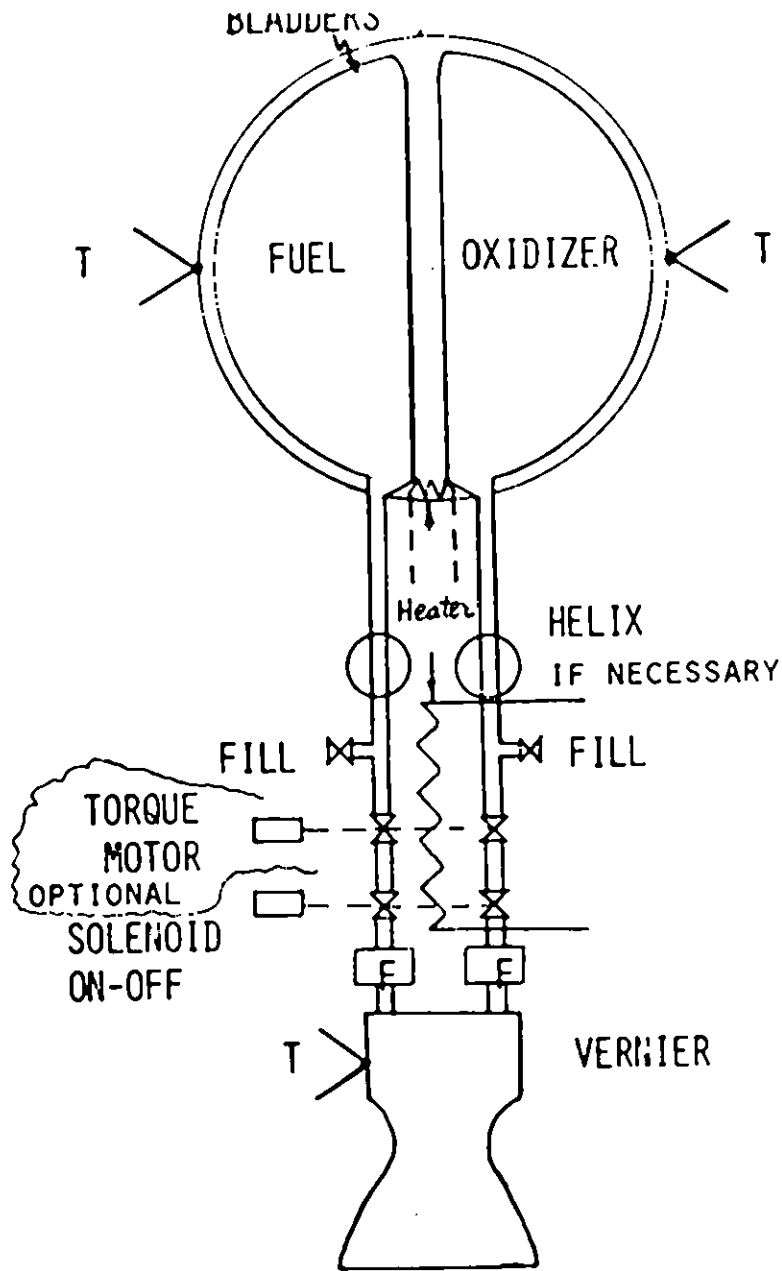
The first figure shows that the fuel and the oxidizer are located in a single spherical tank where they are surrounded by individual expulsion bladders. A proper selection of these bladders will insure no permeability of the propellants into the pressurizing gas.

Pressurization of the propellants may be performed either by hydrazine (N_2H_4) or by a pressurizing gas. When hydrazine flows through a catalyst bed of e.g. Shell 405 pellets, hot decomposition gases are obtained. Prior to entering the spherical propellant tank the gases are cooled by propellants flowing to the vernier and RCS engines.

An alternative pressurization system is shown in Figure 4.3-6. It consists of a GHe sphere with one or more solid gas generators to augment the helium pressure at the time when this pressure becomes low.

An increased hover time from 20 to 30 seconds will require approximately 30 lbs of propellant.

Hop Maneuver. If in future missions a hop to relocate the spacecraft to a distance of one kilometer is required, all verniers will fire to perform such a maneuver. The least amount of propellant (i.e. 203 lbs) is required to ascend almost vertically from the surface, pitching into the proper trajectory, and then perform a




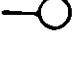
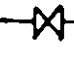

-  T=THERMOCOUPLE
-  P.G.=PRESSURE GAUGE
-  RV=RELIEF VALVE
-  = FILTER

FIGURE 4.3-5. ADVANCED LIQUID PROPULSION SYSTEM
(based on information from the JPL Propulsion Div.)

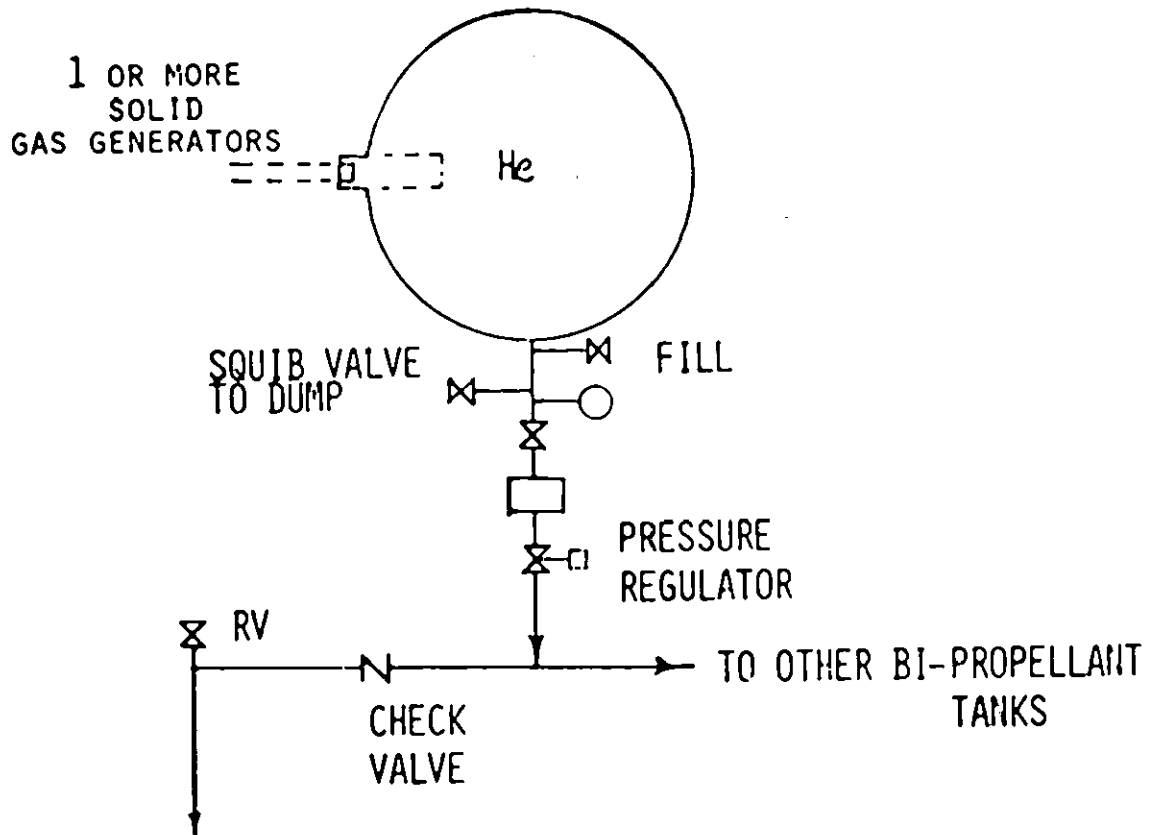


FIGURE 4.3-6. HELIUM PRESSURIZATION WITH SOLID GAS GENERATOR

"short range ballistic trajectory" by firing all the verniers (and four RCS thrusters) for a few seconds. After the powered ascent the spacecraft will coast to the apex and then downrange where the powered descent will slowly bring the spacecraft to the new location. During the coasting part of the trajectory the attitude of the spacecraft must be changed to a proper position of the verniers for descent firing. The ΔV and propellant calculations are performed in Section 3.3. In addition the range in feet (X), the maximum altitude in feet (h), and the flight duration in seconds (t) can be approximated using modified short range ballistic trajectories:

$$X = \left(\frac{\Delta V}{2}\right)^2 \frac{\sin 2\phi}{G_L}$$

$$h = \left(\frac{\Delta V}{2} \sin \phi\right)^2 \frac{1}{2 G_L}$$

$$t = 2\left(\frac{\Delta V}{2}\right) \frac{\sin \phi}{G_L}$$

where, ΔV = total ΔV required for the hop by a ballistic trajectory, ft/sec

G_L = local lunar gravity, ft/sec²

ϕ = launch angle with the local horizontal, degrees

The propellant tanks must be changed to accommodate the increased amount of propellant for the hop.

As the television lens will be covered with dust, the hop should be executed by the astronauts to properly guide the spacecraft to the best location.

4.4 Reaction Control System

Reaction control system consists of 12 thrusters, two propellant tanks, one helium tank, and appropriate tubing, valving, instrumentation, and heaters. The propellant and helium tanks are common with the vernier system.

The thrusters are the Marquardt 4-1E liquid rocket engines each having a thrust of 22 lb_f . Figure 4.4-1 shows ~~this thruster~~. The engines were developed for the Air Force MOL (Manned Orbiting Laboratory) program and do not require additional qualification. The engines can be used in a pulse mode (Figure 4.4-2) or in a steady operation mode.

The delivered specific impulse is between 275 and 289 $lb_f\text{-sec}/lb_m$ depending on the propellant temperature and the mixture ratio, the optimum ratio being 1.7.

The reaction control engines are arranged as shown in Figure 4.3-1. This arrangement permits pitch, yaw, and roll control and also translation, if required. The engines will be used for the following maneuvers:

- a) Posigrade maneuver, which is required to remove the spacecraft from the Centaur stage;
- b) Mid-course correction maneuvers;
- c) Ullage maneuvers to settle LO_2 and LH_2 before firing the RL-10 engine; this maneuver is not mandatory as the RL-10 engine has its own capability to settle LO_2 and LH_2 in their tanks;

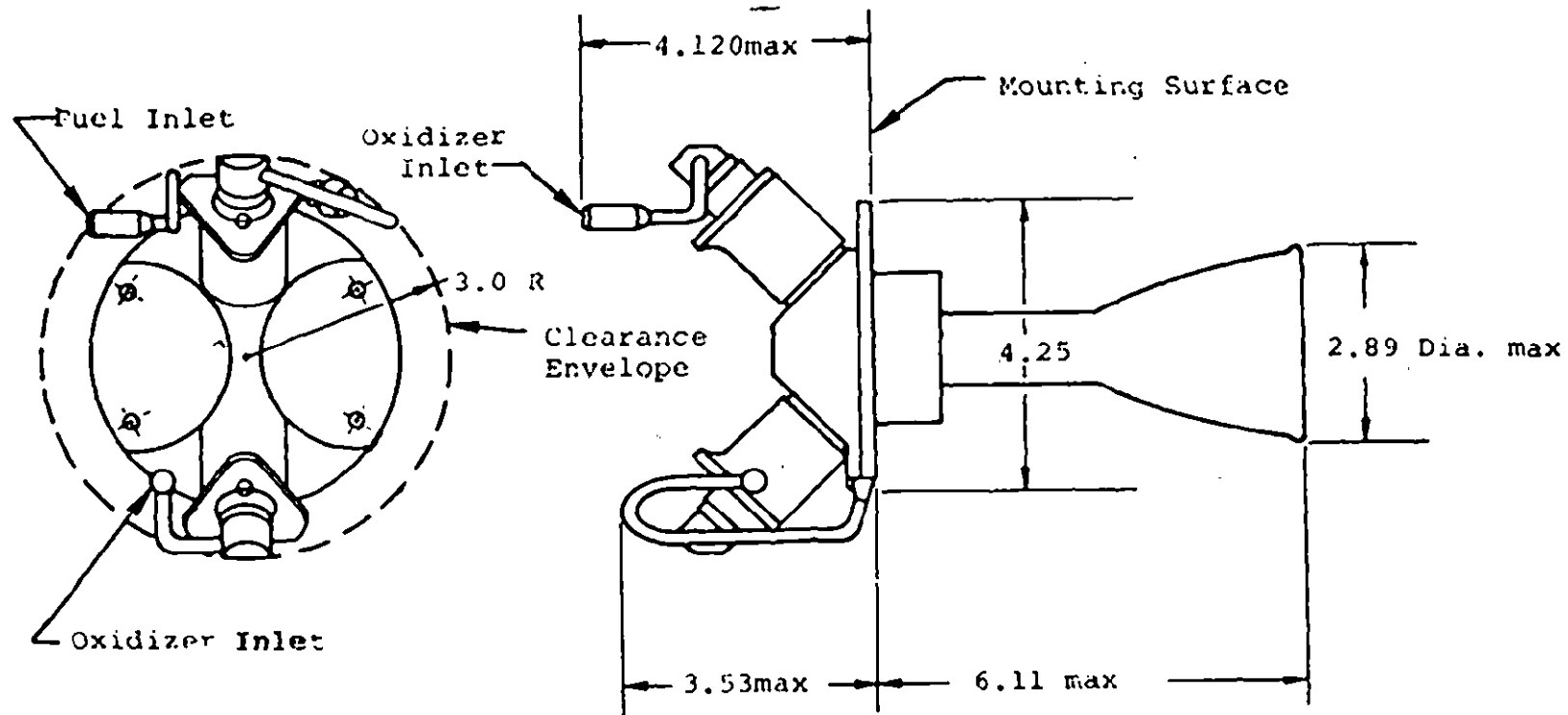


FIGURE 4.4-1 RCS 4-1E ENGINE (by Marquardt Co.)

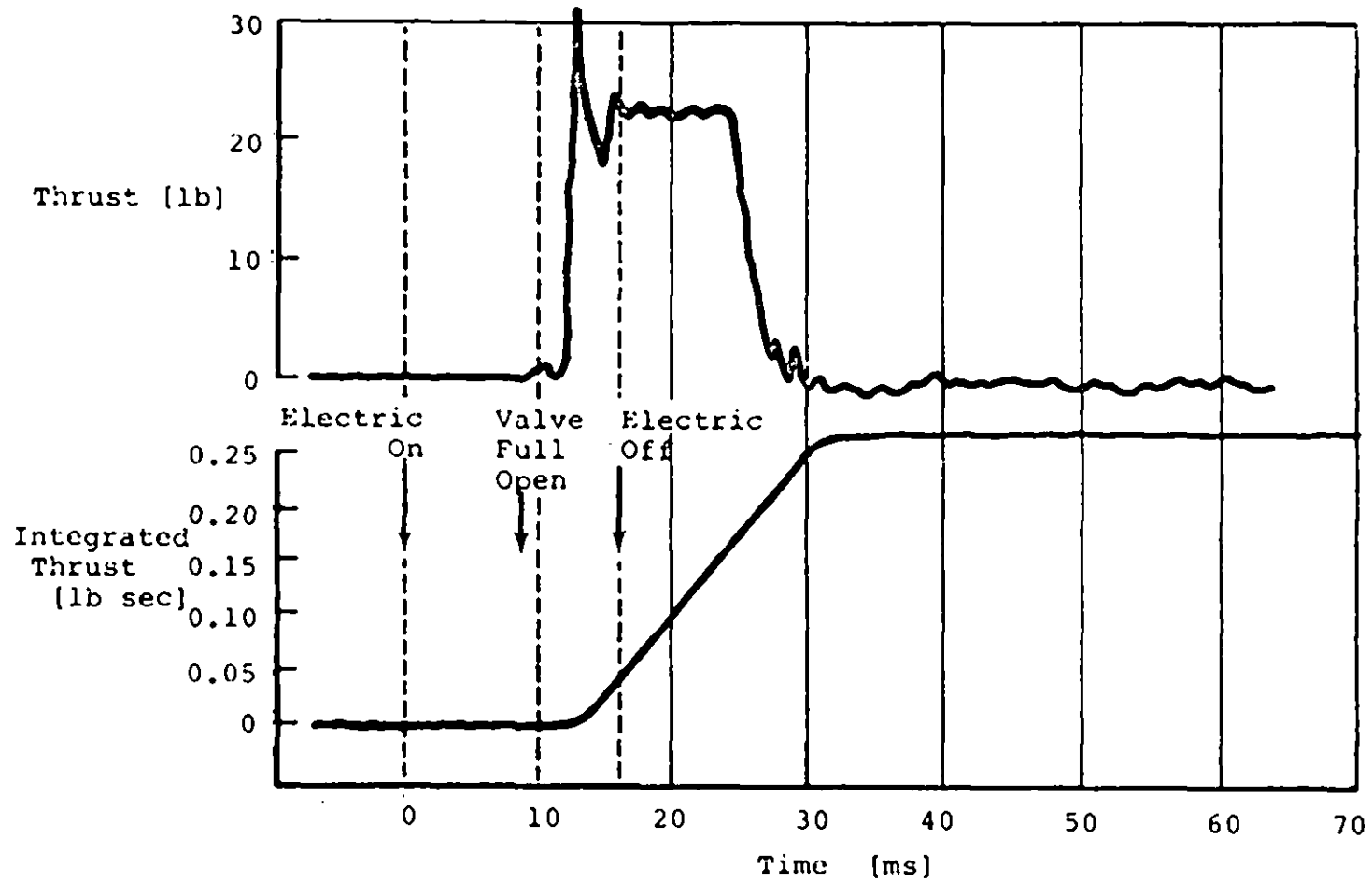


FIGURE 4.4-2 PULSE MODE OF RCS OPERATION (by Marquardt Co.)

- d) Roll control during the RL-10 firing;
- e) Descent to hover (after the retro engine and its tankage has been jettisoned);
- f) Hover above the lunar terrain;
- g) Final descent to the lunar surface;
- h) Hop for relocation on the lunar surface (as growth potential only).

The last four maneuvers will be used in conjunction with the vernier engines.

The RCS engines are located in two quads and two doublets, each quad and doublet in a small structure referred to as the "bird-house". Each bird-house is attached to one "mouse-house" which is a structure for a quad of four verniers. (Figure 4.3-3)

Heating. Fuel and oxidizer lines from propellant tanks to each combination of bird-house and mouse-house are common and have a joint thermal insulation. The insulation and 10 watt electric heaters per fuel-oxidizer line combination will prevent the propellants from freezing during flight and during lunar night[10].

Individual heating of each RCS thruster to 138°-140°F will be done 15-30 minutes before each firing to avoid "spiking" as described in section 4.3. For this purpose each RCS thruster is equipped with a 15 watt electric heater.

Cant. Each RCS thruster is canted (tilted) 10° to prevent as much as possible the impingement of the hot exhaust plume on the neighboring structure. Figure 4.3-3 shows the thermal shield protecting the nearest vernier engine. Such shield should be made of Inconel alloy and padded, if necessary, from inside with

a thermal blanket.

A cant of 10° reduces the 22 lb_f thrust of each thruster by a negligible amount as shown below:

$$F_{\text{net}} = F_{\text{engine}} \times \cos 10^\circ$$

$$F_{\text{net}} = 22 \text{ lb}_f \times 0.9841 = 21.65 \text{ lb}_f$$

4.5 Cold Gas Attitude Control System [17, 18, 19]

The attitude control system uses mass expulsion cold gas jets for obtaining "coasting maneuvers" or maintaining the desired attitude of the spacecraft. The cold gas jets are used only during coasting of the spacecraft; all other engines on the spacecraft obtain the attitude control during powered flight by the appropriate pitch, yaw, and roll control, as discussed in the sections 4.2 through 4.4.

The cold gas sub-system consists of a hydrogen supply and 12 on-off gas jets located at the end of each landing leg. Such a location (high L) permits achieving a large angular impulse per weight of hydrogen expended, as shown in the following equations

$$\text{M.F./cycle} = \frac{W_p}{W} = \frac{4}{I_s} \times \frac{F \Delta t}{W} = \frac{16r^2 \theta}{g I_s L t_c} \quad (4.5-1)$$

$$\Omega/\text{cycle} = 4 F \Delta t L = W_p I_s L \quad (4.5-2)$$

$$\text{M.F./day} = \frac{86,400}{10^6} \left(\frac{F}{W/1000} \right)^2 \left(\frac{Lg}{r^2} \right) \left(\frac{\Delta t^2}{\theta I_s} \right) \quad (4.5-3)$$

where,

Ω = change in angular impulse

M.F. = mass fraction

W_p = GH_2 propellant weight, lb

W = spacecraft weight, lb = 12,000 lb_m

r = radius of gyration, ft, $\left(\frac{L}{\sqrt{2}}\right)$ for a cylinder
 L = radius of jet centerline from c. m. = 117 in = 9.75 ft
 g = 32.2 ft/sec²
 θ = amplitude of motion, radians = (0.04 for coast)
 t_c = period of motion, sec
 F = thrust of jets, lb_f = 0.2
 Δt = on-time of jets, sec

It is anticipated that during coasting the gas jets will "fire" every 10 to 15 minutes depending on the bombardment of the spacecraft by cosmic dust, micrometeoroids, solar wind, solar proton events, solar electromagnetic pressure, and also on the behavior of liquid hydrogen and liquid oxygen in their tanks. The slight evaporation of these cryogenic propellants depending on the heat inputs from outside and from their own circulators and also the periodic mixing of these liquids by the circulators will create some disturbances in the attitude of the spacecraft.

In the Surveyor and Mariner spacecraft the three axes of the vehicle were locked on the star Canopus and on the sun. The dead-band used by the JPL star tracker was less than $\pm 1/2^\circ$ and the gas jets had to "fire" every 15-30 minutes. The maximum possible dead-band for Canopus lock with the JPL star tracker is $\pm 1.0^\circ$ *. It is recommended to use a dead-band between $\pm 1/2^\circ$ and $\pm 1^\circ$ or even a "barbecue" mode of operation during

*Private communication of G Meisenholder of JPL's Star Tracking department to F.J. Hendel

coast, i.e. a very slow roll of the spacecraft having a lock on the sun only. The "barbecue" mode will permit a better equalization of thermal inputs and outputs. The nominal time to re-establish the lock on Canopus by rolling the spacecraft is one hour per 360°.*

The gas jets will be used in couples to provide rotation about the three axes and in pairs to provide translation in six directions (Fig. 4.5-1).

Two gas jet pairs attached to leg 1 and leg 3 will be firing in the x-y or horizontal plane to provide roll control and roll maneuver. Two gas jet pairs attached to the same legs but positioned to fire in the z or vertical plane are for pitch maneuver. Two gas jet pairs attached to leg 2 and leg 4 are positioned to fire also in the z or vertical plane; these jets will execute the yaw control or yaw maneuver.

Supply of Hydrogen Gas. The gas will come from the large LH₂ tank which has a variable but continuous boil-off of gaseous hydrogen due to a heat input from external sources and from the circulator in the tank. The resultant increase in tank pressure above the normal, which is about 35 psia, will cause the relief valve to open and release some of the hydrogen. In weightless conditions the hydrogen will be released either as a liquid and/or gaseous hydrogen. The maximum boil-off of hydrogen is 35 lbs during a 60 hour mission and 70 lbs during a 120 hour mission. It follows that instead of wasting such amount of

*

Ibid. (previous page)

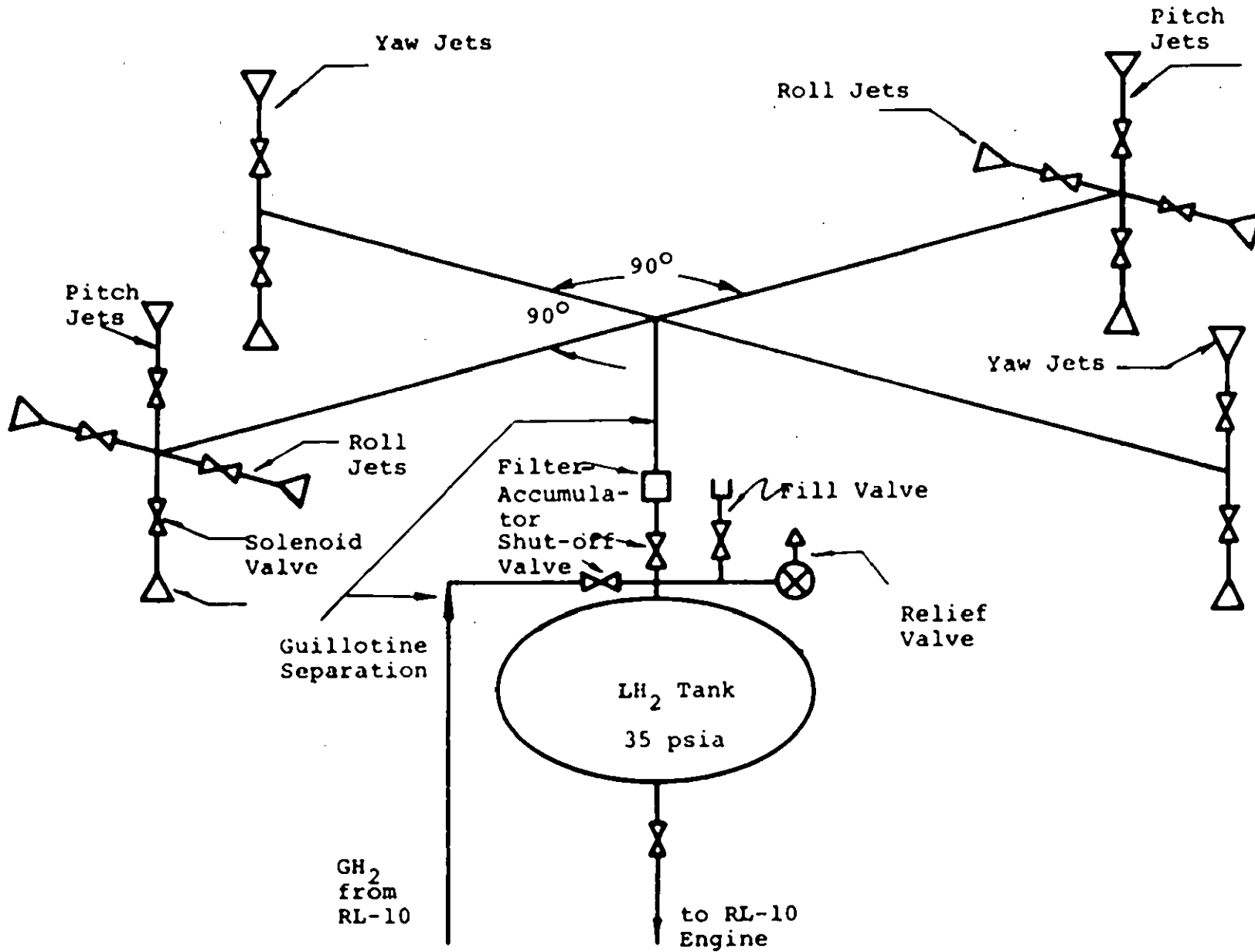


FIGURE 4.5-1. ATTITUDE CONTROL SYSTEM.

propellant the attitude control gas jets should use it. Thus, a separate line from the tank is provided that will supply all gas jets with hydrogen. It is not known in what phase or phases the hydrogen will flow to that line from the tank in zero gravity conditions. However, the uninsulated 3/16 inch lines to gas jets, each 10 feet long, and the uninsulated filter-accumulator tank of 1/2 gallon capacity will insure that all hydrogen will reach the jets in gaseous form at a temperature somewhere between -300° and $+160^{\circ}$ F (160° R and 620° R).

Specific Impulse. The varying temperature of hydrogen will result in a variation of specific impulse (I_s) as calculated from the equation:

$$I_s = \frac{c}{g} = \frac{1}{g} \sqrt{\frac{2k\bar{R}g}{(k-1)M} T_c \left[1 - \left(\frac{P_e}{P_c}\right)^{\frac{k-1}{k}} \right]} \quad (4.5-4)$$

where,

c = effective exhaust velocity, ft/sec

g = 32.2 ft/sec²

k = specific heat ratio of H₂

\bar{R} = universal gas constant, 1545.4 ft-lb_f/°R-lb_m

M = molecular weight of H₂

T_c = chamber temperature, °R

P_e = exit pressure, psia

P_c = chamber pressure, psia

By designing the gas jet nozzle with a 60:1 expansion area ratio the value of

$$\frac{P_e}{P_c} = \text{negligible, and therefore}$$

$$\left(\frac{P_e}{P_c}\right)^{\frac{k-1}{k}} \rightarrow 0$$

Substitution of numerical values into the I_s equation produces

$$I_s = 13 \sqrt{T_c} \quad (4.5-5)$$

then for 160°R, $I_s = 164 \text{ lbf} \cdot \text{sec}/\text{lb}_m$

and for 620°R, $I_s = 300 \text{ lbf} \cdot \text{sec}/\text{lb}_m$

Design of Thrusters The above values of I_s will produce variation of thrust (F) of the gas jets according to the equations:

$$F = I_s \dot{W} \quad (4.5-6)$$

$$F = c_F P_c A_t \quad (4.5-7)$$

where, \dot{W} = mass flow rate of H_2 , lb_m/sec

P_c = chamber, pressure, psia

A_t = throat area, in^2

c_F = thrust coefficient, which is calculated from the following equation

$$c_F = \sqrt{\frac{2k^2}{k-1} \left(\frac{2}{k+1}\right)^{\frac{k+1}{k-1}} \left[1 - \left(\frac{P_e}{P_c}\right)^{\frac{k-1}{k}}\right] + (P_e - P_a) A_c} \quad (4.5-8)$$

in which P_e is a very small number and, hence, the equation abbreviates to

$$c_F = \sqrt{\frac{2k^2}{k-1} \left(\frac{2}{k+1}\right)^{\frac{k+1}{k-1}}} = 1.8 \quad (4.5-9)$$

However, a more conservative value of 1.7 for c_F was adopted.

The pressure drop calculations show that GH_2 will reach the gas jet chamber at a pressure of 10-20 psia. Sizing the gas jet for $P_c = 10$ psia and $I_s = 164$ sec and selecting the gas jet thrust level as $F = 0.2 \text{ lb}_f^*$ we obtain

$$\dot{W} = 0.00122 \text{ lb}_m/\text{sec}$$

$$A_t = 0.0117 \text{ in}^2$$

$$A_c = 60 A_t = 0.702 \text{ in}^2$$

The above values for A_t and A_c were used in the design of the gas jets shown in Fig. 4.5-2.

Each gas jet pair includes two independent solenoid-operated valves mounted back to back. Each gas jet must be preceded by a flip-flop circuit so that the actuation voltage is relatively independent of the individual gas jet characteristics. It is estimated that each gas jet pair will weigh 0.15 lb.

The chamber pressure variations will result from changes of pressure in the cryogenic LH_2 tank and in the filter-accumulator where the varying quality of $\text{LH}_2 - \text{GH}_2$ mixture will change into GH_2 . The changes in demand for attitude control and changes in heating rates of the filter-accumulator and of the uninsulated tubing leading to the gas jets will further influence changes in the chamber pressure.

* This value is a scale-up version of the Surveyor spacecraft gas jets which had a thrust of $0.057 \text{ lb}_f + 30\% - 10\%$ [2].

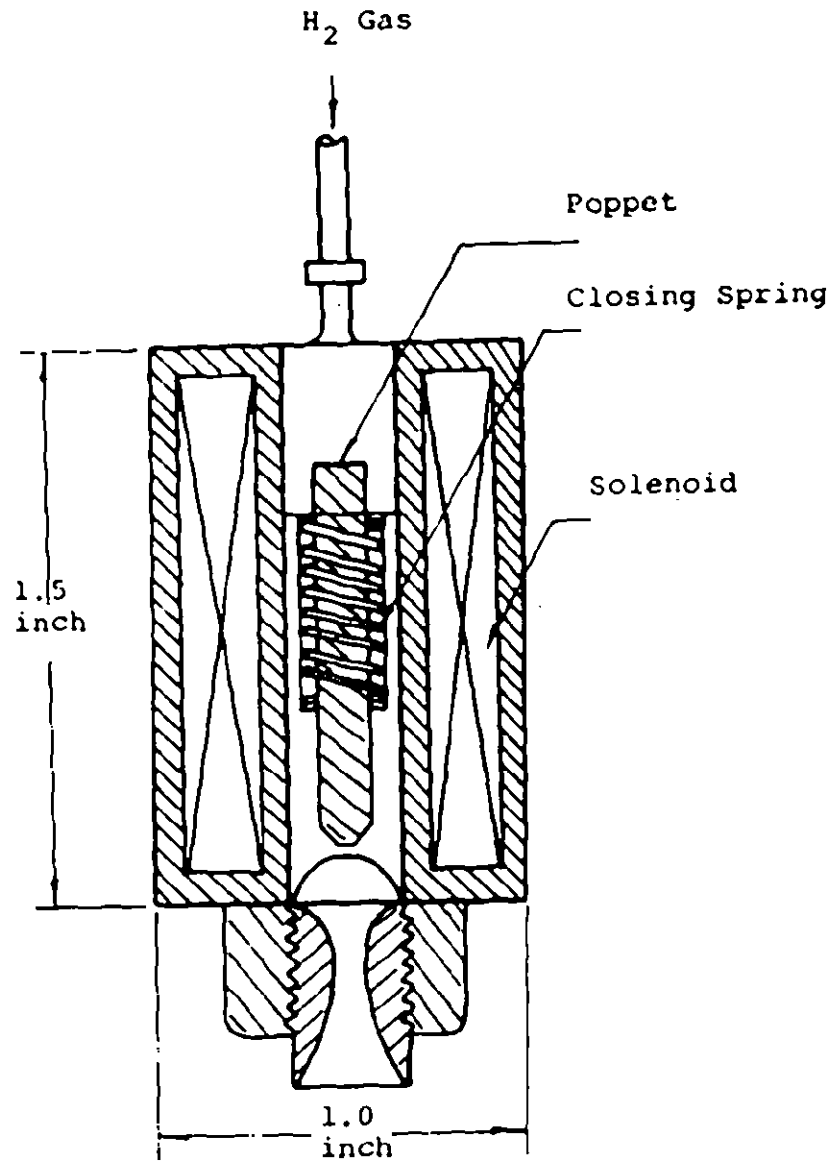


FIGURE 4.5-2. ATTITUDE CONTROL GAS JET THRUSTER

The changes in chamber pressure and the changes of specific impulse will, naturally, cause changes in the thrust levels which will be between 0.2 and 0.4 lb_f . As the radius of the gas jets from the center of gravity is 117 inches the moment capability of the attitude of each jet is between 23.4 and 46.8 in-lb. When jets are used as couples (i.e. when the jet on the other side of c.g. is actuated at the same time) the moment capability is doubled.

By comparison the Surveyor spacecraft (which was six times lighter than the lunar logistics vehicle) had the moment capability of the attitude jet system about each axis of about 4-7 in-lb. Surveyor used GN_2 ($I_s = 60$ sec) in an amount of 4.5 lb. Its nitrogen budget expressed in figures of total impulse was 66.5 lb_f -sec + 13.9 lb_f -sec for 3 σ . This was equivalent to

$$\frac{80.4 \text{ } lb_f\text{-sec}}{60 \text{ } lb_f\text{-sec}/lb_m} = 1.34 \text{ } lb_m \text{ of } GN_2. \quad (4.5-10)$$

This was only 27.9% of the 4.5 lb_m . The value 1.34 lb_m included 0.45 lb_m for ullage and 0.086 lb_m of nitrogen for leakage. The hydrogen budget for LLV jets is shown in Table 4.5-1.

The operating temperature of GN_2 gas jets was in Surveyor [16] between $-40^\circ F$ and $+150^\circ F$ which was the cause of variation in the specific impulse, thrust, and moment of each jet. These variations were not as pronounced as in the present case of GH_2 jets.

Analysis of GH_2 System. The unpredictable thrust and moment

TABLE 4.5-1 GH_2 BUDGET FOR ATTITUDE CONTROL JETS

Event	Impulse/Event $\text{lb}_f\text{-sec}$	No. of Events	Total Impulse $\text{lb}_f\text{-sec}$
Rate dissipation $5^\circ/\text{sec}$ (separation from Centaur)	33	1	33
Sun acquisition	21	3	63
Roll maneuvers	12	6	72
Star mapping	9	3	27
Canopus acquisition	9	3	27
Yaw maneuver	9	3	27
Post midcourse rate dissipation	36	3	108
Coast attitude	160	-	160
Leakage of GH_2	300	-	300
Contingencies		-	200
		Total	<u>1017</u>

$$\text{GH}_2 = \frac{1017 \text{ lb}_f\text{-sec}}{164 \text{ lb}_f\text{-sec}/\text{lb}_m} = 6.2 \text{ lb}_m$$

levels of the gas jets will cause unpredictable changes in:

- (a) mass fraction/cycle (eq. 4.5-1)
- (b) angular impulse (eq. 4.5-2).

The lowest thrust level, however, must still permit the execution of the commanded angular maneuver considering the maximum gyro error.

For pitch, yaw, and roll control the desired attitude is either set in a gyro before flight, acquired by the sensing devices, or telemetered from the ground. This desired attitude may be constant, or may vary according to a preset program.

The current attitude signal is fed back to a synthesizer which computes attitude error, θ . The attitude error is differentiated to give rate of change of attitude $\dot{\theta}$. Finally, the signal $\theta + K\dot{\theta}$ is relayed to a switch; (K is a positive number, typically 0.1 sec). If this signal exceeds a threshold value, it activates a switch for right (if positive) or left (if negative) "rudder"; (the "rudder" is a pair of gas jets which produces a torque, Figure 4.5-1).

Using the sequence of rotations shown in Figure 4.5-3, the spacecraft fixed rates are given in terms of Euler rates and angles (θ, ψ, ϕ)

$$\Omega_x = \dot{\theta} + \dot{\phi} \sin \psi$$

$$\Omega_y = \dot{\psi} \cos \theta - \dot{\phi} \cos \psi \sin \theta$$

$$\Omega_z = \dot{\psi} \sin \theta + \dot{\phi} \cos \psi \cos \theta$$

Considering that the moments of inertia are approximately equal and that the normal body rates are considerably less than 0.1

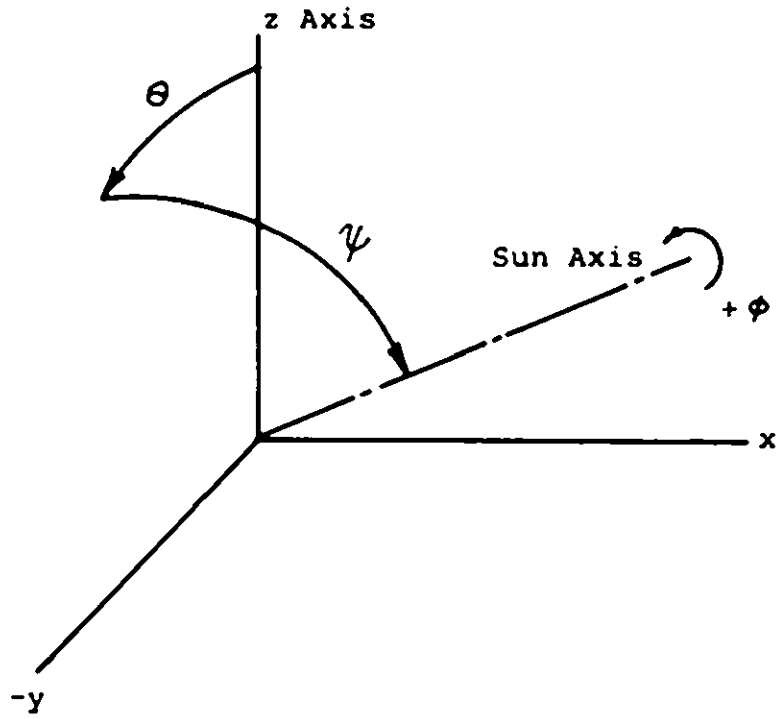


FIGURE 4.5-3. SEQUENCE OF ROTATION FOR EULER EQUATIONS

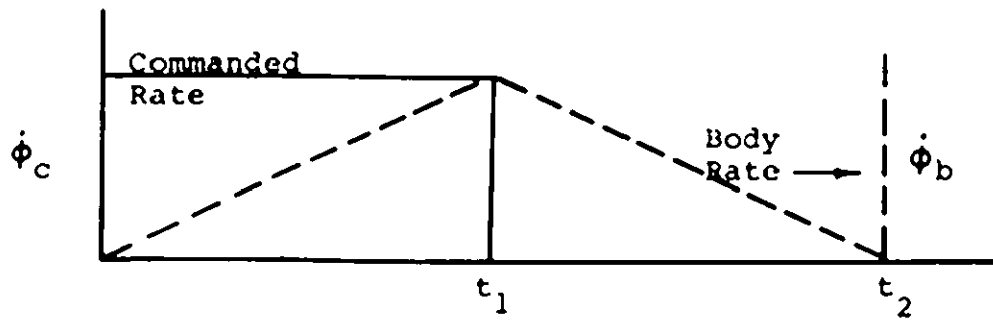


FIGURE 4.5-4. COMMANDED AND BODY RATES vs TIME

rad/sec during the coasting phase, and also that for the normal case where the inertial reference and fixed body reference are in near coincidence (i.e. θ , ψ , and ϕ are small numbers), the body rate equation is

$$\begin{aligned}\Omega_y &= \dot{\psi} \\ \Omega_x &= \dot{\theta} \\ \Omega_z &= \dot{\phi}\end{aligned}$$

The simplified system response to the attitude control commands consists of essentially three parts: (1) The spacecraft moves from zero velocity to the command rate $\dot{\phi}_c$; (2) There is a coasting period; and (3) return to zero velocity. GH_2 is consumed during the first and third parts of the response and consumption is directly proportional to $\dot{\phi}_c$, so it is always desirable that $\dot{\phi}_c$ be kept as small as possible. For large angular maneuvers, the time required for the first and third parts of the response is small compared to the second or coasting period. Thus, the maneuver time could be approximated by

$$t_\phi = \phi / \dot{\phi}_c$$

An error signal in excess of the set dead-band level is applied to a limiting circuit which prevents gas jet operation when a preset angular rate is achieved, thus conserving GH_2 as much as possible and making it possible to use this system of greatly varying specific impulse and thrust.

The main advantage of this system is the partial utilization

of the waste boil-off from the LH_2 tank and that GH_2 has a specific impulse, several times greater than GN_2 .

In addition, any failures of gas jet thrusters could be corrected by firing the RCS bipropellant thrusters.

The growth potential of the GH_2 jet system lies in the possibility of elimination of the RCS thrusters by increasing the thrust level of each gas jet. In this case the moment realized with the gas jets should be as high as the moment realized with the RCS engines. This would reduce the number of propulsion devices while more fully utilizing the waste boil-off of both LH_2 and LOX.

4.6 Propulsion Weights, Power Requirements, and Costs

Weights. Table 4.6-1 shows the overall propulsion system weights which amount to 7470 lbs needed to land LLV on the moon.

The retro system weight is 6727.3 lbs, which consists of 6000 lbs of propellants (LOX 5000 lbs and LH_2 1000 lbs), 665 lbs of inerts, 20 lbs of pyrotechnics (explosive severance devices), and 42.3 lbs of contingencies.

The vernier and reaction control system weight is 673.6 lbs, which consists of 400 lbs of propellants (154 lbs of monomethyl hydrazine, MMH, and 246 lbs of nitrogen tetroxide, N_2O_4), 253.6 lbs of inerts, and 20 lbs of contingencies.

The helium sub-system providing gaseous helium to the RL-10 engine and for the pressurization of the MMH and N_2O_4 tanks weighs 41.1 lbs. This system contains 2.5 lbs of helium under pressure.

The attitude control system weighs only 28 lbs which consists of the hardware only. The 6 lbs of GH_2 gas is included in the RL-10 propellant (in the form of LH_2).

Power. Table 4.6-2 tabulates the power and energy requirements for the propulsion system needed to land the spacecraft on the moon. Time of each event is multiplied by the wattage to obtain the energy.

The circulators for the cryogenic propellants will be used only occasionally for 30-60 seconds.

The attitude control jets will be actuated, at least every 10 minutes. However, before and after each space maneuver this actuation will be much more frequent.

TABLE 4.6-1. PROPULSION WEIGHTS

1. Retro System

RL10A-3-3 engine -----	295 lbs
lines, fittings, valves, instrumentation, LOX evaporator, and their insulation-----	40
LH ₂ tank (for min. thickness of 0.032 inch; good for 50 psia)-----	95
1 inch insulation of LH ₂ tank-----	71
circulator in the LH ₂ tank and valving on the tank--	15
4 LOX tanks (for minimum thickness of 0.032 inch; good for 100 psia) 16 lbs x 4 -----	64
0.7 inch insulation of LOX tanks -----	50
circulators in the LOX tanks and valving on the tanks--	35
propellants (LOX + LH ₂) includes ventage, boil-off, GH ₂ for gas jets, and unusable propellants -----	6000
explosive severance (explosive bolts, guillotines bolt ejectors, flexible linear-shaped charges, and electrical harness)-----	20
contingencies	42.3
Sub-total	<u>6727.3</u>

2. Vernier and RCS Systems

2 tanks for fuel and oxidizer, 21.9" diam. spheres, each 11.5 lbs -----	23
insulation of the tanks-----	5
valve assemblies -----	3
propellants -----	400
lines, fittings, and their insulation-----	25
thermal control and protection from RCS plumes---	14
16 verniers, each 5.25 lbs-----	84
12 RCS, each 3.46 lbs -----	41.6
4 mouse houses (two 15 lbs and two 14 lbs each)---	58
contingencies	20
Sub-total	<u>673.6</u>

3. Helium Sub-System

sphere, 14.2" diam. -----	27.8
valve assembly (includes 2 check valves, filter, squib valve, quick disconnects for fuel and oxi- dizer, and outlet ports for fuel and oxidizer)---	2.8
gaseous helium (2.42 lbs for verniers and RCS and 0.08 lbs for RL-10)-----	2.5
lines and fittings -----	5.0
contingencies	3.0
Sub-total	<u>41.1</u>

TABLE 4.6-1. (Cont'd)

4. Attitude Control System

12 cold gas jets, 2 lbs per pair (including solenoid valves) - - - - -	12
piping, valving, and fittings - - - - -	14
contingencies	2
Sub-total	<u>28</u>

Total Propulsion 7470 lbs

NOTE: Piping, valving, and pyrotechnic severance were estimated using references 20 and 21.

TABLE 4.6-2. PROPULSION POWER AND ENERGY REQUIREMENTS

	Watts	Watt-sec
1. Circulators for Cryogenic Liquids		
LH ₂ : (1 min/12 hrs) x 120 hr x	(30)	18,000
LOX: 4 x (1 min/12 hrs) x 120 hr x	(72)	173,000
2. Posigrade--4 RCS		
4 line heaters: 4 x (15 min) x	(10)	35,000
heat 4 RCS: 15 min x	(7)	6,300
1 He valve: 1 sec x	(28)	28
fire 4 RCS: 4 x (24 sec) x	(15)	1,440
3. Attitude Control Jets		
6 jets: 6(1 sec/10 min)120 hrs x	(28)	121,000
4. Three midcourse corrections (20, 40, 55 hrs)		
4 line heaters: 3 x 4 x (30 min)x	(10)	215,000
heat 12 RCS: 3 x 12 x (30min) x	(15)	975,000
fire 4 RCS: 3 x 4 x (160 sec) x	(15)	28,800
fire 8 RCS: 3 x 8 x (16 sec) x	(15)	5,800
5. Preparation for Retro Fire		
4 line heaters: 4 x (30 min) x	(10)	72,000
heat 12 RCS: 12 x (30 min) x	(7)	151,000
heat 16 Verniers: 16 x (30 min) x	(17.5)	505,000
fire 12 RCS: 12 x (10 sec)	(15)	1,800
5. Retro Fire		
Prestart: 50 sec x	(62)	3,100
Ignition--Start: 10 sec x	(190)	1,900
fire Retro: 250 sec x	(120)	30,000
fire 4 RCS(roll): 4 x (100 sec) x	(15)	6,000
6. Descent to Hover, Hover, and Final Descent		
fire 16 Verniers: 16 x (40 sec) x	(28)	17,900
fire 12 RCS: 12 x (40 sec) x	(15)	7,200
Total Energy Required		<u>2,375,268</u>

The posigrade maneuver, the three midcourse corrections, the preparation for the RL-10 engine to fire (including the ullage maneuver), the descent to hover, the hover, and the final descent to touch-down will occur in the above sequence.

The total energy requirement is 2375.3 kw-sec or 0.64 kw-hr. The highest peak of power requirement starts approximately 35 minutes before landing on the lunar surface.

Cost. Table 4.6-3 gives the estimated cost of all propulsion systems including propellants. The purchase cost of propulsion items per spacecraft amounts to \$810,000. The qualification costs of some of the equipment (RL-10, circulators, cryogenic tanks, LOX evaporator, Vernier, GH_2 jet, and stability motor) amounts to \$11,000,000. This figure divided by eight spacecraft results in approximately \$1,390,000 which when added to the purchase cost gives a grand total of \$2,200,000 per spacecraft.

The stability solid propellant motors may not be required because the verniers may be sufficient for the stabilization of the spacecraft at touch-down (See Section 4.3). Neither the total cost, nor the total weight of propulsion will change as the small figures in cost and weight for these motors are included in contingencies.

TABLE 4.6-3. ESTIMATED COST IN MILLIONS OF DOLLARS

System	No: of Main Items	Purchase Cost/S.C.	Development and Qualification	Total Cost/S.C.
Retro	1	0.5	6	1.25
Vernier	16	0.2	4	0.7
RCS	12	} 0.1	1	0.23
GH ₂ Jet	12			
Stability Motors	4	0.01	0.1	0.02
Totals		0.81	11.1	<u>2.2</u>

4.7 Trade-off Studies of Alternative Propulsion Systems

A lunar landing vehicle which is designed for a soft landing on the surface of the moon must have, at least, two propulsion systems. These are:

1. Main retrograde (retro) rocket which will reduce the great velocity of the vehicle approaching the lunar surface to a small velocity;
2. Small controllable rockets which will permit space maneuvers (mid-course corrections, posigrade and ullage maneuvers, stabilization, attitude control), hover above the landing site and the final descent to touchdown, and also in the future a hop from the landing site to a better location.

Main Retro Criteria. The main retro could be a solid or liquid rocket with a thrust as high as possible to reduce the gravity loss during burning of the retro. The characteristic ΔV_{ch} equation shows that an ideal V_{id} would be the best with respect to the weight of propellant(s):

$$\Delta V_{ch} = \Delta V_{id} + \int_{t_0}^{t_f} g_L (\cos \theta) dt \quad (4.7-1)$$

$$\Delta V_{ch} = c \ln \frac{m_0}{m_0 - m_p} \quad (4.7-2)$$

$$c = 32.17 I_s \quad (4.7-3)$$

where, g_L = local gravity of the moon, ft/sec²

t = burning time (from start, t_0 , to finish, t_f), sec

θ = angle between flight path and the local vertical, degrees

c = effective exhaust velocity, ft/sec

I_s = delivered specific impulse, lb_f-sec/lb_m

m_0 = mass of the spacecraft at start of the retro burn, lb_m

m_p = mass of propellant used, lb_m

It is evident that the gravity loss which is the second term in equation 4.7-1 is the smallest either when the burning time is short or if the angle θ is approaching 90°. The latter approach is achieved during low energy missions (120 hour flight time) when the impact with the lunar surface becomes almost tangential.

A limitation to the high thrust, however, is the requirement that the axial acceleration of the spacecraft will not exceed 6 g i.e. 193 ft/sec². During the burn of the retro the mass of the spacecraft is decreasing because of the propellant consumption. Thus, a constant thrust of the retro will gradually increase the acceleration of the spacecraft. When the 6 g level is approaching the thrust level should be lowered to satisfy the equations

$$F = 6W \quad (4.7-4)$$

$$W = 32.17m \quad (4.7-5)$$

where, F = Thrust, lb_f

W = instantaneous earth weight of spacecraft, lb_f

m = instantaneous mass of the spacecraft, slug

Another very important criterion for the retro rocket is the specific impulse, I_s , which should be as high as possible. A high I_s requires for the same ΔV (equation 4.7-2 and 4.7-3) less propellant mass, or weight, W_p , in order to obtain the required total impulse:

$$I = \int_{t_0}^{t_f} F dt = \int_{W_0}^{W_f} I_s \dot{W} dt \quad (4.7-6)$$

where $\dot{W} = \frac{dW_p}{dt}$

I = total impulse, lb_f -sec

Further criteria for the main retro were:

- (1) The rocket should require none or only little development,
- (2) the rocket including propellants should be inexpensive,
- (3) should be ready available by 1972,
- (4) should be, preferably, small in size,
- (5) should have thrust vector control,
- (6) should be reliable, and
- (7) should be throttleable, if possible (for site redesignation during retro burn).

Taking the above under consideration many rocket power plants were used in trade-off studies.

Retro Trade-off Studies Table 4.7-1 shows the main contenders for the retro rocket. Other readily available rocket power plants were considered, but were eliminated early. These were: Agena engines, LM Ascent engine, several military solid propellant motors (classified), and the Apollo SM main engine.

TABLE 4.7-1 TRADE-OFF ANALYSIS OF RETRO CANDIDATES

Type	Propellant	I_s	F, lb_f	Total Propulsion Weight, lb
RL-10A-3-3	LOX + LH ₂	444	15,000	7550
RL-10A-3-7	LOX + LH ₂	444/434	15,000/2,000	7470
SRM-MSB	Solid	289.8	36,800/32,000	8600
Surveyor 4 + 1	Solid	289.8	36,800/9,200	8800
Surveyor 3 + 1	Solid	289.8	27,600/9,200	8900
LM Descent	N ₂ O ₄ + Aerozine	305-292	10,000/1,000	8900

The Agena engine No. 8096 (single restart) and No. 8247 (multiple restart) weighing 290 lbs and 310 lbs, respectively, each having a thrust of 16,000 lb_f were eliminated because of low specific impulse (293 lb_f-sec/lb_m) and lack of throttleability.

The LM Ascent engine was eliminated because of a low thrust level.

Several military solid motors had a nominal thrust level of about 30,000 lb_f but the burning time and the total impulse were either too low or too high and the thrust curves were occasionally progressively increasing to a level which was not compatible with the 6g constraint.

The Apollo SM main engine requiring heavy tanks for the pressure-fed propellants was considered but because of the high weights was rejected.

Table 4.7-1 shows the main retro candidates arranged in order of total propulsion weights for the 60-hour high energy mission. The weights include not only the retro propulsion but also propulsion for space maneuvers, attitude control, hover, and final descent to landing; hop, however is not included. The trade-off analysis required all these weights because, some retro power plants needed auxiliary propulsion for pitch, yaw, and roll control and also a longer duration of burn from retro burn-out to landing.

NASA-MSD has preformed studies using RL 10A-3-3 engine, the descent engine and the Surveyor motors (in cluster of three or four motors as the first stage and one motor as the second stage). These studies were presented in numerous graphs to the NASA-ASEE Summer Institute [22, 23, 24]. These studies were then further

refined and their results reassessed.* Optimization of stages was performed using the calculus of variation with the Lagrange multiplier.

In addition a study was made of another type of inexpensive solid rocket motor named SRM-MSM which is a military rocket requiring the following changes.

(1) An extension of the nozzle to increase the specific impulse.

(2) A "dual thrust" rearrangement of the propellant grain. A "wagon wheel" configuration of the perforation, without changing the chemical composition of the propellant, can be obtained by inserting a proper core or mandrel into the chamber during casting of the propellant slurry [25,26].

The SRM-MSM has a thrust vector control using fluid injection into the nozzle for pitch and yaw and a solid gas generator for roll control.

In the beginning the thrust of SRM-MSM is up to 36,800 lb_f and after 40 seconds of burn it drops to 32,000 lb_f to meet the 6g maximum constraint at the time when the mass of the spacecraft has decreased after most of the solid propellant has been consumed. The total burn time of the motor is 57 seconds, which is the least time of burn of all retro candidates and, hence, accounts for the smallest gravity loss during any high energy mission.

* Help of M. Lausten of NASA-MSM in the selection of the main retro rocket is gratefully acknowledged.

For low energy missions the SRM-MSD would have to be off-loaded or its thrust termination device for an early burn-out applied.

Table 2.2-1 shows that the RL-10A engines have a much higher specific impulse than the other candidates. However, because the thrust level of the RL-10A engines is much lower than of the SRM-MSD, trade-off and optimization studies were complex. These studies required the following considerations:

(1) total propulsion weight, which is approximately 1,000 lbs lower for the RL-10A system;

(2) complexity, which is much lower in case of the SRM-MSD system;

(3) cost of the system (including development and qualification cost), which is greater for the RL-10A system but is still acceptable;

(4) bulkiness which is much greater in case of the RL-10A system;

(5) reliability, which is lower for the RL-10A system (because of rotating machinery, cryogenic propellants, and presence of large surfaces of tanks which may be punctured by meteoroids).

Of the candidate retro systems the SRM-MSD rocket is probably the most reliable. However, the requirement for a 2500 lbs payload could be met only when RL-10A system is used. As the presently anticipated payload is not too bulky there is enough space for the voluminous RL-10A propulsion. Thus, the trade-off studies indicated that the RL-10A system must be chosen.

The reason why the model RL-10A-3-3 was selected is given in section 4.2. A cluster of two of these engines to reduce the gravity loss during the high-energy missions was also considered but no overall weight gain was achieved.

Small Controllable Rockets' Criteria. The necessity of these rockets in the LLV spacecraft is given in the beginning of this section. The criteria for the selection of these rockets were as follows: (1) ready available, (2) high specific impulse, (3) storable propellants, (4) fine controls, (5) low cost (6) high reliability, (7) very high thrust flexibility, from 1 to 2500 lb_f , (8) little development, if any, (9) rapid response to command, (10) pressure feed to the thrust chamber, and (11) little power and energy requirements, (12) negligible thermal problems.

The latter requirement was further subdivided as follows: (a) no impingement, or at least a negligible impingement of hot rocket plumes (Fig. 4.7-1) on the equipment and structures of the spacecraft, (b) avoidance of freeze-up of the storable propellants, and (c) heating of engines using a propellant from the hydrazine family to prevent "spiking" (see Section 4.3).

In general all the above criteria could be met with one propulsion system except No. 7 and No. 12a criteria.

The reason for the necessity of a very high thrust flexibility are as follows. Very low thrust levels are needed for the attitude control of the spacecraft during coasting (see Section 4.5) On the other hand fairly high thrust levels of 2000 lb_f are needed for the descent to hover (Fig. 4.3-2). Intermediate thrust levels are needed to hover and to descent from hover. Other space

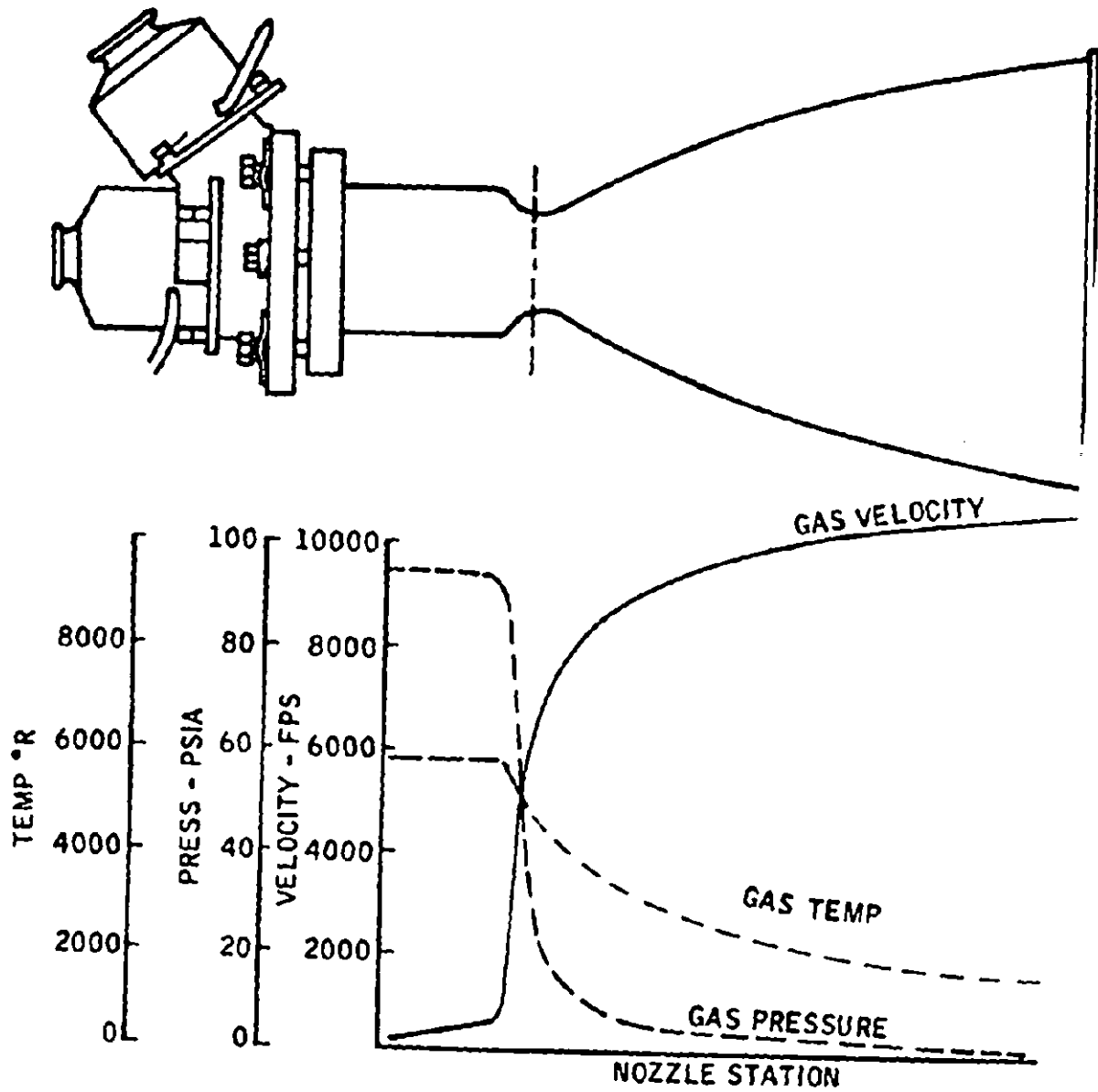


FIGURE 4.7-1 THERMAL CONSIDERATION IN VERNIER DESIGN
 (derived from N.A.-Rockwell training manual)

maneuvers (except retro) can be accomplished with either fairly high or intermediate thrust-level engines (see Section 4.3 and 4.4).

The thermal criterion No. 12a could not easily be met with larger engines performing space maneuvers (mid-course correction etc.) while the LH₂ and LOX tanks were still attached. Hence, for the space maneuvers intermediate size engine had to be used and canted, at least 10° (see Section 4.4).

The possibility of using RCS engines of intermediate thrust levels for both the space maneuvers and attitude control during coasting was considered. This would eliminate the 12 hydrogen jets. However, when the decision was made to utilize LH₂ boil-off for these jets, weight saving and redundancy was achieved.

The hydrogen gas jets have also a growth potential to substitute the RCS engines. This is not feasible in the present design because the LH₂ tank is jettisoned well above the lunar surface making the gas jets inoperable for further controls.

Studies were made whether the cold gas jets could be replaced by hot gas jets (i.e. by very small monopropellant or bipropellant RCS). All these jets, however, require a location on the legs of the LLV (see Section 4.5) to obtain a moment during thrusting. If a storable propellant had to be conveyed so far from the main body of the spacecraft a problem of propellant freezing would be aggravated.

Trade-off Studies of Small Rockets. Taking the above under consideration three auxiliary propulsion systems were decided on*;

* Help of Norman Chaffee in these consideration is gratefully acknowledged (see also Ref. 27).

- (1) larger engines called verniers, (at least one close to each leg);
- (2) medium size engines called RCS (at least two close to each leg);
- (3) very small thrusters for the attitude control system during coasting, (at least two close to each leg).

Section 2.2 lists all the candidates for the auxiliary propulsion systems and the reason for the final selections.

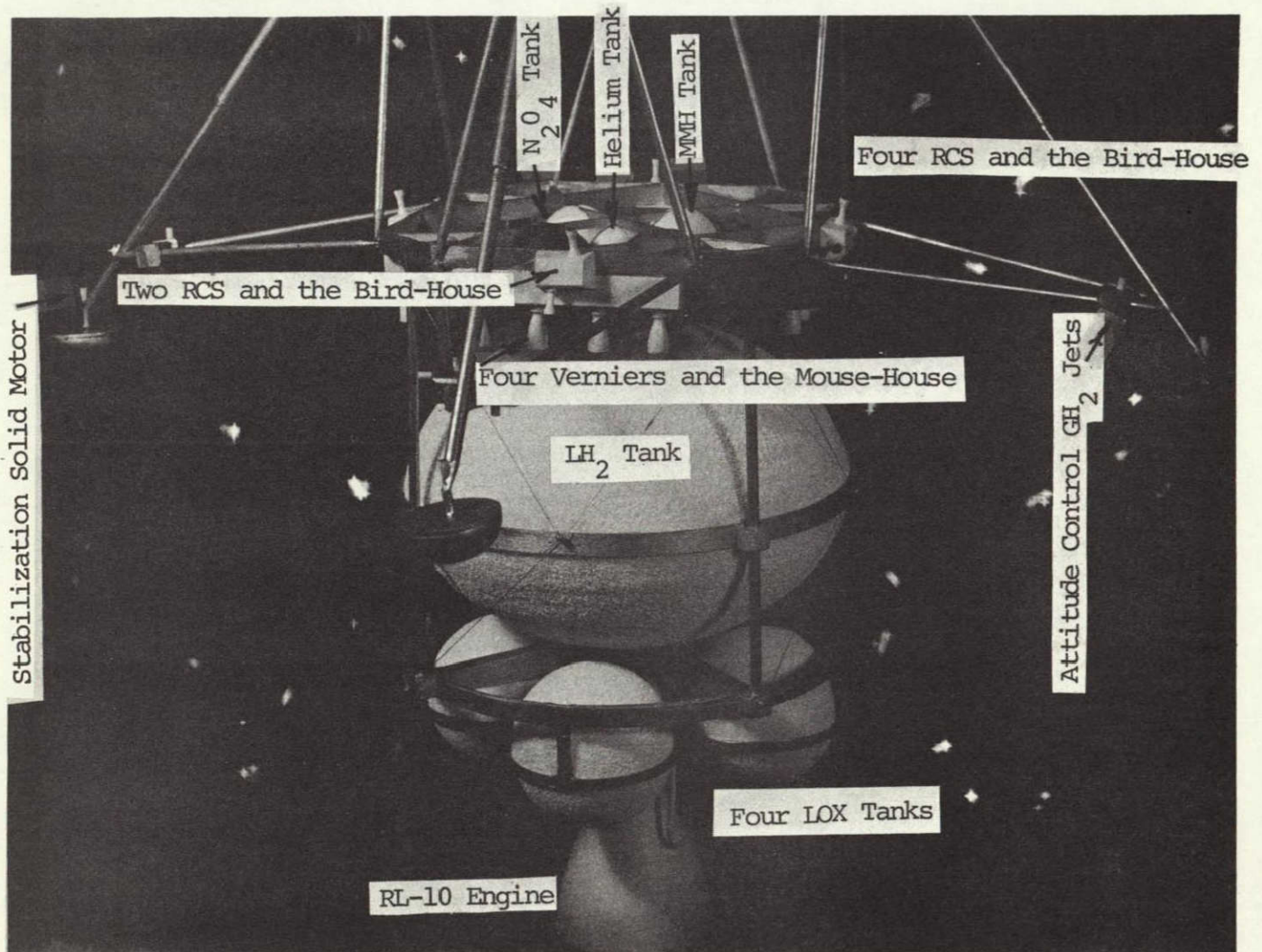


FIGURE 4.7-2. ALL PROPULSION SYSTEMS
(Photograph of a Model)

REFERENCES

1. Pratt & Whitney Aircraft, RL 10 Installation Handbook, July 1, 1966.
2. Pratt & Whitney Aircraft, Discussion of the RL 10 Engine Applied to Apollo Propulsion, PWA FR-918, March 12, 1964.
3. Pratt & Whitney Aircraft, RL 10 Engine for Maneuvering Spacecraft Propulsion, PWA FR-1329, March 17, 1965.
4. Pratt & Whitney Aircraft, Preliminary RL 10A-3-3 Model Specification No. 2265, August 25, 1964.
5. Bullard, B. R., Cryogenic Tank Support Evaluation, Lockheed Missiles & Space Co., Sunnyvale, California, NASA CR-72538, LMSC K-16-68-1, April 15, 1969.
6. Lockheed Missile & Space Co., Thermal Protection System for a Cryogenic Spacecraft Propulsion Module, NASA CR-54879, LMSC-A794993, Vol II, Sunnyvale, California, November 15, 1966.
7. Lockheed Missile & Space Co., LH₂ Storability in Space Propulsion Vehicles, LMSC-685104, Sunnyvale, California, March 14, 1968.
8. Abramson, H. N. (editor), The Dynamic Behavior of Liquids in Moving Containers with Applications to Space Vehicle Technology, prepared by the Southwest Research Inst. for NASA, 1966, contract NASr-94(07).
9. Ring, E. (editor), Rocket Propellant and Pressurization Systems, Prentice-Hall, Inc., Englewood Cliffs, New Jersey, 1964.
10. Hendel, F. J., "Advanced Rocket Propulsion," Chemical Engineering, pp. 131-148, April 3, 1961.
11. Vaugham, C. A., "Apollo Reaction Control Systems," AIAA paper No. 68-566, 4th Propulsion Joint Specialist Conference, Cleveland, Ohio, June 10-14, 1968.
12. The Marquardt Corporation, D. W. Fore and D. C. Sund, "High Pressure Testing of a Modified Model R-4D Engine," MIR#122, October 5, 1967.
13. Hughes Aircraft Co., Surveyor, Final Engineering Report, Vol II, System Design, JPL Contract 950056, June 1968.
14. NASA, "Pressure Vessel Data Sheets," Vol I and II.

15. Pohl, H. O., "Reaction Control Systems" in Manned Spacecraft, Engineering Design and Operation, Purser, E. P., Faget, M. A., and Smith, N. F., Fairchild Publications, Inc., New York, 1964.
16. Hughes Aircraft Com, Surveyor, Final Engineering Report, Vol I and II, System Design, JPL Contract 950056, June 1968, p. 4-1 through 4-76.
17. Olds, R. H., "Attitude Control and Station Keeping of a Communication Satellite in a 24-hour Orbit," AIAA J., 1, 852-858 (1963).
18. White, J. B., "Meteoric Effects on Attitude Control of Space Vehicles," ARS J., 32, 75-76 (1962).
19. Gaylord, R. S., "Differentiating gas Jet for Space Attitude Control," ARS J. 31, 75-76 (1961).
20. Howell, G. W. and Weathers, T. M. (editors), Aerospace Fluid Designer's Handbook, Vol. I and II, revision B, prepared by TRW Systems Group for the Air Force RPL, Air Force Systems Command, Contract No. AF 04(611)-8385 and AF 04(611)-11316, RPL-TDR-64-25, March 1967.
21. Hendel, F. J., Explosive Ordnance for Space Vehicles and Missiles, Blake Printery, San Luis Obispo, Calif., 1969.
22. Abel, R.W. and Bristow,, (both of NASA-MSCF), Presentation to NASA-ASEE Summer Faculty Institute, University of Houston, June 1969.
23. Launey, H. G. and Austin, L. D., Jr., "Preliminary Trajectory and Propulsion System Requirements Analysis for an Unmanned Lunar Logistics Vehicle Utilizing a Solid Retro Motor". Internal Note MSC-EX-69-006, April 4, 1969.
24. Launey, H. G. and Austin, L. D., Jr., "Preliminary Trajectory and Propulsion System Requirements Analysis for an Unmanned Lunar Logistics Vehicle Utilizing a Liquid Retro Propulsion System". Internal MSC Preliminary Note, April 1969.
25. Hendel, F. J., "Review of Solid Propellant for Space Exploration", Jet Propulsion Laboratory TM No. 33-254, October 1, 1965.
26. Hendel, F. J., "Chemical Rocket Propulsion Systems," Chemical Engineering, pp. 99-114, March 6. 1961.
27. Chaffee, N. (of NASA-MSCF), Presentation to NASA-ASEE Summer Faculty Institute, University of Houston, June 1969.

5.2 Power System Requirements

Table 5.2-1 provides a summary of the power and energy requirements for the various phases of the mission. The duty times used as the basis for the estimation of the energy requirements are also shown in the table. Table 5.2-2 lists the energy requirements of the different phases of the mission. Figure 5.2-1 is an approximate power profile for the LLV mission.

TABLE 5.2-2
SUMMARY OF ENERGY REQUIREMENTS

<u>Mission Phase</u>	<u>Energy, w-hr</u>
Pre-Launch and Launch	1940
Trans-Lunar	12294
Course Corrections	2054
Descent and Landing	1981
Post Landing	<u>1196</u>
Total	19,465

The total electrical energy requirements for the mission are 19,465 w-hr. Adding ten percent for wiring and conversion losses results in an energy requirement of 21,412 w-hr. If, in addition, a twenty percent margin allowance is added, the total electrical energy requirements become 25,700 w-hr. The average power requirement during the long duration translunar phase is 106 watts plus losses, or about 120 watts.

5.2.1 Peak Power Requirements

The spacecraft peak power requirements occur during the

CHAPTER V
ELECTRICAL POWER SYSTEM

Floyd Calvert

5.1 Introduction

The LLV power subsystem generates, stores, converts, and controls electrical power for distribution to the spacecraft subsystems. The energy requirements are based on the 120 hour time in the translunar phase of the mission. The ground rules specified in the work statement for the power system are:

Existing, flight proven sub-systems and/or components are to be used to the fullest extent possible

Consideration is to be given to extended survival of the power system for periods of up to ninety days

Consideration is to be given to the possibility of using the power system to provide power to the payload

Thus, since development of new equipment is to be minimized, such alternatives as thermionic and dynamic power systems are not considered for the present application. The spacecraft's power system will supply energy at a nominal 29 volts D C. Alternating current power will be supplied either from a central power conditioner or from individual subsystem power conditioning devices.

TABL
ELECTRICAL

SUB-SYSTEM OR COMPONENT	PRE-LAUNCH AND LAUNCH			TRANS-	
	Avg. Load, watts	Duty Time, hr.	Energy w-hr.	Avg. Load, watts	Duty Time hr.
Guidance and Navigation					
Computer and Celestial Sensors	100	5.0	500	20	115.5
Inertial Measurement Unit	100	5.0	500	-	-
Radar plus Radar Ant. Heater	-	-	-	5	115.5
IMU Pulse Torque Assembly	90	5.0	450	-	-
Coupling Data Units	50	5.0	250	50	115.5
Communications and Telemetry	48	5.0	240	31	115.5
Approach TV	-	-	-	-	-
Retro-Engine					
Circulating Pumps; H ₂ O ₂ Tanks Valves	-	-	-	83	0.17
Vernier Engines, (16 units)					
Heaters	-	-	-	-	-
Valves	-	-	-	-	-
RCS Engines, (12 units)					
Heaters	-	-	-	60	0.25
Valves	-	-	-	180	0.0
Attitude Jets	-	-	-	54	0.1
Hypergolic Line Heaters	-	-	-	40	0.2
Squib Devices	← (Use small in				
Transponder	← (Consider				
SUB-TOTALS	1940				
(TOTAL 19,465 w-hr)					

FOLDOUT FRAME 1

SUMMARY

COURSE CORRECTIONS.			DESCENT AND LANDING			POST LANDING		
Avg. Load, watts	Duty Time, hr	Energy, w-hr	Avg. Load, watts	Duty Time, hr	Energy, w-hr	Avg. Load, watts	Duty Time, hr	Energy, w-hr
100	4.5	450	100	3.0	300	-	-	-
100	4.5	450	100	3.0	300	-	-	-
-	-	-	190	0.5	95	-	-	-
90	4.5	405	90	3.0	270	-	-	-
50	4.5	225	50	3.0	150	-	-	-
48	4.5	216	170	3.0	510	48	24	1152
-	-	-	22	1.0	22	22	2	44
-	-	-	-	-	-	-	-	-
-	-	-	250	0.1	25	-	-	-
-	-	-	280	0.5	140	-	-	-
-	-	-	448	0.05	23	-	-	-
180	1.5	270	180	0.5	90	-	-	-
180	0.1	18	180	0.2	36	-	-	-
-	-	-	-	-	-	-	-	-
40	0.5	20	40	0.5	20	-	-	-
battery) →								
load) →								
<u>2054</u>			<u>1981</u>			<u>1196</u>		

FOLDOUT FRAME 2

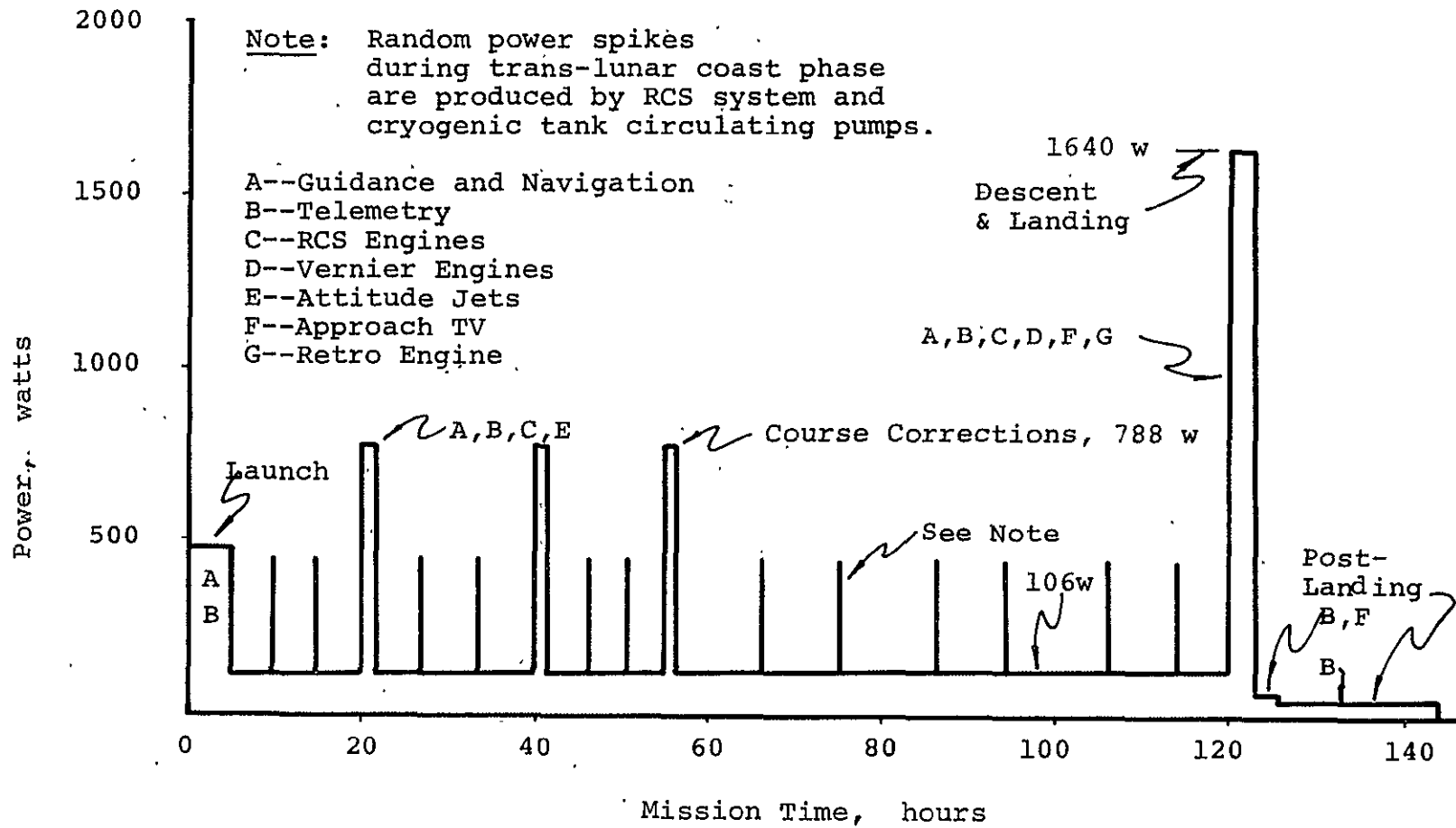


FIGURE 5.2-1 POWER PROFILE (Approximate)

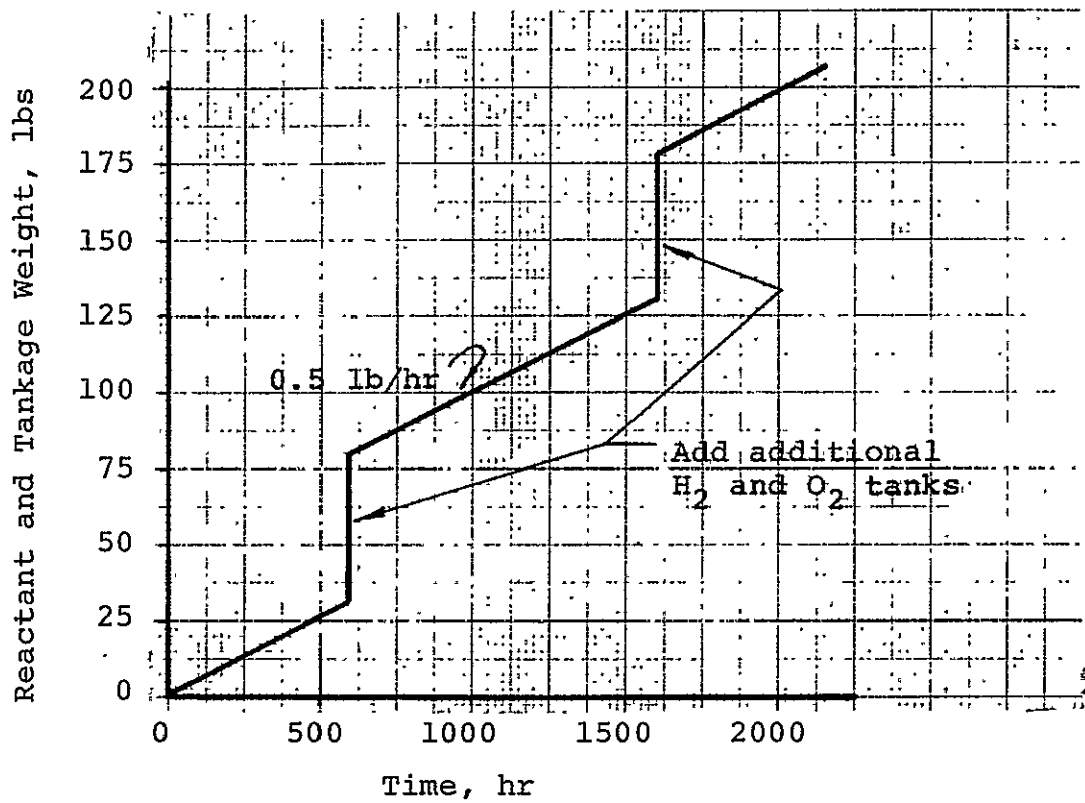


FIGURE 5.2-2 REACTANT AND TANKAGE WEIGHT FOR EXTENDED SURVIVAL (50 watts power)

descent and landing phase of the mission. Table 5.2-3 lists the subsystems which contribute to the power peak for the electrical power subsystem.

TABLE 5.2-3
PEAK POWER

<u>Subsystem</u>	<u>Power, watts</u>
Guidance and Navigation	530
Telecommunications	170
Approach TV	22
Retro Engine	250
Vernier Engines	448
RCS Engines	180
Line Heaters	<u>40</u>
Total	1640

The electrical power system must be able to supply a peak power of 1640 watts. The peak electrical current, at 29 volts, is therefore 57 amperes.

5.2.2 Requirements for Extended Survival

Thermal control calculations (see Chapter VII) indicate that the power required for lunar night survival of the telecommunications and power system are on the order of 50 watts. This power is that required for heater power and/or that required to maintain the telecommunications system at a low operating level. Figure 5.2-2 shows the additional weight of reactants and tanks for extended survival on the surface of the moon (assuming that a Fuel Cell and Battery electrical power system is used).

If the survival time is to be longer than 1200 hours, then a supplementary RTG system (two SNAP-19 modules) would be lighter than the additional weight of reactants and tanks required by a fuel cell system. However, the use of fuel cells is recommended for extended survival since employment of an RTG system involves severe safety, launch, and radiation of electronic component problems.

5.2.3 Payload Support

The importance rating of the payload support criterion has been given a low value in the design of the electrical power system. Fuel cell and RTG power systems are able to provide payload support. (Additional reactants are required for fuel cells.) Solar cell systems may provide some payload support if solar arrays are oriented on the surface of the moon. Support of the payload by solar cell systems during lunar night periods would necessitate use of heavy batteries.

5.3 Candidate Power Systems

Five alternative power systems have been considered and evaluated. The following paragraphs provide a brief description of each of the systems.

5.3.1 Batteries

A battery power system would require three silver-zinc primary batteries. Suitable batteries would be of the type used in the ascent stage of the Apollo LM spacecraft. Each battery will provide 9 kw-hr of energy and is rated 300 ampere-hours at 30 volts. The battery current rating is 50 amperes at 28 volts for 5.92 hours at 80°F. Each battery weighs 130 pounds, [5].

5.3.2 Solar Cells and Battery

This power system concept is based on the use of an orientable solar array or arrays similar to that used on the Surveyor spacecraft. The required solar array area is 30 square feet and the estimated solar array weight is 30 pounds plus 40 pounds for the positioning mechanism. Spacecraft power would be supplied by the solar array during the trans-lunar coast phase. Peak power requirements during the course corrections and descent phases are to be provided by an Apollo LM ascent stage battery of the same description as given in paragraph 5.3.1.

5.3.3 Fuel Cells and Battery

The power generating devices employed in this concept consist of two radiation cooled, capillary matrix type fuel cells as manufactured by the Allis-Chalmers company. Each fuel cell has a nominal power rating of 200 watts at 27 volts dc. Supercritical hydrogen and oxygen are to be utilized. The Gemini RSS two-day

cryogenic tanks are suitable for this application. The hydrogen tank weighs 27.5 pounds and will hold 5.6 pounds of reactant. The oxygen tank weighs 20.5 pounds and will hold 45 pounds of reactant. One fuel cell will supply all the translunar coast phase power; the second fuel cell is redundant.

Peak power loads during the course corrections and descent and landing phases will be supplied by a 300 ampere-hour silver zinc battery of the same description as those in the all battery concept, paragraph 5.3.1.

5.3.4 Radioisotopic Thermoelectric Generators and Battery

This alternative concept employs four SNAP-19 modules which use plutonium 238 as energy source (fuel). Each two-module unit has a power rating of 70 watts for 90 days, [1]. The power rating at the end of five years is 50 watts for each two-module unit. The weight of each two-module unit may be estimated at 105 pounds, [2]. These generators have flown on the Nimbus spacecraft and are expected to be fully qualified for the Pioneer flight by December of 1970. Translunar coast phase power is to be supplied by the RTG units.

Peak power is to be supplied by a 300 ampere-hour battery of the Apollo LM ascent stage type. This battery is described in paragraph 5.3.1.

5.3.5 Fuel Cells

The all fuel cell concept is based on the utilization of two fuel cells each rated at two kilowatts of power. Candidate fuel cells are as follows:

Allis-Chalmers, 2 kw, capillary matrix type, gas/liquid cooled, weight: 169 pounds per module, 100 watts parasitic load

Pratt & Whitney Aircraft, Type PC8B-3, 2 kw, 105 watts parasitic load, weight: 104 pounds per module, liquid cooled, [3].

Two fuel cells are required, one to supply all spacecraft electrical loads and one for redundancy. The Gemini RSS type cryogenic tanks are specified for reactant storage. Noteworthy for this concept is the fact that the magnitude of the fuel cell parasitic load is approximately the same size as the trans-lunar coast phase load. Thus the utilization of the energy content of the hydrogen-oxygen reactants is relatively inefficient during this phase of the mission.

A heat rejection radiator is required for this power system concept.

5.4 Power System Comparison

Table 5.4-1 provides a summary listing of the values for each of the criteria which are considered to be of major importance for this application. Table 5.4-2 lists advantages and disadvantages of the five candidate power systems. Table 5.4-3 lists the weights of the components in the Fuel Cell and Battery concept.

The recommended power system for the Lunar Logistics Vehicle is the Fuel Cell and Battery system. Although the Fuel Cell and Battery (FC/B) concept is slightly heavier than the Solar Cell and Battery (SC/B) concept, it is the preferred choice because of the greater flexibility permitted in the structural

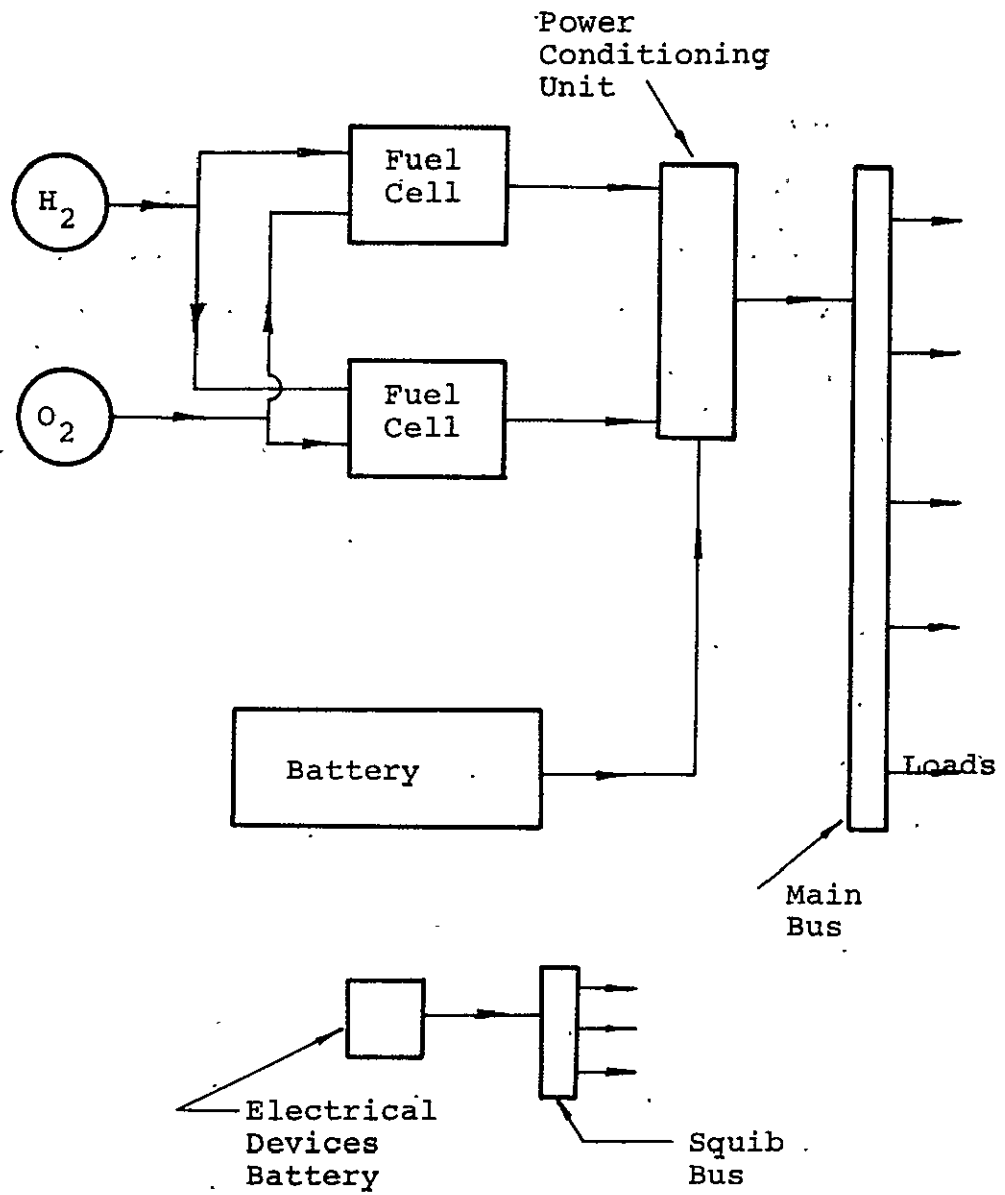


FIGURE 5.4-1. SCHEMATIC ILLUSTRATION--ELECTRICAL POWER SYSTEM.

TABLE 5.4-1 COMPARISON OF CANDIDATE POWER SYSTEMS

	Primary Batteries	Solar Cell and Battery	Fuel Cells and Battery *	RTG and Battery	Fuel Cells
System weight, lbs	490	300	340	384	396
Volume, In ³	8700	8500	10200	22200	37000
Availability	Available 6 Mo.	Available 18-24 Mo.	Available 18 Mo.	Available 24 Mo.	Available 18 Mo.
Growth Potential Beyond 120 hr Mission	Add Batteries, 12 lb/kw-hr	Continuous in lunar day if oriented	Add cryo. @1.0 lb/kw-hr.	Inherent in system type	Add cryo. @1.0 lb-kw-hr.
Cost, \$, (Qual./Shipset)	100K/75K	3M/250K	3M/300K	5M/2M	3M/400K
Payload Support Potential	None	Yes, lunar day	Yes, add cryo.	Yes, 100w/5yr	Yes, add cryo.
Interface Problems	Minor	Major	Moderate	Major	Moderate
Number of Modules	3 Battery	Solar Array, 1 Battery	2 F. C. 1 Batt.	4 RTG 1 Batt.	2 F.C.
Lunar Night Survivability	No	Yes, if batt. recharged prior to lunar night	Yes, provide cryogenics	Yes	Yes, provide cryo.

*Selected System: Fuel Cells and Battery

TABLE 5.4-2 ADVANTAGES AND DISADVANTAGES

CANDIDATE POWER SYSTEMS

Electrical Power Source	Advantages	Disadvantages
Primary Battery	<ul style="list-style-type: none"> · Low cost · High reliability · Low volume · Minor spacecraft structure interface problems 	<ul style="list-style-type: none"> · High weight · No payload support · No lunar night potential
Solar Array and Battery	<ul style="list-style-type: none"> · Low weight · Low volume · Extensive flight experience · Payload support potential 	<ul style="list-style-type: none"> · Structural interface problem, constrains spacecraft design flexibility · Spacecraft must be oriented · Complex system
*Fuel Cells and Battery	<ul style="list-style-type: none"> · Low weight · Redundant fuel cells · Possible payload support · Potential to survive lunar night · Greater flexibility in spacecraft configuration design · High overload capability 	<ul style="list-style-type: none"> · Complex system, supercritical cryogenics required
RTG and Battery	<ul style="list-style-type: none"> · Long life · Payload Support potential · Lunar night survivability 	<ul style="list-style-type: none"> · High heat rejection · Nuclear radiation of electronic components · Adds launch pad complexity · Safety questions · High cost · High volume
Fuel Cells	<ul style="list-style-type: none"> · Redundant system · Potential payload support · Potential to survive lunar night · High overload capability 	<ul style="list-style-type: none"> · Large volume · Low efficiency at translunar power load level · May require liquid heat rejection loop · Requires cryogenics

TABLE 5.4-3 POWER SYSTEM WEIGHT
FUEL CELL AND BATTERY

Item	Weight, lbs
(2) Fuel Cells	60
Gemini RSS H ₂ Tank	27.5
Gemini RSS O ₂ Tank	20.5
H ₂ Reactant	2.3
O ₂ Reactant	17.7
Battery, 9 kw-hr	130
Power Conditioning	60
Battery Support and Thermal Control	12
Fuel Cell Supports	<u>10</u>
Total	340

configuration design of the spacecraft. Also eliminated is the necessity for orientation of the spacecraft with respect to the sun's rays. In addition, the FC/B concept has improved potential for lunar night power supply over that provided by the SC/B system.

The solar cell-battery electric power system alternative involves the following interface problems that may prove to be difficult to overcome:

1. A problem of deployment
2. Fuel penalties are incurred as a consequence of the necessity to compensate for the various static and dynamic perturbations that are caused by the solar cell array
3. The problem of orientating the solar array both in space and on the surface of the moon

For example, when the solar array tries to orient itself with respect to the sun, a reaction results on the spacecraft. The spacecraft will try to correct for the perturbation forces that the array has introduced. The reverse is also true: when the spacecraft moves to orient itself toward the earth, it will tend to disorient the array and thus introduce perturbations into the solar array servo loop. These particular problems are not associated with the fuel cell-battery alternative.

The FC/B concept is based on the use of one Apollo LM ascent stage type battery. An alternate battery choice is that of two modified Surveyor batteries, [4]. Each battery would weigh 73.5 pounds and would have a capacity of 6.1 kw-hr.

Figure 5.4-1 is a schematic illustration of the recommended power system.

5.5 Electrical Devices Battery

Electrical power for the Explosive Devices Subsystem is provided by a single 20 cell silver oxide-zinc battery of the type used on the Apollo LM vehicle. Performance and design data for the battery are shown in Table 5.5-1.

TABLE 5.5-1
PERFORMANCE AND DESIGN DATA
EXPLOSIVE DEVICES BATTERY

Battery rating	37.1 volts dc, open-circuit voltage 0.75 ampere-hour, 75 amperes for 36 seconds
Height	3.03 inches
Width	2.75 inches
Length	6.78 inches
Weight	3.50 pounds

5.6 Summary

Table 5.6-1 is a summary listing of the specifications for the recommended power system.

TABLE 5.6-1 DESIGN SPECIFICATIONS
 FUEL CELL AND BATTERY ELECTRICAL POWER SYSTEM

Item	Specifications
Two fuel cells	Each: Allis Chalmers, 200 w, radiation cooled, 27 v dc, weight 30 lbs, size 7" x 7" x 17", H ₂ and O ₂ reactants, 2w parasitic power, 200°F operating temperature, 180°F to 230° F operating range.
Gemini RSS H ₂ Tank	Supercritical storage, empty tank weight 27.5 lb, hydrogen capacity 5.6 lbs, 250 psia operating pressure.
Gemini RSS O ₂ Tank	Supercritical storage, empty tank weight 20.5 lbs, oxygen capacity 45 lbs, 850 psia operating pressure.
Battery	Apollo LM ascent stage type, 9 kw-hr capacity, rated 300 ampere-hours at 30 volts, current rating 50 amperes at 28 volts for 5.92 hours at 80°F, weight 130 lbs
Power Conditioning	30 v dc to 400 Hertz, 115v ac, reverse current control, dc voltage boost, 60 lbs weight
Electrical Devices Battery	See Table 5.5-1

CHAPTER V

REFERENCES

1. Conference, July 1969, at Manned Spacecraft Center attended by Cliff Robinson, William Remy, and Floyd Calvert.
2. Arthur W. Fihelly, Herbert N. Berkow, and Charles F. Baxter, "Snap 19/Nimbus B Integration Experience", Intersociety Energy Conversion Engineering Conference, Boulder, Colo., IEEE report number 68 C 21, volume 1, page 158.
3. Pratt and Whitney Aircraft, "Fuel Cells for LM-Derivative Spacecraft", reference number 69-1287, prepared for Grumman Aircraft Engineering Corporation, March 19, 1969
4. Bendix Corporation, Aerospace Systems Division, "Solar Power Subsystem for Apollo Lunar Surface Experiments Package, Alternate Thermal Study", (Contract NAS 9-5829, CCP 97/510-40 and 130), Final Report Volume II, Appendix D, page D-49
5. Grumman Aircraft Engineering Corporation, "Apollo Operations Handbook, Lunar Module, Volume I, Subsystems Data", NAS 9-1100, 15 Dec. 1968, page 2.5-23.

CHAPTER VI

TELECOMMUNICATIONS

George Gless 6.1-6.3

Frank Swenson 6.4

6.1 Telecommunication Subsystem Requirements

The general requirements of the communication, instrumentation and video subsystems were discussed in Section 2.5 and outlined in Table 2.5-1. The first two subsystems are so closely related that they are both discussed under the title of telecommunications in the first section. The separate subsystems are then described in more detail in the following sections.

In addition to the broad general requirements as listed in Table 2.5-1 there are several more specific items shown in Table 6.1-1. Initial acquisition of the spacecraft on earth is facilitated by the use of Surveyor type omnidirectional antennae and high power from the transmitter. After initial acquisition, the LM steerable S-band antenna is automatically controlled by the receiver as indicated in the block diagram of Figure 6.1-1. Initial acquisition may be controlled by commands from the ground or the guidance computer.

Part b of Table 6.1-1 indicates the various items to be measured and telemetered to MSFN or DSIF via the S-band communication subsystem. Very little design effort was devoted to determining the actual measurement items needed. An estimate of 150 analog channels and 150 digital channels was used as the basis for the selection of the components shown in the block diagram of Figure 6.1-2.

A possible mission objective was to provide an active or,

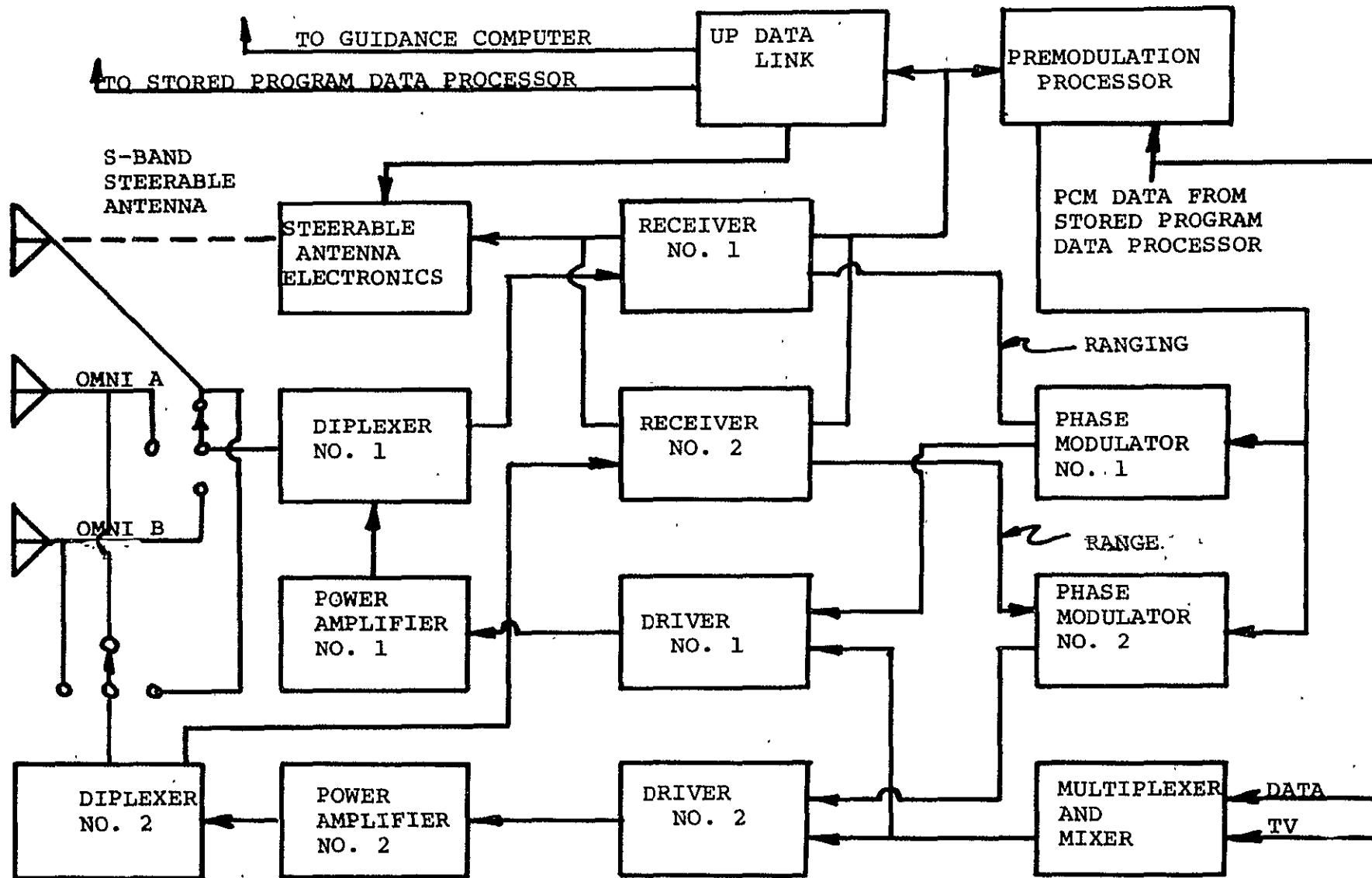


FIGURE 6.1-1 BLOCK DIAGRAM OF TELECOMMUNICATIONS SYSTEM

TABLE 6.1-1 ADDITIONAL TELECOMMUNICATION
SUBSYSTEM REQUIREMENTS

a. Communications

Mission Phase	Function
Launch	Establish communications between MSFN or DSIF and the tumbling LLV
Lunar Approach	Align high gain antenna so as to maintain television transmission to MSFN. LLV may maneuver at rotation rates up to 5°/sec. Provide high frame rate television video signals to MSFN to reduce control delay time.

b. Instrumentation

Mission Phase	Function
Launch	Measure temperatures, pressures, voltages, frequencies, valve positions, antenna and landing gear deployment, switch positions, attitude information, etc.
Coast	All above less deployment
Mid-course	All above plus engine thrust
Landing	All above plus landing gear stress

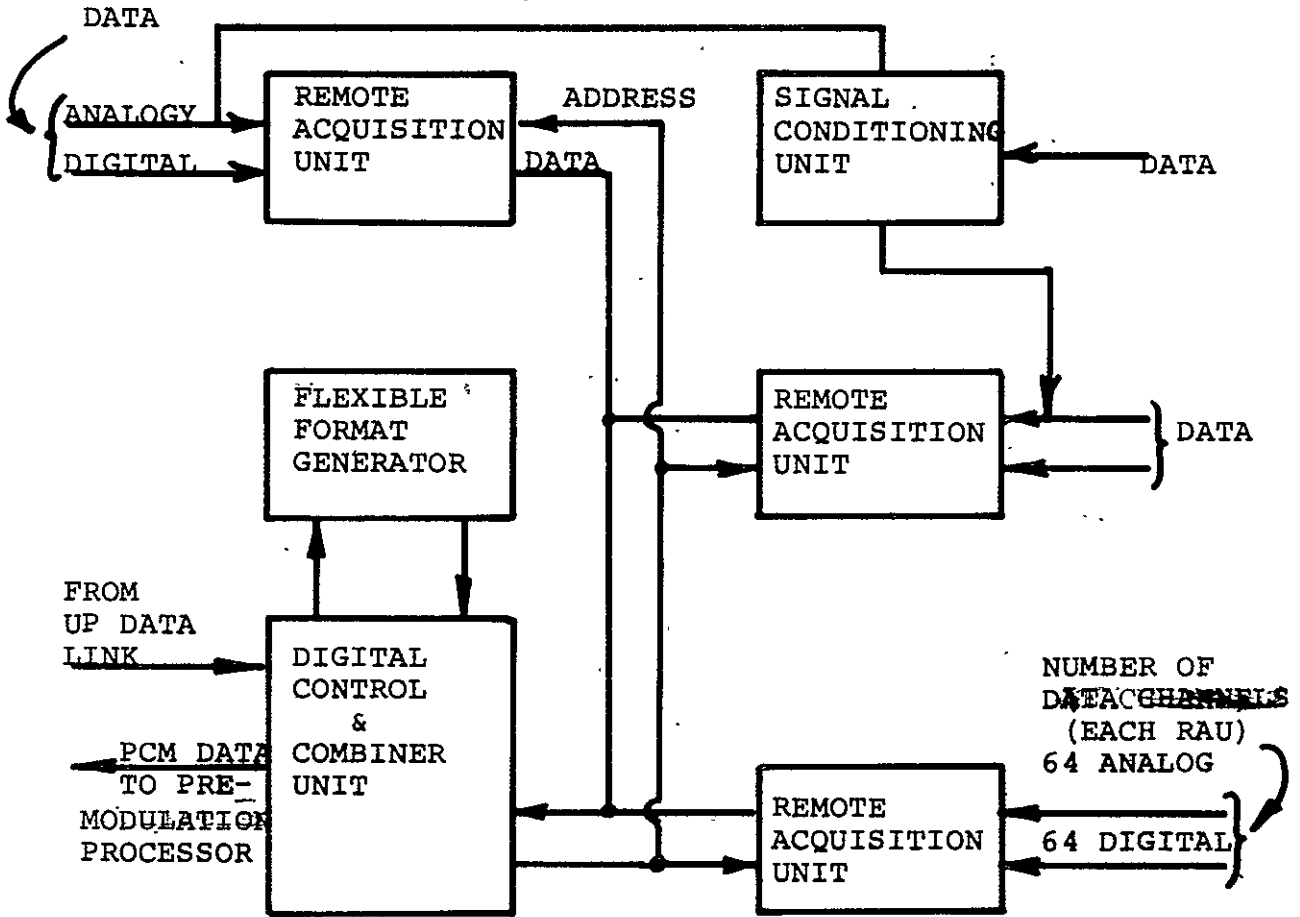


FIGURE 6.1-2 BLOCK DIAGRAM OF STORED PROGRAM DATA PROCESSOR AND SIGNAL CONDITIONING UNIT

passive transponder on the LLV to aid in making subsequent landings in its vicinity. Because of the requirement that the electronics components be placed below the payload, it appears that it will be difficult to maintain a suitable thermal environment for the electronic packages during the lunar day. If the landing is made shortly before the lunar night, then it is possible to maintain the electronics compartments at a suitable temperature (at the cost of the weight of reactants for the fuel cells) until the next lunar day. If an active transponder is to be used or a passive device, it is recommended that it be mounted with the payload. This will result in a better viewing angle and improved thermal environment for the transponder antenna and electronics.

A summary of the design parameters is presented in Table 6.1-2. Some of the requirements are estimated and are marked with an asterisk. The second column gives the capability of the equipment specified as the preferred subsystem. The DC to 2 megahertz modulation capability meets the requirements of the television system as described in Section 6.4.

The high gain antenna is used during television transmission. It is steered automatically by signals from the receiver once the signal from MSFN is acquired. Automatic tracking is possible if the antenna is within 12° of the line of sight to the transmitting antenna on earth. Original positioning of the antenna to enable acquisition would be on command from the earth or the computer on board the LLV.

The maximum rate of uplink command transmission would occur

during the use of the television system. Use of the high rate during television command guidance would aid in keeping the time delay to a minimum. The maximum downlink rate would occur while measuring engine thrust and landing gear stresses.

TABLE 6.1-2 COMMUNICATION AND INSTRUMENTATION
DESIGN PARAMETERS

Item	Required	Capability
Transmitter	2280 Mhz*	2280 Mhz
Frequency	DC to 2 Mhz	DC to 2 Mhz
Modulation	0.4 & 10 μ	0.4 & 10 μ
Power Out		
Receiver		
Frequency	2100 Mhz*	2100 Mhz
Ranging	Yes	Yes
Steerable Antenna		
Gain	19.5 db (transmit)	19.5 db
Slew Rate	5°/sec	20°/sec
Multiplex TV		
Video and Data	Yes	Yes
Up Data Link	1000 bits/sec* (peak)	1000 bits/sec
Down Link Data	5x10 ³ bits/sec* (peak) 5 bits/sec (ave.)	1.024/102.4 kbits/sec
Data Channels		
Analog	150*	192
Digital	150*	192

* Estimated values - transmitter and receiver frequencies must be compatible with MSFN/DSIF

6.2 Communication Subsystem

The alternative communication subsystem candidates presented in Table 2.5-2 are here reduced to two, and the detailed tradeoffs made are discussed. The candidate subsystems selected for study in depth were Surveyor and the Modified Lunar Rover. These two systems have a distinct weight advantage and are less complex than the LM and CSM versions.

6.2.1 Alternative Communication Subsystems

The components for the best two candidates are listed in Table 6.2-1 with the Modified Lunar Rover being the recommended system. Using the criteria of Section 2.5.2, the two sets of components may be compared as in Table 6.2-2.

The Surveyor system is quite attractive if the inadequate television capability and uplink data rates could be improved at low cost. If the sixty pound weight penalty could be tolerated and the television capability improved [7] the Apollo LM equipment would be usable.

If the television capability of the Surveyor or LM equipment is used without improvement [7], the television signal will no longer be compatible with commercial equipment and additional ground conversion facilities will be needed. The conversion time along with low frame rates would introduce additional time delays of the order of 1 or 2 seconds into the television command guidance system which has an inherent 5 or 6 second delay due to signal transmission time, operator reaction time, etc.

The Multiplexer and Mixer unit which makes possible the transmission of video and telemetry simultaneously uses the "back porch"

of the video signal as pictured in Figure 6.2-1. The figure illustrates just one horizontal "line" of the 525 possible in each frame. The frame rate is 30 per second with a 2 to 1 interlace. As indicated in Reference 7, a PCM TM data rate of up to 3×10^5 bits per second may be transmitted along with a 2 Mhz video picture (4 Mhz equivalent because of interlace.)

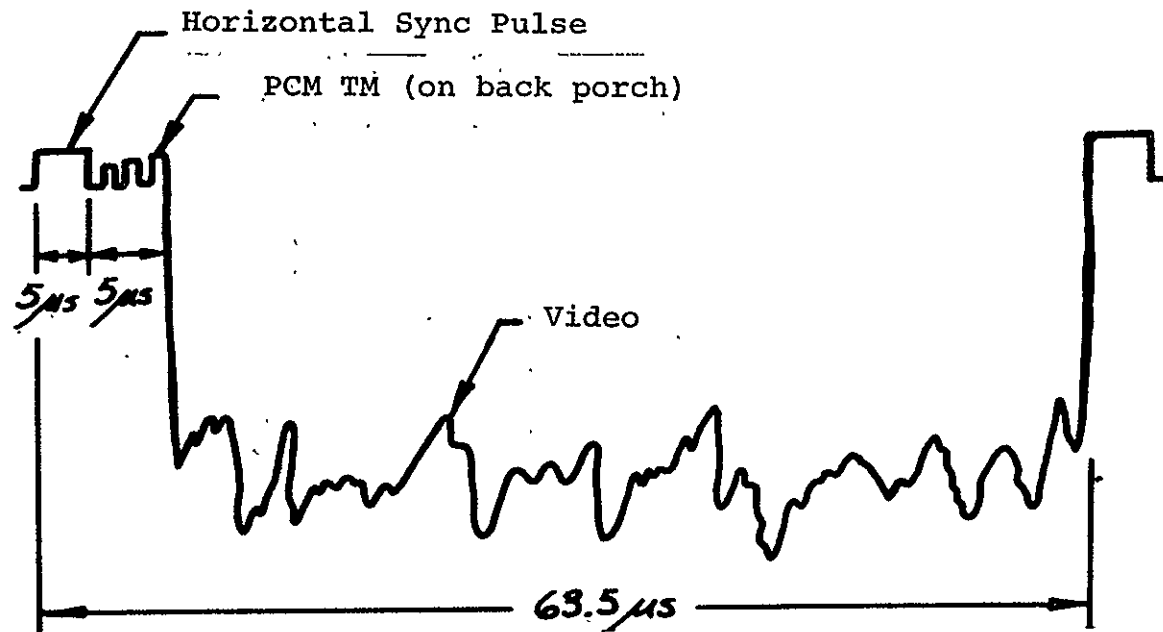
6.2.2 Communication Subsystem--Interface Problems

Because of the requirement that the electronics be located below the payload, two rather serious problems immediately arise. The first, thermal environment, has been mentioned previously and is discussed in Section 7.1. The second has to do with antenna placement and cable losses. The best location for the steerable antenna appears to be on top of the LLV. This location calls for a long cable run which may cause sufficient losses so as to degrade the television transmissions. The omni antenna locations will have to be studied further to insure adequate gain margins.

6.2.3 Communication Subsystem - Equipment Mounting

The communications equipment is to be mounted in compartment A which is a compartment much as used on Surveyor with thermal trays, switches, insulation, radiators, heaters, and mounting hardware to provide a proper environment. The estimated size of the compartment is 20 x 15 x 12 inches overall with a total weight of 52.5 pounds including equipment and internal cabling. The compartment is to be located in one corner of the space beneath the payload as indicated in Figure 8.5-1. The particular location chosen enables the radiators to "see" free space.

6.2.4 Communication Subsystem Development and Qualification



ONE HORIZONTAL " LINE " OF TELEVISION SCAN SIGNAL SHOWING MIXED VIDEO AND PCM TM DATA

FIGURE 6.2-1

TABLE 6.2-1 COMMUNICATION SUBSYSTEM--DETAILED DATA

ITEM	SURVEYOR	MOD. LUNAR ROVER ✓
S-Band Steerable Antenna*		
Size (inches)	46 x 26 x 15	46 x 26 x 15
Volume (in ³)	17,940	17,940
Weight (lb) = (W/O boom)	27.4	27.4
Voltage	28VDC; 115 VAC 400 Hz; 3φ	28VDC; 115 VAC 400 Hz, 3φ
Power (watts)	4.5 - 29	4.5 - 29
Slew Rate (°/sec)	20	20
Gain (db)	19.5	19.5
Modes	Auto Tracking Man. Acquisition	Auto Tracking Man. Acquisition
Heaters (watts)	51.7	51.7
S-Band Omni Antenna		
Size (inches)		
Cone	4.5 x 6.9	4.5 x 6.9
Arm	2 x 42	2 x 42
Volume (in ³)	150	150
Weight (lb)	3	3
S-Band Transponder***		
Transmitter Size (inches)	4 x 6 x 15	5 x 5 x 4
Volume (in ³)	360	100
Weight (lb)	7	5

Transmitter (Contd)		
Power (watts) Input	9/70	15/130
Output	0.1/10	0.4/10
Frequency (est. MHz)	2280	2280
Modulation Video Baseband	DC to 0.22 MHz	DC to 2.0 MHz
Receiver		
Size (inches)	3 x 6 x 8	5 x 2.5 x 1.6
Volume (in ³)	144	20
Weight (lb)	4	1
Power (watts)	2	5
Frequency (est. MHz)	2100	2100
Multiplexer & Mixer (TV Auxiliary)		
Size (est. inches)	3 x 6 x 8.5	3 x 4 x 2
Volume (est. in ³)	153	24
Weight (est. lb)	4.5	1
Power (est. watts)	2	1
(See Section 6.4)		
Updata Link**** (Command Decoder)		
Size (inches)	5.3 x 6 x 13.3	6 x 4.7 x 8.6
Volume (in ³)	240	242
Weight (lb)	5.7	5
Power (watts)	1.9	4.4
Bit Rate (bits/sec)	48	1000

Updata Link (Contd)		
Data Rate (bits/sec)	20	200
Word Length (bits)	24	16-24
Premodulation Processor* (Sur. Central Signal Processor)		
Size (inches)	5.3 x 5.7 x 8.8	6.75 x 7.5 x 8
Volume (in ³)	173	405
Wright (lb)	4.8	10.5
Power (watts)	2.2	4.3

✓ Recommended Subsystem

* Apollo LM item

* Surveyor item--2 used

*** For each unit--2 used. Transmitter includes high and low power units, modulators and dixer.

**** See Reference 5.

1. S-Band Transponders - develop and qualify
2. Television - Data Mixer and Multiplexer - qualify
3. Updata Link - qualify
4. Compartment A - develop and qualify

The estimated cost of development and qualification is indicated in Chapter 10.

6.3 Instrumentation Subsystem

The original four instrumentation subsystem candidates presented in Table 2.5-2 are here reduced to the best two and further details in the selection process are outlined. The Surveyor and Modified Lunar Rover were the two selected primarily on the basis of low weight and simplicity. A block diagram of the recommended design is shown in Figure 6.1-2.

6.3.1 Alternative Instrumentation Subsystems

The items which compose the best two candidates are listed in Table 6.3.1. The Modified Lunar Rover is the recommended subsystem as it must be closely coordinated with the communications equipment. The actual comparison as shown in Table 6.3-2 indicates that the Surveyor subsystem is lighter in weight and lower in power required and the recommended system has more versatility and growth potential in the area of data format and number of inputs. The Stored Program Data Processing Unit has great flexibility in that it can change data format on command thru the Flexible Format Generator and can easily be expanded by adding Remote Acquisition Units up to a total of 16 [6]. If the added flexibility is not needed, the Flexible Format Generator may be eliminated by storing a format in the Digital Control and Combiner Unit.

TABLE 6.3-1 INSTRUMENTATION SUBSYSTEMS - DETAILED DATA

Item	Size in	Volume in	Weight lb.	Power w	Channels	Bit Rate kbits/sec
SURVEYOR						
Signal Processor Auxiliary Engineering	1.8x2.4x2.4	10	0.34	0.15		4.4/1.1/0.55
Signal Processor Aux. Engineering	5.3x8x8	260	6.1	3.9	179 Analog	
Signal Processor Low Data Rate	5.2x5.7x9.9	198	6	6	144 Analog	
Auxiliary	2.4x3.0x5	21	0.55	0.1		0.55/0.1375/ 0.0172
MOB: LUNAR ROVER						
Stored Program Data Processor* Flexible Format Generator	5x9x10	447	11.5	10		102.4/1.024
Digital Control & Combiner Unit	3 x 6 x 10	180	9.5	5		
Data Acquisition Unit (each .3 used)	1.1x4x5	42	1.8	1	64 Analog 64 Digital	
Signal Condi- tioning Unit (est.)	7x8x8	448	4	12		

✓Recommended Subsystem

*Includes first three items listed immediately below. Yields 192 Analog and 192 digital channels.

TABLE 6.3-2 INSTRUMENTATION SUBSYSTEM COMPARISON OF
CANDIDATES

SURVEYOR	MODIFIED LUNAR ROVER
Less weight, size and power	Has remote acquisition units
Less flexible	More flexible
Little growth potential	Simple to expand by adding small remote acquisition units May easily be used to monitor launch vehicle and/or payload [6]
Complicates thermal control to some degree	Aids in thermal control of compartments

The large number of conductors entering the telemetry system causes considerable heat loss during the lunar night. This loss may be minimized by placing two of the remote acquisition units in the Guidance and Navigation compartment which is to be shut down after touchdown. Only four twisted pairs of wires are needed to connect the remote units to the control unit (DCCU). The third remote unit would be mounted in compartment B and its chief function would be to monitor activity in compartments A and B while the other two would service all equipment external to those compartments.

6.3.2 Instrumentation Subsystem - Signal Conditioning and Wiring

The Instrumentation Subsystem design will have a great effect on the weight and complexity of the signal conditioning equipment and the interconnecting cables. Most of the measurements of temperature and pressure do not need to be made with high accuracy and thus would not require extensive shielding and sophisticated signal conditioning. Much of the information is digital bilevel as in the case of valve and thermal switch positions, etc., and thus the signal level may vary by several percent as long as the actual level is sufficiently far from the 3.0 volt switching point of the Remote Acquisition Unit. Based on the assumption that the accuracy requirements will be kept low, it is estimated that the sensors and interconnecting cables will weight 85 pounds.

6.3.3 Instrumentation Subsystem - Equipment Mounting

The Instrumentation Subsystem is mounted in compartment B which is similar to compartment A as described in Section 6.2.3. As indicated earlier, two of the Remote Acquisition Units are

located with the Guidance and Navigation equipment. The estimated size of the compartment is 22 x 15 x 16 inches overall with a total weight of 64.3 pounds.

6.3.4 Instrumentation Subsystem Development and Qualification .

1. Stored Program Data Processor - qualify
2. Signal Conditioner - develop and qualify
3. Cable and Sensors - develop and qualify
4. Compartment B - develop and qualify

The estimated cost of development and qualification is presented in Chapter 10.

6.4 Operational Considerations

The use of video data in approach navigation and the avoidance of hazards constrains the lunar landing times to those with satisfactory lighting conditions at the landing area. The LLV guidelines are the 7° and 20° range of sun angles at the landing area that is recommended for Apollo missions [8]. The low sun angles would be preferable to give long shadows in landing areas of low relief. The higher angles in this range would be preferred to reduce the shadowed area classified as unknown hazard for high relief areas.

As a logistics vehicle, the LLV could land either at sunrise or dusk of a lunar day. In Apollo support missions where the Lunar Module must land in the sunrise of a lunar day due to LM design limitations, the LLV could be landed either at sunrise or dusk of the preceding lunar day. An LLV dusk landing may be preferred to reduce the minimum required survival time until the LM landing from 28 days to 16 days.

The LTVS is not operated post-landing so that survival requirements do not extend beyond the landing. The thermal survival requirements are satisfied by exterior thermal control coatings and the inclusion of a vidicon heater and an electronic heater in the camera. The power requirements for these heaters are discussed in Section 7.2.

Approach navigation requirements provide that the camera must be on the side of the vehicle facing the lunar surface during the terminal descent phase. The limited camera field-of-view also contains the permissible roll angle range during the early portion of the powered descent for near-horizontal trajectories.

TABLE 6.4-1 CANDIDATE LANDING TELEVISION SYSTEM CAMERAS

<u>CAMERA</u>	<u>CAMERA WEIGHT (lbs)</u>	<u>CAMERA POWER (WATTS)</u>	<u>RESOLUTION (RASTER LINES)</u>	<u>FRAME RATE (FRAMES/sec)</u>	<u>BANDWIDTH (HERTZ)</u>
Surveyor	6.9	14.1	600	0.28	0.07
Lunar Module	4.5	6.5	1280	0.62	0.68
Lunar Rover	9.0	20.0	800	0.31	0.13
Cammand Module	11.2	20.0	200	30.0	0.80

<u>REQUIRED SCAN CONVERSION</u>	<u>SPACE QUALFEED</u>	<u>GROWTH POTENTIAL</u>
96-to-1	Yes	Limited
108-to-1	Yes	Limited
48-to-1	No	Limited
None	For Interior Use	Good

An optical field seen by the camera may be distorted by refraction in passing through the exhaust plumes of the main and vernier engines. A preferred location for the television camera is near the bottom of the upper stage of the vehicle at a location that maximizes the size of the clear fields-of-view. A study should be made of the visibility of lunar terrain viewed by a television system through exhaust plumes in outer space.

Lunar dust particles moving in the region of soil disturbance by the vernier engines can obscure the lunar surface and prevent an accurate visual determination of relative velocities. It is recommended that the hover maneuver be performed at an altitude for which the disturbance of the lunar soil is still negligible.

Recommended Tasks and Studies

The following tasks and studies are recommended in addition to those of Section 3.4 for the development of the Landing Television System.

1. Qualification of a black-and white version of the Command Module television camera for exterior use.
2. Continued development of the multiplexer for the time multiplexing of telemetry and video data. (Section 6.3).
3. System-level flight acceptance testing which includes solar-thermal vacuum profile, and vibration-shock environments at expected upper bound flight levels.
4. Study of the optical distortion, if any, of viewing through the plumes of the RL-10-3-3 and the LLV vernier engines in outer space. A multiple-burn descent may be advisable to permit periodic undistorted video-viewing.
5. Operational experience with the Landing Television System prior to the first LLV flight by flight of the system in LM's of the schedule 1971-1973 Apollo Missions.

REFERENCES

1. Apollo Operations Handbook, Lunar Module, Volume I, Subsystems Data, NAS 9-1100
2. Conferences with Olin Graham, C. R. Edmiston, Norman B. Farmer and Richard Sinderson of NASA-MSD, July 30 and August 5, 1968, Topics discussed were NASA unmanned lunar rover concept with two television cameras, S-band communication and a video - PCM TM multiplexer [7].
3. Surveyor, Final Engineering Report, JPL Contract Number 9500056, Hughes Aircraft Company, June 1968, Volume II, Systems Design
4. Advanced Logistics Spacecraft System, Volume V, Subsystems and Weight Analyses, October 31, 1967, Final Report No. F-738, McDonnell Astronautics Company
5. Final Report on IC application to Apollo UDL Motorola 3030-1-10, July 28, 1968 NAS 9-3458 and 9-5366.
6. William E. Mallery and Mark C. Smith, The Stored Program Data Processor for Post-Apollo Applications, NAS 9-7785.
7. MSD Internal Note MSD EE 69-, "Time Multiplexing Low Frequency Data Into The Television Waveform, Space Electronics Systems Division, Flight Data Systems Branch.
8. A. V. Bernard, Jr., "Landing Site Selection Criteria", Apollo Lunar Landing Mission Symposium, NASA TM X -58006, June, 1966.

CHAPTER VII
THERMAL CONTROL

Clift Epps

7.1 Thermal Control Requirements

7.1.1 Subsystem Functional Description

Thermal control of the LLV is required to maintain the temperature of each subsystem within specified operating limits for each critical phase of spacecraft operation. An open system configuration is selected with individual temperature control requirements for each subsystem. Although this configuration increases the thermal control hardware design complexity, with its resulting increase in analytical complexity, it minimizes insulation weights as well as power requirements for the lunar night.

To maintain each subsystem within specified temperature limits, a variety of control systems are necessary. To minimize weight, maximum use should be made of completely passive systems, which includes paints, various metal surface treatments, reflecters and insulation. Whenever normal environmental heat inputs are insufficient to maintain operating temperatures, active thermal control heaters are required in combination with passive control to minimize energy requirements. For those subsystems that have large heat rejection requirements, the use of semiactive variable conductance thermal switches, as used on Surveyor [1], is recommended.

Thermal control requirements for the LLV may be subdivided into four phases:

1. Transit coast
2. Terminal descent
3. Lunar day

4. Lunar night

Each subsystem operating during each of the four phases has its own unique thermal control requirements. Unfortunately requirements for the lunar day and lunar night are basically incompatible with each other and subsystems that must survive a lunar day-night cycle have different control requirements. The terminal descent phase differ from the coast in that the terminal descent requires a large heat dissipation rate from the electronics and battery subsystem compartments.

The primary subsystems that require active or semiactive thermal control considerations are:

1. Electronic compartments .
2. Fuel cells
3. Battery compartment
4. Guidance equipment compartment
5. Approach television
6. Vernier and RCS engines

Other systems may be maintained between operating temperature limits by the use of passive control techniques. Preflight conditioning is also required for the propellant tanks of the vernier and RCS propulsion subsystems. Further consideration of the thermal control design for several of the above subsystems is given in Section 7.2.

Of the subsystems listed above, the first two require thermal control during post-landing operation. Thus, more consideration must be given to the lunar environment exposure of these subsystems.

7.1.2 Lunar Day Environment

The most severe thermal control requirements imposed on the spacecraft is the survival of electronics and power subsystems through the hot lunar day. The variation of the lunar surface temperature, neglecting uneven terrain [2], with solar elevation angle may be represented by the equation,

$$T_m = 673 \sin^{1/6} \phi \quad ^\circ\text{R} \quad (7.1-1)$$

where the noon lunar surface temperature at the equator may be expected to be about 673°R .

Lunar day survival capability of the electronics and power subsystems depends on the ability of these subsystems to reject heat during the lunar day. The cooling loads placed on these subsystems depends on the following factors:

1. Required operating temperature
2. Location of the principle radiator surface relative to the lunar environment
3. Energy dissipation rate

Of these, the controlling factor is the temperature of the radiator through which the internally generated energy is dissipated. As an initial estimate of the heat dissipation ability of the radiator, an equilibrium temperature of the radiator surface may be calculated. This equilibrium temperature, at a zero internal power generation rate of the electronic equipment, is given by the equation, [2]

$$T_{s,r} = \left[F_{a,r} T_m^4 + \frac{S_c \alpha_{s,r} \cos \theta}{\sigma \epsilon_r} \right]^{1/4} \quad (7.1-2)$$

$$S_c = 443 \text{ BTU/hr-ft}^2$$

$$\sigma = 0.1714 \times 10^{-8} \text{ BTU/hr-ft}^2 \text{ } ^\circ\text{R}^4$$

- $\alpha_{s,r}$ = 0.11, solar absorbtivity of radiator surface
 ϵ_r = 0.79, emissivity of radiator surface
 $F_{a,r}$ = 0.5, configuration factor between vertically oriented radiator surface and lunar terrain
 $\theta_{s,r}$ = angel between incident solar radiation and, outer normal of the radiator

Actual temperatures inside the electronic compartments are greater than the equilibrium temperature of the radiator surface. This increase in temperature is caused by the temperature drop, ΔT , required to transport heat. Much of the temperature drop in the LLV is across the thermal switches and assorted heat flow paths to the radiator surface. An estimate of the equilibrium temperature of the radiator is given in [Fig. 7.1-1] for a radiator oriented vertically with respect to the lunar surface angles relative to the East-West direction at the lunar equator and solar elevation angel. Also presented is an estimate of the temperature inside a typical electronic compartment for an estimated ΔT of 50°F and asimuthal angles of 0° and 90°. The maximum estimated electronic compartment temperature of 167°F occurs at a solar elevation angle of 60° and an asimuthal angel of 90°. For an asimuthal angel of 0° and a solar elevation angel of less than 45°, the electronic compartment temperature remains less than 125°F, which corresponds to the maximum electronic operating temperature used in the Surveyor Spacecraft [1]. For a horizontal radiator that can "see" free space over a 180° angel, the equilibrium radiator temperature equals -25°F and the compartment temperature equals 25°F at lunar noon. Although a radiator placed at the top of the spacecraft greatly

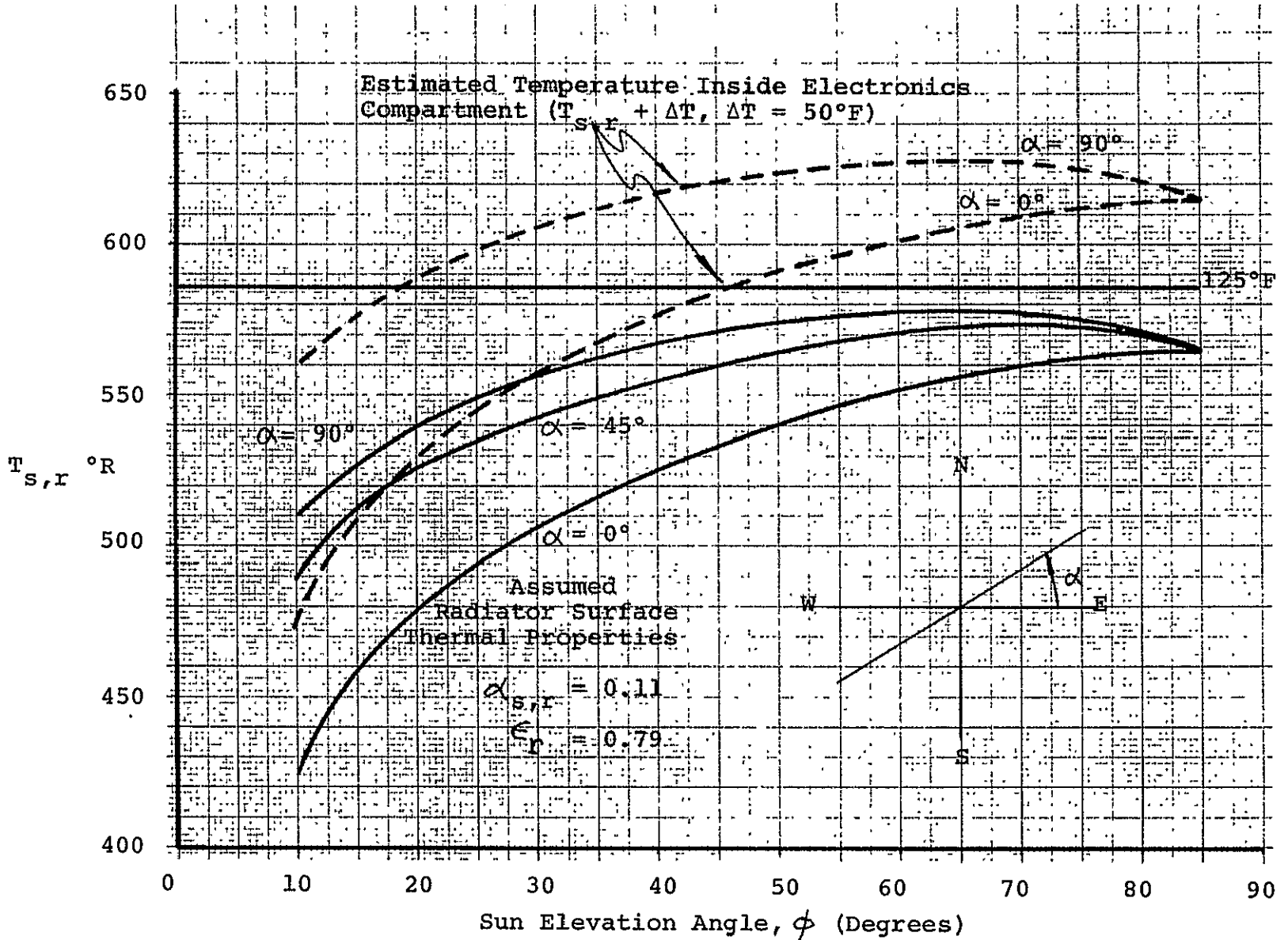


FIGURE 7.1-1 SURFACE TEMPERATURE FOR VERTICAL ORIENTED RADIATOR

improves the heat dissipation capability of the electronic compartments, other design considerations require that the electronic compartments be placed near the bottom of the spacecraft with a vertical oriented radiator. In conclusion, the electronic equipment may be expected to be operational 45° before sunset or after sunrise for an azimuthal angle of 0° and 20° before sunset or after sunrise for an azimuthal angle of 90° . For other periods of the lunar day, marginal operation may be expected. The number of thermal switches required for adequate heat dissipation from the electronic compartments is further discussed in Section 7.2.

The other subsystem that must survive a lunar day is the fuel cell power system. This system is an Allis Chalmers, 200 watt, radiation cooled fuel cell that uses proportionally controlled louvers for temperature control [3]. Fig. 7.1-2 depicts the maximum allowable power output permissible for 200°F operation against solar elevation angle. As expected, the effectiveness of heat dissipation capability of the module decreases with increasing solar elevation angle resulting in a restricted power capability near lunar noon of 150 watts for an azimuthal angle of 90° . Since the nominal power output is 200 watts, it is concluded that the fuel cell power system will survive through the lunar day if operated at a power output of less than 150 watts, which will meet post-landing power requirements.

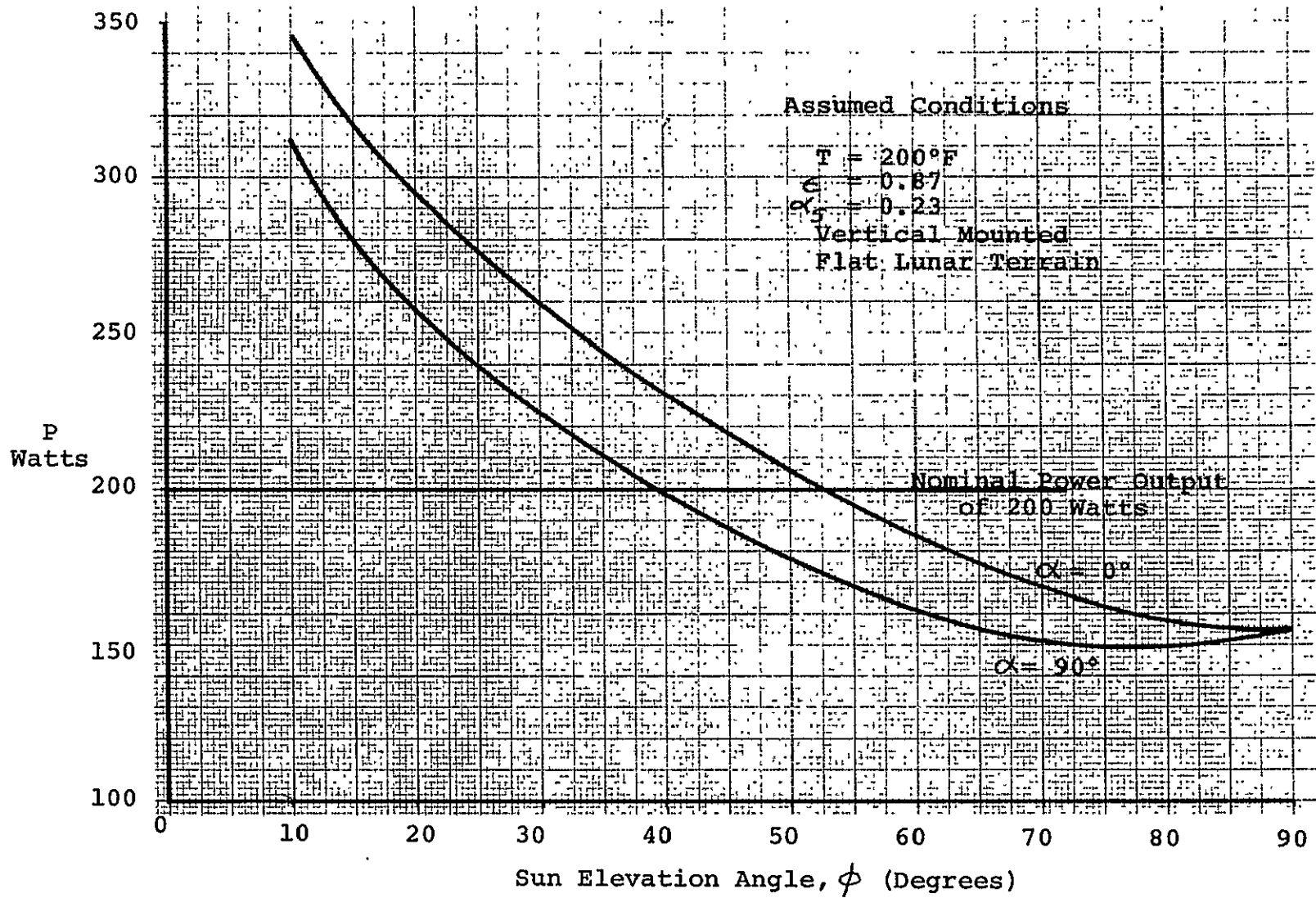


FIGURE 7.1-2 MAXIMUM FUEL CELL POWER OUTPUT PERMISSIBLE DURING LUNAR DAY

7.1.3 Lunar Night Environment

Electronic compartments A and B and the fuel cell power system must survive the lunar night temperature of $\approx 250^{\circ}\text{F}$. The fuel cell module operates during the lunar night at reduced power loads by having the louvers in a closed position and by having standby heaters using part of the power drain to help maintain operating conditions [3]. The electronic compartments may be isolated from the cold lunar night by the use of superinsulation blankets made of multiple layers of double aluminized mylar. Internal energy generation of the electronics and standby heaters provide the energy required to maintain the temperature above minimum operational level of 0°F . The sizing of the heaters is further discussed in Section 7.2.

7.1.4 Coast and Terminal Descent Phase Environment

During the coast phase, the spacecraft will nominally be aligned with a fixed attitude with respect to the sun (except during midcourse correction maneuvers). Because power requirements for the electronics during coasting are at low levels, electronic compartments A and B may require power to help maintain the temperature at operating conditions. To control the effects of solar radiation on critical subsystems, passive control techniques are used. For example, those subsystems that require minimum solar heat inputs should use surface coatings with low values of the solar absorptivity-emissivity ratio while those subsystems that face 0°R space require surface coatings with low values of emissivity. Those subsystems that require precise thermal control for the entire transit phase, such as guidance equipment, vernier propellant tanks, cryogenics propellant tanks, electronics, and batteries, require superinsulation for extreme isolation so as to minimize effects from the external environment. Other subsystems such as the approach television, vernier engines, RCS engines, require passive control techniques plus heaters to bring the subsystems to operating conditions for that particular part of the mission in which the subsystem will be operating.

During the terminal descent phase the electronic and power subsystems operate at high power loads, which may require additional heat dissipation capability. Estimates of the number of thermal switches required for heat dissipation from the electronic compartments should be based on worst case conditions of maximum power dissipation existing during the terminal descent and conditions existing at lunar noon.

7.2 Thermal Control System Design

7.2.1 Electronic compartments

To aid in estimating the cooling and heating loads through the insulation during lunar day and lunar night operation, a parametric study was performed. The effects on heat transfer through the insulation is predicted for different compartment sizes, surface coatings, number of radiation shields, lunar environmental conditions, and average compartment operating temperatures. For the lunar day, the external environmental heating load through the insulation must be added to the internal electronic energy generation load to determine the total heat to be dissipated to the external radiator and, consequently, the number of thermal switches required for each compartment. For the lunar night the external heat loss through the insulation must be added to the loss through the supporting structure, wire harness, and thermal switches in the open position to determine the heating requirements for the electronic compartments during the lunar night.

Based on a model presented in [2], an equation is developed for the average electronic compartment temperature;

$$\begin{aligned}
 T = & \left[\frac{P_{ins} n}{A} \left(\frac{2 - \epsilon_{sh}}{\sigma \epsilon_{sh}} \right) + \frac{1}{6} \frac{T_m^4 \sum F_a}{\text{all surfaces}} \right. \\
 & + \frac{1}{6} \frac{S_c}{\sigma} \left(\frac{\alpha_{s,r}}{\epsilon_r} \right) \cos \theta_{s,r} \\
 & \left. + \frac{1}{6} \frac{S_c}{\sigma} \left(\frac{\alpha_s}{\epsilon} \right) \sum \cos \theta_s \right]^{1/4} \quad (7.2-1)
 \end{aligned}$$

other surfaces
except radiator

where:

P_{ins}	The heat transfer through the insulation, BTU/hr.
n	The number of shields in the insulation blanket.
A	The total surface area of the compartment, ft^2 .
ϵ_{sh}	The emissivity of the shield equals 0.05.
ϵ	The emissivity of the other surface equals 0.87
α_s	The solar absorptivity of the other surfaces equals 0.23.

The configuration factor, F_a , has values depending on the orientation of the various surfaces with respect to the lunar terrain, degree of blockage caused by payload and vehicle support structure, and geometry of lunar terrain. The surface coating properties of the radiator are assumed to be for aluminized Vycor mirrors and the surface coating properties of the other surfaces are assumed to be for inorganic white paint [1]. Equation (7.2-1) also assumes that the compartments are cubic in shape. Only minor variation may be expected from a model that includes rectangular compartments.

Results of the analysis for the lunar day conditions are given in Fig. 7.2-1 where the average compartment temperature is plotted against the quantity $P_{ins}n/A$ for various external environmental conditions. The results include the effect of blockage of part of the compartment external surfaces by payload and vehicle support structure, location of the vehicle in a crater, and variation of solar elevation angle. The blockage factor, BF , is assumed to be approximately fifty per cent as viewed from a horizontal plane looking upward past the payload to

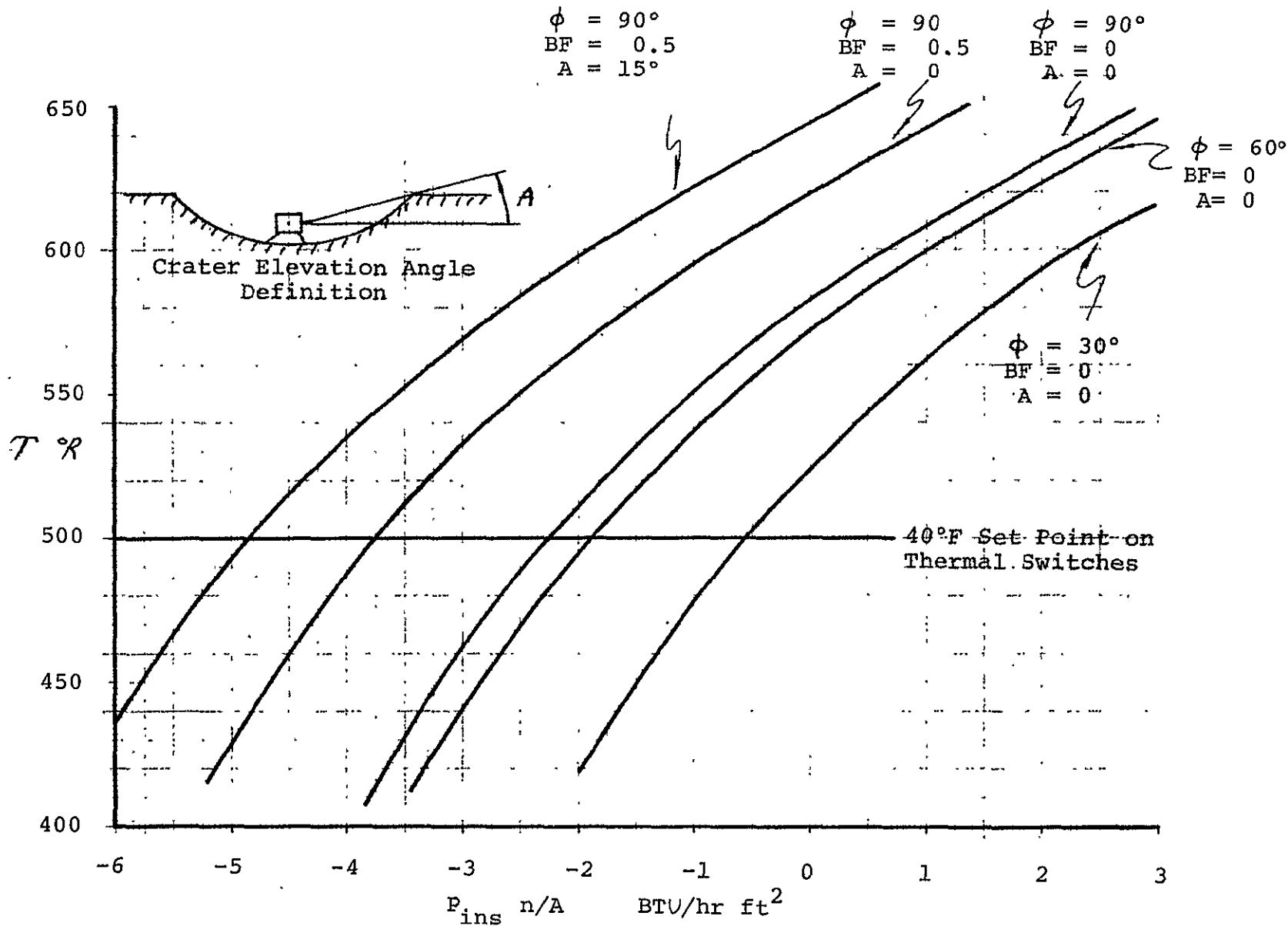


FIGURE 7.2-1 INSULATION HEAT GAIN FOR LUNAR DAY

free space. The crater elevation angle, A , is assumed to have a value of 15° . For these conditions at lunar noon and a closure point temperature of 40°F on the thermal switches, a value of $P_{\text{ins}}n/A$ of -4.85 is selected for design purposes.

Results of the analysis for a lunar night temperature of -250°F are given in Fig. 7.2-2 where the compartment temperature is plotted against $P_{\text{ins}}n/A$. For a heater set point of 40°F , a value of $P_{\text{ins}}n/A$ of 2.7 is selected for design purposes. Also plotted in this figure is the average compartment temperature during the transit phase for an orientation of the radiator normal to the solar incident direction. A comparison of this curve with the lunar night curve indicates that the transit phase may require some internal heating either from heaters or electronic equipment to keep the compartment at normal operating temperatures.

Table 7.2-1 presents the results of the thermal control design for lunar day conditions for electronic compartments A and B, and Table 7.2-2 presents the results of the thermal control design electronic compartments A and B for lunar night conditions. A one inch layer of double aluminized nylon, 70 layers per inch, is used to isolate the compartments from the surroundings. Thermal switch properties [1] are given in Fig. 7.2-3 from which estimates of the number of thermal switches per compartment are made. The large number of switches for compartment A results from the large dissipation of 155 watts required during the terminal descent phase. Values of the thermal losses through the structure, wire harness, and thermal tunnels during the lunar night are estimated from data from [1]. To allow for uncertainties in estimating thermal losses

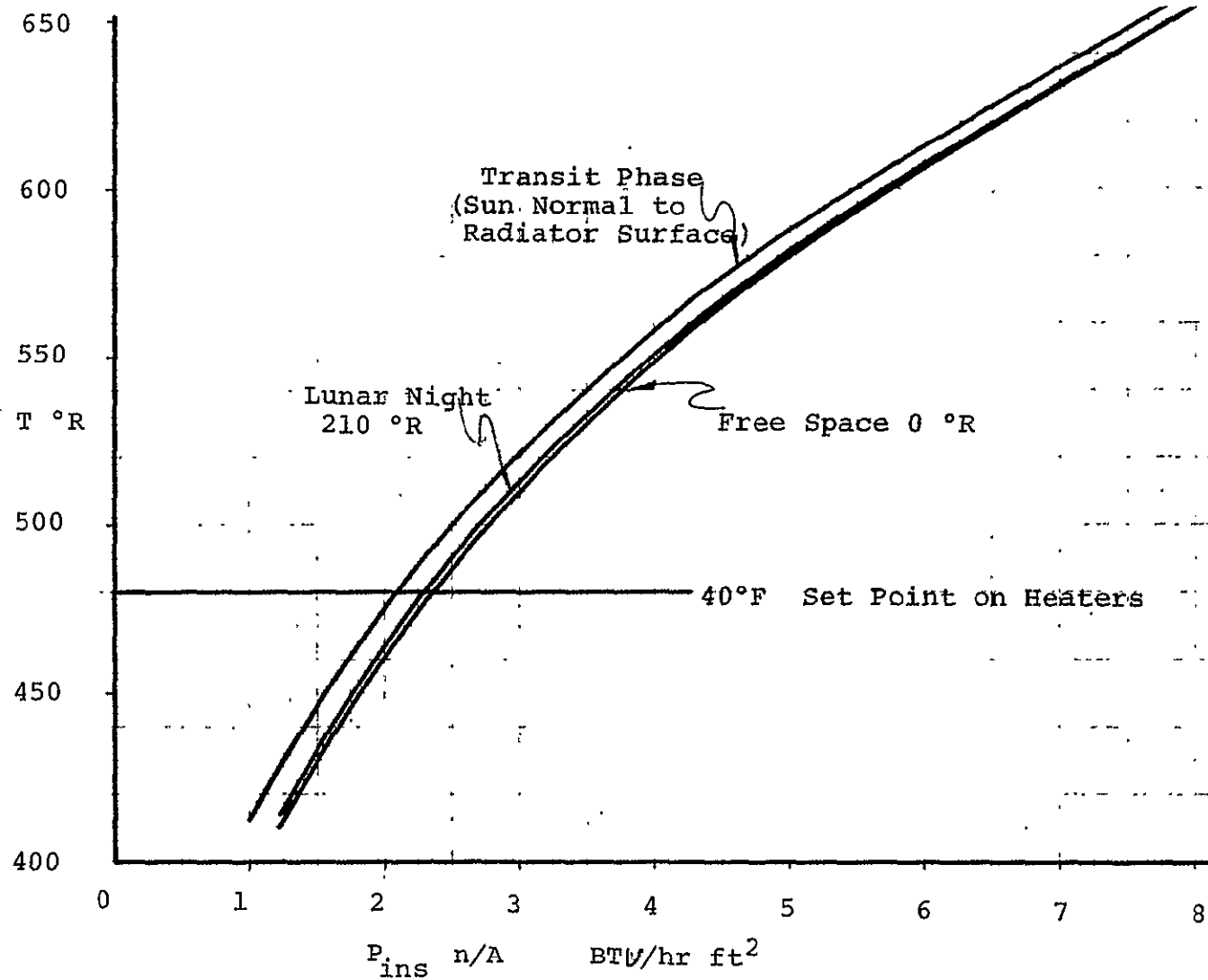


FIGURE 7.2-2 INSULATION HEAT LOSS FOR LUNAR NIGHT AND TRANSIT PHASE

TABLE 7.2-1 ELECTRONIC COMPARTMENTS A AND B THERMAL
CONTROL DESIGN FOR LUNAR DAY CONDITIONS

	Compartment A	Compartment B
Dimensions	20 x 15 x 12 in	22 x 15 x 16 in
Thermal Switch Closure Temperature	40°F	40°F
Maximum Power	152 Watts	20 Watts
Minimum Power	15 Watts	20 Watts
Insulation Heat Gain	2 Watts	3 Watts
Other Heat Gains (Estimated)	1 Watt	1 Watt
Total Dissipation Load	155/18 Watts	24 Watts
Number of Thermal Switches	19	6

TABLE 7.2-2 ELECTRONIC COMPARTMENTS A AND B THERMAL
CONTROL DESIGN FOR LUNAR NIGHT CONDITIONS

	Compartment A	Compartment B
Heat Loss Summary		
Insulation	1.13 Watts	1.45 Watts
Structure (Estimated)	1.00 Watts	1.00 Watts
Tunnel (Estimated)	2.00 Watts	1.00 Watts
Thermal Switches	2.85 Watts	.90 Watts
Wire Harness (Estimated)	5.00 Watts	5.00 Watts
Total Heat Loss	11.98 Watts	9.35 Watts
Electronic Load	14.0 Watts	20.00 Watts
Heater Set Point Temperature	40° F	40° F

Recommendations:

Compartment A	Operate Electronics and Provide a Backup Heater of 10 Watts
Compartment B	Do Not Operate Electronics and Provide Two 10 Watt Heaters (Use One As a Backup System)

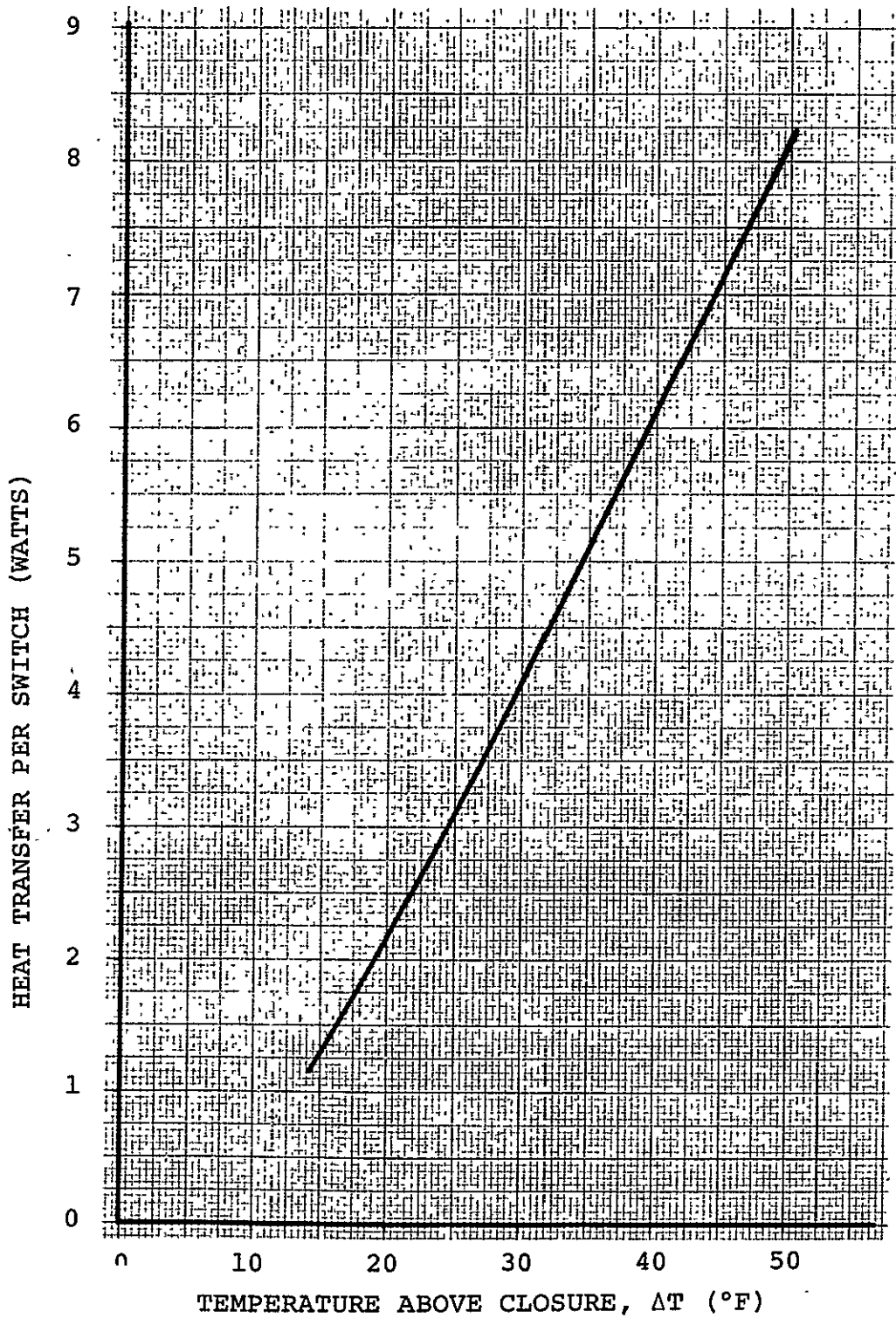


FIGURE 7.2-3 THERMAL SWITCH PROPERTIES [1]

during the lunar night, the thermal loss through the insulation is increased by a factor of ten and the overall loss is increased by a factor of two.

7.2.2 Battery Compartment

The battery must provide power during the terminal descent phase to satisfy peak power loads from other subsystems. After the vehicle has landed, the battery is no longer needed so that it does not need thermal protection during the lunar day and night. Table 7.2-3 presents the thermal control design for the battery compartment for the terminal descent and the coast phases. Heaters are provided during the coast phase and thermal switches during the terminal descent phase to keep the battery at an operating temperature of near 80°F. A battery heat generation rate of fifteen per cent of the peak power requirements is assumed during the terminal descent phase while the heaters are sized for the assumption of no battery dissipation and deep space operation at 0°R, which corresponds to worst case conditions that would be experienced by the battery compartment. A one inch layer of insulation is used to keep the battery compartment isolated from the surrounding environment.

7.2.3 Landing Television Subsystem

The landing television subsystem must operate during the terminal descent phase. From a scaleup of heater requirement of the Surveyor television system [1], the LLV vidicon heater power is approximately 3 watts and the television electronics is approximately 9 watts. The vidicon tube and electronic chassis temperatures are sensed by thermocouples whose signals are telemetered to Earth, and the heaters are turned on and off from Earth as needed to

TABLE 7.2 -3 BATTERY COMPARTMENT THERMAL CONTROL DESIGN

	Transit Coast Phase	Terminal Descent Phase
Dimensions	9 x 6 x 40 in	9 x 6 x 40 in
Battery Heat Dissipation	0	216 Watts
Number of Thermal Switches	27 (Open Position)	27 (Closed Position)
Thermal Switch Closure Point Temperature	60°F	60°F
Insulation Heat Loss	1.1 Watts	1.1 Watts
Other Heat Losses (Estimated)	3.0 Watts	3.0 Watts
Total Heat Loss	4.1 Watts	4.1 Watts
Heater Set Point Temperature	50°F	50°F

Recommendation: Provide an 8 watt heater to keep battery warm during transit coast phase and 27 thermal switches to remove heat during terminal descent phase.

maintain the temperature above the minimum survival temperature of -180°F during the coast phase and above the minimum operational temperature of -20°F prior to terminal phase operation.

7.2.4 Guidance Subsystem Compartment

The guidance subsystem compartment must operate during the coast and terminal descent phase. The compartment has the dimensions of 15 x 16 x 52 inches. The heat dissipation rates of the IMU, flight computer, and other electronics located in this compartment ranges from a minimum value of approximately 75 watts during the coast phase up to 500 watts during the terminal descent phase. Because of the large differences between peak power and minimum power, it is suggested that 61 thermal switches (8.21 watts dissipation per switch at full closure) be used on all surfaces of the compartment to maintain the equipment at proper operating conditions. The closure point of the switches should be set at about 40°F , located between the switches will blankets of double aluminized nylar supersulation. The outer surface of the compartment should be coated with white inorganic paint to minimize solar radiation heat inflow.

7.3 Future Development

During the course of this investigation several ideas were considered that may be of use in the development of the LLV or any other space vehicle. The requirement that the electronic compartments be located near the bottom of the spacecraft created some difficult problems in thermal control. As discussed in section 7.1.2, the operation of the electronics through the lunar noon is marginal because of the high radiator surface temperature of near 100° F for level terrain. For this condition an electronic compartment temperature of near 150° F may be expected. Unless the electronics are qualified to operate at these higher temperatures, marginal operation is expected.

One solution to cool the electronic compartments is to use a stored liquid. By venting the liquid into the compartment, the latent heat of vaporization keeps the electronic at nominal temperatures. Water, with a latent heat of vaporization of near 1075 BTU per pound at very low pressures, has the advantage of ease of storage with minimum thermal insulation requirements. Liquid hydrogen has a combined latent and sensible heat of approximately 1900 BTU per pound. The main disadvantages are the severe thermal insulation problems at cryogenic temperatures and the large storage volume necessary. The main advantage is the possible onboard availability from a fuel cell power system.

A unique radiator design that may have good heat rejection capability at high lunar surface temperatures is presented in Fig. 7.3-1. A radiator surface oriented vertically with respect to the lunar surface may be expected to have a temperature of 106° F at lunar noon (see Fig. 7.1-1). If a radiator could be

designed that blocked a large percent of the lunar thermal radiation from the main radiator surface but still allowed a large emittance to free space, then a radiator surface temperature low enough to allow for adequate cooling of the compartment may be expected.

The design of a directional emissivity wall, as depicted in Fig 7.3-1, accomplishes this by using a parabolic reflecting mirror to reflect up to ninety-five percent of the lunar thermal radiation away from the main horizontal radiator surface. A three zone radiosity network for lunar noon conditions yields the following equations for the equilibrium temperatures of the mirror and radiator, respectively:

$$T_{\text{mirror}} = \left(\frac{F_{23}}{1 - \epsilon_2 F_{12} F_{21}} \right)^{1/4} T_{\text{moon}} \quad (7.3-1)$$

$$T_{\text{radiator}} = (\epsilon_2 F_{12})^{1/4} T_{\text{mirror}} \quad (7.3-2)$$

where:

- F_{12} The configuration factor between the radiator and mirror equals 0.618.
- F_{21} The configuration factor between the mirror and radiator equals 0.269.
- F_{23} The configuration factor between the mirror and free space equals 0.352.
- ϵ_2 The emissivity of the mirror is assumed to equal 0.04.

A calculation of the mirror and radiator surface temperature yield values of 59° F and -253° F, respectively. The low radiator

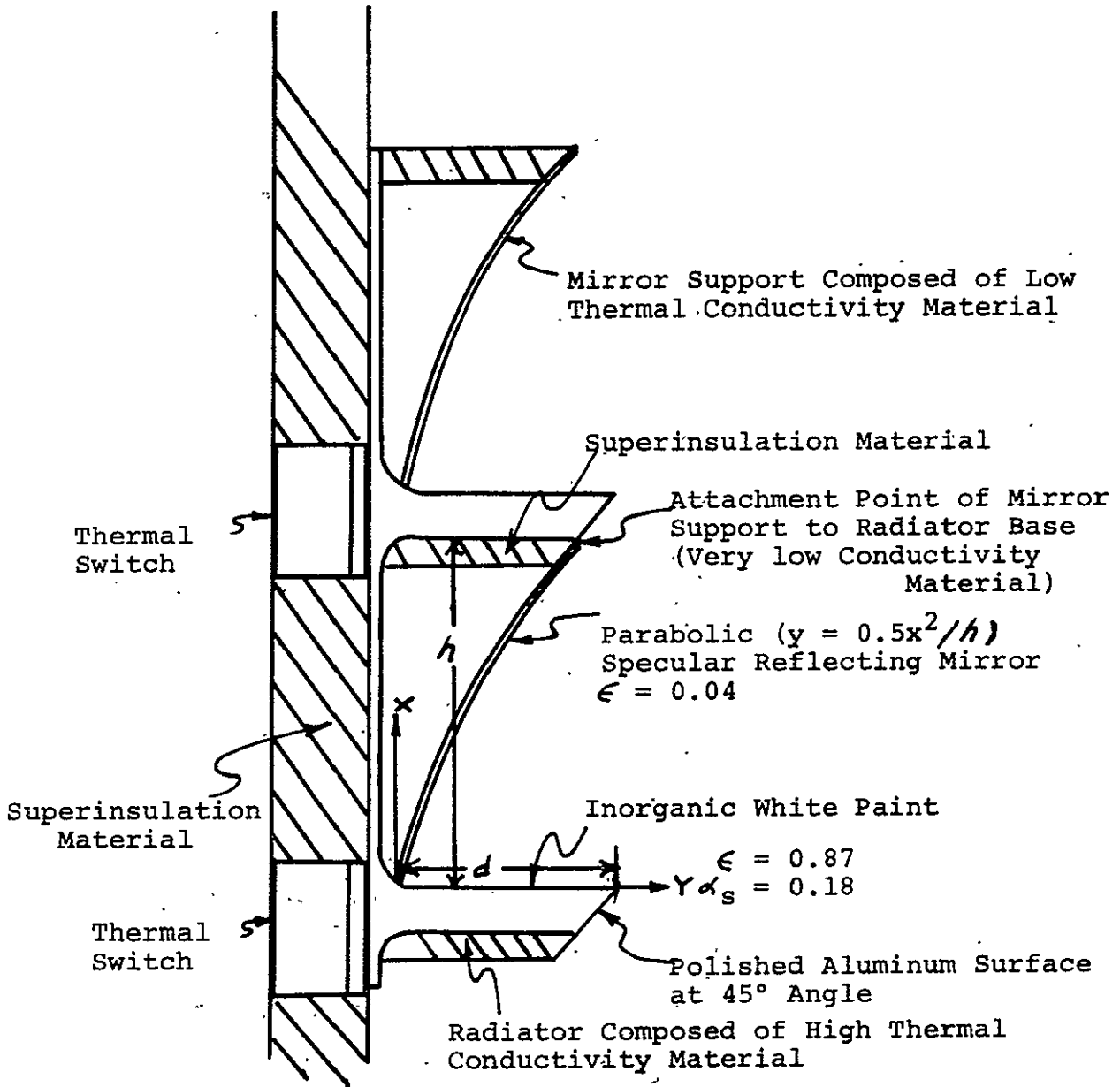


FIGURE 7.3-1 SUGGESTED CONFIGURATION OF DIRECTIONAL EMISSIVITY WALL ORIENTED VERTICALLY WITH RESPECT TO LUNAR SURFACE

surface temperature is caused by the lack of direct "view" of the radiator surface with the hot lunar terrain. Only emitted radiation from the mirror arrives at the radiator surface. Theoretically, if the mirror were a perfect reflector (ϵ_2 equal to 0.0) and the lunar terrain were completely flat, the radiator surface would have an equilibrium temperature of -460° F at lunar noon. Further investigation is needed to determine the heat rejection capability of this type of radiator for other solar elevation angles, lunar terrain features, and heating loads from the compartment.

References

1. Surveyor, Final Engineering Report, JPL Contract Number 950056, Hughes Aircraft Company, Vol II, June, 1968.
2. MacKay, Donald B., Design of Space Power Plants, Prentice Hall Inc., Englewood Cliff, New Jersey, 1963.
3. Platner, John L., "Allis-Chalmers Capillary Matrix Fuel Cell Systems on Advanced Aerospace Power Source", Inter-society Energy Conversion Engineering Conference, Boulder, Colorado, IEEE Report Number 68-CC21, Volume 1, page 52, August 13-17, 1968.

CHAPTER VIII

VEHICLE STRUCTURES AND SUBSYSTEMS

8.1	J.E. Rozenberg
8.2	B. Koo
8.3	I. Eisenstein
8.4	J.H. Cole
8.5	G. Pincus

8.1 Thrust-and Retro-Structure

Most studies made assume the lander vehicle and landing gear to be connected to the retro structure [1,2]. Since one of the most important requirements is ease of deployment of the payload, both retro and thrust structures are to be separated from the lander vehicle.

One study made by Lockheed Missiles and Space Co. [3] assumes a separate cryogenic vehicle, but consists of a proposal beyond the state of the art for such structures.

The proposed configuration of the thrust-and retro-structure is shown on Figure 2.6-1. It consists of a combination of tubular columns and tension cables, connected to the Centaur interface at the lower end, to the lander vehicle at the upper end, and to space rings supporting the propellant tanks at intermediate stations. The RL-10 engine is connected to the frame by four I-beams, rigidly connected to it and to the space ring supporting the four LOX tanks. The total weight of the thrust structure is estimated to be about 250 lbs.

This structure was designed on the basis of a vertical lift-off acceleration of 6 g. Its configuration is laterally stable but horizontal loading was neglected in this preliminary design. A summary of the design of the various members is given in Table 8.5-1. The material used is Al-7075-T6.

Separation of the Centaur from its payload and separation of the lander vehicle from the retro structure will be effected by pyrotechnic devices at the Centaur interface and at the payload support plane respectively.

8.2 Lander Structure

8.2.1 Objectives of Structure

The lander structure carries the payload, vernier engines, propellant tanks, electric power, telecommunication, and thermal control systems with a total approximate mass of 4400 pounds. It is a space structure with top and bottom platforms connected together by diagonal members from the peripheries of two platforms as shown in Figure 2.6-1. The structure is supported by four landing gears (which are described in Section 8.3). It can accommodate payload volume of 9 feet diameter by 7.5 feet high, and payload mass of up to 2500 pounds. Types of payload that may be accommodated include a lunar surface roving vehicle; service stations for returning environmental data to earth; a large stationary geological/geophysical package; an astronomical observatory; an expandable shelter to extend the astronauts' surface staytime; lunar flying units; mobility supplies and propellants; life support equipment and various tools and equipment to be utilized by the crew. Various combinations (within the mass and volume constraints) of the above payload units may be delivered during any one lunar mission.

8.2.2 Structural Arrangement

The main load carrying structural system is the bottom frame consisting of a square frame circumscribed by an octagonal frame as shown in Figure 2.6-1. The square frame is divided into four equal

parts by two intersecting interior members. The frame is supported by four posts of the thrust structure in the boost stage and by four landing gears in the landing stage. The top platform shown in Figure 2.6-1 consists of two main compression members crossing each other at the center. These two members serve as diagonals for a square frame formed by four tension rods, and transmit the compression force from the main landing gear strut. The top and bottom platforms are joined by four pairs of tubular members. Each of these diagonals spans from the top of a main landing gear to the end point of a tension strut. These members also serve to resist twisting of the vehicle during lift-off and trans-lunar flight.

8.2.3 Structural Material

In structural design, the selection of material is usually made on the basis of weight, strength, stiffness, cost, and experience in design and fabrication. The aluminum alloy Al-7075-T6 provides a high strength to weight ratio, large stiffness to weight ratio, well known mechanical and physical properties, and good behavior in fabrication and manufacturing [4]. Based on these considerations, it was chosen as the main structural material. In addition, the effects of space environment on materials have been considered. These effects include the magnetic field, vacuum, radiation and meteorites. The proposed material is non-magnetic. It is found that in a very low pressure environment, material loss through sputtering or evaporation may be possible but the effect on the aluminum alloy is insignificant. From the information available, the effect of penetrating particle radiation in space on the metal is expected to be negligible [5,6,7,8,]. The effects of erosion, spalling and per-

foration upon impact are difficult to evaluate because of many uncertainties in size, composition, weight, flux density and velocity of meteorite particles. The effects of meteorites are omitted in the structural analysis.

8.2.4 Design Conditions

The lander structure was designed for two critical loading conditions. The first one, lift-off, is predicated on a vertical acceleration of 6 g, resulting in an equivalent static load of six times 4400 lbs. The second condition, landing on two of the four gears, results in the loads described in Section 8.3, which are determined by crushing of the shock absorbing material within the main landing gear struts. In addition to the landing gear, discussed in the next section, the top frame elements and the diagonals were designed for this latter loading condition, while the payload support frame, like the thrust structure discussed in the preceding section, was designed for the lift-off forces. The payload was assumed applied at the third points of the perimeter beam of the payload support frame. The vehicle support equipment was assumed distributed over the platform frame, so that the design does not depend on the exact arrangement shown in Figure 8.5-1.

Table 8.5-2 summarizes the design of the lander structure. The results shown include a factor of safety of 1.1, applied to the minimum guaranteed yield strengths for Al-7075-T6 (shapes).

8.2.5 Design Detail

Since this report represents a preliminary design study, the analysis is only intended to give engineering estimates for dimensions and weights. Loads may be imparted to the space frame through several paths. Boost loads from the Centaur vehicle are

transferred at four peripheral points of the load platform, separated by 45° from the landing gear centerlines. During mid-course correction, vernier engine thrust loads are transmitted through engine mounting brackets into the outer octagonal ring girder in the lower platform. During landing, loads are transmitted from the landing gears into the upper and lower platforms of the space frame. Each member is sized according to its maximum axial force or bending moment, to obtain minimum structural weights. The members selected are summarized in Table 8.5-2.

The selected shapes include channels, rods and tubes. In the framed structure, channels provide simple connections between members. Loads in the channel are assumed to act through the shear center creating only bending but no twisting moments. For flexural members, local buckling of flanges and webs is considered. The limiting values are established such that the ratio of flange width to its thickness is less than or equal to 10 and the ratio of depth of web to its thickness, less than or equal to 30. The rod is a convenient shape for a tension member. Tubular sections provide a large radius of gyration and are therefore used extensively as compression members. They also have large torsional rigidity. To prevent local buckling of tubes, the wall thickness to diameter ratio is kept within safe limits.

8.3 Landing Gear

8.3.1 General Design Requirements

The landing gear configuration for the Lunar Logistics Vehicle (LLV) is determined to major extent by the following general design requirements or constraints:

1. The available space for stowability of the landing gear system in the shroud of the Centaur.
2. Terrain characteristics: the lunar surface is assumed to include slopes of up to 35 degrees, boulders of up to one-foot diameter, low density of 1.2 to 1.5 gr/cm³, and a bearing strength of 8 psi at 2 inches depth and 12 psi at 3 inches depth.
3. Landing velocities:

maximum vertical velocity	15 fps
maximum lateral velocity	5 fps
4. Landing deceleration (of payload):

maximum vertical deceleration	6g
maximum lateral deceleration	2g

To assure a successful lunar landing the landing gear system must provide:

1. Shock attenuation for protection of the structure and payload.
2. Stability against overturning after touchdown.

It is also desirable that the landing be accomplished with gear loads as small as possible to minimize the loads acting on equipment, structure and payload.

8.3.2 Alternatives and Selection

The following concepts and approaches for design of the landing gear for the LLV were considered, and used;

1. Landing device configuration
 - a. Three-leg (tripod) type landing gear system, e.g. Surveyor.
 - b. Four-leg (quadpod) type landing gear system, e.g. Apollo LM.
 - c. Crushable pad with stabilizing arms.
 - d. Stub legs with stabilizing arms.
2. Shock absorption devices
 - a. Multi-stage crushable material
 - b. Hydraulic systems
 - c. Gaseous systems
 - d. Cantilever leaf springs
3. Self-leveling landing gear systems
 - a. Active hydraulic system
 - b. Passive hydraulic system
 - c. Gaseous (explosive) system

Examination of these various approaches led to the selection of a four-leg type landing gear system with telescoping main struts and two stage crushable honeycomb material. Self leveling devices were omitted because of the associated weight penalty and their questionable value. The selected landing gear configuration is shown in Figures 8.3-1 and 2.6-1. The total weight of landing gear is approximately 1180 pounds.

8.3.3 General Description of the Landing Gear

The landing gear system comprises four foldable leg assemblies, each assembly consisting of three struts in an inverted tripod

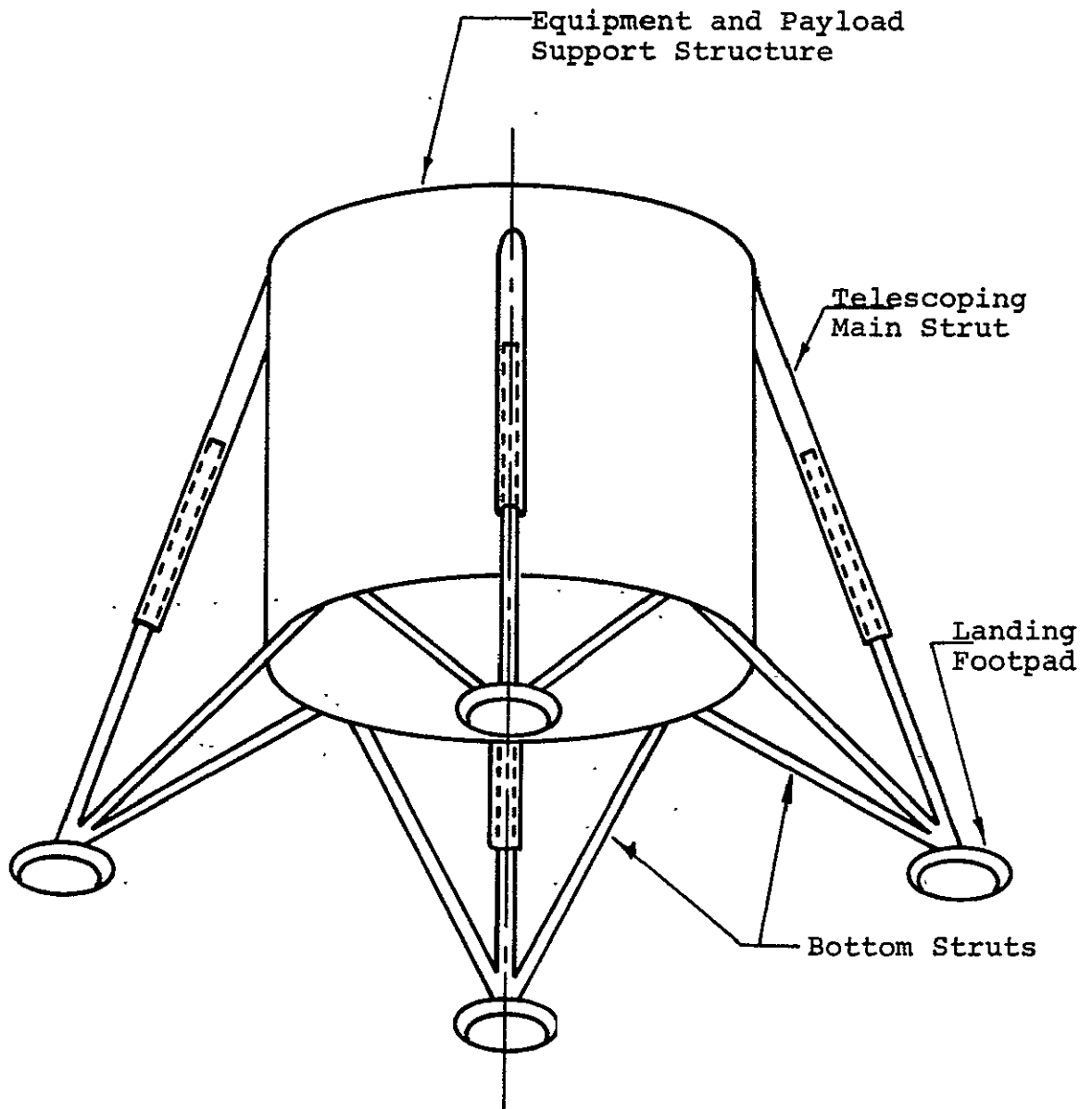


FIGURE 8.3-1 LLV--GENERAL LANDING GEAR CONFIGURATION

arrangement, as illustrated in Figure 8.3-1. Each leg assembly consists of a telescoping main strut or shock strut, two bottom struts, and a footpad.

The struts are connected individually to the equipment and payload support structure. The bottom struts are joined to the main strut at its lower end. The lower end of the main strut carries a landing footpad. The landing gear is stowed within the shroud with the main strut in an elongated (telescoped) position. It remains retracted until the shroud of the centaur is opened. The deployment from the retracted position is accomplished automatically by a spring deployment device installed inside the ram of the main strut. Once extended, each gear assembly is locked in place by a latch pin mechanism.

8.3.4 The Main Strut or Shock Strut

The telescoping main struts consist of a lower ram and an upper cylinder. Both are made of Al-7075-T6 alloy. The ram is a tube 3.5 inches outside diameter and .146 inches wall thickness, the cylinder ~~attaches to the top frame~~ of the payload support structure and the lower ram has a ball joint support for the footpad. The two bottom struts are connected to the lower ram through a hinged pin joint.

Two stage crushable honeycomb material located inside the upper cylinder and crushable material in the pad are used as the shock absorbing medium. The crushable material is assumed to absorb energy with essentially a constant-load-stroke relationship. At touchdown, a strut compresses until the load reaches the level at which crushing of the ~~honey~~ honeycomb begins. The main struts are subjected to column loads at touchdown.

8.3.5 The Bottom Struts

The bottom strut attaches to the main strut and to the payload support structure. These struts are 2.0 inches outside diameter tubes having 0.10 inch walls and made from 7075-T6 aluminum alloy.

8.3.6 The Landing Footpad

The landing footpad has area and sufficient strength to provide flotation and small penetration into the lunar surface. It is attached to the lower end of the main strut by a ball joint that permits the pad to align itself with the lunar surface. The footpad has an outside diameter of 20 inches and an outer shell made of 7075-T6 aluminum alloy. This shell is filled with crushable honeycomb material 4 inches thick and 8 psi strength. The footpad honeycomb is assumed to crush under a uniform loading.

8.3.7 Shock Absorption

It is assumed that:

1. The LLV lands on two adjacent legs.
2. Three inches of crushing thickness of honeycomb material cover the footpads.
3. Fourteen inches of crushing length of honeycomb material is provided in the main strut of the leg assemblies. This includes two stages of crushing: eight inches for lower crushing strength and six inches for higher crushing strength.
4. Both main struts of the contacting leg assemblies crush equal amounts.
5. Total kinetic energy of the vehicle is absorbed by crushing the two leg assemblies.

The kinetic energy of the vehicle is given by the equation:

$$KE = 1/2 MV^2 = 17,080 \text{ ft-lb}$$

where M is the total landed mass and V is the resultant velocity of landing.

This amount of kinetic energy must be absorbed by two leg assemblies at touchdown. Table 8.3-1 shows the contribution to total energy absorption of each of the three deformation devices, i.e. footpad as well as first and second stage crushing in the telescoping legs. It is seen that the total energy absorbed by one landing gear assembly is 8545 ft-lb, so that two legs give a total of 17,090 ft-lb, which is satisfactory.

	<u>Footpad</u>	<u>1st Stage</u>	<u>2nd Stage</u>
Strength (psi)	8	500	850
Area (in)	314	10	10
Force (lb)	2500	5500	8500
Stroke (in)	3	8	6
Energy (ft-lb)	625	3610	4250

TABLE 8.3-1 ENERGY ABSORPTION IN ONE LANDING GEAR

Simultaneously it may be noted that the energy absorbed by the footpad and first stage crushing total 4295 ft-lb, so that four legs in concert are capable of absorbing the total energy without second stage crushing.

Inspection of the forces in the struts under landing conditions of various velocities and attitudes with respect to the tension indicates decelerations well within the design limits.

8.3.8 Structural Proportioning

The material used is Al-7075-T6 i.e. with the following properties.

Modulus of elasticity $E = 10.5 \times 10^3$ Ksi

Yield strength (Compression) $\sigma = 71$ Ksi

Yield strength (Tension) $\sigma = 64$ Ksi

MAIN STRUT:

Both ends of the main strut have pin connections. The applied column load is 8,000 lbs and the length is 150 inc. The main strut is analyzed for:

- (1) Local buckling allowable stress.
- (2) General buckling critical load.

For a thin cylindrical tube subject to uniform axial compression the local buckling stress is conservatively expressed as

$$\sigma_{cr} = 0.12 E \frac{t}{R}$$

where σ_{cr} - critical stress in psi

t - thickness of tube wall in inches

R - the mean radius of tube in inches

so that for σ_{cy} the limit $\frac{t}{R} = .059$.

A tube with an outside diameter of 3.5 in and a wall thickness of .146 in satisfies this requirement. Such a section has a radius of gyration of about 1.25 in and thus a slenderness ratio of 120. A check reveals buckling to take place in elastic range and solution of Euler' equation yields a critical stress of 7.0 Ksi. The cross-sectional area being 1.53 in², the buckling force is 10.7 Kip. Since the actual maximum force is 8.5 Kip, a factor of safety of 1.25 is achieved. Thus both local and general stability are achieved.

BOTTOM STRUTS:

The bottom struts normally act as tension members but may, under severe and unusual landing conditions, be subjected to compressive forces of up to 5 Kip. This condition, it appears, governs their design. The length is 85 in.

A tubular cross-section with an outside diameter of 2 in and a wall thickness of .100 in may be chosen. A radius of gyration of about .71 in and thus a slenderness ratio of 120 result. Again, Euler's equation applies and yields a critical stress of 7.0 Ksi. With a cross-sectional area of .76 in², each strut, acting as a pinned column, can withstand 5.3 Kip. The safety factor for this rare condition is 1.06.

The ultimate tensile load is 48.7 Kip, which clearly cannot be approached under any conditions. Also, it is easily shown that the chosen section is not subject to local buckling.

8.4 Payload Deployment

Two methods available to facilitate payload deployment are shown in Figure 2.6-2.

The method at the left permits unloading the rover and other relatively narrow payloads. The two diagonals are disconnected from the top structure by pyrotechnic devices. Diagonals A are then rotated about their lower hinge points until they contact the lunar surface. If desired, cross members may be attached to the diagonals to form an off-loading ramp. Lowering the diagonals may be done manually, automatically, or by remote control.

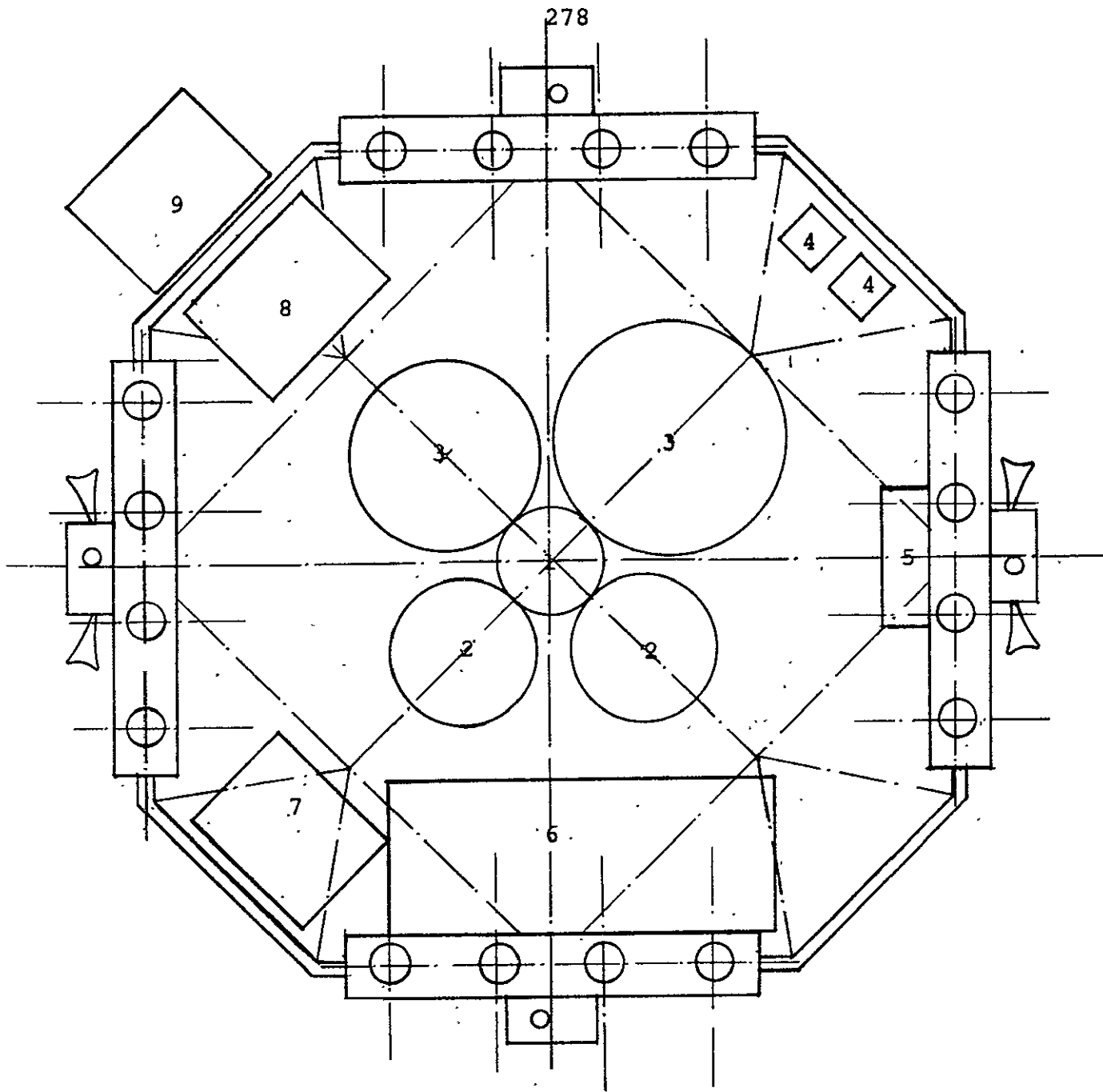
For wide payloads, such as the lunar shelter, the method at the right of Figure 2.6-2 may be needed. This technique requires manned assistance. First, auxiliary supports D are lowered and secondary struts B are disconnected from the lower end of primary strut C. The free ends of the struts are then lowered to the lunar surface. Next a suitable device separates diagonals A and main strut C from the upper cross structure. However, diagonals A and strut C remain pinned together. The footpad end of strut C is moved away from the vehicle, rotating the diagonals downward. After lowering, members A, B, and C may be completely removed, if desired.

8.5 Vehicle Summary

A detailed summary of member sizes and weights for the thrust and retro-structure is presented in Table 8.5-1 while the lander structure (including landing gear) member summary is given in Table 8.5-2. These tables include; the calculated design force or bending moment for each typical member; the loading condition for calculating the loads; the length, shape, size, area and number of members and the total weight for all elements of each type within the structure. All the structural elements were designed of Al 7075-T6 alloy. The MIL-HDBK-5A specification, "Metallic Materials and Elements for Aerospace Vehicle Structures", was used for the vehicle's structural design. Member sizes are also depicted in Figure 2.6-1.

A breakdown of the subsystems weights by individual components is presented in Tables 8.5-3 through 8.5-9. These subsystem totals have been summarized in Table 2.6-1.

The vehicle subsystems are attached primarily to the payload support octagon frame. The components are arranged so as to minimize thermal control problems and to equalize the weight distribution about the center of the vehicle. A bottom view of the subsystem configuration is shown in Figure 8.5-1. The landing radar antenna is shown in the deployed position to one side of the vehicle. The fuel cells are placed between two sets of verniers and close to the fuel cell tanks. The batteries are also placed in the general vicinity of the other power components. The common vernier and RCS propellant tanks are placed in a central location. The navigation and control subsystem is placed behind a vernier "mousehouse" while electronic



1. Gaseous helium tank
2. Vernier and RCS propellant tanks
3. Fuel cell tanks
4. Fuel cells
5. Batteries
6. Guidance and Navigation System
7. Electronics, Box A
8. Electronics, Box B
9. Landing radar antenna (deployed)

SUBSYSTEMS CONFIGURATION

FIGURE 8.5-1

boxes A and B placed at two short-sided corners. All communications antennas and directional sensors are attached to the vehicle top frame, while the TV camera is attached to one short side on the upper part of the payload support frame.

TABLE 8.5-1 THRUST-AND RETRO-STRUCTURE MEMBER SUMMARY

MEMBER DESCRIPTION	FORCE/MOMENT		LENGTH	SHAPE	SIZE	AREA	No.	WEIGHT
	[Kips/Kip-in]		[in]		[in]	[sq in]		[lbs]
THRUST STRUCTURE (Centaur to Lower Ring):								
Verticals	9.0	C,LO (1)	75	Tube	3.0 OD x.05 WT	0.463	4	14.1
Diagonals	4.09	C,LO	81	Tube	3.0 OD x.04 WT	0.377	8	24.7
Connections and Contigencies								20.0
RETRO STRUCTURE (Lower Ring to Payload Support Frame):								
Verticals, Lower	9.75	C,LO	26	Tube	2.0 OD x.05 WT	0.306	4	3.2
Diagonals, Lower	8.67	T,LO	47	Cable	0.500 D.	0.196	8	7.5
Verticals, Upper	6.60	C,LO	63	Tube	3.0 OD x.04 WT	0.377	4	9.6
Diagonals, Upper	4.03	T,LO	77	Cable	0.375 D.	0.110	8	6.9
Lower Space Ring	31.6	BM,LO	367 (2)	Tube	4x4x.100 WT	1.560	1	57.8
Retro Cross Beams	208.0	BM,LO	120	WF	4x4 (3)	0.316	2	51.2 (3)
LO ₂ Hangers	2.6	T,LO	26	Bar	1.0 x.125	0.125	12	3.9
LH ₂ Ring	3.0	BM,LO	367 (2)	Tube	2.0x1.0x05 WT	0.290	1	10.8
Connection and Contigencies								40.3
Total Weight Thrust-and Retro-Structure								<u>250.0</u>

- (1) C= Axial compression force
T= Axial tension force
BM= Maximum bending moment
LO= Lift-off loading, 6g vertical
- (2) Circumferential length
- (3) Wide-flange beam, 4 in deep, 4 in flange width, 0.290 in web thickness, 0.270 in. flange thickness, tapering to 2 in depth over outer 40 in each side.

TABLE 8.5.3

PROPULSION SYSTEM WEIGHT

ITEM	WEIGHT [lbs]
RL-10-3-7	315
Lines, Fittings, Valves, Instruments	35
LOX Evaporator	
LH ₂ Tank	95
Circulator in LH ₂ Tank & Valving	15
LOX (4) Tanks	64
Circulators in LOX Tanks & Valving	50
Explosive Severance Devices	20
Contingencies	27.3
14.2" Diam Spherical He Tank	27.8
He Valve Assembly	2.8
Gaseous He	2.5
Lines & Fittings	5.0
Contingencies	3.0
Vernier Oxidizer & Fuel Tanks (11.5)	23
Valve Assemblies	5
Line & Fittings	20
16 Verniers (5.25 Each)	84
12 RCS, (3.46 Each)	41.6
4 Mouse Houses	58
Contingencies	10
12 Gold Gas Jets	12
Piping, Valving, Fittings	14
Contingencies	23
	<hr/>
Total Propulsion System	<u>933</u>

TABLE 8.5.4

PROPELLANT WEIGHTS

ITEM	WEIGHT [lbs]
Reserve Propellant	90.9
Inflight Losses	70.0
Thrust Decay Propellant	46.0
Full Thrust Propellant	5770.6
Vernier, RCS, and ACS Propellant	<u>400.0</u>
	<hr/>
Total Propellant Weight	<u>6378</u>

TABLE 8.5-5

GUIDANCE AND NAVIGATION SYSTEM WEIGHT

ITEM	WEIGHT [lbs]
IMU	42
IMU Mounting Frame	3
IMU Pulse Torque Ass.	15
Coupling Data Unit	35
Flight Computer	50
Landing Radar Elect	25
TV Camera	11.4
TV Auxiliary	1.7
TV Mtg ADW	2.0
Celestial Sensors	5.0
Box Structure & Mounts	20.0
Wiring	15
Total Guidance and Navigation	<u>225</u>

TABLE 8.5-6

POWER SYSTEM WEIGHT

ITEM	WEIGHT [lbs]
Fuel Cells (2)	60
Gemini RSS H ₂ Tank	27.5
Gemini RSS H ₂ Tank	20.5
H ₂ Reactant	2.3
O ₂ Reactant	17.7
Battery 19 KW-Hr	130
Battery Support	9.0
Fuel Cell Support	10
Wiring	20
Power Converter and Distributor	60
Total Power	<u>357</u>

TABLE 8.5-7

COMMUNICATION SYSTEMS WEIGHT

ITEM	WEIGHT [lbs]
Structure & Mtg.	9
S-Bank Transmitter & Modulator A	3
S-Bank Transmitter & Modulator B	3
S-Bank Receiver A	1
S-Bank Receiver B	1
Diplexer A	2
Diplexer B	2
Antenna Switch	2
TV & PCM Data Mixer	.5
Transponser	4
Digital Uplink Assembly	5
Pre Modulation Precessor	10.5
S-Bank Omni Antenna A	3
S-Bank Omni Antenna B	3
S-Bank Steerable Antenna	32.4
Wiring	30
	<hr/>
Total Communication	<u>111</u>

TABLE 8.5-8

INSTRUMENTATION SYSTEM WEIGHT

ITEM	WEIGHT [lbs]
Structure & Mtg	14
Stored Program Data Processor	23
Signal Conditioning Assembler	10
Engineering Sensors	10
Wiring	10
	<hr/>
Total Instrumentation	<u>67</u>

TABLE 8.5-9

ENVIROMENTAL CONTROL SYSTEM WEIGHT

ITEMS	WEIGHT [lbs]
Telecommunications	11
Instrumentation	17
Guidance	4.35
Battery	3
Propellant Lines	5
Lh ₂ Tank	71
LOX Tank	50
2 Vernier Tanks	5
Vernier Lines	5
Thermal Control Heater	.5
Thermal Control Heater	.5
	<hr/>
Total Enviromental Control	<u>196</u>

REFERENCES

1. "Improved Lunar Cargo & Personnel Delivery System", Lockheed Missiles and Space Co., Sunnyvale, Calif.; (Contract No. NAS-8-21006), 1968, Volume IV.
2. "Surveyor, Final Engineering Report", Hughes Aircraft Co., (JPL Contract NO 950056), 1968.
3. "Cryogenic Tank Support Evaluation", Lockheed Missiles & Space Co., Sunnyvale, Calif.; (Contract No. NAS-3-7979), 1969.
4. "Metallic Materials and Elements for Aerospace Vehicle Structures," Dept. of Defense, Washington, (MIL-HDBK-5A), 1966.
5. Purser, Eaget & Smith, "Manned Spacecraft--Engineering Design and Operation," Fairchild Publications, Inc., New York, 1964.
6. Osgood, "Spacecraft Structures," Prentice-Hall, 1966.
7. Abraham, "Structural Design of Missiles and Spacecraft," McGraw-Hill Book Company, 1962.
8. Orlando, Meyers & Breehn, "Missile Structures--Design and Analysis," Tri-State Offset Company, Ohio, 1967.

CHAPTER IX
SOFT LANDING ANALYSIS

Charles Gilbert Richards 9.1,9.3
Thomas Perkins 9.2,9.4
Steve Dickerson 9.5
Sam Kozak 9.6

9.1 Introduction

The primary objective in the analysis of the landing dynamics of the LLV was the determination of the conditions that would produce a stable landing on the lunar surface. Three types of analyses were carried out to determine landing stability criteria for the LLV.

9.2 Static Stability

The static stability of the spacecraft was analyzed for surface slopes which varied from zero to 35 degrees. The variation of the static stability angle β with center of gravity height to landing-gear radius ratio, H/R , is presented in Figure 9.2-1. It is evident that as the H/R ratio increases the static stability angle, β , decreases. At a surface slope of 35 degrees the static stability angle becomes zero for a value of $H/R = 1.42$. Therefore, to prevent the spacecraft from statically tipping over on a surface slope of 35 degrees an H/R of less than 1.42 must be incorporated into the final design of the LLV.

9.3 Dynamic Stability -- Energy and Momentum Methods

The landing stability of the LLV can be improved by, (1)

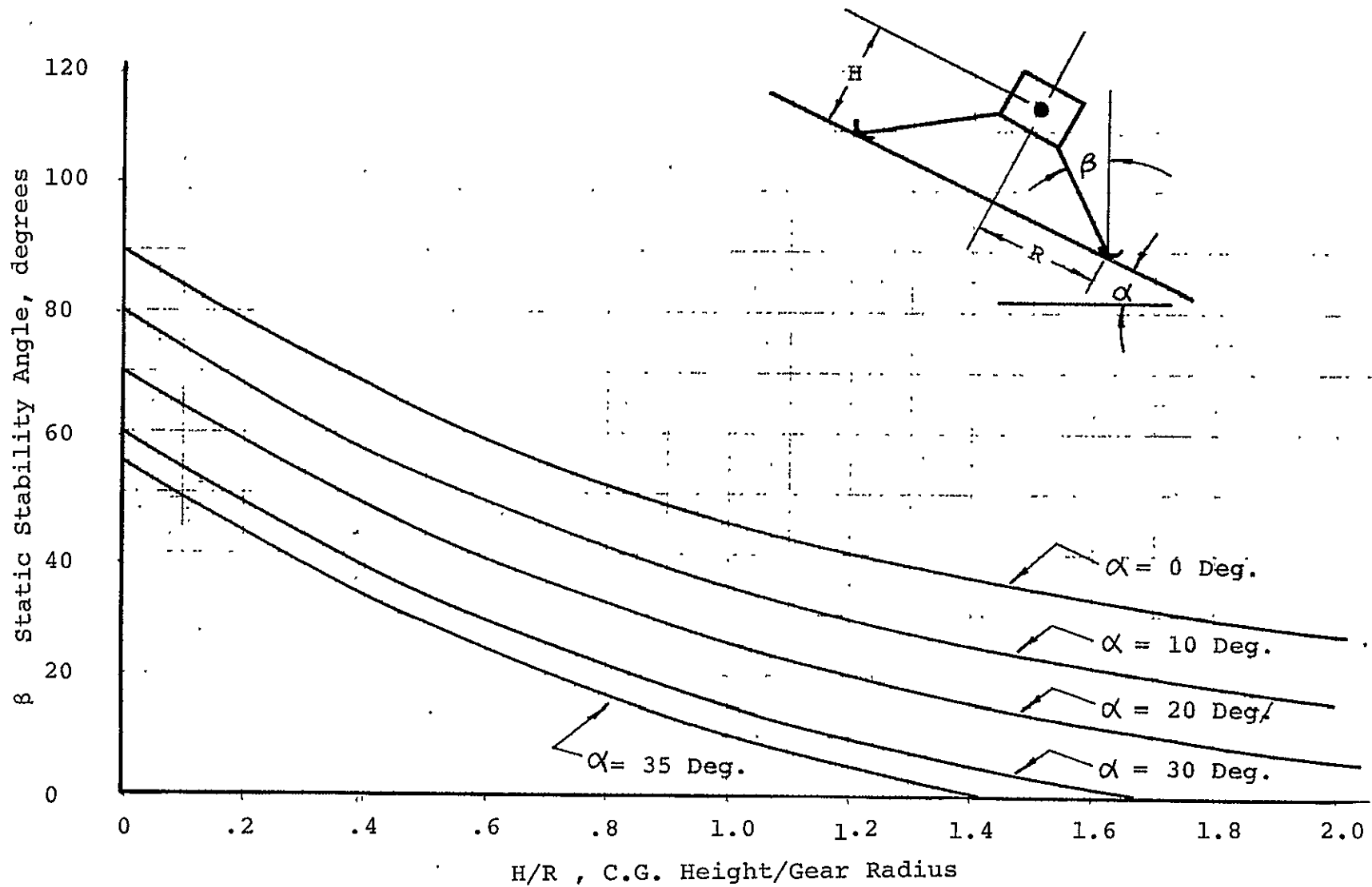
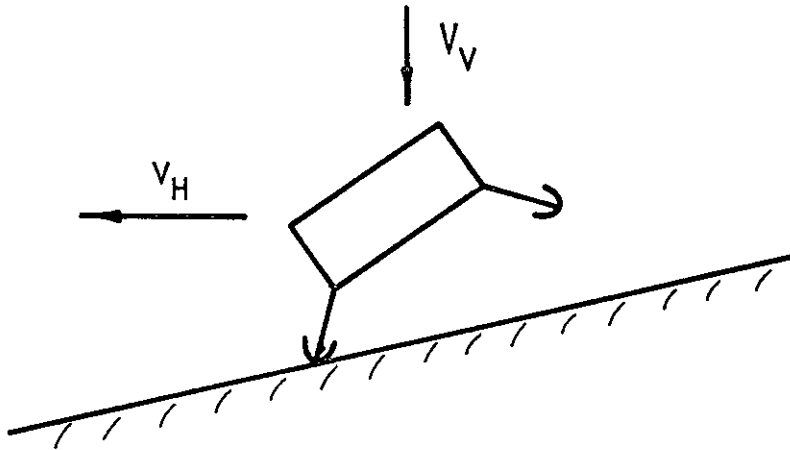


FIGURE 9.2-1 VARIATION OF THE STATIC STABILITY ANGLE WITH C. G. HEIGHT TO LANDING GEAR RADIUS RATIO.

reducing the impact velocity, (2) use an energy absorbing device, and (3) the use of a rocket motor to force the vehicle downward upon impact. A simplified mathematical analysis was carried out with the use of a digital computer to obtain rough estimates of the values of energy absorption and thrust required to prevent the vehicle from toppling over upon landing.

In order to make a realistic analysis, it was necessary to consider the sequence of events during impact. The landing gear legs were assumed to contact the lunar surface in pairs (i.e., the study is restricted to two dimensions). There are two cases which require study; case 1 in which the front legs hit first, and case 2 in which the back legs hit first. These two cases are illustrated in Figure 9.3-1. In case 1 it is desirable to give the vehicle a downward thrust immediately upon initial contact with the lunar surface so that a clockwise restoring moment results. In case 2, a reverse reaction is required in order to reduce the probability of tipping the vehicle over. In either case a stability rocket should be fired when the front legs contact the surface.

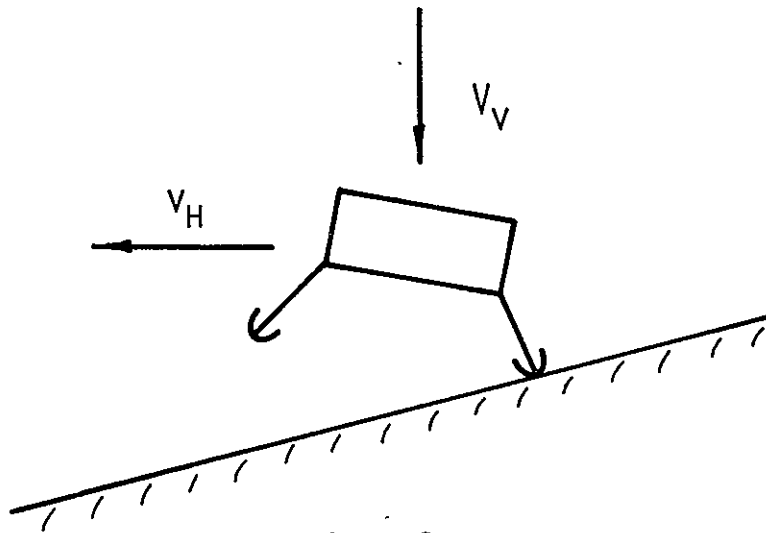
A single stability rocket may be mounted on the top of the vehicle over the C.G. or four rockets, one on each footpad (or side) of the vehicle may be used. The four rockets can be such that they supply one fourth the thrust of this single rocket. The total propellant required and torque supplied will be about the same in the two cases. The four rocket motor casings, controls, etc., will weigh slightly more than the single casing,



CASE 1

FRONT LEG CONTACTS

INITIALLY

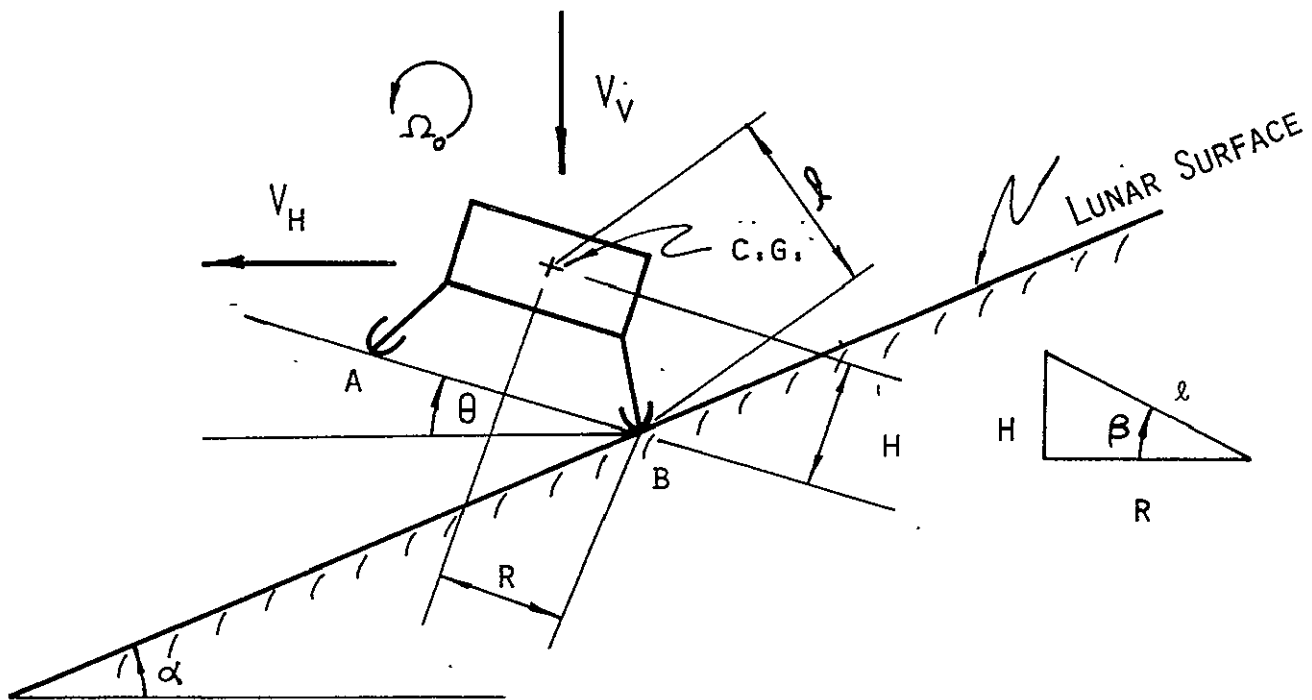


CASE 2

BACK LEG CONTACTS

INITIALLY

FIGURE 9.3-1



VEHICLE ATTITUDE AT INITIAL CONTACT

WITH THE LUNAR SURFACE

(REAR LEG HITS FIRST)

FIGURE 9.3-2

etc., of the centrally located rocket. The ignition circuitry for the single rocket will probably be less complex than that for four rockets. A single rocket will require additional supporting structure whereas four rockets can be mounted on existing structural members.

The dynamic stability analysis described below was intended to give "ballpark" estimates from which trends could be seen and trade-offs could be made. The dynamic model used was as follows: the vehicle approached the lunar surface with a horizontal velocity component, V_H , a vertical velocity component, V_V , an angular velocity component, Ω_O , about an axis through the vehicle's C.G., and a pitch angle, θ . The surface slope angle is α . The model is two dimensional and is shown in Figure 9.3-2.

There are basically two steps in the analysis:

1. The vehicle impacts legs "B" (i.e., the rear legs in Figure 9.3-2) first. The footpad is assumed to be pinned upon impact at point B, and angular momentum about an axis through B is conserved [1].

2. The total energy after impact at B is conserved as the vehicle continues to rotate about B until legs "A" contact the surface. (See Figure 9.3-3) At this time, an amount of energy, ΔW , is assumed to be absorbed by some dissipation device in each leg, e.g., crushable honeycomb. A single stability rocket, with thrust, T , mounted over the C.G.* is simultaneously ignited.

*This is dynamically equivalent to four rockets, each with one fourth the thrust, mounted symmetrically about the c.g.

The vehicle continues to rotate about an axis through A. The work-energy relationships are used to determine the thrust, T , which is required to just keep the vehicle from tipping over.

The equations used are given below:

For conservation of momentum at B, one has

$$I\Omega_B = I_{CG}\Omega_O + m[V_H \ell \sin(\beta+\theta) + V_V \ell \cos(\beta+\theta)] \quad (9.3-1)$$

The energy after impact at B is given by

$$E_B = 1/2 I\Omega_B^2 + mg_{\text{moon}}[\ell \sin(\beta+\theta) + 2R \sin\alpha] \quad (9.3-2)$$

where the datum plane is shown in Figure 9.3-3.

The energy absorbed by a crushable device at A is denoted by ΔW and is added to the energy "taken out" by the stability rocket and crushable material.

$$W_{\text{out}} = TR\left(\frac{\pi}{2} - \alpha + \beta\right) + \Delta W \quad (9.3-3)$$

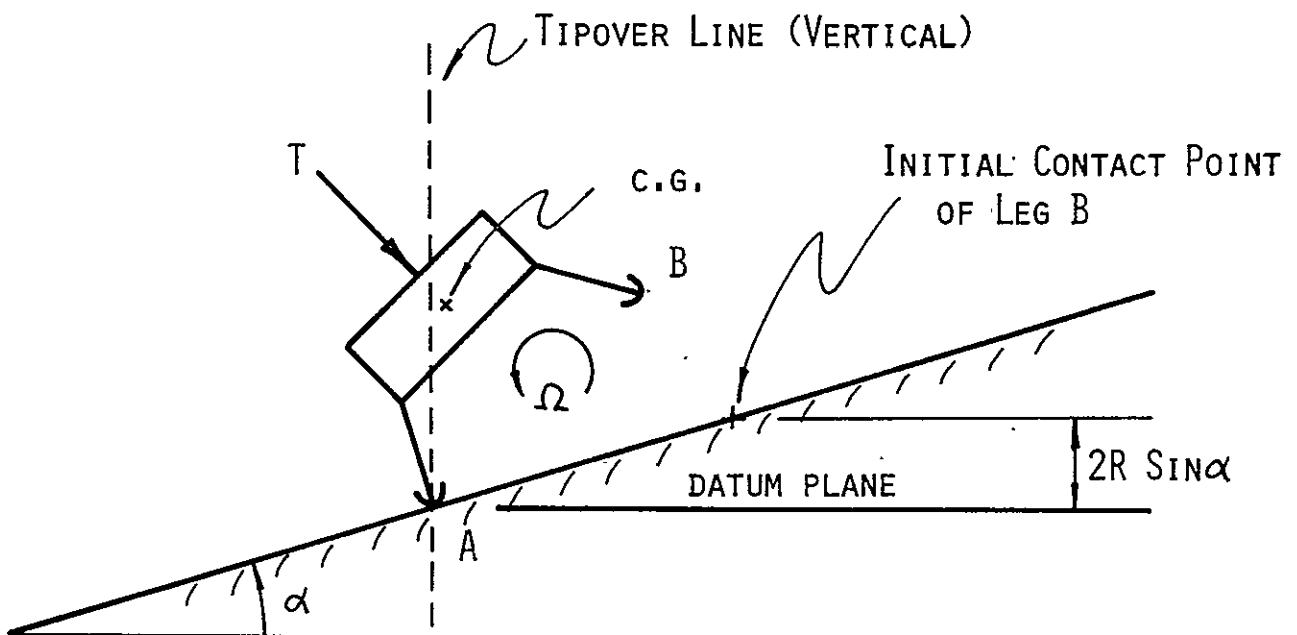
If the assumption is made that the vehicle just reaches the tipover line (shown in Figure 9.3-3) with a zero angular velocity, the energy of the vehicle consists only of potential energy and is given by

$$E_A = mg_{\text{moon}} \ell$$

the work-energy relationships then give

$$E_B = E_A + W_{\text{out}} \quad (9.3-5)$$

Substitution of E_B , E_A and W_{out} substituting into (9.3-5) and solving for T yields



VEHICLE ATTITUDE DURING STABILITY

ROCKET FIRING (ENERGY IS ABSORBED

BY LEG A)

FIGURE 9.3-3

$$T = \frac{1}{R(\frac{\pi}{2} - \alpha - \beta)} \left\{ \frac{1}{2I} [I_{CG} \Omega_o + m \left(\ell V_H \sin(\beta + \theta) + \ell V_V \cos(\beta + \theta) \right)]^2 + mg_{moon} [\ell \sin(\beta + \theta) - \ell + 2R \sin \alpha] - \Delta W \right\} \quad (9.3-6)$$

In the case where the front legs hit first at A (see Figure 9.3-4), the analysis is similar. As a conservative estimate, it is assumed that ΔW is zero in this latter case. The resulting equation for the thrust, T , is

$$T = \frac{1}{R(\frac{\pi}{2} - \beta + \theta)} \left\{ \frac{1}{2I} [I_{CG} \Omega_o + m (V_H \ell \sin(\beta + \theta) - V_V \ell \cos(\beta - \theta))]^2 + mg_{moon} \ell [\sin(\beta - \theta) - 1] \right\} \quad (9.3-7)$$

where $\theta < 0$.

The symbols, as can be seen in the preceding figures, are defined to be

R = footpad radius

H = CG height

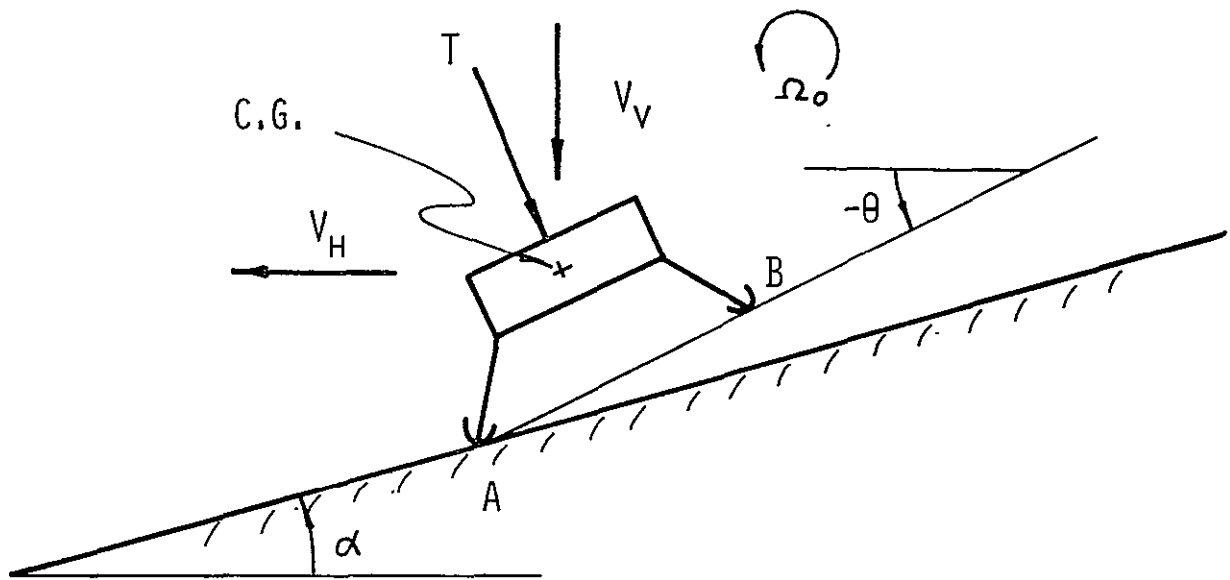
$\ell = \sqrt{R^2 + H^2}$

$\beta = \arctan H/R$

θ = pitch angle

I_{CG} = mass moment of inertia about the CG

$I = I_{CG} + m\ell^2$



VEHICLE ATTITUDE AT INITIAL CONTACT
WITH THE LUNAR SURFACE
(FRONT LEG HITS FIRST)

FIGURE 9.3-4

Ω_0 = angular velocity at touchdown

V_H = horizontal component of the touchdown velocity

V_V = vertical component of the touchdown velocity

m = total mass of the vehicle at touchdown

$g_{\text{moon}} = 5.31 \text{ ft/sec}^2$

ΔW = energy absorbed by crushable devices

T = thrust required to prevent tipping

α = slope angle of the lunar surface at touchdown

Equations (9.3-6) and (9.3-7) were solved for realistic values of the parameters, α , θ , Ω_0 , ΔW , V_V , and V_H on a digital computer. It was found that the results from the solution of Equation (9.3-7) were always below those from Equation (9.3-6). The latter was used to predict the thrust because the values were more conservative and because it seems more probable that the rear legs will hit first when moving downhill. Moving uphill is essentially the case given by Equation (9.3-7). The results of these runs are presented graphically in Figures 9.3-5 through 9.3-10. The value of I_{CG} used was 3700 slug-ft², and the weight used was 4440 lbs. These were estimated to be the approximate values at touchdown.

The results show that the pitch angle, θ , and the angular velocity, Ω_0 , at touchdown, do not significantly alter the thrust requirements to prevent tipover. However, the utilization of energy absorption devices and the reduction of touchdown velocities (by the vernier engines) can result in a sizeable reduction in the required thrust, T . The reduction of the

vertical velocity component appears to be the simplest parameter variation to implement. The reason for this is that the vernier rockets already present can be used to reduce the touchdown velocity. For example, one can see from Figure 9.3-7 that reducing the vertical component of the velocity from 15 fps to 2.5 fps on a 35° slope (worst case) reduces the required thrust from 5400 lbs to 1600 lbs.

Use of a crushable energy-absorption device which absorbs 12,000 ft-lbs will reduce the required thrust from 5400 lbs to 1400 lbs, for a vertical velocity of 15 fps, and a 35° slope, as can be seen from Figure 9.3-6.

If one were to combine these two features - reduction of the vertical velocity component and use of an energy absorber - the above analysis indicates that no stability rocket is needed even on a 35° slope! (It should be re-emphasized that the above analysis is based on very elementary considerations, and the conclusions should be interpreted in a qualitative sense only.)

A computer run was made for landing at a reduced vertical velocity ($V_H = 5$ fps) and utilizing energy absorbers. The results for lunar slopes of 35° and 25° are shown in Figure 9.3-11 and 9.3-12, respectively. A velocity reduction to 10 fps coupled with an energy absorption of 10,000 ft-lbs allows a stable landing without the use of the stability rocket on a 35° lunar surface slope. For lower values of the slope, a higher vertical velocity component for the same energy absorption

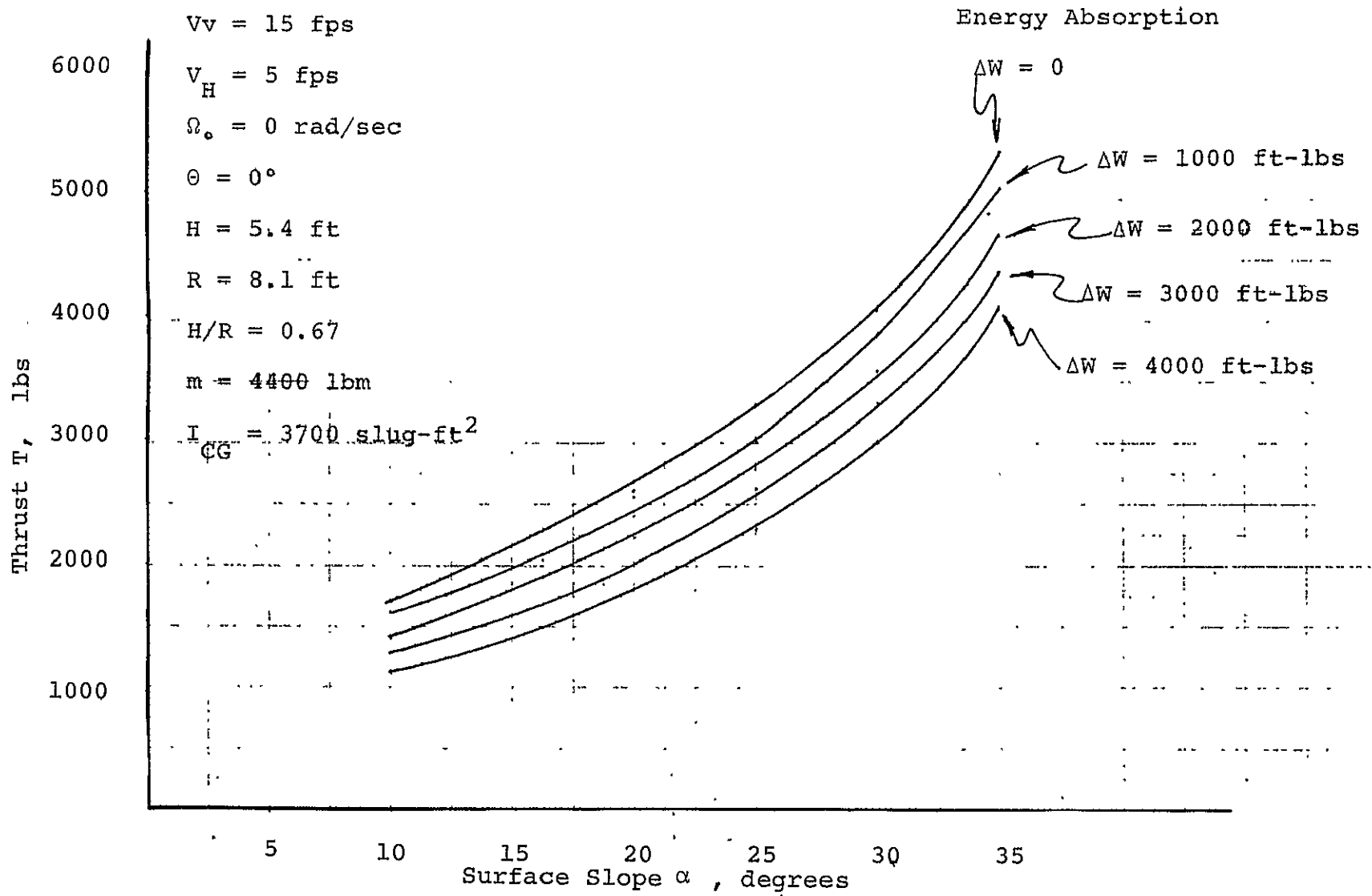


FIGURE 9.3-5 STABILITY ROCKET THRUST T vs SURFACE SLOPE ANGLE

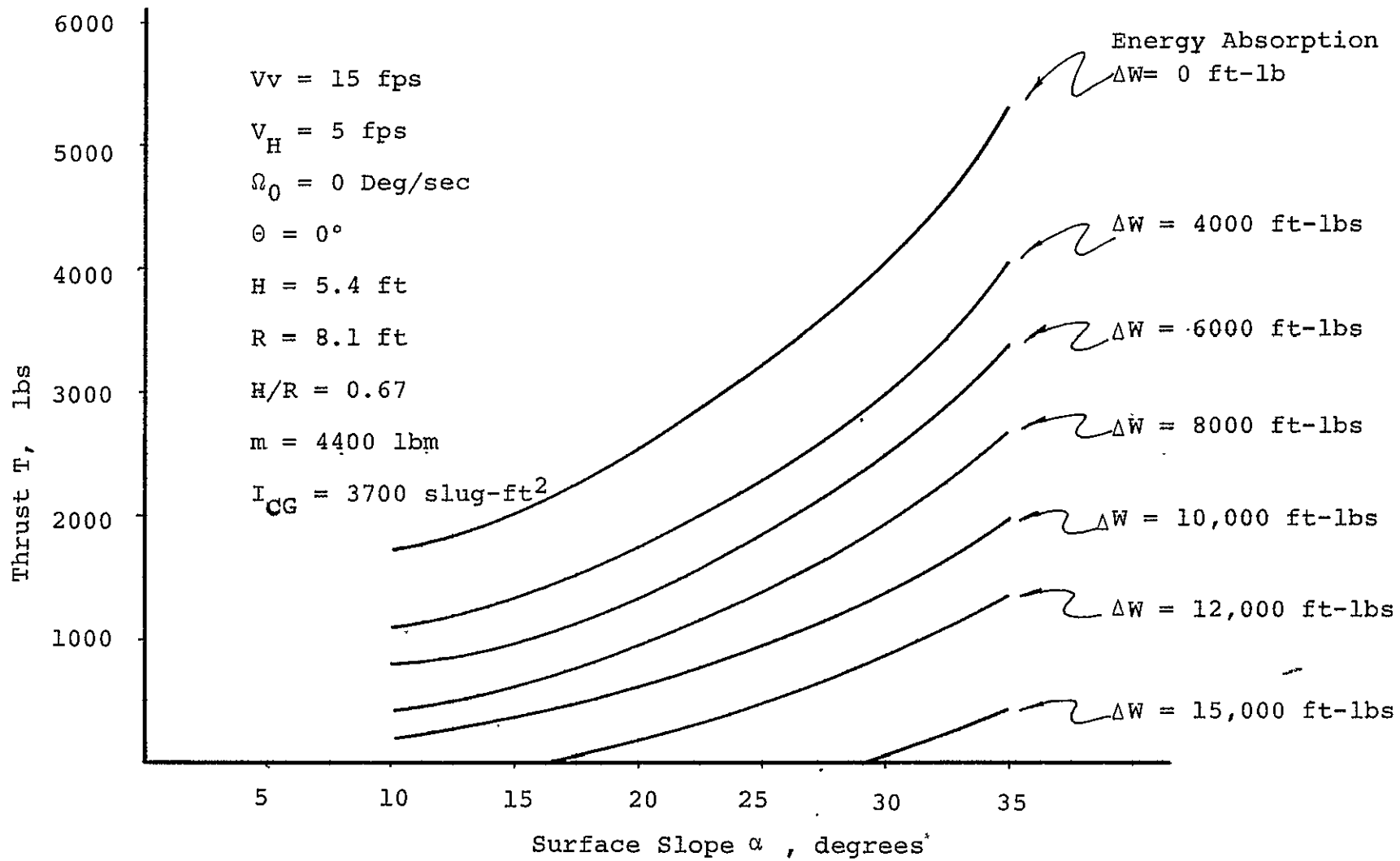


FIGURE 9.3-6 STABILITY ROCKET THRUST T vs SURFACE SLOPE ANGLE α

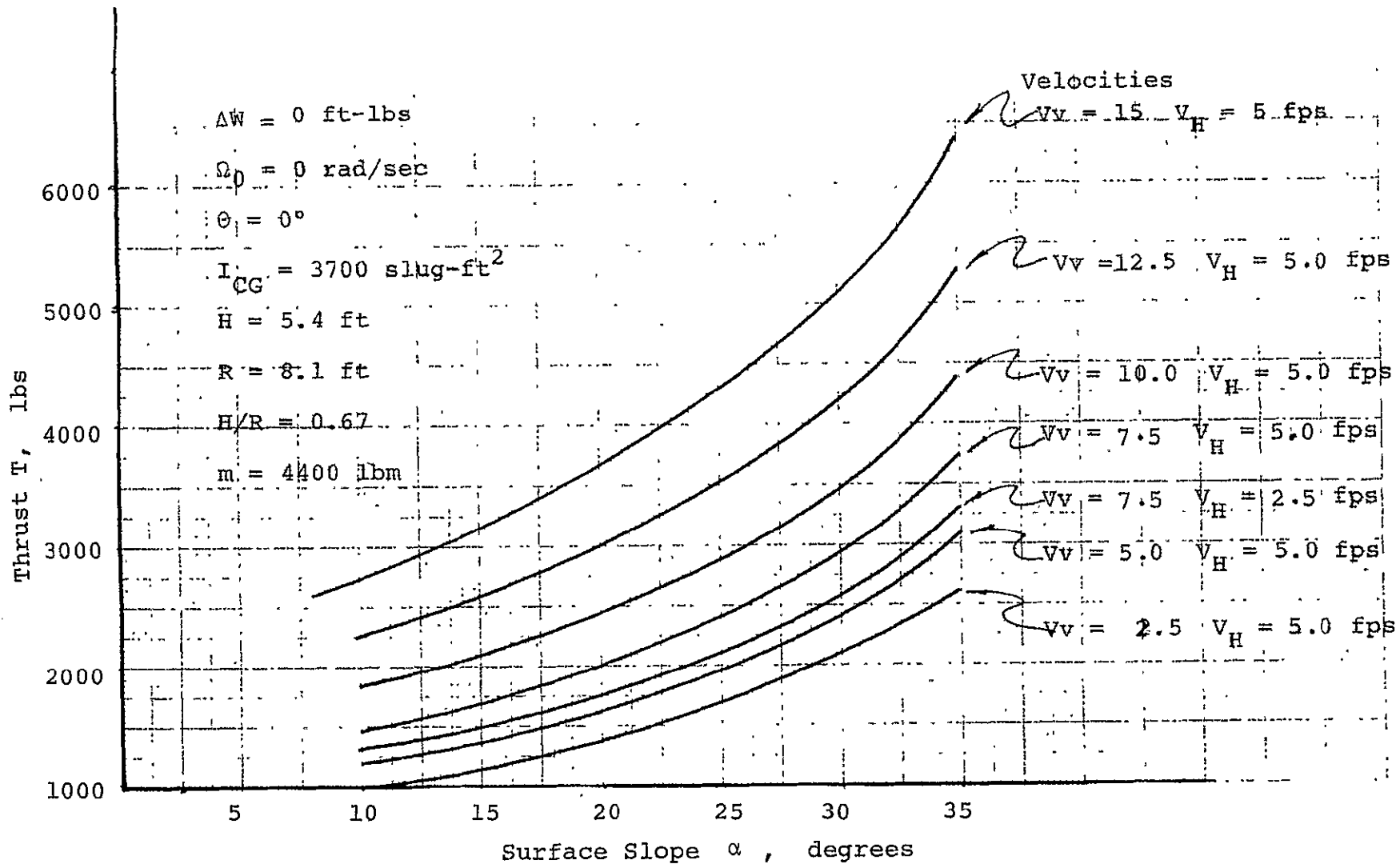


FIGURE 9.3-7 STABILITY ROCKET THRUST T vs SURFACE SLOPE ANGLE α

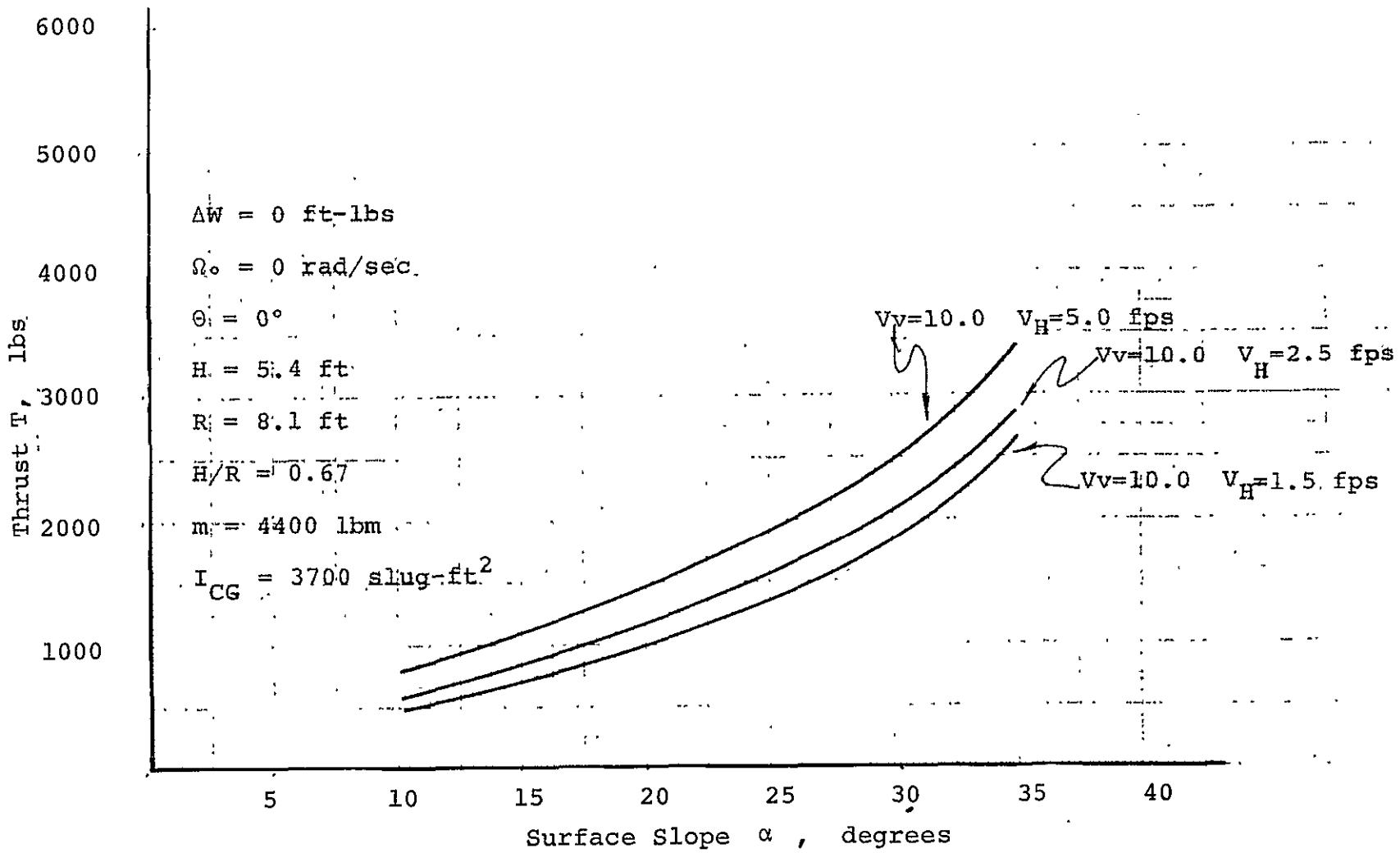


FIGURE 9.3-8 STABILITY ROCKET THRUST T vs SURFACE SLOPE ANGLE α

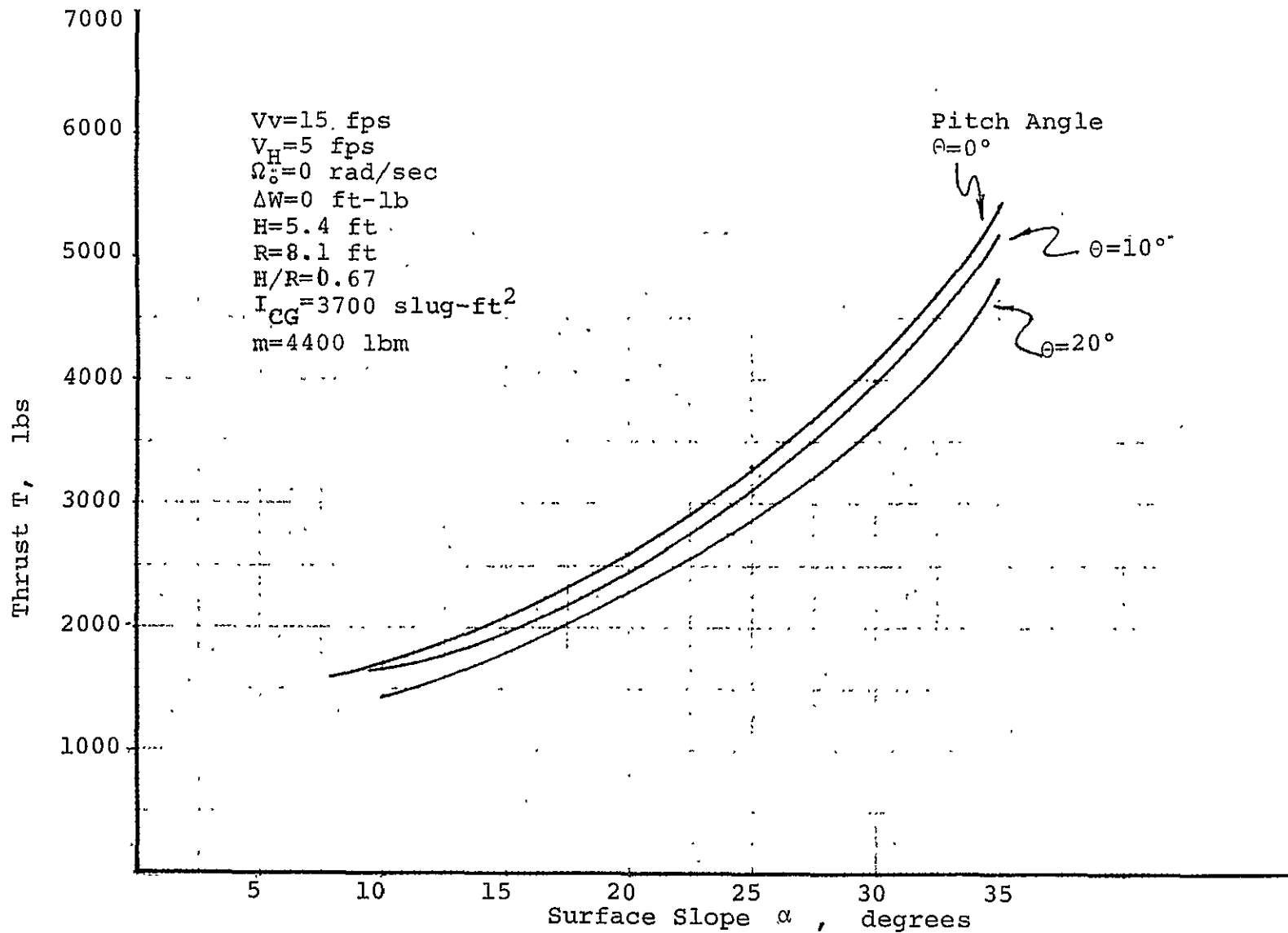


FIGURE 9.3-9 STABILITY ROCKET THRUST T vs SURFACE SLOPE ANGLE α

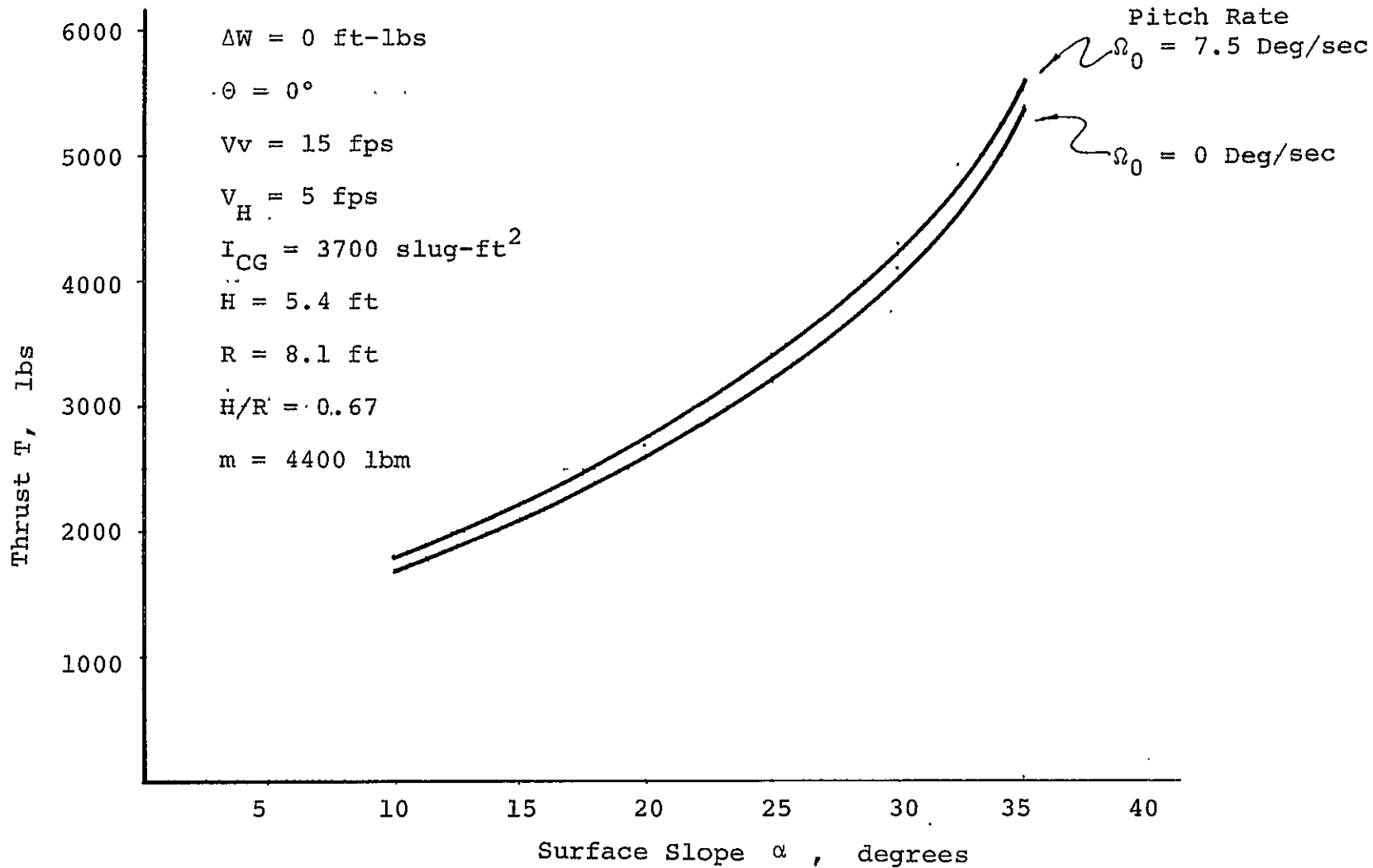


FIGURE 9.3-10 STABILITY ROCKET THRUST T vs SURFACE SLOPE ANGLE α

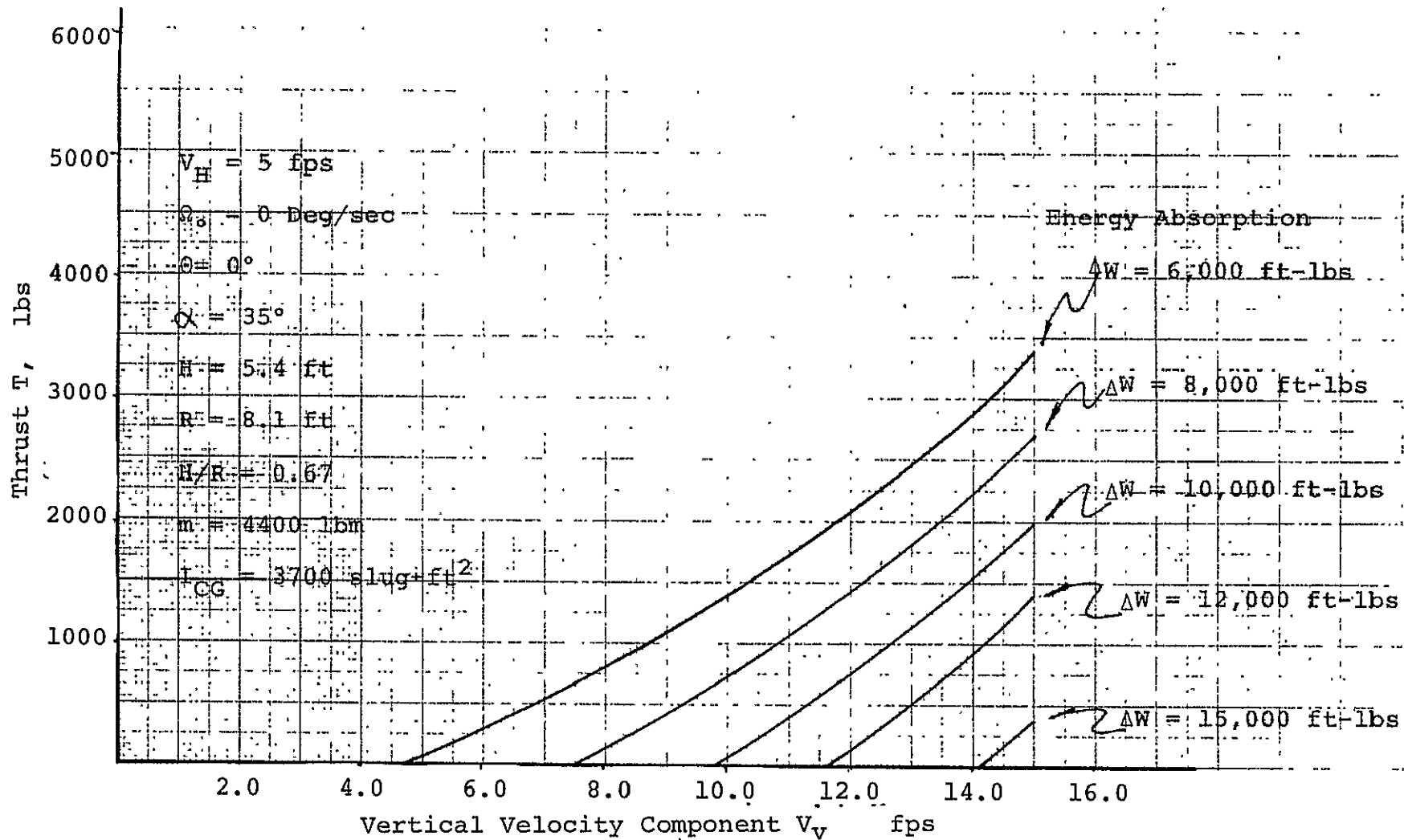


FIGURE 9.3-11 STABILITY ROCKET THRUST T vs VERTICAL VELOCITY COMPONENT V_v

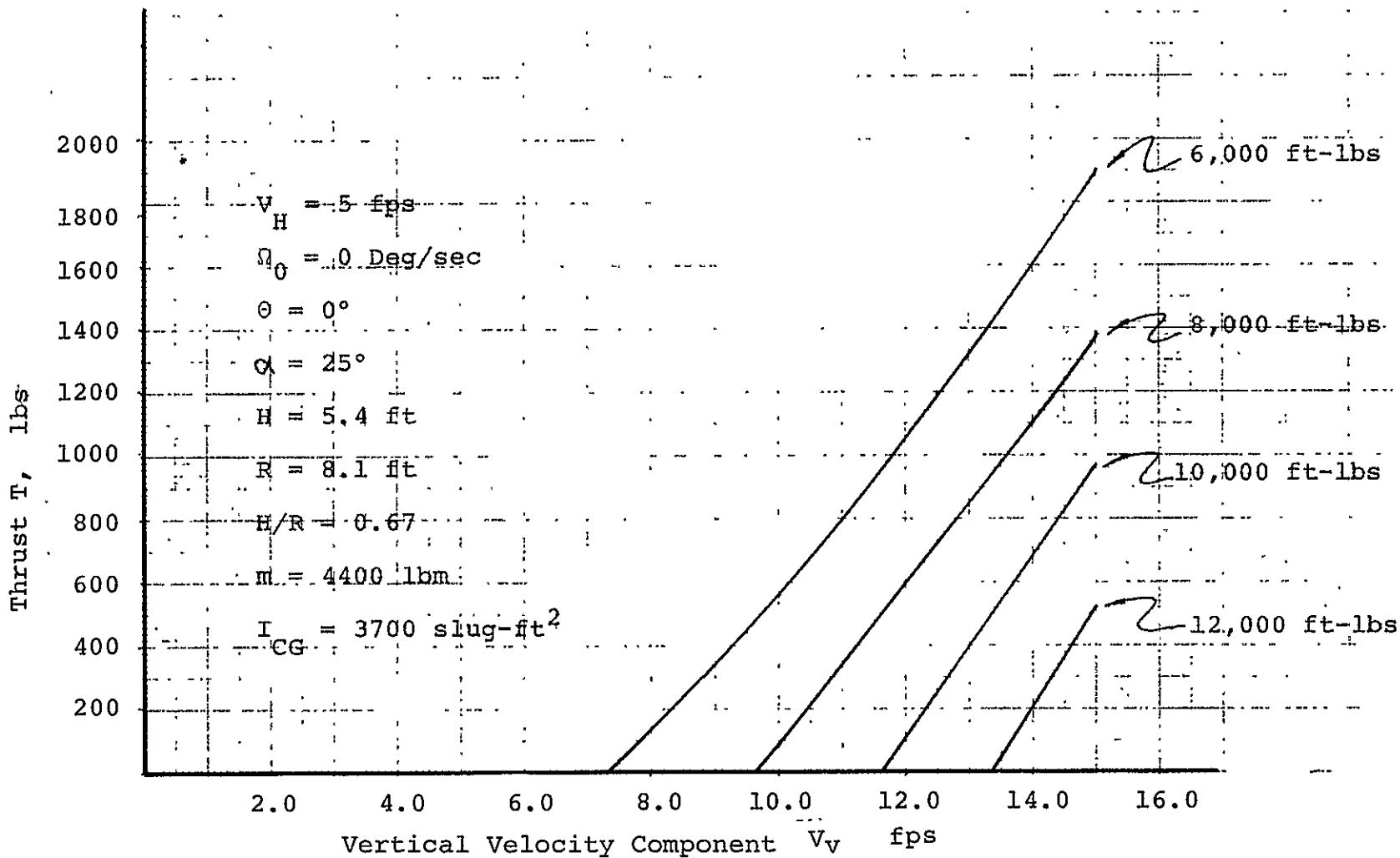


FIGURE 9.3-12 STABILITY ROCKET THRUST T vs VERTICAL VELOCITY COMPONENT V_v

will still give stability, e.g. on a 25° slope, an absorption of 10,000 ft-lbs will allow an 11.4 fps vertical component of velocity. These values are for the case of no thrust from the stability rocket.

Figure 9.3-6 indicates that an energy absorption of 13,400 ft-lbs will allow the vehicle to land on a 21° surface slope without the use of a stability rocket.

Figures 9.3-13 and 9.3-14 show values of the stability rocket thrust required for a stable landing on a 35° slope for two other values of I_{CG} and H/R ratios.

If a stability rocket were to be used, the figures show that the thrust should be of the order of 500 lbs. or greater in order to significantly reduce the crushable energy - absorption capacity and/or allow higher impact velocities.

If a stability rocket is used, it is necessary to know the length of time for which the rocket must be operated. An order-of-magnitude time estimate is obtained by finding an estimate of the elapsed time between the initial contact of a footpad with the lunar surface (see Figure 9.3-2) and the time at which the vehicle CG reaches the "tipover" line; see Figure 9.3-3). This time is estimated by finding the total angle, γ , through which the vehicle must rotate to reach the "tipover" line, where

$$\gamma = \frac{\pi}{2} + \theta - \beta \quad (9.3-8)$$

At the beginning of the motion, the angular velocity is Ω_B and is found from Equation (9.3-1). Assuming a constant angular deceleration, the average angular velocity is $\Omega/2$. Dividing γ by $\Omega/2$ yields the estimate of the total time from touchdown to

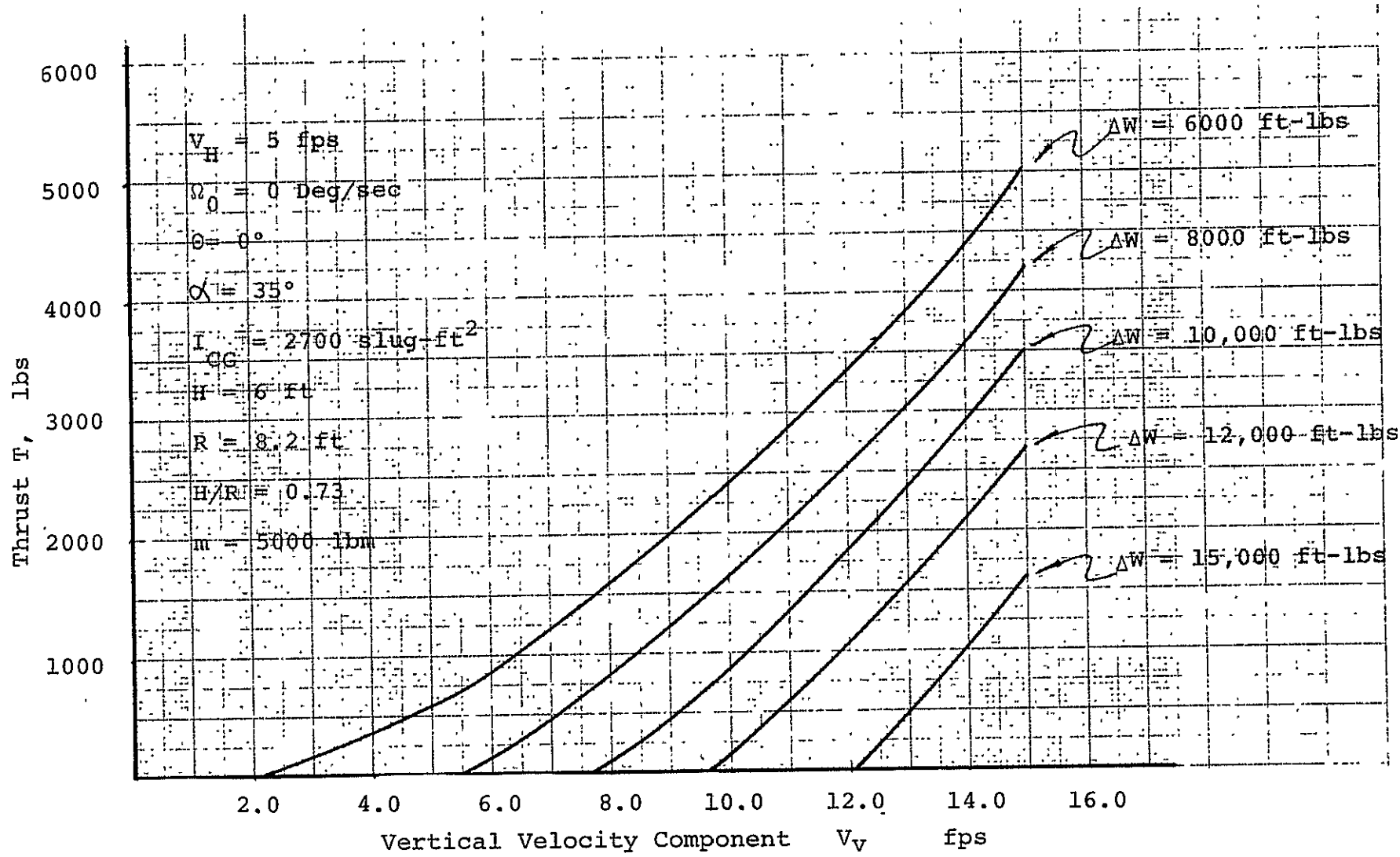


FIGURE 9.3-13 STABILITY ROCKET THRUST T vs VERTICAL VELOCITY COMPONENT V_v

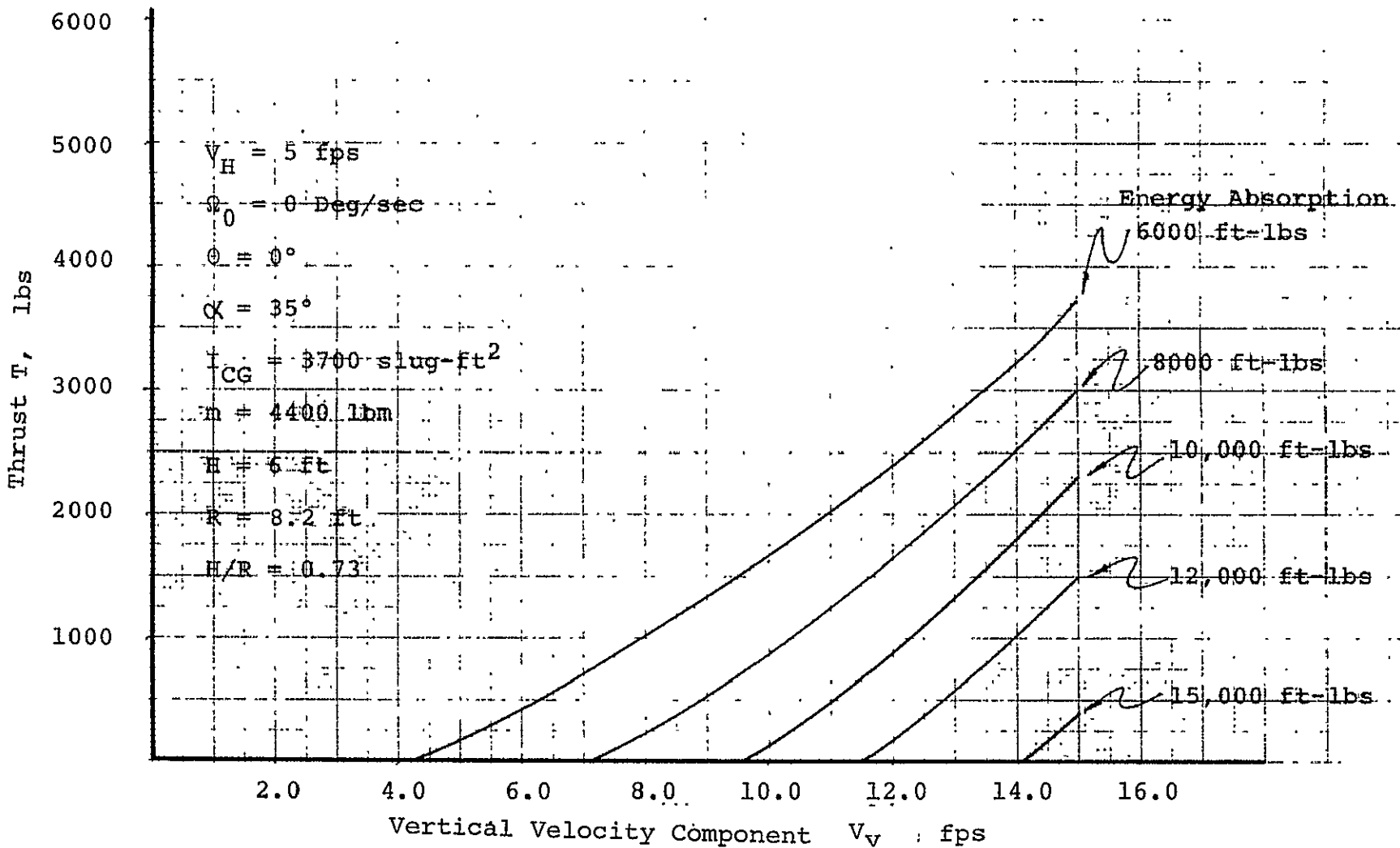


FIGURE 9.3-14 STABILITY ROCKET THRUST T vs VERTICAL VELOCITY COMPONENT V_v

tipover. Thus

$$T = \frac{2\gamma}{\Omega_B} = \frac{[\pi + 2(\theta - \beta)] I}{I_{CG} \Omega_0 + [V_H \sin(\beta + \theta) + V_V \cos(\beta + \theta)] m \ell} \quad (9.4-9)$$

Values of this time are of the order of 5 secs or less. Since the stability rocket should fire for only that portion of the rotation which takes place about legs A (see Figure 3.9.3-3), the time of firing has been assumed to be one half the total rotation time or approximately 2 1/2 secs. A calculation using a specific impulse of 290 lb_f-sec/lb_m, shows that 4.3 lbs of propellant are required for 500 lbs of thrust for 2 1/2 secs. Solid rocket motors will provide thrusts from 500 lbs to 1000 lbs for 4 secs and nominally have a total weight of 25 lbs including the safety and arming devices. So, for a weight penalty of about 25 lbs, the probability of a stable (i.e., upright) landing could be increased by the inclusion of a centrally mounted stability rocket with a thrust of up to 1000 lbs or four stability rockets mounted symmetrically about the vertical C.G. axis with a total thrust of 1000 lbs.

9.4 Solutions of Landing Equations of Motion

A mathematical procedure for computing the touchdown dynamics of a soft-landing on the lunar surface has been derived by NASA-MSFC [2]. This computer program was used to calculate the dynamic stability boundaries incurred for the Lunar Logistics Vehicle for a symmetric 2-2 landing on surface slopes which ranged from zero to 35 degrees and touchdown velocities which varied from 0 to 15 fps vertically and ± 5 fps horizontally. The spacecraft must be statically and dynamically stable for these landings, and the landing forces must not exceed 6 g. (g = earth gravitational acceleration).

The LLV is approximated by a rigid body of constant mass that has four identical landing gear assemblies attached to it. The mass of each landing gear assembly is assumed to be a point mass concentrated at its respective footpad. The landing gear system is composed of telescoping struts that house crushable honeycomb material as shown in Figure 9.4-1. The forces that act on the idealized vehicle during landing result from the vehicle's landing gear system, reaction control system, and gravity. The elastic properties of the vehicle structure and landing gear system are approximated by assuming a linear structure.

Touchdown analyses were restricted to landings on a rigid uniform surface and do not include effects due to soil properties and crater dispersions. The surface slope angles were varied from 0 to 35 degrees with a two foot barrier inserted ahead of the front legs as they touched the lunar surface. This prevented the spacecraft from sliding down the slope. All solutions

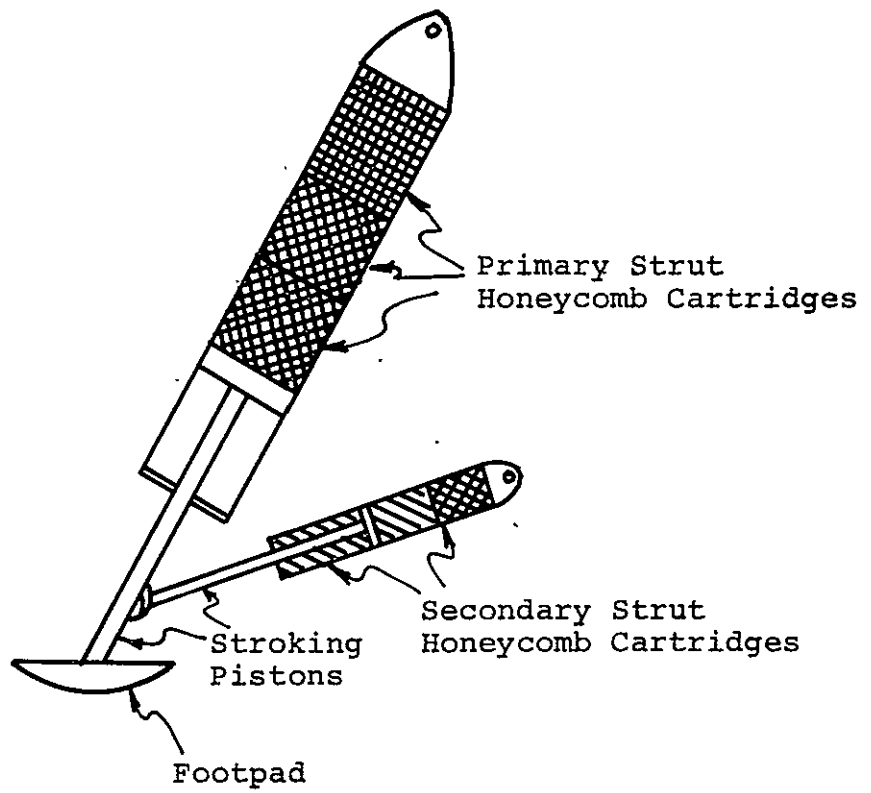


FIGURE 9.4-1 PRIMARY AND SECONDARY STRUT CONFIGURATION

presented were for a 2-2 landing which allows the rear footpads to strike the surface first and absorb energy as rotation occurred about the rear footpads. After the front footpads struck the surface, energy absorption occurred simultaneously in both front legs as rotation occurred about the front footpads, which are not allowed to slide. The footpads are free to translate vertically above the surface. However, if the front footpads translate above the 2 foot barrier the run is declared unstable.

Figure 9.4-2 presents a drawing of the model geometry as represented on the NASA-MS-1108 computer, and Figure 9.4-3 presents a sequence illustration of the 2-2 landing made and the corresponding location of the stability walls.

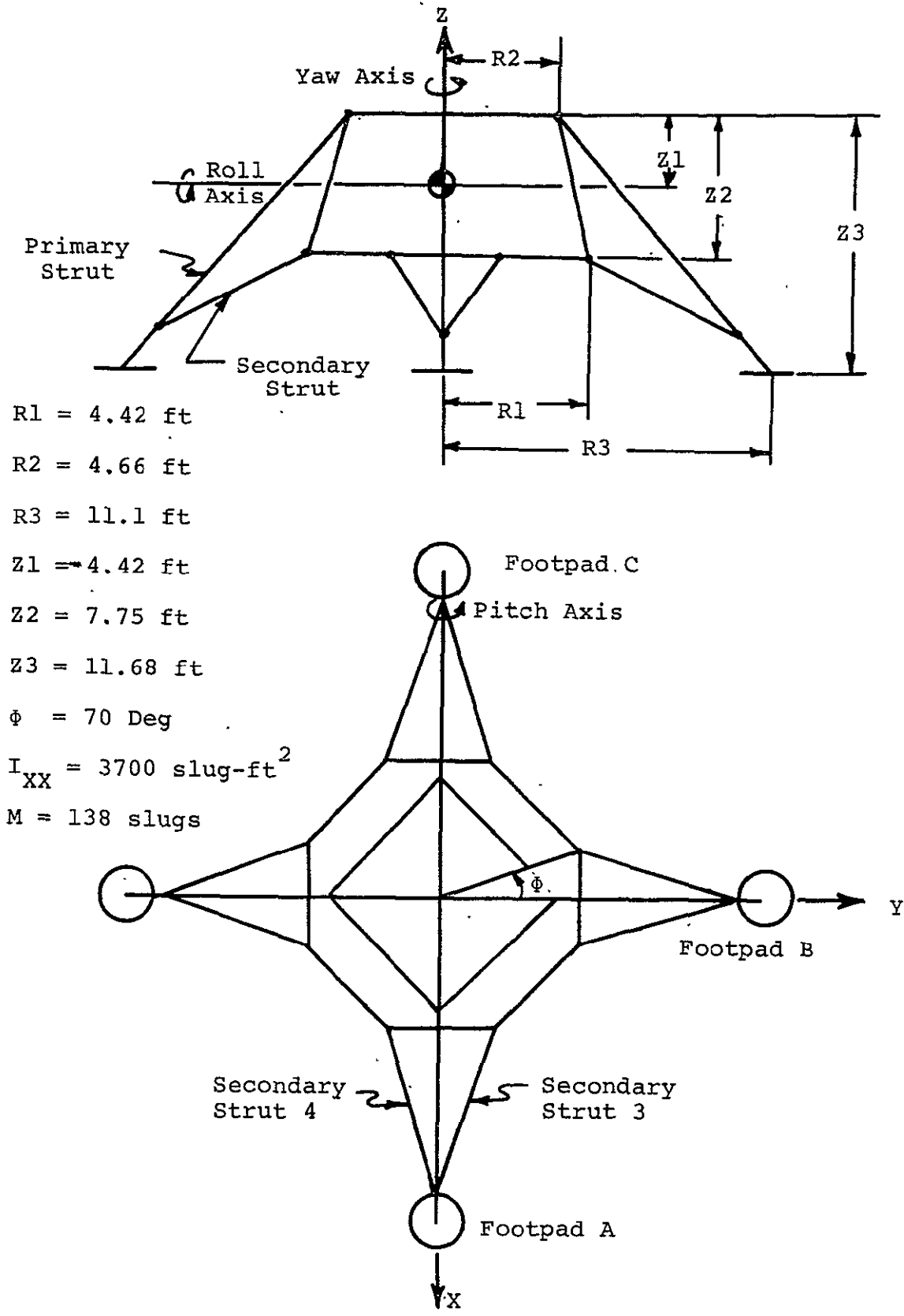


FIGURE 9.4-23 COMPUTER MODEL GEOMETRY

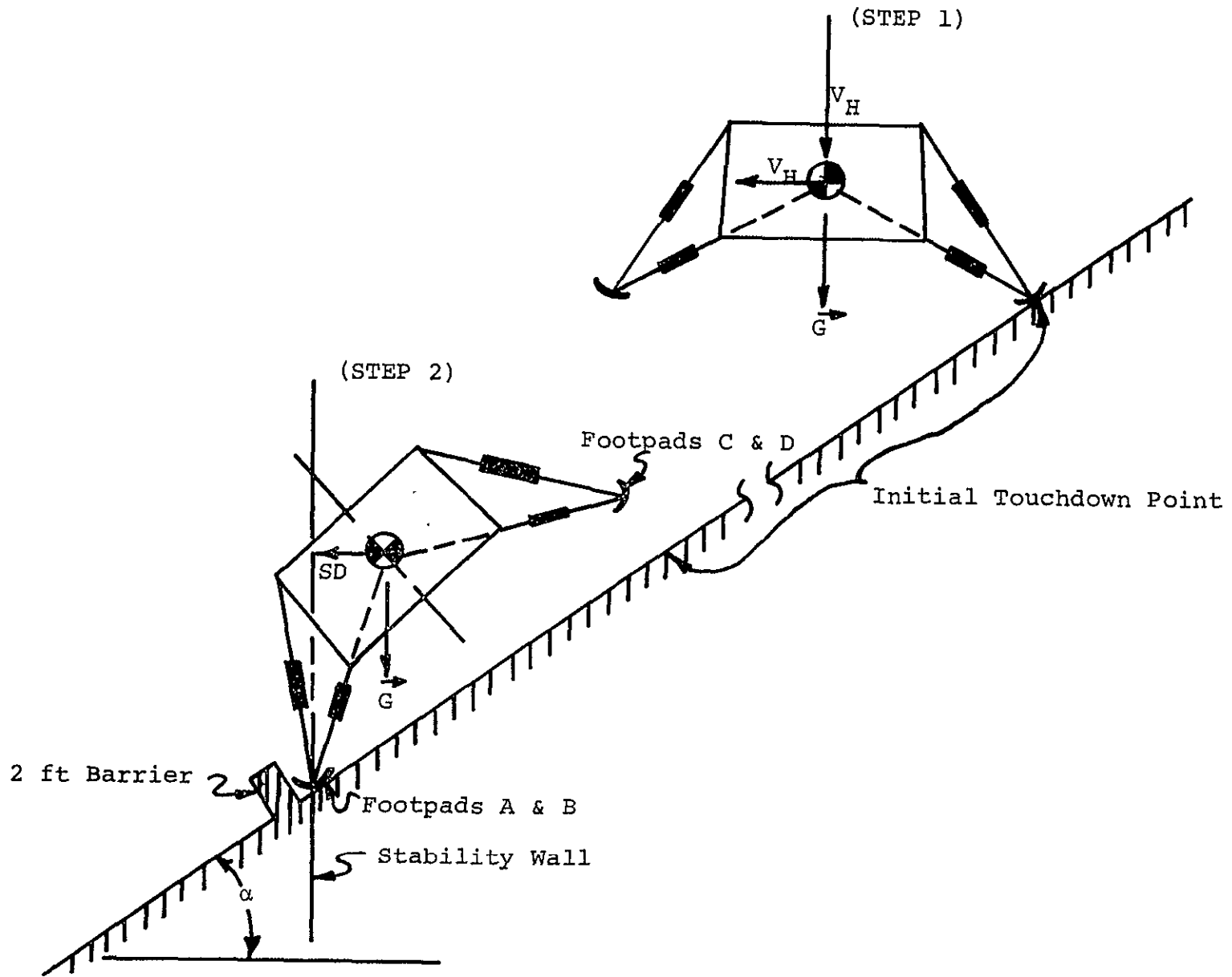


FIGURE 9.4-3 , TOUCHDOWN SEQUENCE & STABILITY CRITERIA

Stability Criteria. A performance evaluation of a soft landing system required the simulation of many touchdown conditions. When a large number of touchdown simulations are required, the speed at which the computer can execute these simulations became a factor in the problem. In the evaluation of this soft-landing system for stability (tip-over) performance, the computer running time was reduced by defining a stability criteria such that the computer could make the decision as to whether the landing simulated was stable or unstable. After making this decision the computer simulation was terminated.

A parameter representative of the state of stability of a landing is the magnitude of the "stability distance." The stability distance is the shortest distance between the vehicle center of mass and a plane parallel to the gravity vector, passing through two adjacent landing gear footpads. This plane is defined as the "stability wall." The vector definition of the stability distance is presented in Figure 9.4-3. The length of vector (\vec{SD}) is the stability distance.

If the vehicle center-of-mass is within an enclosure defined by stability walls and lunar upslope, then the gravitational action on the vehicle will stabilize it. If the vehicle's center-of-mass is outside this enclosure, the gravitational action on the vehicle will cause it to be unstable. When the vehicle's center-of-mass is outside the stability walls, the landing is declared unstable. If the vehicle is unstable, the degree of instability can be estimated by the magnitude of the "overturning velocity" at the instant the vehicle's center-of-mass passes through the stability wall.

A stable landing may also be determined by the vehicle's kinetic energy. At the instant a landing gear footpad makes contact with the landing surface, the vehicle has a given kinetic energy. The subsequent motion will increase or decrease the initial vehicle kinetic energy depending on the amount of energy dissipated by the landing gear system or the energy gain due to the lowering of the vehicle's center-of-mass. When the vehicle's kinetic energy has been dissipated to the point that is less than approximately 10 percent of the initial vehicle's touchdown kinetic energy, the landing gear struts have generally undergone maximum stroking. The resulting vehicle motion, after maximum stroking occurs, will generally be rigid body rotation about two adjacent landing gear footpads on the landing surface. A landing is declared stable when the following conditions are satisfied:

1. The vehicle's center-of-mass is inside the stability walls.
2. The vehicle's landing-gear footpads are on the landing surface (Figure 9.4-3).
3. The vehicle's center-of-mass is moving away from the stability wall.

Dynamical Equations of Motion. The instantaneous position coordinates of the rigid vehicle's center-of-mass (X, Y, Z) together with the instantaneous values of the Euler angles ($\theta_x, \theta_y, \theta_z$) specified the orientation of the rigid vehicle. The instantaneous position coordinates of the n^{th} landing gear footpad in the inertial coordinate system (XP_n, YP_n, ZP_n) allowed the determination of the instantaneous geometry of the n^{th} landing gear assembly. The equations of motion which were solved in this simulation of the landing impact dynamics were the three translational equations of motion of the rigid vehicle's center-of-mass, three rotational equations of motion of the idealized rigid vehicle, and three translational equations of motion for each of the four landing gear footpads.

The three translational equations of motion of the rigid vehicle were obtained by summation of all forces acting on the rigid vehicle and the application of Newton's Laws of Motion:

$$\ddot{X} = \frac{FX}{M} \quad (9.4-1)$$

$$\ddot{Y} = \frac{FY}{M} \quad (9.4-2)$$

$$\ddot{Z} = \frac{FZ}{M} \quad (9.4-3)$$

where,

FX, FY, FZ

summation of forces on the idealized rigid vehicle resolved along the X, Y, Z inertial coordinate axes.

M

mass of the idealized rigid vehicle.

X, Y, Z inertial accelerations of the rigid vehicle's center-of-mass.

The three rotational equations of motion express the time rate of change of the angular momentum vector of the rigid spacecraft in terms of Euler angles and Euler angular rates. These equations of motion are developed in Reference [2].

$$\ddot{\theta}_x = (\dot{\omega}_x \cos \theta_z - \dot{\omega}_y \sin \theta_z - 2\dot{\theta}_x \dot{\theta}_y + \dot{\theta}_z \omega_z) \cos \theta_y \quad (9.4-4)$$

$$\ddot{\theta}_y = \dot{\omega}_x \sin \theta_z + \dot{\omega}_y \cos \theta_z + \dot{\theta}_z \dot{\theta}_x \cos \theta_y \quad (9.4-5)$$

$$\ddot{\theta}_z = -\ddot{\theta}_x \sin \theta_y - \dot{\theta}_x \dot{\theta}_y \cos \theta_y + \dot{\omega}_z \quad (9.4-6)$$

where $\dot{\omega}_x, \dot{\omega}_y, \dot{\omega}_z$ are the components of the angular acceleration vector expressed in the body coordinate system and are determined by solving the familiar Euler moment equations for rigid bodies:

$$\begin{aligned} T_x = I_{xx} \dot{\omega}_x - I_{xy} \dot{\omega}_y - I_{xz} \dot{\omega}_z + (-I_{xy} \dot{\omega}_x + I_{zz} \dot{\omega}_z) \omega_y \\ - (-I_{xy} \omega_x + I_{yy} \omega_y - I_{yz} \omega_z) \omega_z \end{aligned} \quad (9.4-7)$$

$$\begin{aligned} T_y = -I_{xy} \dot{\omega}_x + I_{yy} \dot{\omega}_y - I_{yz} \dot{\omega}_z + (I_{xx} \omega_x - I_{xy} \omega_y - I_{yz} \omega_z) \omega_z \\ + (I_{xz} \omega_x + I_{yz} \omega_y - I_{zz} \omega_z) \omega_y \end{aligned} \quad (9.4-8)$$

$$\begin{aligned} T_z = -I_{xz} \dot{\omega}_x - I_{yz} \dot{\omega}_y + I_{zz} \dot{\omega}_z + (-I_{xy} \omega_x + I_{yy} \omega_y - I_{yz} \omega_z) \omega_x \\ + (-I_{xx} \omega_x + I_{xy} \omega_y + I_{xz} \omega_z) \omega_y \end{aligned} \quad (9.4-9)$$

where,

$\omega_x, \omega_y, \omega_z$ angular rate vector components of the rigid vehicle expressed in the body coordinate system.

I_{xx}, I_{yy}, I_{zz} mass moments of inertia about the

	X, Y, Z body coordinate axes
I_{xy}	cross product of inertia with respect to the X-Y plane in the body coordinate system
I_{xz}	cross product of inertia with respect to the X-Z plane in the body coordinate system
I_{yz}	cross product of inertia with respect to the Y-Z plane in the body coordinate system
T_x, T_y, T_z	sum of the torques about the X, Y, Z body coordinate axes.

The footpad equations of motion were obtained by summing all forces acting on the effective footpad masses. These equations have the general form given below although the actual equations solved may vary depending on the specific type of landing surface assumed.

$$\ddot{X}_{P_n} = \frac{1}{PMASS} \left(FXP_n - \frac{FGRND_n \dot{X}_{P_n}}{\sqrt{(\dot{X}_{P_n})^2 + (\dot{Y}_{P_n})^2}} \right) + g_x \quad (9.4-10)$$

$$\ddot{Y}_{P_n} = \frac{1}{PMASS} \left(FYP_n - \frac{FGRND_n \dot{Y}_{P_n}}{\sqrt{(\dot{X}_{P_n})^2 + (\dot{Y}_{P_n})^2}} \right) + g_y \quad (9.4-11)$$

$$\ddot{Z}_{P_n} = \frac{1}{PMASS} (FZP_n) + g_z \quad (9.4-12)$$

where,

$X_{P_n}, Y_{P_n}, Z_{P_n}$ inertial coordinates of the n^{th} footpad

PMASS	effective mass of each footpad.
FGRND _n	magnitude of a drag force on the n th footpad with direction opposite to the instantaneous sliding direction of the footpad in the inertial X-Y plane.
FXP _n , FYP _n , FZP _n	forces on the n th footpad in the X, Y, Z inertial directions which were independent of the instantaneous sliding direction of the footpad.
g _x , g _y , g _z	components of the gravitational acceleration vector expressed in the inertial coordinate system.

The equations of motion (9.4-1) - (9.4-12) were solved by a numerical integration procedure. The initial conditions for these equations were specified in the following manner. The spacecraft attitude at the instant of impact was specified by the three Euler angles θ_x , θ_y , and θ_z . These angles determined which footpad was initially in contact with the landing surface. This initial point of contact was taken to be the origin of the inertial coordinate system. The position of each footpad in the body coordinate system prior to impact was specified by known vehicle geometry. The vector expressed in body coordinates directed from the origin of the body coordinate system (located at the rigid vehicle center of mass) to the footpad in the surface contact was denoted by \vec{BN}_n . Then the vector joining the origin of the inertial coordinate system and the origin of the body coordinate system was given by the vector transformation

$$\begin{bmatrix} X \\ Y \\ Z \end{bmatrix} = - [T_{BI}] B\vec{P}_n \quad (9.4-13)$$

since the tip of the $B\vec{P}_n$ was located at inertial coordinates (0, 0, 0). The three velocity components of the rigid vehicle center-of-mass were specified in the gravity coordinate system and then transformed into inertial components. Thus the three initial inertial coordinates of the rigid vehicle center of mass given by equation (9.4-13) together with the three velocity components at impact comprised the initial conditions for the numerical integration of equations (9.4-1) through (9.4-3).

The angular rate vector components of the spacecraft at impact were initially specified in the body coordinate system and then transformed to Euler rates. These Euler rates together with the initially specified Euler angles provide initial conditions for the integration of equations (9.4-4) through (9.4-6). Equations (9.4-7) through (9.4-9) were solved as a set of simultaneous algebraic equations for the quantities ω_x , ω_y , and ω_z at each integration step prior to the numerical integration of equations (9.4-4) through (9.4-6). After equations (9.4-4) through (9.4-6) were integrated, new values of ω_x , ω_y , and ω_z were computed by transforming the new Euler rates.

The positions and velocities of the landing gear footpads were determined by integration of equations (9.4-10) through (9.4-12) only if the n^{th} footpad was in contact with the surface. The initial conditions for these equations were taken to be the inertial position and velocities of each footpad at the moment the inertial Z coordinate of the respective footpad was computed

to be less than or equal to zero with the assumption that the footpad was rigidly connected to the rigid vehicle's center of mass. If a footpad broke contact with the surface, the landing gear geometry was assumed to remain unchanged from the moment the pad left the surface until it reestablished contact. During the period of no contact with the surface, the position and velocity of the pad was computed as though the pad were rigidly connected to the vehicle. At the moment of recontact with the surface, the footpad equations of motion were again initialized as before.

Results of Computer Study. The results of fifteen runs which comprised three landing configurations on NASA-MSD's 1108 computer are presented in Figures 9.4-4, 9.4-5, and 9.4-6. The object of this study was to soft land a vehicle of 138 slugs on the lunar surface without tipping over or damaging the payload. In Figure 9.4-4, the dynamic stability boundary is shown for a surface slope of only 15 degrees. This is due to the original landing gear design which had no crushable material included in the secondary strut and not enough stroke length in the primary strut. The entire landing gear system was too rigid, thereby tipping the spacecraft over when impacted on a slope of only 15 degrees with a vertical velocity of 10.8 fps and zero horizontal velocity.

Figure 9.4-5 was the first attempt at reducing the rigidity of the primary strut and including crushable material in the secondary strut. As can be seen, considerable improvement was achieved since a surface slope of twenty-five degrees could now be negotiated for identical touchdown velocities, as shown in Figure 9.4-4. The primary and the secondary struts were again too stiff and higher stroking of the primary strut was deemed necessary for a stable landing at velocities of 15 fps vertically and 5 fps horizontally.

Therefore, the crushable material was again redesigned in order to provide a longer initial stroke to the primary strut. The results of this redesign of the energy absorption capability of the landing gear is presented in Figure 9.4-6. These results clearly indicate that a stable landing could be made on a 35 degree

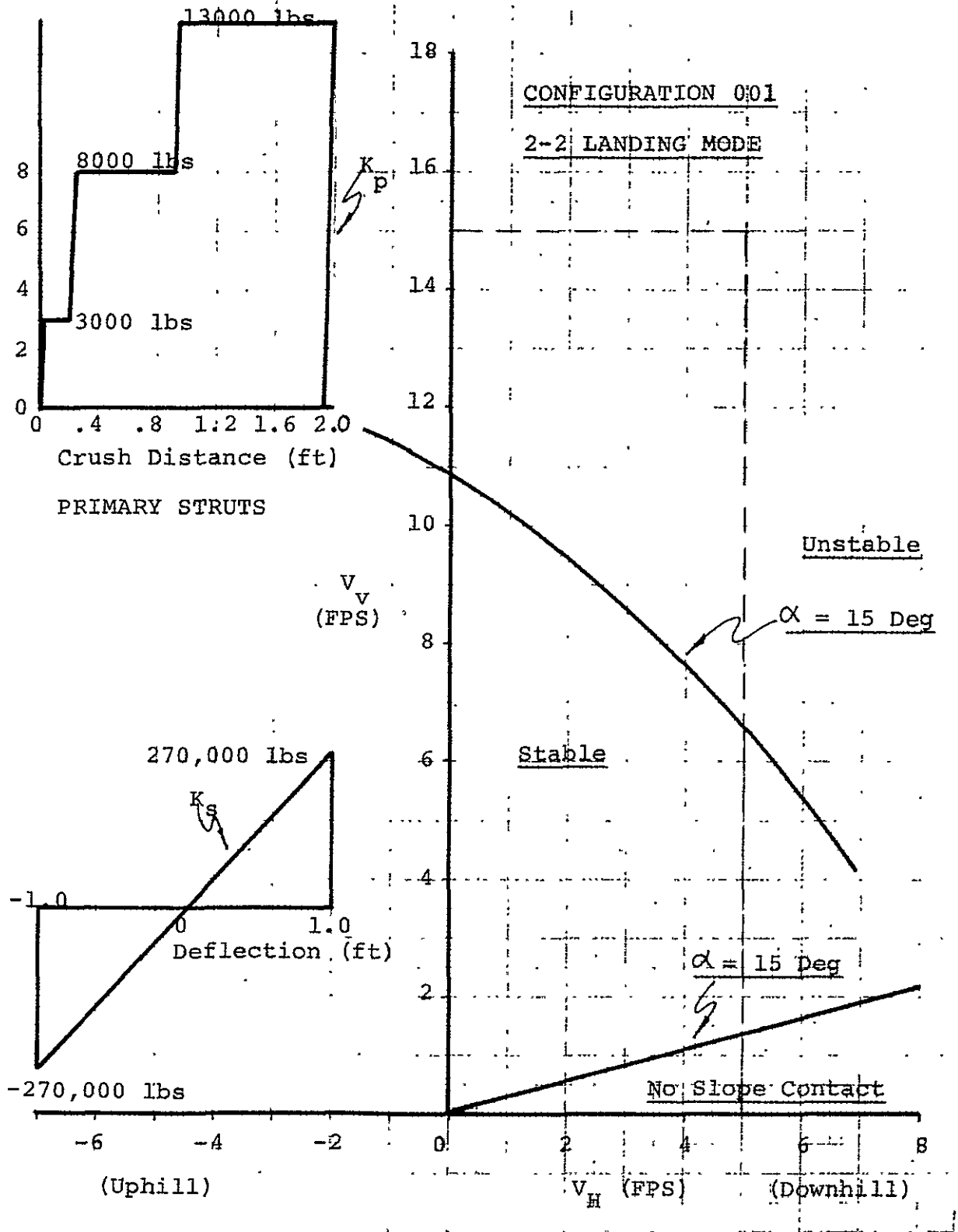


FIGURE 9.4-4 VARIATION OF LANDING STABILITY BOUNDARIES WITH TOUCHDOWN VELOCITIES

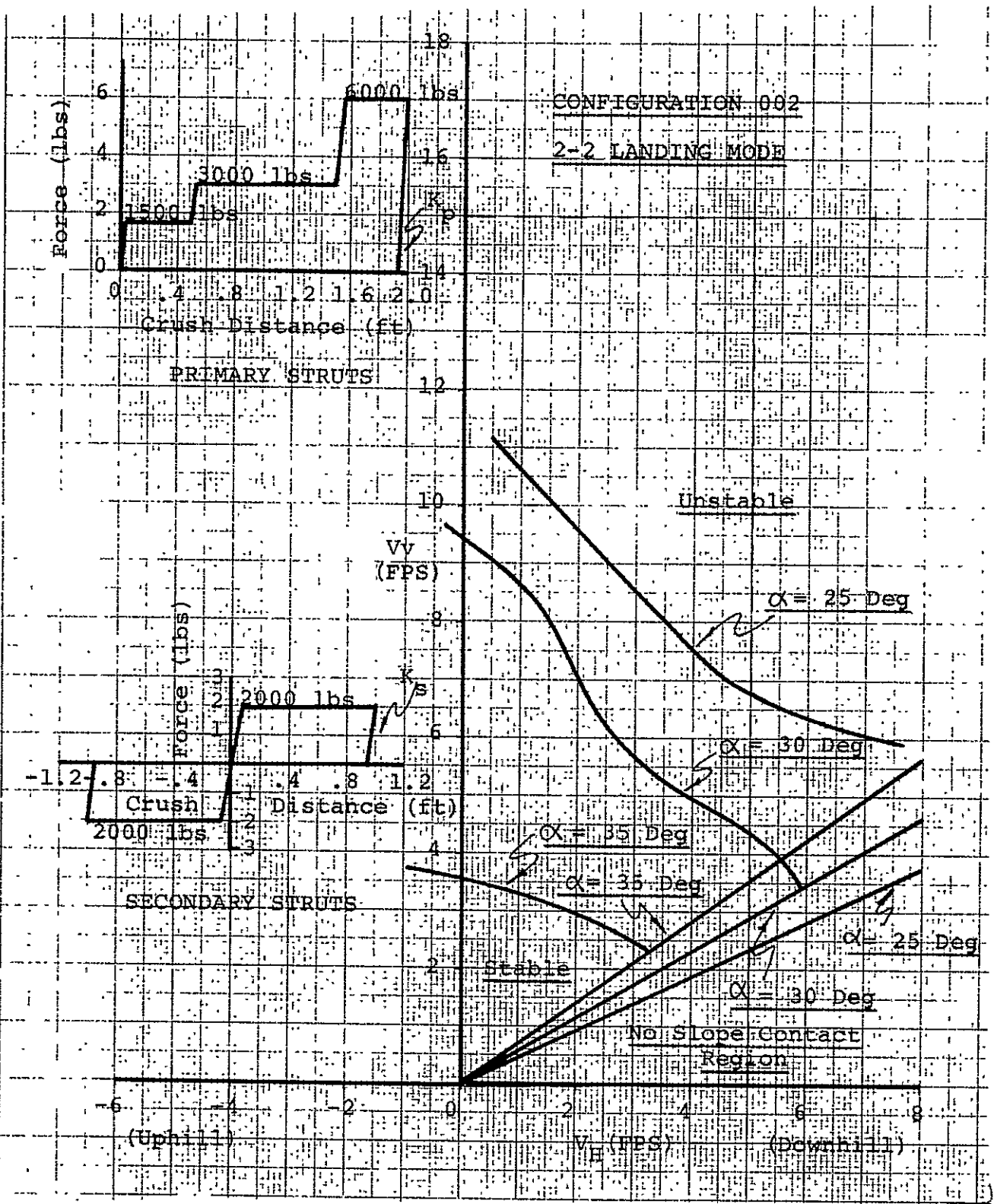


FIGURE 9.4-5 VARIATION OF LANDING STABILITY BOUNDARY WITH TOUCHDOWN VELOCITIES

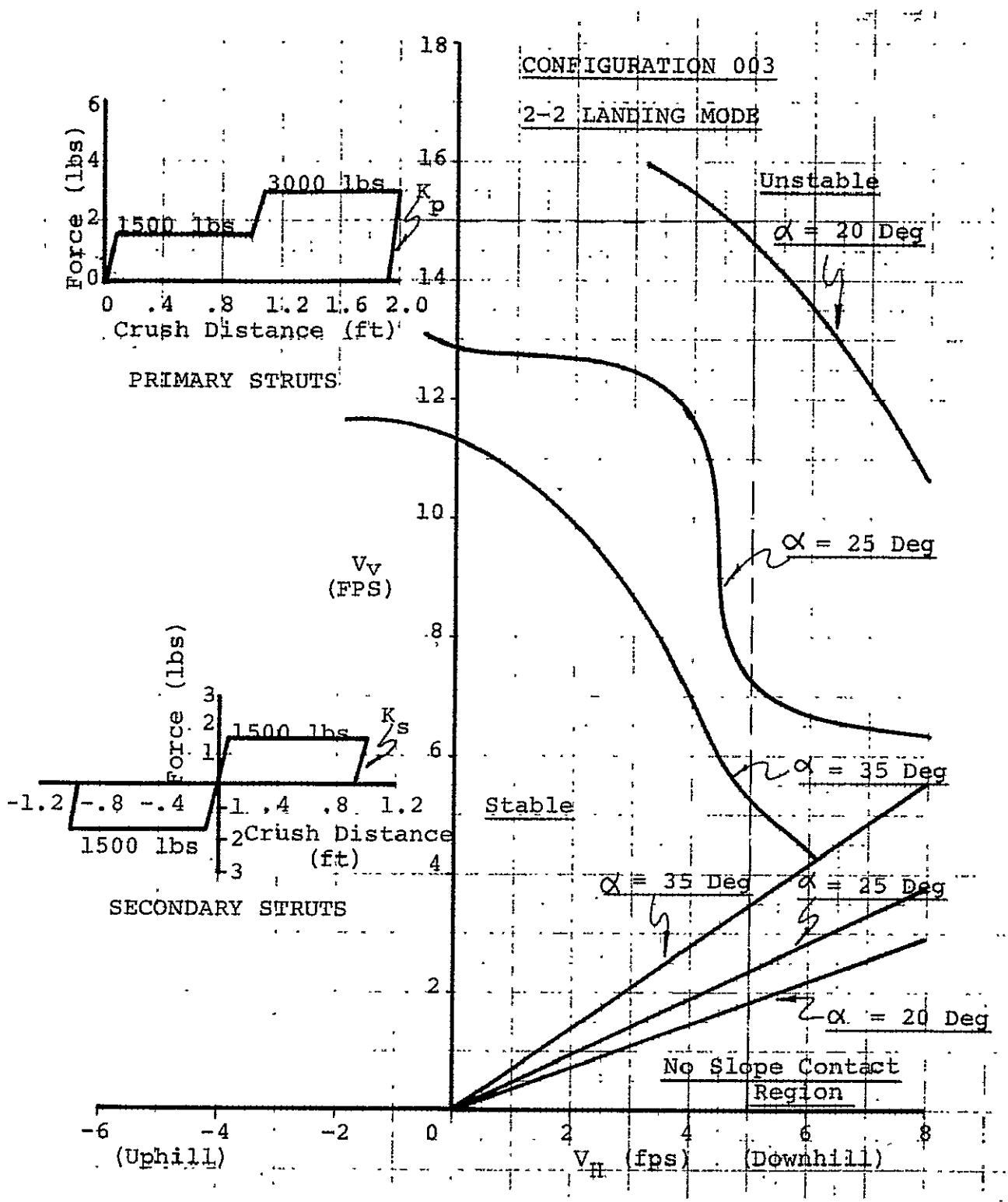


FIGURE 9.4 -6 VARIATION OF LANDING STABILITY BOUNDARIES WITH TOUCHDOWN VELOCITIES

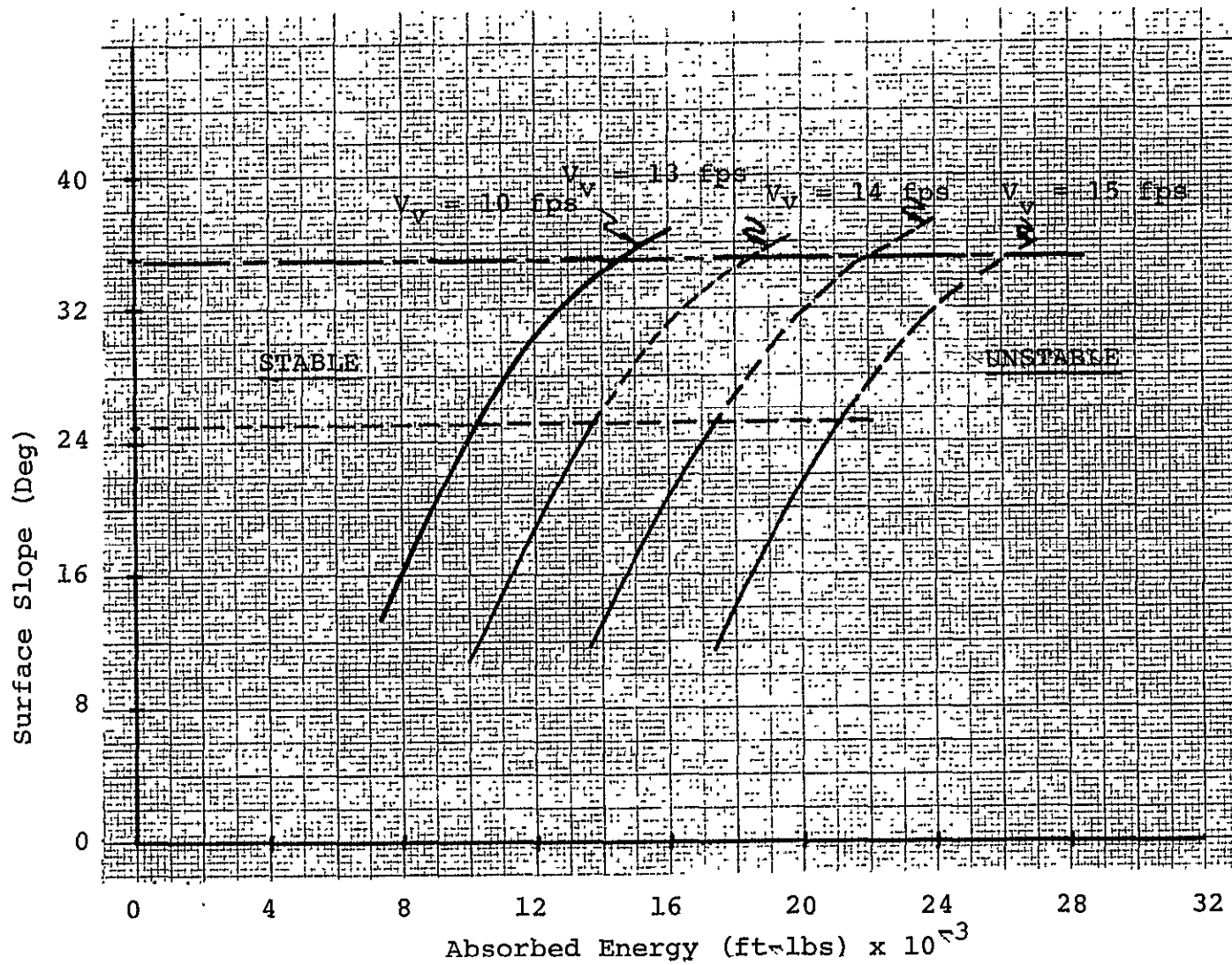


FIGURE 9.4-7 VARIATION IN TOUCHDOWN ENERGY ABSORBED WITH SURFACE SLOPE AND VERTICAL VELOCITY

slope if the vertical and horizontal velocities were reduced to more reasonable levels such as 8 fps vertically and ± 3 fps horizontally. However, even for the 15 fps and ± 5 fps case, the system would probably be stable on a 20 degree slope when the coefficients of friction and restitution were included in the analysis. It is recommended that an energy absorption versus increased landing gear weight trade-off study be conducted as the final step in the design of the landing gear system. Figure 9.4-7 presents the variation in energy absorbed for the various landing configurations and surface slopes that were shown in figure 9.3-7. It appears that approximately 26,000 ft-lbs of energy must be dissipated by the primary and secondary struts for a stable landing on a 35 degree slope. If the unrealistic requirements of 15 fps vertical and ± 5 fps horizontal are reduced, a much lower level of absorbed energy would be required for a stable landing. This reduction would also result in a reduced stroke length and therefore lower landing gear structural weight.

9.5 Dynamic Landing Model Tests

9.5.1 Experiment Description

To obtain an approximate correlation with theoretical landing stability results, a model of the LLV was constructed and landings simulated. The model (Figures 9.4-1 and 9.4-2) had only one degree of freedom in each leg and tests with it attempted to achieve dynamic similitude with regard to the acceleration due to gravity, g ; vertical and horizontal components of the impact velocity, V_V and V_H ; mass, m ; mass moment of inertia, I ; radius of footpad from vehicle centerline, R ; C.G. height, H , above undeflected footpad plane; and vertical component of the crushing force in each of the four legs, F .

TABLE 9.5-1 SIMILITUDE PARAMETERS

<u>Parameter</u>	<u>Units</u>	<u>LLV</u>	<u>Simulator</u>	<u>Est. Expr. Error</u>
g	ft/sec ²	5.31	32.2	
V_V	ft/sec	<15	<7.68	10%
V_H	ft/sec	<5	<2.56	50%
m	lb sec ² /ft (slugs)	138.	0.0329	2%
I	lb sec ² /ft	3640.		30%
R	ft	11.1	0.48	4%
H	ft	7.26	0.314	5%
F	lb	6700	9.6	+0,-100%
gR/V_V^2		0.262		
H/R		0.655		
mg/F		0.1093		

$$mR^2/I \quad 4.67 \quad \left(\frac{R}{r_g} = 2.16\right)$$

While the listed parameters are among the more important, it is apparent that others should be included for an accurate simulation. Foremost among these are lunar suit characteristics, spring rate of the legs, footpad size and shapes, and increased degrees of freedom of the legs.

The test apparatus is shown in Figure 9.5-3 and 9.5-4. Vertical velocities were achieved by dropping the model from a calculated height, d_v , and horizontal velocities by adjusting the walking speed of the experimenter. Release of the model at the proper point was facilitated by a marker, which consisted of a horizontal string with a flag attached both of which were properly located relative to the impact point. The impact point was chosen so that the model's landing legs struck the obstacle immediately after touchdown. It was found experimentally, as would be expected intuitively, that this condition was more severe than allowing the leading leg to slide. A greatly improved experiment would result from replacement of the manned drop with an automatic mechanism since the present results were very dependent upon the manual dexterity of the test engineer.

In all tests an attempt was made to have impact occur with the vehicle horizontal and with no pitch, yaw, or roll rates. Tests were conducted with several yaw orientations, two different footpad designs, three different types of landing surfaces, and four velocity combinations. All horizontal velocities were directed downhill.

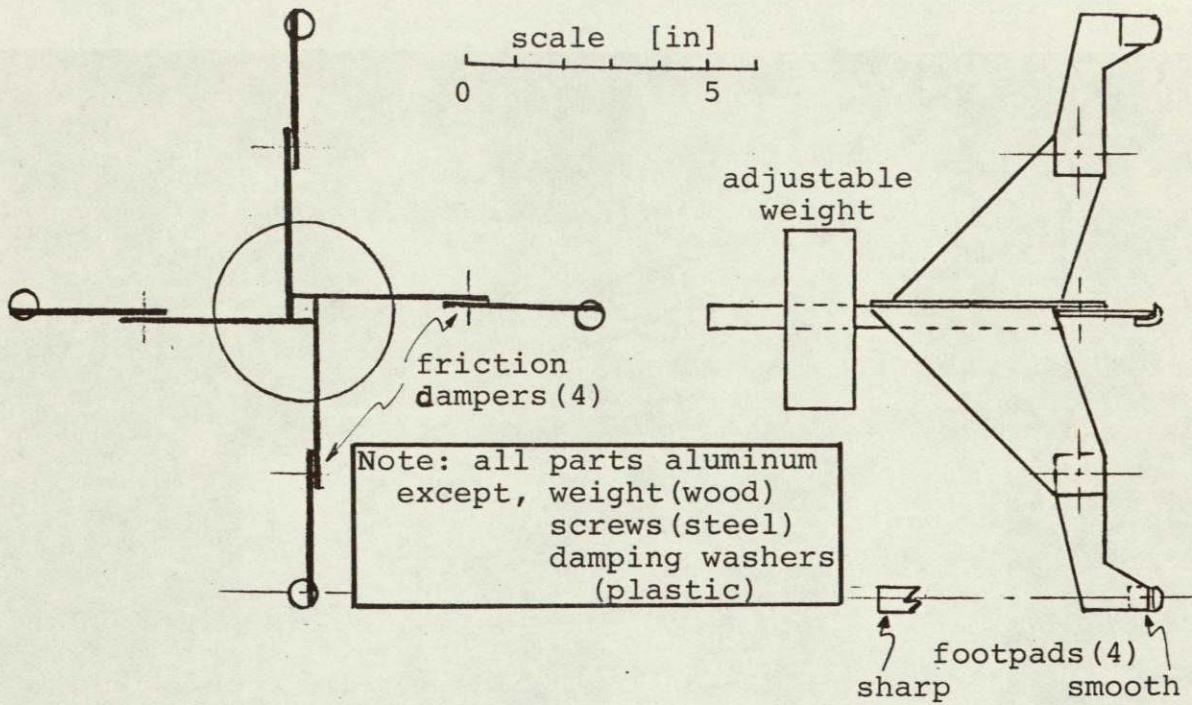


FIGURE 9.5-1 LANDING DYNAMIC MODEL

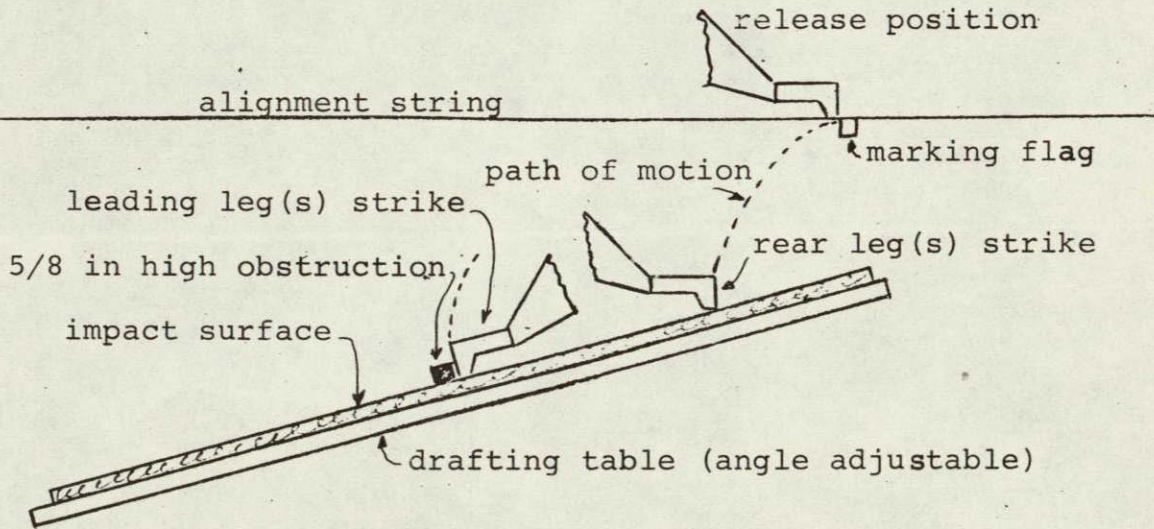


FIGURE 9.5-3 LANDING DYNAMICS TEST APPARATUS

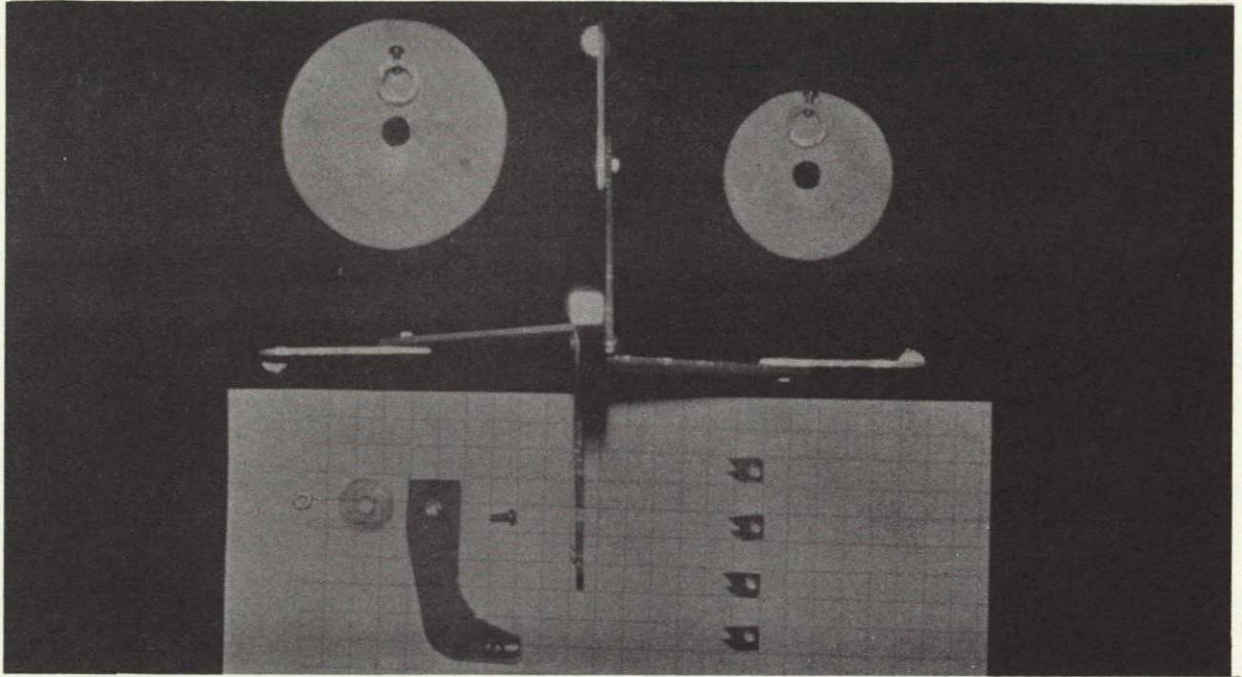


FIGURE 9.5-2 Dynamic Model Photograph

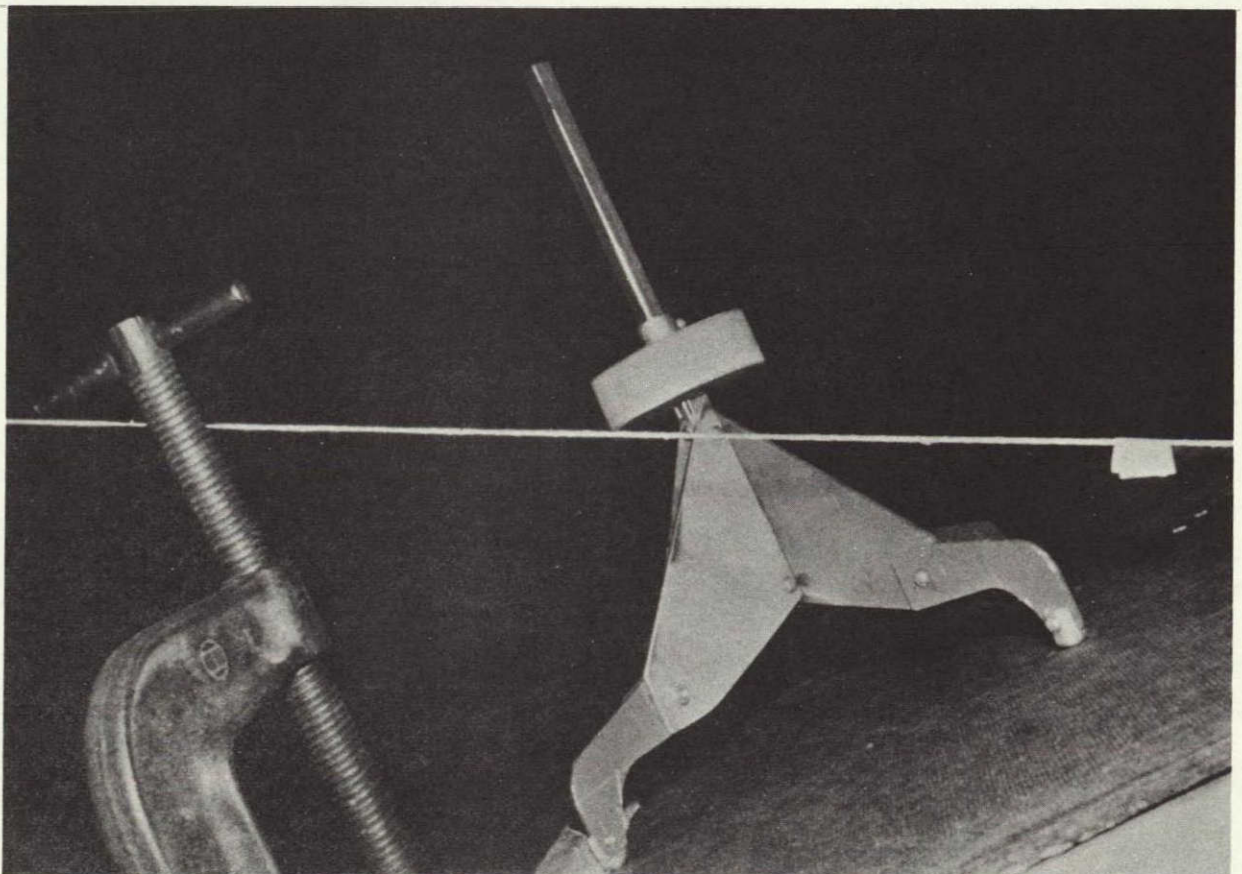


FIGURE 9.5-4 Dynamic Test Apparatus Photograph

TABLE 9.5-2 PARAMETER VARIATIONS

<u>Parameter</u>	<u>Variations</u>
Yaw Orientation (Figure 9.5-3)	1 leg directed downhill 1 leg at an angle of 45° with the downhill direction 1 leg at an angle of 22.5° with the downhill direction
Footpad Design (Figure 9.5-1)	Elliptical Sawtooth
Landing Surface	Smooth pine drafting table top Rough side of 3/16" Masonite hardboard Asphalted side of 1/2" celotex fiberboard
Input Velocity (LLV equivalent)	$V_V = 15 \text{ fps}$, $V_H = 5 \text{ fps}$ $V_V = 15 \text{ fps}$, $V_H = 0 \text{ fps}$ $V_V = 10 \text{ fps}$, $V_H = 3 \frac{1}{3} \text{ fps}$ $V_V = 10 \text{ fps}$, $V_H = 0 \text{ fps}$

9.5.2 Experimental Results

The results are summarized in Figure 9.5-5 which indicate that the proposed vehicle can safely land on a slope of 20° . if $V_V < 15$, $|V_H| < 5$. If $V_V < 10$ and $|V_H| < 3 \frac{1}{3}$ then safe landings may be made on slopes up to 28° .

A landing mode was considered unstable if any yaw attitude was unstable. An interesting anomaly in the data was the very unstable results given by the fiberboard surface, particularly when the sawtooth footpads were used. This was unexpected, but may be the result of (1) a greater coefficient of restitution on impact due to the low spring constant of the fiberboard and (2) the low damping of horizontal motions because of the single-degree-of-freedom landing legs and/or the effect of the sawtooth

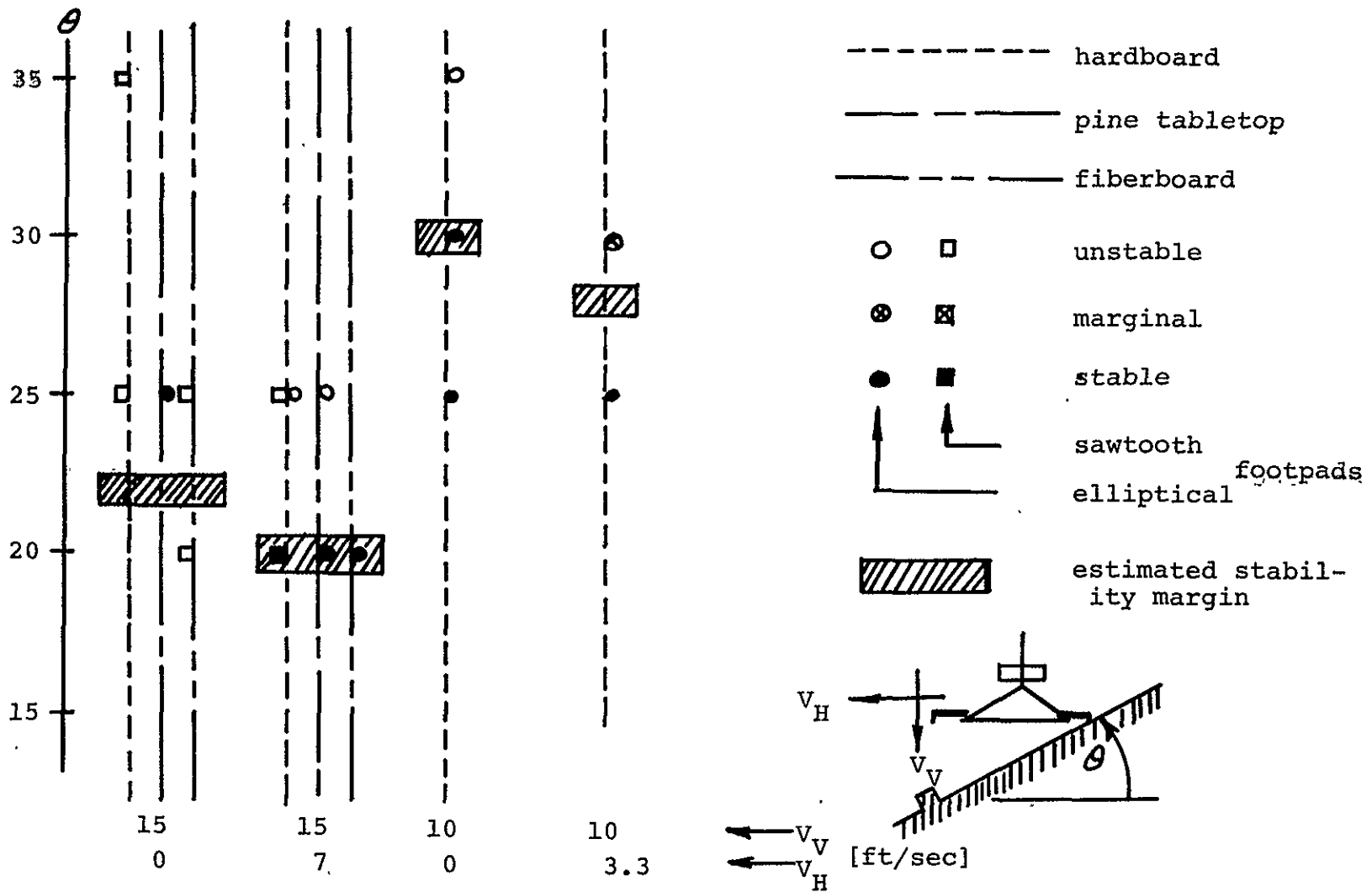


FIGURE 9.5-5 EXPERIMENTAL RESULTS OF DYNAMIC MODEL SIMULATION

~~foot~~ ~~as~~ ~~biting~~ into the surface.

These experimentally determined stability margins are crude estimates based on sparse data and a simplified experimental approach. However, taken together with the analytic results presented they give increased confidence in the capabilities of the LLV. Referring to Figures 9.4-6 and 9.5-5 the close agreement between simulated and experimental results can be verified.

9.6 Probability of Safe Landing Analysis

The potential for a safe LLV landing is dependant upon the interaction between vehicle configuration and lunar surface characteristics. Lunar surface characteristics which influence the probability of a safe landing are considered to include the areal distribution of slopes and the size-frequency distribution of craters and boulders. Probability values for the lunar surface features considered in this section were derived from curves presented in a review of lunar surface models by Hutton [3].

9.6.1 Landing Hazards

The probability, P , of a landing in a hazard-free area is equal to the area unoccupied by hazards divided by the total area. Craters ranging in diameter between 2 and 34 meters are considered to be large enough and abundant enough to constitute landing hazards to the LLV. In order to insure that the area considered unharzarded by the craters is free of craters, the diameter of each crater was increased by the diameter of a circle circumscribing the LLV landing gear, 25 feet. Thus, any point excluded from the area considered hazardous represents a point at which the center of the LLV footprint can be placed without impinging on a crater. The range of diameters for craters considered hazardous was subdivided into classes at two meter intervals. The hazardous area occupied by each class was calculated by multiplying the number of craters per square kilometer times the area occupied by a crater with the midclass diameter increased by

the landing footprint diameter. A uniform crater distribution was assumed, and the total hazarded area was calculated by adding to the sum of hazarded area that area of each succeeding smaller class which under assumed uniform distribution lay in previously unhazarded area. These calculations indicate that approximately 25 percent area is unoccupied by craters ranging from 2 to 34 meters. This percent unhazarded area is the same for both mare and highland areas [1-Figure 6]

Boulders constitute an additional hazard to landing. Unlike craters, the relative abundance of boulders varies between area characterized by different topographies. Three general topographic areas were distinguished by Hutton [3]; minimum, nominal, and maximum. These correspond to smooth mare, rough mare and hummockly upland, and rough upland. The number of boulders per square kilometer was determined for boulders larger than 1, 2, 3, 4, 5, and 6 feet in diameter for each of the three types of topographic areas. A uniform distribution of the boulders were considered to constitute additional hazards to landing. Each of these became the center of a hazard circle equal in size to the landing gear footprint. The new hazard area thus developed was subtracted from the 25 percent of the original one square kilometer remaining unhazarded by craters and boulders. The results of these calculations are presented in Table 9.6-1. These values represent the probability for an unmanned LLV, without an approach television camera of landing on an unhazarded area. The range of probabilities is sufficiently

low to demand a television approach system.

TABLE 9.6-1

PROBABILITY OF UNHAZARDED AREA

Boulder Size = >	<u>Minimum</u>	<u>Nominal</u>	<u>Maximum</u>
1'	.000	.000	.000
2'	.154	.000	.000
3'	.211	.000	.000
4'	.227	.136	.045
5'	.234	.193	.141
6'	.238	.212	.189

9.6.2. Probability of finding one hazard free site

In a consideration of safe landing probabilities using TV control to avoid ground hazards, account should be taken of the TV display screen measurements. An analysis of this problem was carried out by Swaney [4] for the LM system equipped with an approach TV. It was determined that for such a combination, the contour on the lunar surface containing 99.7 percent of all touchdown points is an ellipse centered at the nominal touchdown point, with a semi-major axis of 15.8 feet along track and a semi-minor axis of 12.8 feet crosstrack. This elliptical touchdown error footprint is approximated by a circular footprint of diameter 30 feet. When the 25 foot landing gear footprint is added to this a circular total landing uncertainty footprint 55 feet in diameter is obtained. The crater and boulder hazarded area can now be recalculated by enlarging each crater diameter by the new landing uncertainty circle. Calculations based

on the 55 foot uncertainty circle resulted in zero percent crater un hazarded area. Figure 9.6-1 summarizes the percent area left un hazarded by craters with various uncertainty footprints. The minimum uncertainty footprint possible is 25 feet, the landing gear footprint. The maximum is on the order of 35 feet. Thus, a guidance uncertainty footprint circle with a radius of five feet, is the maximum allowable to maintain a point on the lunar surface as hazard free. This circle should include the uncertainty of altitude determination and dispersion of thrust in the vernier system during descent. It is obvious from the preceding discussion that the percent of area un hazarded by craters alone will approach zero, even without considering the effect of boulders. The propability of un hazarded areas is likely to be extremely small.

The view area required to find at least one hazard free landing site can be expressed as a function of the probability of at least one hazard free site and the probability of hazard free area as indicated by Equation 9.6-1.

$$A = \frac{D^2 \text{Log}_{10}(P_1)}{\text{Log}_{10}(1-P_2)} \quad (9.6-1)$$

where A = area required

D = landing uncertainty footprint

P_1 = probability of finding at least one hazard free site

P_2 = probability of un hazarded area

Figure 9.6-2 presents the results of calculations based on a required probability of .99 of finding at least one unhazarded landing site. Area has been expressed in terms of the radius of a circle necessary to supply the required area. The radius of the scan area circle can be determined for a range of probabilities of unhazarded lunar surface. Figure 9.6-3 presents various effective scan radii as a function of TV lens view angle at various altitudes.

Slope Probabilities : Figure 9.6-4 presents the relationship of probability of occurrence of effective slope angles. Effective slopes were considered to be generated by a combination of general slopes and craters. This combination was chosen as a worst case since the probability of boulders is less than that of craters. Combinations of boulders and craters on general slopes were not considered because the probability of such a combination is extremely low. Comparison of 9.6-2 with data presented in the sections on vehicle stability will allow determination of the approximate probability of finding slopes within the values required for LLV landing stability.

9.6-3: Summary

1. On the basis of assumed uniform distribution of craters and boulders, the probability of an LLV landing in a hazard-free area without TV guidance is less than .25.
2. Presence of a TV guidance system requires the addition of a landing uncertainty circle due to limitations on the measurement of altitude and velocity, and upon thrust

dispersion in the vernier system. This component of the total landing uncertainty circle diameter must be less than ten feet in order that the area not be completely hazarded by craters alone. This appears to be an impossible with the present design to insure at any probability level the presence of even one unhazarded area large enough to land the LLV.

3. The above conclusions are based on a uniform hazard distribution and serve to indicate that under the assumptions made it is unlikely that an unhazarded landing area can be found. It should be **emphasized**, however, that under the conservative assumptions made, safe landings are possible even in hazarded areas. Furthermore, detailed terrain analysis preceeding actual LLV missions should define unhazarded areas as was done for Apollo landing mission.

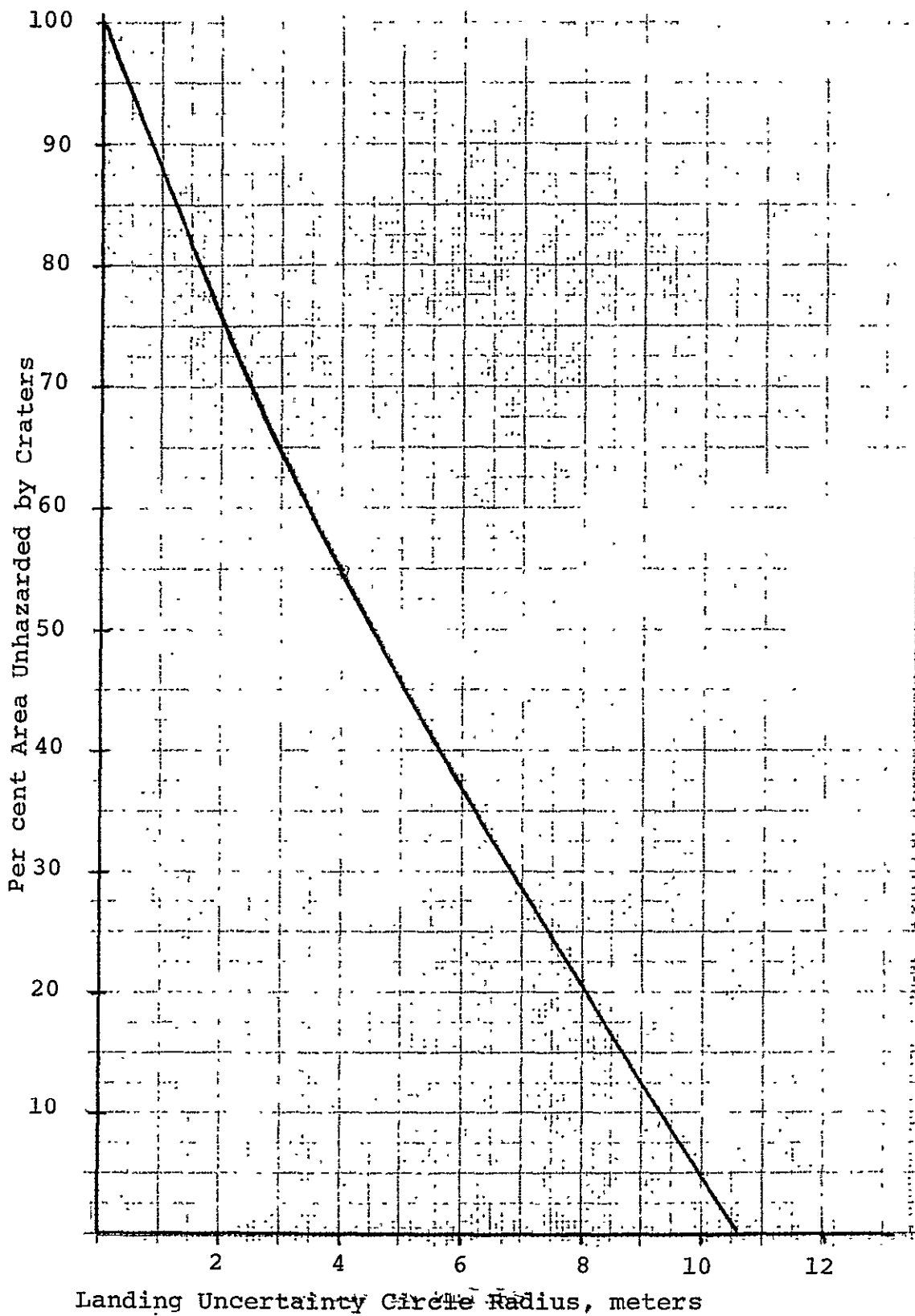


FIGURE 9.6-1

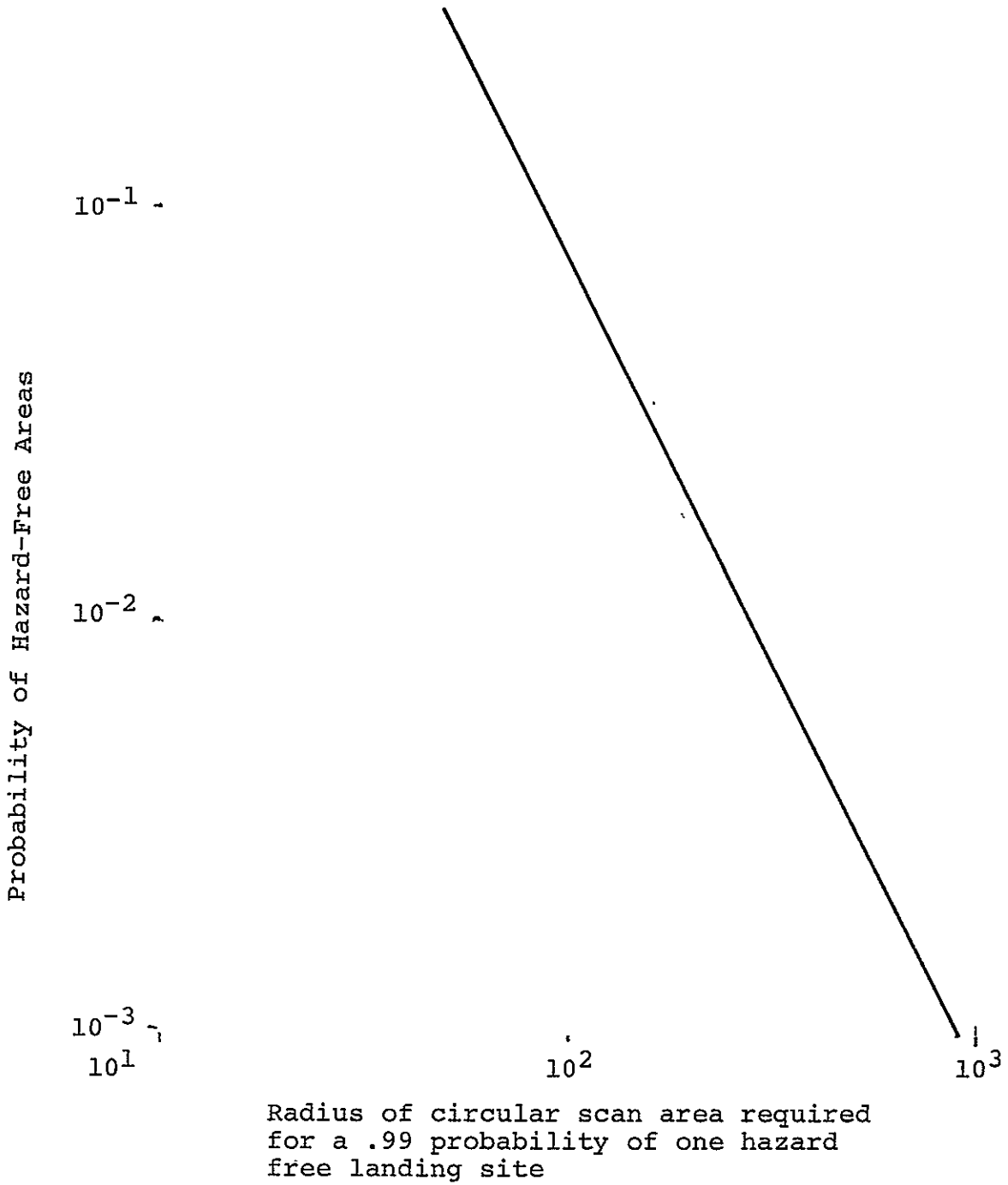


FIGURE 9.6-2

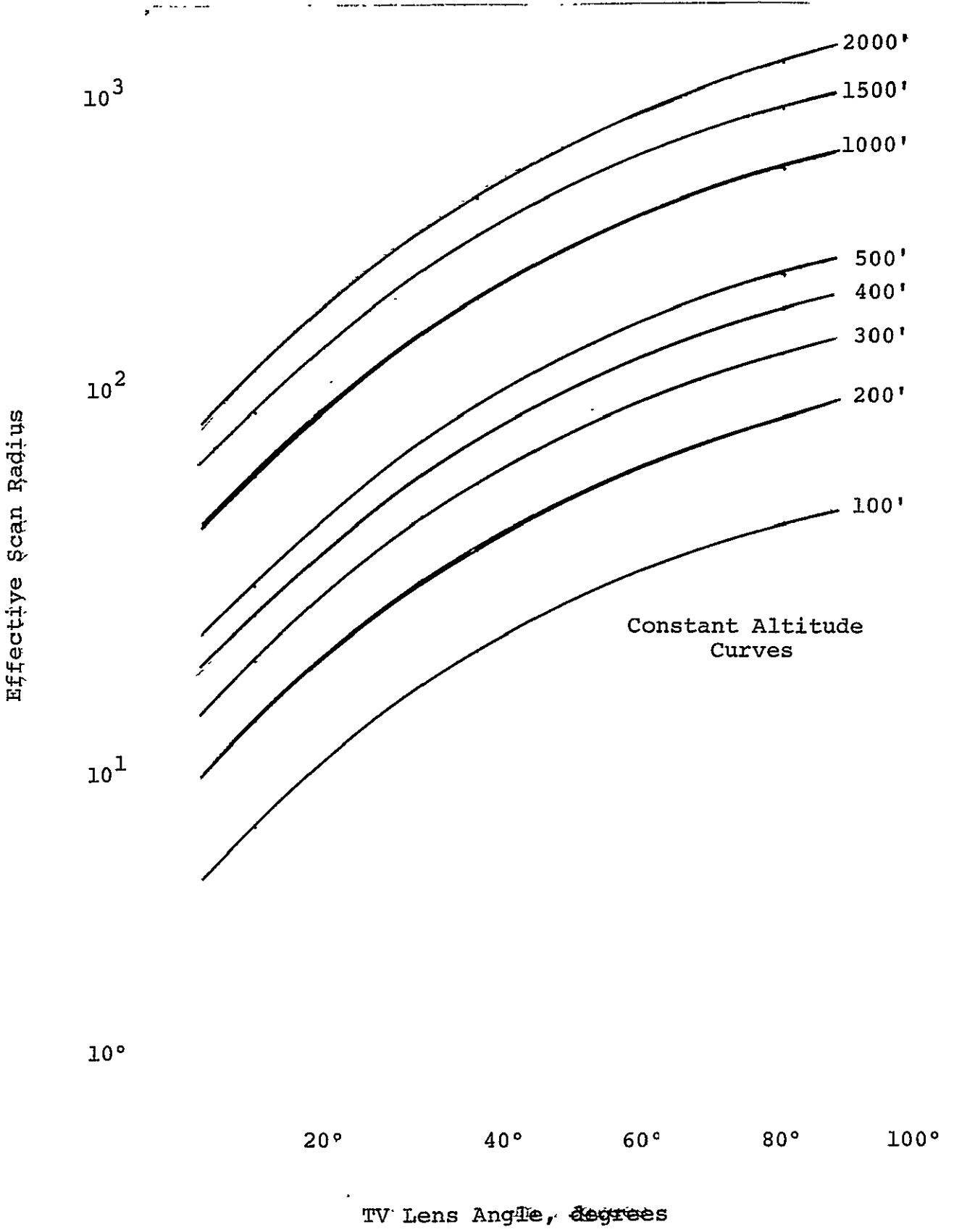


FIGURE 9.6-3

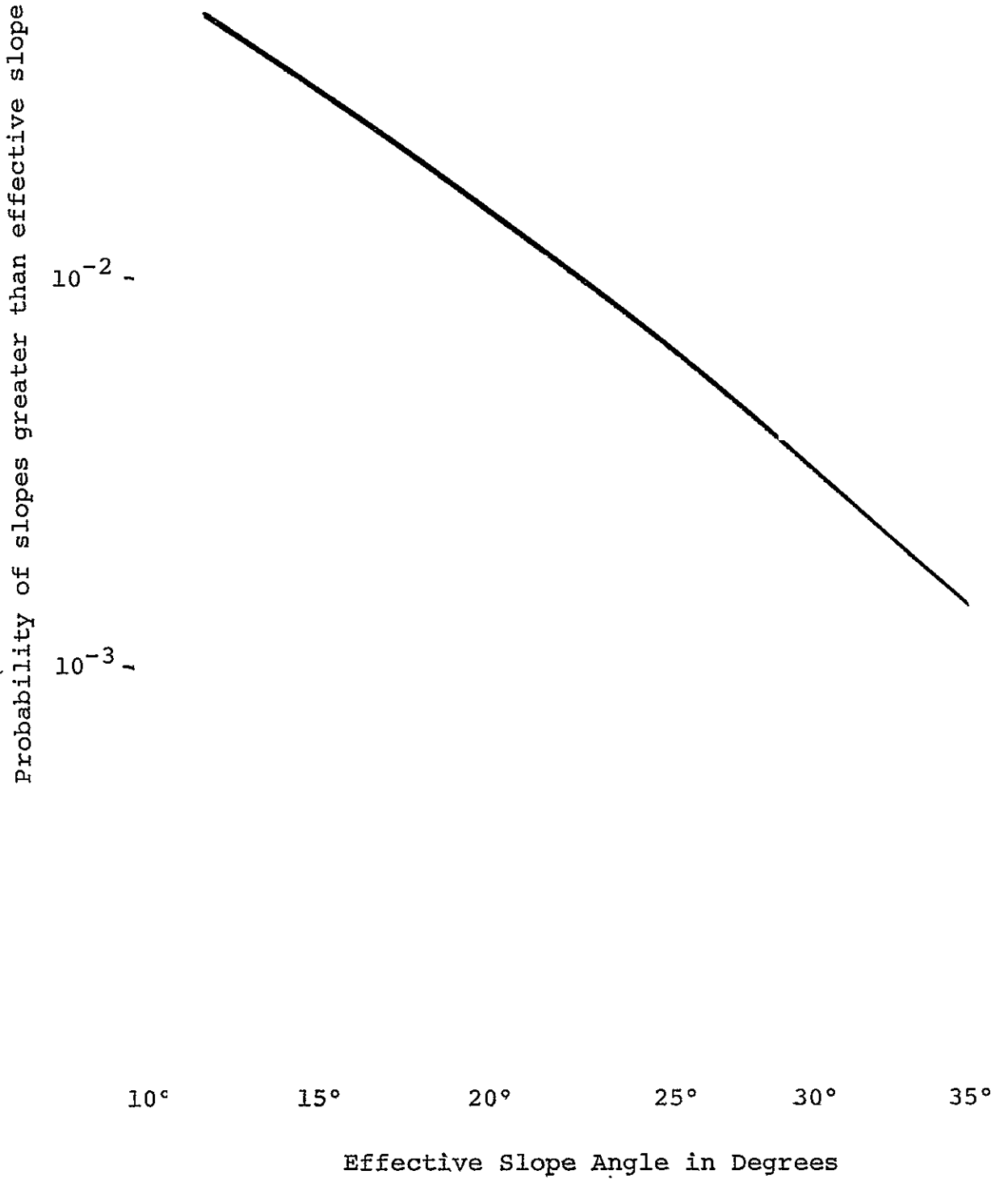


FIGURE 9.6-4

REFERENCES

1. Meriam, J. L., Statics and Dynamics, John Wiley & Sons, Inc., N. Y., 1966, p. 228.
2. Zupp, G. and Doiron, H., "A Mathematical Procedure for Predicting the Touchdown Dynamics of a Soft-Landing Vehicle." (unpublished technical note) NASA-MSC, June, 1969.
3. Hutton, R. E., Contract Number NAS8-21427, TRW Systems Group, Redondo Beach, California, March, 1969.
4. Swaney, D. C., LM Landing, Section 4, in Study Report, Apollo Applications Program, Lunar Surface Mission Planning, Volume 2, Supplementary and Detailed Studies, Bell Telephone Laboratories, November, 1967.

CHAPTER X
SYSTEM COST, SCHEDULE, AND RELIABILITY

Jesse Wampler 10.1-10.2
Alvin Strauss 10.3

10.1 Cost Summary

The basic level for cost estimation in this report is the subsystem level (NASA Standard Level 5). In some cases we have been able to collect cost data at the component level, but these data are generally not sufficiently complete to serve as the basis for cost estimation. The estimates of the subsystem level costs are presented in Table 10.1-1

TABLE 10.1-1 ESTIMATED SUBSYSTEM COSTS (MILLIONS)

<u>SUBSYSTEM</u>	<u>FIRST ITEM COST</u>	<u>NON-RECURRING COSTS</u>
Structure	0.3	3
Guidance and Navigation	1.5	6
Electrical Power	0.3	3
Communications	1.9	4.3
Instrumentation	0.7	3.3
Retro Propulsion	0.5	6
Vernier Propulsion	0.2	4
Reaction Control and Attitude Control	0.1	1
	5.5	30.6

There is considerable uncertainty in the choice of appropriate relationships for estimating module level costs from the subsystem level costs, for this spacecraft. The module level first-item costs have been estimated from the sum of the subsystem costs, using a factor of 1.6, based on historical data from manned

spacecraft programs [1]. The appropriateness of this factor is open to question in light of the range of ratios for manned spacecraft (from 1.3 for Gemini to 2.0 for the Apollo CSM , and because the LLV is not to be a manned spacecraft.

The greatest uncertainty in estimating module level costs is in the non-recurring cost category. The extensive use of qualified components has reduced the subsystems non-recurring costs relative to historical programs, so the well-defined relationship between subsystems and module non-recurring costs for manned spacecraft [1] is not applicable in this case. An alternative approach is to use the historical relationship between module-level first-item costs and module-level non-recurring costs [1]. Unfortunately, this relationship is very poorly defined, ranging from a factor of 8 for Gemini to as much as 43 for Apollo. Since the LLV is unmanned, it is reasonable that the appropriate factor should be toward the low end of this range. For illustrative purposes we have chosen a factor of 10, recognizing a great deal of uncertainty. An earlier proposal involving a spacecraft in many ways similar to the LLV [2] estimated module-level non-recurring costs 10 times greater than module-level first-item costs.

Table 10.1-2 presents a summary of the cost buildup estimates. For reference, we have also included an estimate of the cost of the launch vehicle, to provide a rough picture of the total cost of the LLV program, exclusive of payload.

TABLE 10.1-2 COST BUILDUP SUMMARY (IN MILLIONS)

	FIRST ITEM COSTS	NON-RECURRING COSTS	TOTAL 8 MISSIONS	TOTAL PER ITEM
1. Sum of Subsystem Level Costs	5.5	30.6	71.6	9.0
2. Estimated Module Level Costs	8.8	88	158	20
3. Cost of Launch Vehicle	30-40	(Not applicable)	240-320	30-40
Total, 2 & 3	39-49		400-480	50-60

10.2 Development Schedule

A proposed development schedule for this program is given in Figure 10.2-1.

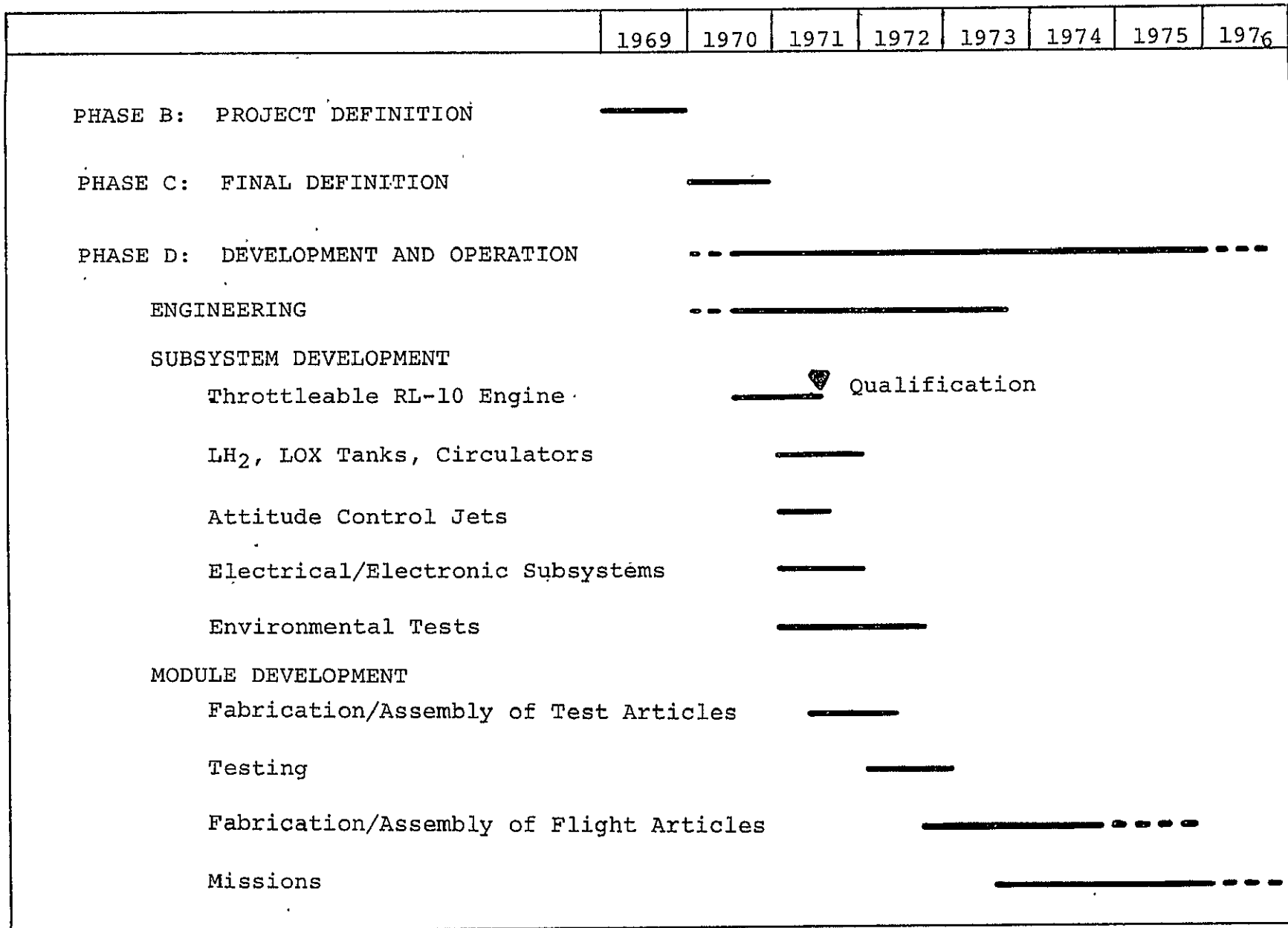


FIGURE 10.2-1 DEVELOPMENT SCHEDULE

On the whole, therefore, a critical evaluation of the LLV will reveal an exceptionally reliable spacecraft on the subsystem level. The less reliable items on the LLV appear to be the interfacing, connections (electronic, mechanical, plumbing), and the deployment of the various subsystems.

Aside from the equipment there is another area where it appears that the reliability of the LLV can be maximized. This area is in the sequencing of events and the mode of operation of the LLV subsystems. For example, it is possible to eliminate certain single point failures by resequencing certain events. Thus one could significantly increase the reliability of the LLV by determining the optimum sequence of events, and mode of operation. It is recommended that this type of study be undertaken.

Also, since the study of single point failures undertaken here is necessarily incomplete, it is recommended that an extensive failure mode and effects analysis be undertaken when all the LLV components have been specified.

As a final recommendation, it is suggested that a criticality analysis be performed in conjunction with the failure mode analysis. In other words, it should be determined just how many failures can be tolerated.

10.3.2 Basic Principles and Definitions

The object of this section is to present the basic principles in the analysis and standardize all terms in order to eliminate any confusion which may arise as to terminology or method of attack.

10.3 Reliability

10.3.1 Introduction

The reliability of the LLV is of ultimate significance to the systems design engineer. The object of his labors is to design a reliable system capable of attaining a desired goal. A number of other considerations enter into the design, and the reliability of the system must be compromised with respect to these considerations. The factors which compromise or detract from the reliability of the LLV are cost, weight and a variety of specific secondary considerations. In this investigation into the reliability of the LLV, reliability is considered a synonym for operating efficiency and is used as primitive measure of the effectiveness of the system.

As is well known, the system effectiveness is defined as the product of system capability and system reliability. Thus an attempt was made to increase the reliability of the LLV design (or component, or subsystem) without lowering the system capability.

Taking into account the fact that the LLV contains as much qualified hardware as is consistent with the work statement, most of the components in the LLV are extremely reliable. In many cases, man-rated subsystems and components were specified for the LLV. The reliability of some of these man-rated items has been somewhat reduced, however, by removing certain redundancies. The removal of redundancies tends to increase the system capability in a number of ways, of which the increase in landed payload weight is the most important.

First, because of time and manpower considerations, it was not considered practical to obtain actual values for the reliability of the LLV subsystems or components. For this study, a failure mode and effects analysis yields immediate information concerning the single point failures in the system and also provides one with a platform from which an upgraded study of the LLV can be launched.

Since a failure free system of this complexity cannot be built, an attempt must be made to design a system where if any of the components fail the system will go on functioning, or if a component failure would cause system failure to provide a very reliable component. This can be accomplished best by a combination of two considerations. First, to provide redundancy and second to grossly overdesign the system for its intended use. The failure mode analysis will give a clear indication as to where the LLV needs redundancy and where it needs to be overdesigned. It is felt that overdesigning is equivalent to redundancy, in its overall effect on system reliability in most cases, and in the LLV one finds that overdesigning yields significant weight savings over redundant design. This point will be discussed below, but first the terminology used here needs clarification.

In general, one classifies failures into two categories. First, one has the category comprised of tolerance failures. In this case the functional characteristics of the system change gradually in time to the point where failure occurs. The second category is comprised of those failures where the system functional characteristics change abruptly and drastically. One calls this type of failure catastrophic. In this study the primary

concern centers about catastrophic failures. Tolerance failures are considered only when the effect of a tolerance failure is felt by systems in a catastrophic manner. Thus one considers tolerance failures, but in a manner which removes the time dependence from consideration.

In order to dispel any subsequent confusion over terminology it is appropriate that two terms which have, to this point, been used somewhat loosely and imprecisely be fixed: failure and system.

A system is defined to mean that particular collection of items (hardware and/or software) to which a prediction pertains. A subsystem will be considered to be a system when the failures inherent in that collection of items are under consideration. Indeed, if a piece of equipment performs many functions (such as the IMU) and a failure prediction can be made for each function, then that piece of equipment will be considered to be comprised of several systems. Hence defining a system consists of describing the functions of the items which comprise the "system."

Failure is defined as the occurrence of any condition which tends to affect the system in a manner which renders the system incapable of performing the operations for which it was designed.

The system-failures which can possibly occur in the LLV are generally time-dependent. The longer the system operates the greater the probability of that system failing. In this study, however, one does not consider the operating times of the various items in the system. This emphasizes the fact that one just looks into the possibility of system failure and not the probability of

the system failing. In a manner of speaking, time-dependence is taken into consideration. This occurs in dividing each system function into three basic operational modes. For most systems the three are: start, operation, and shutdown. In general, different mechanisms, or different equipment are used for each phase, or there exist different modes of operation for each phase.

In applying these three basic operational modes in analyzing the failures of the system one looks for the following occurrences possible in each of the operational modes. First, for the start mode, one looks at the possibility of (a) failure to start, (b) premature start, (c) catastrophic start. For the operational mode one looks for the possibility of (a) inability to operate, (b) sub-standard operation, (c) catastrophic operation. Third, or the shutdown case, one looks for (a) failure to shutdown, (b) premature shutdown, (c) catastrophic shutdown. In many systems all nine of these failure modes may lead to single point failures. However, there are significant exceptions to this classification of system failures. For instance, all one shot devices, a category into which the pyrotechnics fall, form a special classification for which different ground rules must be set down.

The analysis which will be performed will consist in establishing the failure modes of the system functions and at the same time identifying the specific failures of the functional hardware set which are capable of causing failures of the system functions.

In accordance with the work statement directive the main object is to locate and describe all possible single point failures. This consists in performing a failure mode analysis and pointing out all possible Criticality I failures.

The criticality of the failure modes is subsumed into three classifications. The first class comprises Criticality I failures. Criticality I failures are defined as those single point failures which cause the mission (or LLV) to be classified a failure.

The second class is called the class of Criticality II failures. Criticality II type failures are defined as those single point failures which, if they occur, would cause the system to be in a new failure mode and effect state such that another associated failure would cause the mission to fail.

The last class, or the class of Criticality III failures, encompasses all situations which cannot be classified as either Criticality I or Criticality II failures.

The purpose of this study is to point out all Criticality I single point failures. Some Criticality II type failures are occasionally described and Criticality III type failures are ignored in the analysis.

In reality, however, one cannot delineate all single point failures in this manner for the LLV: In the case of the LLV the criticality of the failure may be dependent on the payload. Thus far in the space program the mission objectives have been man-associated (Apollo) or man-independent (Surveyor). In this situation, the LLV has both man-associated and man-independent

objectives. For example, the man-associated case may be a payload of a lunar roving vehicle to be used for transportation by an astronaut, and the man-independent case may be a payload of an unmanned lunar roving vehicle to be controlled from Earth.

In these two cases the failure of a certain item can attain different criticalities dependent upon the mission objectives. An example of payload dependent criticality is the beacon which will be used by an astronaut to locate the exact position of the LLV after it has landed and to beam in on the signal to land in the near proximity of the LLV in order to obtain use of the rover. If the beacon fails and the astronaut cannot land close enough to the LLV the payload becomes useless and the mission (man-associated) must be declared a failure.

In the man-independent case the beacon can fail resulting in an uncertainty in the location of the LLV, but the unmanned lunar rover can be deployed nonetheless and the mission will be a complete success. Thus it is evident that in the former case the failure of the beacon is of Criticality I while it is of Criticality III in the latter situation.

The man-associated mission is the more severe case, and hence, all criticalities will be based on this type of mission. In most cases the criticalities will be the same. The major exceptions will be in the equipment which insures the accuracy of the landing and communications.

10.3.3 Assumptions and Method of Attack

An assumption which is necessary to restrict the problem to one which is tenable is that all human operational procedures in

assembly, prelaunch activity, checkout, loading, fueling up, etc. are correct and that no equipment has been left out or misconnected. It is further assumed that all instructions from Earth to the LLV will be correct and in the right sequence.

Insofar as the structure is concerned, it is assumed that passive structural failures of the LLV basic structure will not occur when the LLV is functioning within normal mode of design. This assumption is made because it is assumed that the properties of the structure and the structural materials have been experimentally determined and exhaustively tested under conditions simulating those the vehicle will see in cislunar space and the Lunar surface. Supplementing these tests it is further assumed that a sufficiently large factor of safety has been used to compensate for any unforeseen events or stresses.

It is further assumed that all LLV components are adequately designed. All equipment is assumed to be, at the least, adequate to perform the function for which it was designed. The pumps will produce the required flow, the electronic components will produce the desired signal, and the engines will provide the desired thrust.

The type and quantity of information which should be taken into account in order to perform an adequate failure mode and effects analysis of the LLV is now discussed. First, all requirements for the performance of the LLV subsystems must be established and the failure modes of each component determined. Second, the margin of safety (or safety factor) for each component and system

should be determined. This must be done if one is to evaluate the seriousness of the failure and also get an indication as to the probability of the failure occurring.

Also concerning the probability of failure one should determine whether or not a particular system is qualified, man-rated, flight proven, or has even been built. In this manner an immediate indication as to the potentially unreliable systems and components can be obtained.

A related study which could improve system effectiveness and reliability would be to determine where below-state-of-the-art components or procedures were being used on the LLV. A study of this type is not only important from a reliability point of view, but is extremely valuable to the engineer who seeks to determine the upgrading potential of the LLV, or to update the design, or to extend the capability of the lunar landing vehicle. It is therefore recommended that a below-state-of-the-art study be made on the LLV design.

In somewhat the same vein as the structural assumptions, one assumes that all heat transfer devices, thermal insulation, and reflective coatings are adequately designed and will not fail to provide the necessary heating and cooling to the LLV systems which require it.

Finally, the last consideration will be to determine whether or not the existing safety factors are sufficient to offset the threat of any possible single point Criticality I failure.

10.3.4 LLV Environment

In order to better evaluate the single-point failures and overall reliability of the LLV, cognizance should be taken of the environment the LLV will experience. Included here are considerations of the lunar surface environment since a study of that environment and its effects on the LLV falls within the realm of two of the system design groups who were evaluating the effects of a ninety day lunar survival capability on the LLV. Another reason for not considering the lunar surface environment is that only a nominal amount of equipment will be required to operate and that their failure will normally fall within the category of Criticality III. Hence the discussion is restricted to the cislunar environment where all systems must function. This environment must be considered to see what possible effect it can have on the LLV systems and their failure modes.

The first consideration is the almost perfect vacuum experienced by the LLV. In this vacuum materials with high vapor pressures will sublime or evaporate rapidly, with the magnitude of the effect increasing with increasing temperature. In plastics, the loss of plasticizers by evaporation causes cracking, shrinking, and a significant increase in brittleness.

In the cislunar vacuum, adjoining solid surfaces can become cold-welded after losing their absorbed gases. Thin films of soft metal must be used to prevent this from occurring. Also, inorganic coatings with low vapor pressure should be applied to materials particularly susceptible to evaporation. One can conclude that the cislunar vacuum condition does not appreciably

affect either the LLV or its reliability.

The second consideration is the problem of solar electromagnetic radiation. The solar constant has the value $0.14W/cm^2$. Most of this energy in the solar spectrum is generated by particles having associated wavelengths of 0.3 to 4.0 microns with only one per cent of the solar energy falling outside of those bounds.

The ultraviolet and soft X-ray components of the solar spectrum do not fall within the category of what one classifies as penetrating radiation. The properties of metals are not significantly changed by these radiations. However, this radiation is intense enough to cause damage (failure) to organic polymers and certain unprotected glasses. Since there is no susceptible material on the unprotected surfaces of the LLV one concludes that solar electromagnetic radiation will not be responsible for any single point failures.

The third environmental consideration is that of penetrating radiation. Penetrating radiation is comprised of cosmic rays, and solar flare radiation. One differentiates penetrating radiation from the above-mentioned solar electromagnetic radiation, because the penetrating radiation is capable of passing through the exterior of the LLV and damaging the electronics and other sensitive internal systems. Semiconductors and organic materials are particularly susceptible to failure due to the effect of the penetrating radiation. The effect of the penetrating radiation on the LLV semiconductor devices results in an increase in the current leakage (Gamma ray effect). The lattice structure of the

semiconductors can also be damaged by the remaining components of the penetrating radiation. High energy protons, electrons, and fast neutrons are capable of penetrating the LLV to cause atomic displacement and damage to the lattice structure of the semiconductor devices. In organic materials drastic physical changes in the cross-linking and scission molecular bonds occur. The electronic circuits are affected by a lowering of input and output impedances.

Thus it is recommended that all non-redundant semiconductor electronics be given some degree of shielding from the effects of the penetrating radiations. The energy of these penetrating particles can attain energies of 10^{10} Bev and travel with velocities approaching the speed of light. Fortunately most of the penetrating particles--mainly protons--have somewhat lower energies. It should be noted that after a solar flare intense fluxes of these particles appear in cislunar space.

The final consideration is that of the meteorite problem. Micrometeorites are of the order of a micron in diameter and travel with velocities up to 70 km/sec. A micrometeorite collision with the LLV will result in the explosion of the micrometeorite on contact. This will lead to pitting of the LLV surface, but no system failure. The probability of a single point failure due to a micrometeoritic impact is virtually nonexistent.

A single point failure due to a collision with a larger particle, or meteorite, is also an event of extremely low probability even though meteor showers capable of causing such damage have

been detected by earth orbiting satellites. Thus a statistically calculated risk is involved. It is recommended that sensitive equipment be placed in a protective configuration in order to protect the equipment from possible failure due to meteoric collision without having to increase the weight of the LLV.

10.3.5 Single Point Failure Significance

The most important objective a study of this type can achieve is the elimination of certain single point failures which can be achieved without significantly affecting the landed weight or capability of the LLV. Usually this would consist in removing poorly designed, for a specified mode of operation, components from the LLV and replacing them with better designed items. On the whole, this has been accomplished in the design of the LLV as a consequence of the utilization of a large quantity of off-the-shelf qualified hardware designed for similar purposes. The hardware in these components are extremely reliable. The systems on the LLV, where correctible single point failures appear more frequently, are associated with the new portions of the design such as the landing gear deployment mechanism. These single point failures are not due in any way to some inefficiency on the part of the designer, but to a lack of qualification testing. The qualification testing would point out the weak points in the design and give the designer an indication as to what subsystem should be redesigned, or where to add redundancy.

On the LLV most single point failures are associated with grossly overdesigned systems. For instance, there are a number of single point failures associated with the helium supply system. Most of these failures are caused by bursting or leakage. However, the maximum operating pressure of one of the vernier system helium tanks is 4500 psig while the burst pressure is 8900 psig and the tank has been proofed at 6670 psig. Thus, this single point failure associated with the helium tank constitutes a single point failure for which no redundancy need be provided. It would be a case of poor engineering design to provide a redundant helium tank to eliminate this single point failure.

There are also single point failures associated with what is probably the safest and most reliable piece of equipment on the LLV; the high pressure tubing. The situation in this case is just an exaggerated example of the single point failure conditions associated with the vernier helium tank. The maximum operating pressure of these high pressure lines is 4150 psig, the proof pressure is 9000 psig, and the demonstrated burst pressure is 36,200 psig. Thus in this case one deals with a system in which the force, required to bring about a single point failure by rupture, is more than eight times the maximum force the system sees when it is operating. Here again it would be ridiculous to include redundancy in order to eliminate the single point failure mode.

To further illustrate the point of view adopted here, it will serve to present the example of the vernier engine system. It is assumed that the loss of any one of the four vernier engine clusters would result in the loss of the spacecraft. A study of the

dynamics of the spacecraft yields the result that in certain situations it will be possible to complete the mission (primarily the landing) with one vernier cluster inoperable. In doing so, however, one puts an excessive burden on the RCS system for stabilizing the LLV, puts an excessive burden on the fuel reserves, due to the LLV now having to overcome large gravity losses, and precludes a program of sufficient complexity to control the LLV under these conditions. Other problems also appear such as, the LLV will not be able to land as accurately as with all four clusters operating, will not be able to perform the hover operation, or have adequate site redesignation capability. Thus one must assume that the failure of a single vernier engine cluster induces a spacecraft failure of Criticality I.

Some other worst case assumptions that are made here are that fuel or oxidizer leakage (in the RL-10, vernier, or RCS engine systems) is a single point Criticality I failure. Also, the explosion of any engine (Vernier, RCS, RL-10) is a Criticality I single point failure.

10.3.6 Discussion of the LLV Single Point Failures

The problem of bursting occurring in the helium high pressure system has already been considered from a failure standpoint. The problem to be considered here is that of leaking in any of the helium common manifolds of the regulator bellows, valves, pressure transducers, or high pressure lines associated with the vernier or RCS engine systems. A failure in any of the above mentioned items could cause propellant backflow leakage from the propellant tank bladders through the check valves. This leaked propellant will eventually enter the common manifold. If, on the other hand, the helium isolation solenoid valve is opened subsequent to the above leakage, some of the propellant which has accumulated in the common manifold will be injected into the wrong tank causing a hypergolic explosion and loss of the LLV.

Even if no failure of the common manifold occurs, a comparable explosion may occur. In this situation either the tank bladder, or the check poppet valve may fail. This induces a pressure differential, due to the thermal expansion, between the fuel and oxidizer. This induces a transfer of fuel or oxidizer through the common manifold to the complementary tanks, initiating the hypergolic explosion.

These single point failures can, for the most part, be eliminated. The removal of this type of Criticality I single point failure can be accomplished in a number of ways such as positive separation of fuel and oxidizer. This results in increased mission reliability with no significant increase in weight or complexity.

TABLE 10.3-1 FAILURE MODE AND EFFECT ANALYSIS (page 1 of 8)

Name	Failure Mode	Failure Effect	Failure Cause
<p>This column identifies the hardware set to accomplish the function.</p>	<p>This column is related to the system function. Generally, the failure modes can be classified into three classes:</p> <ul style="list-style-type: none"> a)Function failure b)Premature function shutdown c)Inadvertant function operation 	<p>This column lists the effect of the function failure on the LLV and/or its subsystems, and indicates the criticality.</p>	<p>This column lists the possible means of inducing the failure, or what hardware must fail to produce loss of function.</p>

Name	Failure Mode	Failure Effect	Failure Cause
RL-10, Vernier, RCS Thrust Chamber	Rough combustion: Injector failure: Burn through:	Loss of thrust (I)	Various subsystem inadequacies
Vernier, RCS, helium tanks fill and drain coupling (used for filling and draining the helium tanks)	Rupture	Depletion of helium in tank, loss of propellant supplies (I)	Understrength materials and processes
Helium Solenoid isolation valve (Vernier-RCS)	Rupture	Depletion of helium supply; loss of propellant (I)	Substandard processes and materials
Helium Pressure Regulation	Rupture	Depletion of helium and loss of propellant (I)	Substandard materials and processes
Expulsion Tanks Oxidizer and fuel	a)Rupture of oxidizer tank wall b)Rupture of fuel tank wall c)Leakage or rupture of propellant outlet or propellant vent connection d)Bladder leakage	a)Loss of propellant system Probable rupture of adjacent tank (I) b)Same as a) (I) c)Loss of propellant system, explosion of propellant d)Excessive helium in the propellant supply lines (Critical engine condition Filling of propellant manifold with helium (loss of system) (I)	a)Stress Corrosion Temperature changes Overpressure Understrength materials and processes b)Same as a) c)Manufacturing, installation, or handling error. d)Flexing, sharp edges, Metalchips, Pressure differential, Sloshing Stress.

Name	Failure Mode	Failure Effect	Failure Cause
RL-10, Vernier, RCS Engine assembly	a) Explosion b) Engine valve rupture or external leakage	a) Loss of Engine or Cluster, Shrapnel damage (I) b) Loss of Engine or Cluster, Possible explosion (I)	a) Substandard material and processes: Rough combustion: loss of fuel lead b) Substandard material and processes
Vernier-RCS-RL-10 Switches	One of the engines is not inhibited during the power phase up.	Engine coils have power supplied and are capable of premature operation if a second failure or transient occurs during warmup (II)	Failure of an engine on switch in the closed circuit position, or premature computer command.
RL-10 Gimbal	Gimbal actuator clutches are not energized	Loss of Redundancy in Pitch and Yaw control during the main retro phase (excessive burden on RCS system) (II)	Defective electronics or lack of commands.
RL-10 Separation Pyrotechnics	a) Premature firing b) Failure to separate or late separation.	a) Failure to complete main retro phase (I) b) Inability to land (I)	a) High temperature, auto ignition; electrostatic discharge, b) Degradation of charge during boost heating, no firing current, structural failure (stress corrosion)
Helium Tanks (Vernier-RCS)	Rupture/Gross external leakage	Loss of system due to Shrapnel damage-- structural damage to payload (I)	Overpressure, under-strength due to solar heating, defective materials and processes

Name	Failure Mode	Failure Effect	Failure Cause
Helium high pressure tubing and components	Rupture/Gross external leakage	Loss of system due to Shrapnel damage of LLV (I)	Overpressure, under-strength, substandard materials and processes
Helium low pressure lines and compartments	Rupture	Shrapnel damage to LLV (I)	Overpressure
Propellant supply tubing and components (RL-10-Vernier-RCS)	Rupture/Gross external leakage	Damage to LLV systems and payload. Danger due to exposure and/or fire and explosion. Loss of function (I)	High pressure, solar heating, substandard materials and processes
Propellant isolation Diaphran valve	Fails closed	Discharge of propellant through engine (II)	Electronic failure, substandard materials and processes
Positive expulsion system	Rupture/Gross external leakage	Fire, explosion (I)	Overpressure, under-strength materials, stress corrosion, solar heating
Positive expulsion tank	Bladder rupture or gross external leakage	Discharge of propellant through engine (II)	Pressure differential, materials and processes
RL-10 Propellant valves and lines	Rupture	Explosion, shrapnel damage	High pressure, vent failure, solar heating Stress concentrations

Name	Failure Mode	Failure Effect	Failure Cause
RL-10 Gimbal actuator, gear-train and asso. Gimbal components	Jamming	Loss of ability to gimbal the RL-10 engine (no pitch or yaw control) (II)	Foreign matter, sub-standard materials and processes, solar heating
RL-10 Gimbal actuator rod	Frozen	Loss of RL-10 pitch and Yaw control (II)	Metal chips, inadequate materials and processes, high or low temperatures
Helium Pressurization system valves and pressure regulators	Clogging, freezing	No Pressure (I)	Foreign material, temperature effects, electronics failure
RL-10 turbopump assembly	Mechanical failure (explosion)	Loss of propellant pressure (explosion) leakage (I)	Impeller sear failure
RL-10, Vernier, RCS shutoff valves and pump valves	a) fail open: valve rupture, jamming b) fail closed: jamming, gate deformation	a) Engine flames out (I) b) Fuel loss, thrust chamber cool down prior to spark (II)	Electronics failure, computer signal failure, substandard materials and processes
Engine pressure relief valves	a) fail closed: mechanical jamming b) fail open: mechanical jamming	a) Excessive pressure Possible bursting (II) b) Loss of pressure	a) Freezing or contamination b) Freezing or contamination
Automatic sequencer	Relay open, closed or shorted. Diode open or shorted.	Sequencing function failure (i.e. failure to pressurize open or close propellant isolation solenoid valves; backflow of propellant	Substandard materials and processes, vibration and shock

Name	Failure Mode	Failure Effect	Failure Cause
Automatic sequencer (contd)		into empty tank, loss of pressure and engine shutdown, premature sequencing. (I)	
LLV Shroud	Fail to separate from LLV	Inability of LLV to function (I)	Explosive bolt failure
RL-10 Umbilical Guillotine (Disconnect)	a) Shattering of backplate or head assembly by explosive charges b) Rupture; deformation of housing c) failure to fire d) Premature firing	a) failure to separate (I) b) Blast or shock damage to LLV (I) c) Failure to separate (I) d) Loss of RL-10 function (I)	Temperature effects, vibration, electrostatic charge, substandard materials and processes, etc.
Landing gear	Fails to deploy in landing configuration	Inability to land	

The failure of any unit of the LLV structure at any time jeopardizes the mission success of the LLV and may lead to a failure of more critical structural components. Thus any structural failure is Criticality (I).

Name	Failure Mode	Failure Effect	Failure Cause
Oxygen and hydrogen tanks, high pressure lines, fittings for fuel cells.	Rupture/excessive external leakage	Structural damage due to fire and explosion (I)	Substandard materials and processes, high temperature, sloshing stress
Circuit Breakers	Fail shorted to ground	A sustained short drops voltage on AC busses to a value where AC loads cannot continue to operate (I)	
Diode	Fail shorted to ground	A sustained short would result in loss of DC main bus or loss of battery relay bus with loss of fuel cell	
General Electronics	Inability to turn switches off	Excessive power drain (I or II depending on the specific occurrence)	Faulty switch(es)
Antenna	Structural or material failure, bad breakage	Loss of Earth communication (I man-asso. II man-independent)	Substandard materials and processes, stress corrosion
IMU	a) Loss of power failure to powerup b) Failure to command IMU to action c) IMU fail to provide total attitude and ΔV info d) IMU program loss of function or improper function	a) Does not provide ΔV parameters, retros burn time, Gimbal positioning, etc. b) Loss of function c) Loss of altitude information, loss of thrust information, loss of steering control	a) Power supply failure, broken wire(s), over heating b) Power supply failure, switch/relay fail in open position, broken wire(s) c) Temperature control failure, electronic mechanical failure of

Name	Failure Mode	Failure Effect	Failure Cause
IMU (Contd)		d)IMU could be torqued or will not yield correct parameters (I)	platform stabilizing circuits, failure of 800 cps power which excites resolvers, failure of IRIG torque circuit, 52 fail open d)Defective power supply; logic, switch, or wiring defective
Celestial Sensor	a)Failure of dust cover to eject b)Shaft and trunion drive fails	a)Loss of function b)Loss of function (II)	a)Dust cover mechanism mechanical failure b)Mechanical gear box failure, electronic failure of motor drive system
Flight Computer	Failure to provide ΔV, altitude and engine commands	Inability to control LLV (I)	IMU failure, associated subsystem failure, power failure
Fuel Cell	Loss of power	Loss of redundant power (II)	Value failure, sub-standard materials and processes
Battery	Loss of power	Insufficient power for peak demand period (I)	Temperature control failure, Diode failure

The major items on the LLV have now been covered in the failure mode analysis. It was not possible to cover all the components involved in the LLV design. The systems which remain to be looked into in detail are the interface, landing equipment, telecommunications, power, sequence and timing, guidance and control, radar, thermal control, retropropulsion, reaction control system, gas jet system, packaging and cabling, and the data coupling unit.

In order for the failure mode analysis to be used for minimizing mission failures, the failure mode analysis should be carried to the detail level. The failure causes should be traced down to the components responsible, and the single point failure should be corrected there, if possible.

This is not possible in our study. Making a conservative estimate, there will be approximately 100,000 parts on the LLV and 35,000 of these will be electronics parts. Thus it is obvious that not only is it impossible to do a failure mode analysis on all these items, but it is doubtful whether or not they could even be itemized.

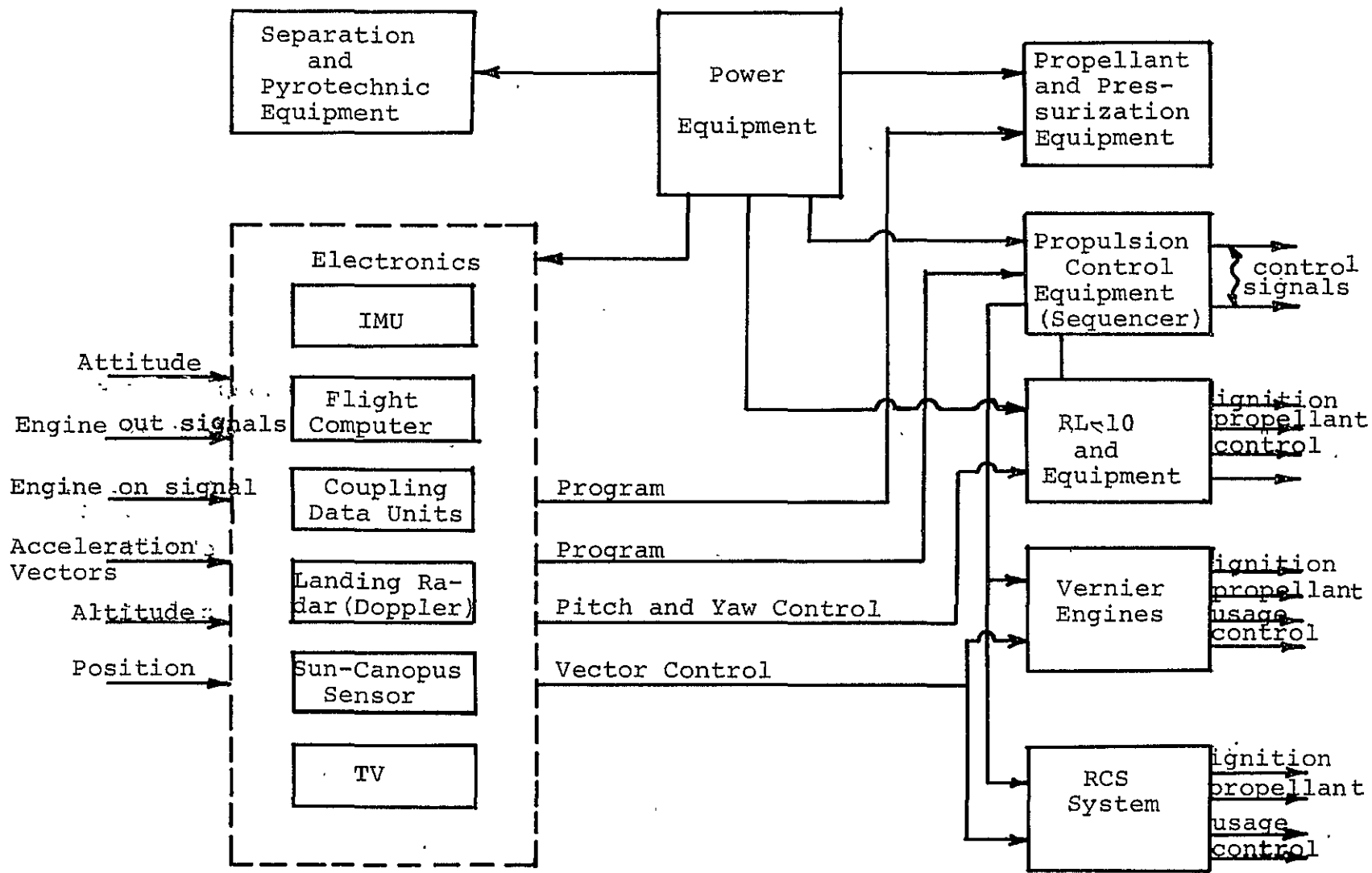


FIGURE 10.3-1 FUNCTIONAL DIAGRAM

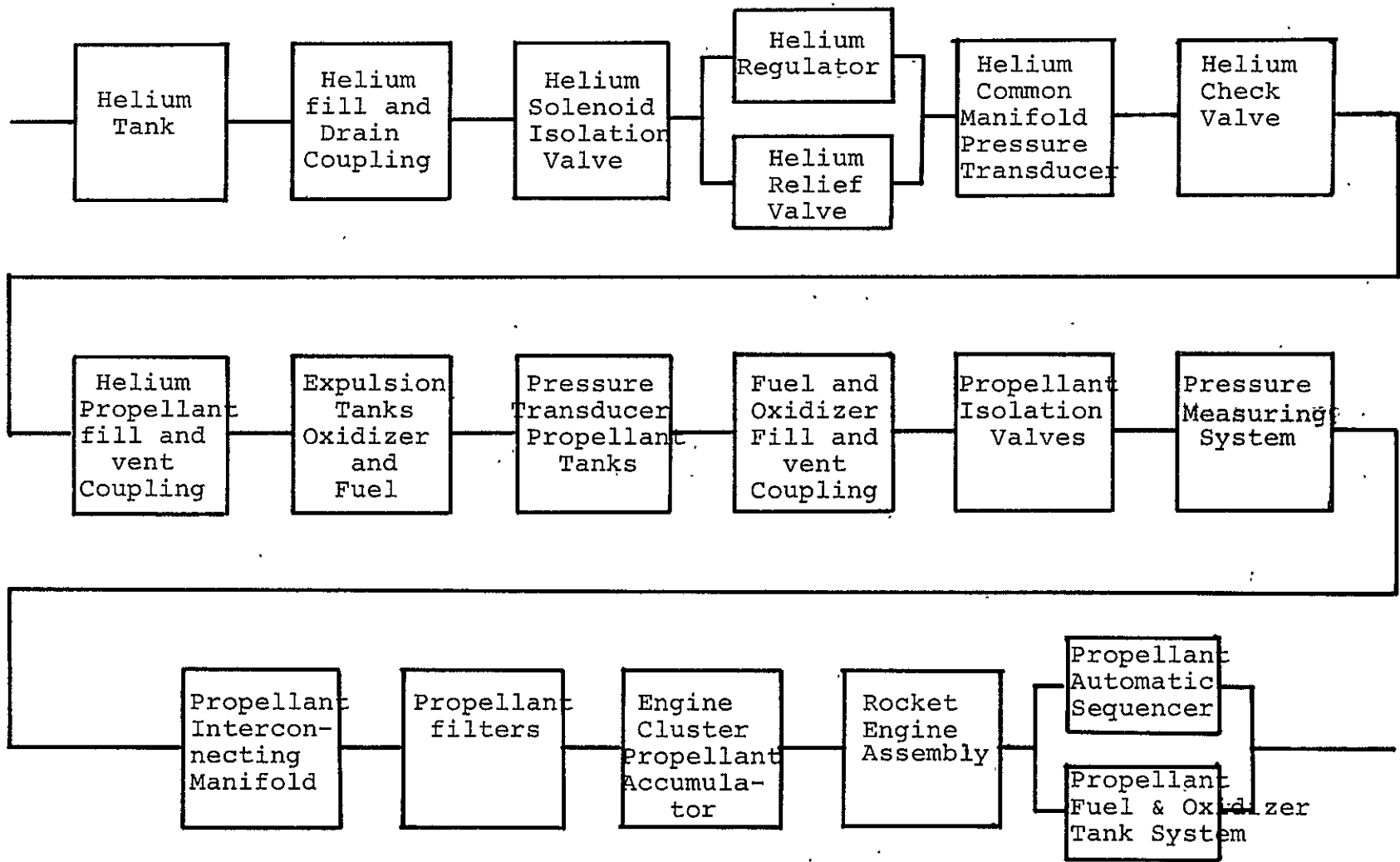


FIGURE 10.3-2 LOGIC DIAGRAM [BASIC VERNIER SYSTEM]

REFERENCES

1. Mandell, H. C., "A Graphical Costing Procedure for Advanced Manned Spacecraft (Mascot G)", NASA TM X-58012, Oct. 1967.
2. Lockheed Missiles & Space Co., "Improved Lunar Cargo and Personnel Delivery System Study", Contract NAS 8-21006, March, 1968.
3. "Mission Module Functional Failure Mode and Effects Analysis", (D-CSM-104), NAS9-150/SA300.
4. Rew, D. M., and N. A. Samuels, "Apollo Applications Program Failure Mode Analysis", Vol. 12, SM Reaction Control Subsystem, NAS9-6593, Jan 27, 1969.
5. Adelstone, J., "CSM 104 Criticality I and II Single Point Failure Summaries", NAS9-150, Sept, 1968.
6. Society of Environmental Engineers, "Environmental Engineering and Its Role in Society", Vol 5, London, 1966.
7. ARINC Research Corp, "Reliability Engineering", Prentice Hall, 1964.
8. McDonnell Astronautics, "Voyager Capsule Phase B Final Report", Vol 2, Capsule Bus System. Part E (Reliability), Report No. F694, N67-40051, August 31, 1967.
9. General Motors Corp, "Surveyor Lunar Roving Vehicle", Final Report, Phase I, Vol 2, Section IV (Reliability), N66-15481, April 23, 1964.